August 2010

Measurement of Temperature and Soil Properties for Finite Element Model Verification

Final Report

Prepared By:
Margaret M. Darrow, Ph.D.
Institute of Northern Engineering

Prepared By:

Alaska University Transportation Center
Duckering Building Room 245
P.O. Box 755900
Fairbanks, AK 99775-5900

Alaska Department of Transportation
Research, Development, and Technology
Transfer
2301 Peger Road
Fairbanks, AK 99709-5399

REPORT DOCUMENTATION PAGE

Form approved OMB No.

1. AGENCY USE ONLY (LEAVE BLANK)	2. REPORT DATE	3. REPORT TYPE AND DATES COVERED
FHWA-AK-RD-12-06	August 2012	Final (7/1/08-6/30/10)

4. TITLE AND SUBTITLE	5. FUNDING NUMBERS
Measurement of Temperature and Soil Properties for Finite Element Model Verification	T2-08-04 AUTC # RR08.11
6. AUTHOR(S) Margaret M. Darrow, Ph.D	DTRT06-G-0011

7. PERFORMING ORGANIZATION NAME(S) AND ADDRESS(ES) Alaska University Transportation Center P.O. Box 755900 Fairbanks, AK 99775-5900	8. PERFORMING ORGANIZATION REPORT NUMBER INE/AUTC 11.19

9. SPONSORING/MONITORING AGENCY NAME(S) AND ADDRESS(ES) Alaska Department of Transportation Research, Development, and Technology Transfer 2301 Peger Road Fairbanks, AK 99709-5399	10. SPONSORING/MONITORING AGENCY REPORT NUMBER FHWA-AK-RD-12-06

11. SUPPLENMENTARY NOTES

Performed in cooperation with the U.S. Department of Transportation, Federal Highway Administration.

12a. DISTRIBUTION / AVAILABILITY STATEMENT No restrictions	12b. DISTRIBUTION CODE

13. ABSTRACT (Maximum 200 words)

In recent years, ADOT&PF personnel have used TEMP/W, a commercially available two-dimensional finite element program, to conduct thermal modeling of various embankment configurations in an effort to reduce the thawing of ice-rich permafrost through thermally stable embankment designs. This modeling was done with historic air temperature data and input parameters derived from the literature, since site-specific data is typically not available. The overall goal of this study was to verify the thermal modeling results produced by TEMP/W. Temperatures and soil properties were measured at two different sites underlain by permafrost in Interior and Southcentral Alaska. A sensitivity analysis of certain input parameters was conducted on models of each site. Analysis indicates that the most critical input parameter is air temperature. While historic air temperature data provided an approximation of the regional climate, this data produced model results that were too cold by several degrees. Using air temperatures measured at each site resulted in models that closely matched the measured soil temperatures, and either matched or overestimated active layer depths. Using the overestimated active layer depth for design purposes would result in a more conservative embankment construction, which is a favorable approach if a warming climate is considered.

14- KEYWORDS: Permafrost (Rbespfp), Embankments (Pdxe), Embankment foundations (**Pdxte**), Thermal properties (**Rkt**) , Frozen soils (**Rbespfh**), Computer models (**Xbkpm**), Temperature sensors (**Dmgut**) , Temperature measurement (**Gmcn**) Frigid regions (Vcrf), Thermistors (**Qtbcit**) Ground settlement (**Jbgpw**)	15. NUMBER OF PAGES 295
	16. PRICE CODE N/A

17. SECURITY CLASSIFICATION OF REPORT	18. SECURITY CLASSIFICATION OF THIS PAGE	19. SECURITY CLASSIFICATION OF ABSTRACT	20. LIMITATION OF ABSTRACT
Unclassified	Unclassified	Unclassified	N/A

NSN 7540-01-280-5500

STANDARD FORM 298 (Rev. 2-98)
Prescribed by ANSI Std. 239-18 298-1

Changing the thermal conductivity input parameter had little effect on the model results for either location. The model results from the Richardson Highway research location indicate that using a soil- and site-specific unfrozen water content function improves the model accuracy when soils demonstrating a high unfrozen water content (i.e., clay) are present.

Of the two research sites investigated, the Dalton site is more critical in terms of thaw settlement, since the embankment directly overlies ice-rich permafrost. The final model for the Dalton Highway 9 Mile Hill research site, using site specific air temperatures and adjusted *n*-factors, produced active layer depths that closely matched those indicated from measured temperature data.

To reiterate, the driving input parameter is the surface boundary condition. Determining the surface temperatures for a project location will produce the most benefit in the thermal modeling of future embankment designs in permafrost regions. This can be accomplished by installing a weather station to measure air temperature. Additionally, measuring soil surface temperature to calculate representative *n*-factors for a surface type will help to improve the model. If thermal modeling is planned for a project location, the geotechnical field investigation and sampling program can be improved by collecting soil samples for determination of dry unit weight, percent ice, and unfrozen water content.

Although climate warming scenarios were not included in the present analysis, these research results suggest that such scenarios should be considered given the importance of the surface boundary condition. Finally, both of the sites modeled consisted of long-established embankments that may have finally reached a thermal equilibrium with the foundation soils. To further investigate modeled embankments, a newly constructed embankment over permafrost should be instrumented and modeled.

TABLE OF CONTENTS

TABLE OF FIGURES

TABLE OF TABLES

APPENDICES

CHAPTER 1 – INTRODUCTION

1.1 Background

Areas of Alaska's highways experience distress due to the thawing of ice-rich permafrost below the highway embankment. This has been recognized as a maintenance problem for many years and by many individuals with the Alaska Department of Transportation and Public Facilities (AK DOT&PF). In the early 1990's, AK DOT&PF designers began to use an MS-DOS computer program, MUT1D (Multilayer User-Friendly Thermal Model in 1 Dimension), to conduct thermal analysis of embankment designs. MUT1D uses implicit finite difference techniques to estimate the thermal regime of a multilayered model in one dimension (Braley and Zarling 1990). Using this program, designers analyzed different embankment heights, with and without layers of insulation, to determine the effects on the thermal regime of the foundation soils. Although the MUT1D model yields results with acceptable accuracy (Braley and Zarling 1990), it is limited to producing the depth of phase change along a single line of analysis.

In contrast, two-dimensional (2-D) finite element programs provide heat flow analysis for an entire cross-section. The author, while employed with AK DOT&PF, began to use TEMP/W in 2006, which is a commercially available 2-D finite element program. The model results can be viewed in a variety of ways, including as heat flow vectors and as color temperature contour plots. Because this model incorporates 2-D boundary effects, it is more accurate than a 1-D model.

For a typical analysis using TEMP/W, the author would find collected air temperature data as close to the project site as possible; in many cases, the nearest collection point would be more than 50 miles from the project site and/or more than 30 years out-of-date. The soil input parameters (e.g., frozen and unfrozen thermal conductivity) and surface boundary condition modifiers (i.e., *n*-factors) would be selected from charts and tables of representative values available in the literature. In other words, these input parameters are "educated guesses." The modeling results of such an analysis suggest a typical temperature configuration within/and below the embankment and at the embankment toe, which is grossly consistent with visual observations of embankment performance, as well as with the measured thaw depth progression at certain locations (Esch 1994). These modeling results, however, have not yet been checked for accuracy against actual field conditions. Gosink et al. (1986), in their testing of two computer models for the ground thermal regime, indicated that "…a complete data set including the thermal and hydrological regimes and measurements of all model parameters is urgently required to test numerical models of heat and mass transport." These authors recommended that a research program be initiated to measure these needed input parameters, specifically thermal and hydrological parameters such as thermal conductivity and unfrozen water content.

1.2 Objectives

The overall goal of this study is to ground-truth the 2-D thermal modeling results. The objectives of this study are: 1) to measure temperatures from within existing embankments and the underlying foundation soils at two permafrost locations with differing climates and soils; 2) to measure the thermal and hydrological properties of the soils at these locations; and 3) to conduct a review of previously measured temperature data from other locations within AK

1

DOT&PF's Northern Region, against which further 2-D thermal modeling results may be compared.

To achieve these objectives, this study consisted of the following tasks:

- Conducting field programs for the Richardson Highway mile post (MP) 113 location and the Dalton Highway 9 Mile Hill location, which included soil collection and installation of thermistor strings to measure soil temperatures.

- Performing standard AK DOT&PF laboratory testing and specialized testing on the acquired soil samples.

- Comparing model results from the TEMP/W program produced using both the "educated guesses" as input parameters and those produced using the measured soil properties, to the measured soil temperatures.

- Summarizing previously measured temperature data, and associated literature, from other locations within AK DOT&PF's Northern Region.

Chapters 2 and 3 of this report summarize the field programs, soils, and laboratory results for the two research locations, Richardson Highway MP 113 and Dalton Highway 9 Mile Hill, respectively. Chapter 4 summarizes the measured temperatures from both locations, and Chapter 5 reviews the thermal modeling procedures and results. Chapter 6 details the archived temperature data from previous research and associated literature; updated Excel spreadsheets of the temperature data, copies of the associated AK DOT&PF reports, and the original data files are included on CD media at the end of this report. Several appendices contain test hole logs, laboratory data, ADAS parts lists, raw thermal conductivity data, modeling results, and a user's guide to selecting input parameters for thermal modeling using the TEMP/W program.

2.1 Site Location, History, and Soil Characteristics

We chose the Richardson Highway MP 113 location because of previous and ongoing work in the area, fine-grained foundation soils, and the presence of permafrost. This research site is located approximately three miles south of the intersection of the Glenn Highway with the Richardson Highway, which lies about 189 road miles from Anchorage and about 247 road miles from Fairbanks.

2.1.1 History of road work

The oldest as-built plans on file in Northern Region for this portion of the Richardson Highway date from the 1950's, when the centerline of the highway was approximately 90 ft from the bluff edge overlooking the Copper River in the MP 113 area (see Figure 2.1). In 1965, this portion of the highway was realigned away from the bluff edge. The new alignment required a deep cut and a high side-hill fill where the highway descended from the top of the bluff to the Tazlina River to the south, an area known as Simpson Hill. During the fill construction, a slope failure occurred in which a portion of the embankment moved up to 30 ft horizontally and dropped up to 20 ft vertically. Platts (1965) attributed the failure to excessive loading of a saturated clay foundation, causing excessive pore pressures and loss of strength. Platts suggested that the source of water was melting of massive ice exposed in the cut, as well as water introduced by construction. The slope failure mitigation consisted of building a soil buttress along the toe of the embankment and adding underdrains to direct excess water down slope into the ditch.

In 1977 and again in 1993, this section of highway was rehabilitated and repaved. Prior to the 1993 project, the Simpson Hill area again experienced a small slope failure, which disturbed the existing buttress and part of the roadway embankment. Similar to the 1965 mitigation, the 1993 slope failure was corrected by rebuilding the soil buttress. Underdrains were extended to the north along both sides of the highway beyond the crest of the hill. Figure 2.2 is a schematic of the underdrain design, modified from the relevant as-builts on file with Northern Region.

Since the 1965 realignment, the bluff at the MP 113 location (roughly 2000 ft north of the Simpson Hill area) has experienced significant erosion, with westward progressing gullies eradicating portions of the abandoned highway. AK DOT&PF Northern Region Materials Section (NRMS) personnel have investigated the Richardson Highway MP 113 area three different times in the past two decades. In 1991, NRMS personnel drilled 25 test holes in the MP 113 slide area, and installed casing for three water observation wells. In 2003, NRMS personnel drilled eight test holes in the area, installing Slope Indicator (SI) casing in five of these borings (03-01, 03-02, 03-03, 03-04, 03-05), and casing for water observation wells in four of these borings (03-02, 03-06, 03-07, 03-08). During the winter of 2005, one SI casing (03-05) and water observation well casing (03-07) were broken off at the ground level. Because this SI casing was in a critical location for slope movement measurements, NRMS decided to replace it with a new installation. Two additional SI casings (07-1710 and 07-1711) were installed during November 2007 to the west and east of the highway (see Figure 2.1).

Figure 2.1. Location of the Richardson Highway MP 113 research location, including 2003, 2007, and 2009 test hole locations. Inset shows the project location relative to Fairbanks and Anchorage.
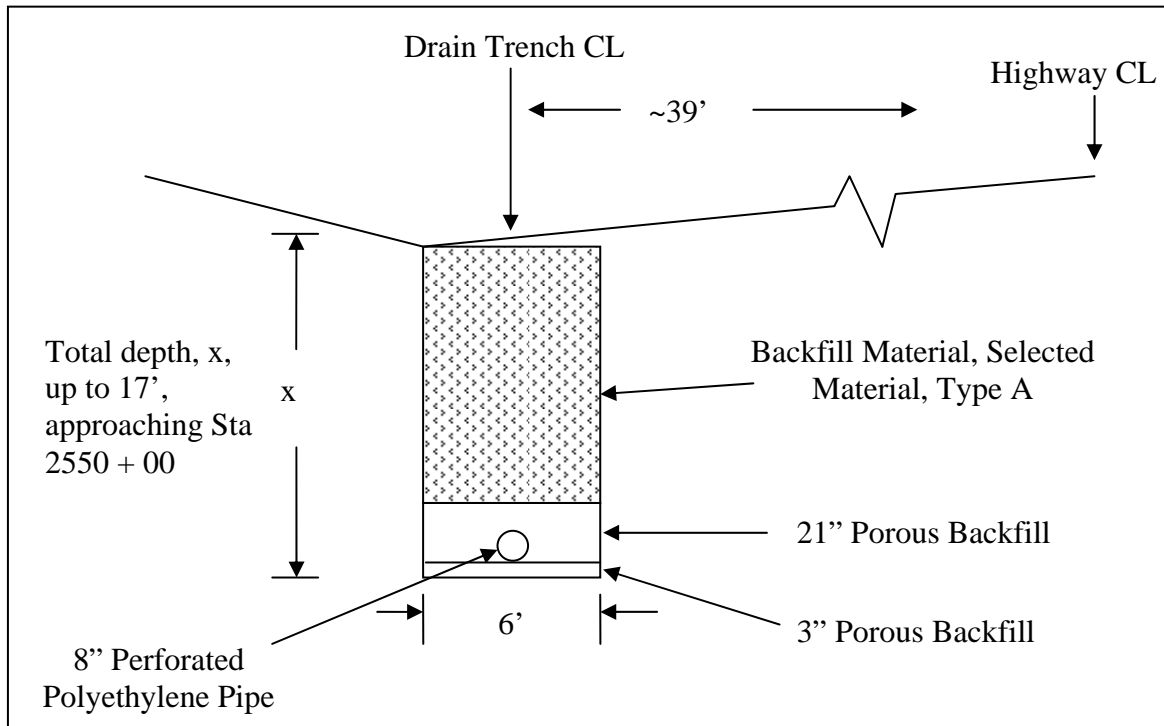
Figure 2.2. A detail of the underdrain present in the Richardson Highway MP 113 area; Station 2550+00 is approximately at the 113 mile marker (modified from the "*Richardson Highway Mile 106 to 155, Rehabilitation, Bike Path and Paving F-071-2(30)/65197, 1992*" as-builts available from AK DOT&PF).

2.1.2 Foundation soils and permafrost

During the late Pleistocene, glaciers originating in the mountains surrounding the Copper River Lowland coalesced and blocked the drainage of the Copper River to the south. This resulted in the formation of a large proglacial lake, Lake Atna. The most recent formation of Lake Atna was during the Last Glacial Maximum (i.e., roughly 20,000 yr BP), when the lake covered more than 2,000 mi^2 of the lowland (Ferrians, Jr. et al. 1983). The lacustrine deposits in the lowland are laminated lake sediments, as well as nonsorted deposits, referred to as glaciolacustrine diamicton deposits, with ice-rafted sediments throughout. The deposits mostly consist of silty clay and clayey silt with pervasively scattered sand and gravel. Radiocarbon dates of the organic material at the top horizon of the lacustrine deposits indicate that Lake Atna drained around 9,400 ± 300 yr BP (Ferrians, Jr. et al. 1983).

Permafrost is ubiquitous throughout the Copper River Lowland. It typically ranges from 100 to 200-ft thick, and is considered to be "warm permafrost," with temperatures in the range of 31.3°F to 29.3°F (Ferrians, Jr. et al. 1983). Shur and Zhestkova (2003) presented a summary of drilling done in the Copper River Lowland. As indicated by these previous borings, the frozen soils may contain ice as stratified ice lenses or as massive ice up to 15-ft thick.

2.2 2008 Fieldwork Program

The PI and a NRMS drill crew (T. Johnson, S. Parker, J. Cline) conducted a drilling program at the Richardson Highway MP 113 location from November 6 to November 10, 2008. P. Calvin, a UAF Masters student at the time, aided in the field work, and M. Lilly of Geo-Watersheds Scientific oversaw the installation of the Automated Data Acquisition System (ADAS).

Maintenance and Operations (M&O) personnel from the Tazlina maintenance station began the fieldwork by using a tracked excavator to dig a trench in which the cables would be buried (see Figure 2.3). Once the trench was completed, NRMS personnel centered the truck-mounted CME-45B drill over the trench to drill the boring for the undisturbed location, the ADAS, and for the boring at the toe of the slope (see Figure 2.4). In total, we drilled six test holes (TH), five with hollow-stem (HS) auger and one with solid-stem (SS) auger. Logs for each of these test holes are located in Appendix A and AK DOT&PF laboratory results are summarized in Appendix B. Drilling in the winter months is rarely routine, as the freezing temperatures take their toll on the equipment and personnel. An extended narrative of the November 2008 drilling is included here to detail the added complexities of recovering samples and installing instrumentation during winter.

2.2.1 Drilling details, foundation soils, and AK DOT&PF laboratory results

The first boring completed was TH08-1650, which was located in the stand of spruce to the east of the highway (see Figure 2.4). This is referred to as the "undisturbed" location in what follows, as it most closely resembles the *in situ* conditions that would exist without anthropogenic disturbance. On November 7, we drilled TH08-1650 with HS auger to 34.5 ft, and intercepted 3.8 ft of silt, underlain by fat clay with areas of sand and gravel to the bottom of the hole (BOH) (see Figure 2.5a). The upper 0.5 ft of the soil contained seasonal frost, while the permafrost table was at 6.5 ft below the surface. We observed ice veins and random crystals in soil samples (see Figure 2.5b), and drill reaction suggested the presence of massive ice from 30.5 to 31.5 ft and again from 32.5 to 33.5 ft. While sampling at a depth of 22.0 ft, the continuous sampler sheared off at the bottom of the test hole. The drillers had to advance the hole to 25.0 ft in order to recover the sample. Once the sampler was retrieved from the boring, drilling was discontinued for the night. Early on November 8, we installed the thermistor string to a depth of 30 ft below the ground surface (bgs), backfilling with commercially-available bagged sand to the depth of the bottom of the trench. The thermistor installation procedures are detailed in a separate section of this report.

The truck-mounted drill was moved forward along the trench by about 10 ft, and a shallow test hole, TH08-1651, was drilled with HS auger for the installation of the 4 in. by 6 in. post that served as the mounting surface for the ADAS.

In the afternoon of November 8, 2008, NRMS personnel moved the drill truck to a location along the roadway, positioning the drill at 40 in. from the pavement edge right at the upper break in slope along the top of the embankment. This boring, TH08-1652 drilled with HS auger, would have served as the location for the shoulder thermistor installation. The driveline on the drill broke at around 2 pm, however; drilling was stopped to repair the driveline. The following day, the drill truck could not be repositioned over TH08-1652 as it continued to slide down the embankment. TH08-1652 was abandoned.
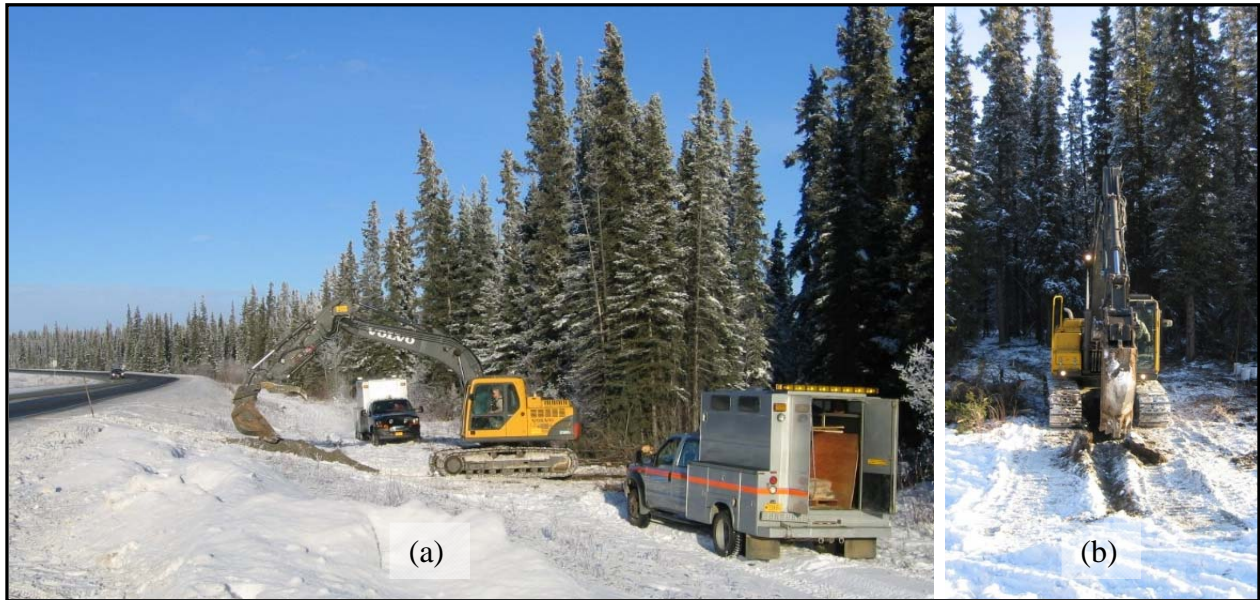
Figure 2.3. Tazlina M&O personnel digging the trench for cables: (a) view to the north, showing the research location relative to the Richardson Highway; (b) view to the east from the highway along the trench.

Figure 2.4. NRMS truck-mounted CME 45B drill centered over the trench at TH08-1650.
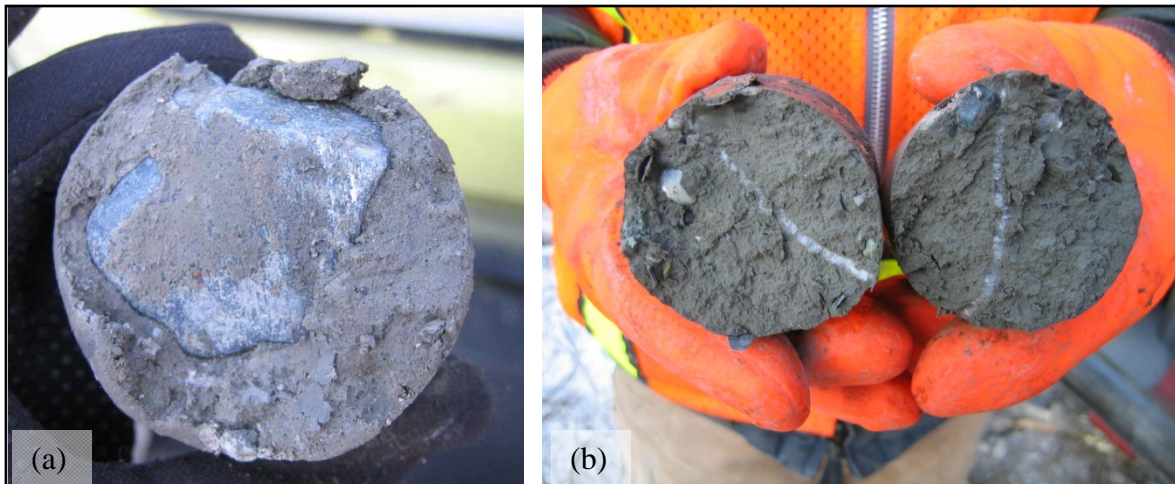
Figure 2.5. Split-spoon samples from TH08-1650: (a) clayey soil containing gravel; (b) clayey soil containing sand and gravel and visible ice vein.

On November 9, 2008, we began drilling the new boring for the shoulder thermistor installation, TH08-1652b. This test hole, drilled using HS auger, was located at the edge of the pavement, with the upper four inches consisting of asphalt-concrete (see Figure 2.6). At this location, the embankment was 6.5 ft thick, and consisted of well-graded sand with gravel and silt, underlain by well-graded gravel with sand and silt. The foundation soils were 2.5 ft of silty sand with gravel, underlain by sandy silty clay and sandy lean clay, with gravel scattered throughout. Only the upper five feet of the test hole were frozen, which was drilled to 40.0 ft bgs. A thermistor string was installed to 30.0 ft bgs, and the boring was backfilled with sand from the Tazlina M&O station. This installation will be referred to as the "embankment" location.

The final thermistor installation originally was located at the base of the embankment, or at the toe. NRMS personnel backed the drill truck up to this location along the trench during the afternoon of November 9, 2008 (see Figure 2.7). This boring, TH08-1653, was drilled with HS auger. We intercepted 5.0 ft of well-graded gravel with sand, silt, and cobbles, underlain by well-graded sand with gravel to a depth of 25.5 ft. This was underlain by sandy lean clay. A water table was intercepted at 24.0 ft. Only the upper 5.0 ft of the test hole were frozen. Based on its grain size and location at the toe of the embankment, this sandy material is interpreted as one of the underdrains emplaced during the 1993 construction project. Because of the loose sand and water table, the test hole collapsed at 24.0 ft. Despite our efforts, we could not install the thermistor string to the required depth. We abandoned and backfilled this boring. Additionally, a portion of the safety hammer broke during the retrieval of a soil sample.

The final boring, TH08-1654 or the "toe" location, was located within the trench roughly nine feet from the toe of the embankment. Without the safety hammer, samples were limited to collecting auger flight; thus, this test hole was drilled using solid-stem (SS) auger for expediency. We intercepted 10 inches of silty gravel, followed by 1.2 ft of gravelly silt, and sandy silty clay with cobbles to BOH at 35.5 ft. The upper 2.5 ft of the test hole were frozen; the permafrost table and massive ice were inferred at 34.5 ft based on drill reaction. After removing the auger, a

Figure 2.6. Location of TH08-1652b at the edge of pavement.

Figure 2.7. Position of TH08-1653 within the trench.

clay plug formed at 23.0 ft; we were able to push the thermistor through the clay to a depth of 30.0 ft. We backfilled with sand from the Tazlina M&O station.

A total of 32 samples were transported to the AK DOT&PF NRMS laboratory for testing. Laboratory results are summarized on the test hole logs in Appendix A, as well as on summary sheets in Appendix B. Table 2.1 is a list of the laboratory testing performed by AK DOT&PF personnel for this project.

Table 2.1. Summary of laboratory test methods used by AK DOT&PF

Test Name (*short description or common identifier)*	ASTM Test Number
Moisture Content of Soils (*Natural Moisture*)	D2216
Sieve Analysis of Fine and Coarse Aggregates (*Gradation*)	C126/C117
Determining the Liquid Limit of Soils (*Liquid Limit*)	D4318
Determining the Plastic Limit and Plasticity Index of Soils (*Plastic Limit/PI*)	D4318
Organic Content of Soils by Ignition (*Organic Content*)	D2974
Specific Gravity of Soils (*Fine Specific Gravity*)	D854

2.2.2 Thermistor installation

Once the drillers removed the auger from the completed boring, we began to stage the associated thermistor for installation. The first step was to stretch the thermistor string out along the ground; because of the sub-freezing temperatures, uncoiling the thermistor string before installation helped with its maneuverability (see Figure 2.8a). Next, we assembled threaded steel rods, attaching them together with couplers and set screws. We greased the end of the steel rod before "lightly" attaching a coupler (i.e., the coupler was mated to the rod by only two threads). We then securely taped the down-hole end of the thermistor string to the coupler (see Figure 2.8b).

The rod/thermistor string assembly was lowered into the boring. While applying tension to the thermistor string, we positioned the assembly so that the thermistor beads were at the correct depths relative to the ground surface. We then began to backfill the boring. Once the thermistor string was anchored at the correct depth, we carefully backed off the steel rod from the coupler at the base of the boring (see Figure 2.9a). The rod was removed from the test hole and the remainder of the boring was backfilled with sand, which was tamped at intervals throughout the process (see Figure 2.9b). Tamping was accomplished using fiberglass rods.

Each of the thermistor strings was installed in a similar fashion. After installation, the cables were laid into the trench and routed to the ADAS location (see Figure 2.10). Above each thermistor string, we installed a CS107 sensor. These temperature sensors were placed approximately 0.25 ft below the surface at TH08-1650, and 0.33 ft below the surface at both 08-1652b and 08-1654; the exact depth was determined during the final backfilling of the trench. Initially, we lightly covered the cables with sand using shovels or a bucket (see Figure 2.11a). Once the cables were secured, M&O backfilled the rest of the trench with a loader (see Figure 2.11b). We backfilled by hand around each of the CS107 sensors and at the ADAS location in order to anchor the ends of the Liquid Tight conduit (see Figure 2.12).

2.2.3 ADAS set up

Geo-Watersheds Scientific designed and installed the ADAS for this research location. The overall system, shown in Figure 2.13, can be separated into the power and enclosure components, the data acquisition components, and the telemetry components.

Figure 2.8. Staging a thermistor for installation: (a) extending the thermistor string along the steel rod; (b) thermistor end attached to the "sacrificial" coupler.

Figure 2.9. Installing a thermistor string: (a) backing off the steel rod (red in color); (b) backfilling and tamping the test hole.

Figure 2.10. Thermistor cables at the bottom of the trench at the TH08-1654 location, prior to backfilling. Note the CS107 sensor laying on the sandy backfill. Its exact placement occurred during the final backfilling of the trench.
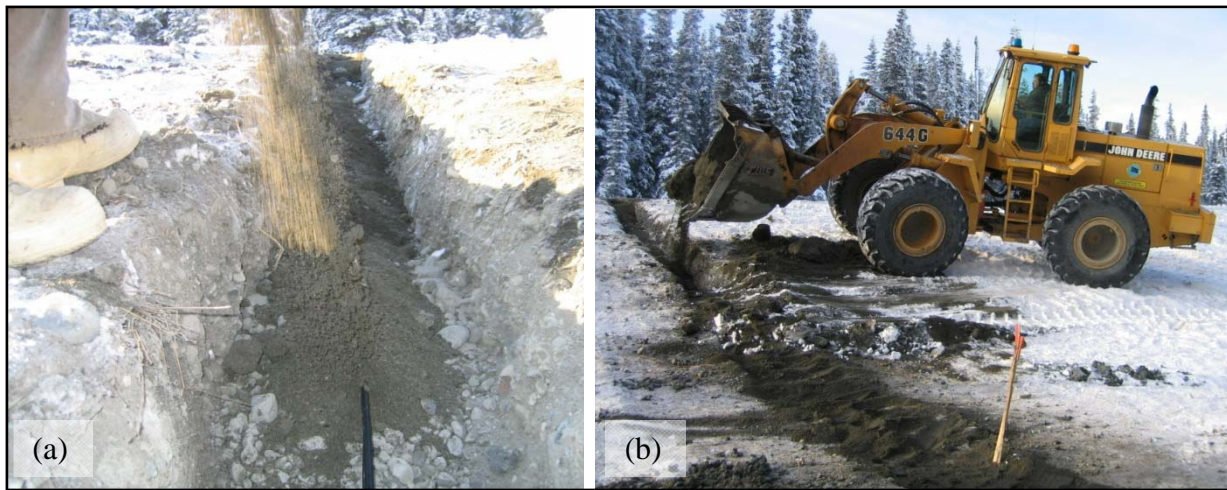
Figure 2.11. Backfilling the trench: (a) anchoring the cables using buckets and shovelfuls of sand; (b) M&O making short work of the backfilling with a loader.

The power is provided by a 20 Watt solar panel that powers the system during most of the year, and charges three 100 Amp-Hr deep cycle batteries, which are housed in a battery enclosure resting on the ground (indicated as (e) in Figure 2.13). The data acquisition components are housed within a weather-resistant enclosure (indicated as (d) in Figure 2.13), and consist of a Campbell Scientific (CS) CR1000 datalogger and a CS AM16/32B multiplexer (see Figure 2.14).

The telemetry components at the field site consist of a RF450 900 MHz 1W spread spectrum radio (see Figure 2.14) and a 900 MHz omni antenna (indicated as (a) in Figure 2.13). This radio

Figure 2.12. Thermistor cables and Liquid Tight conduit routing into the ADAS system.
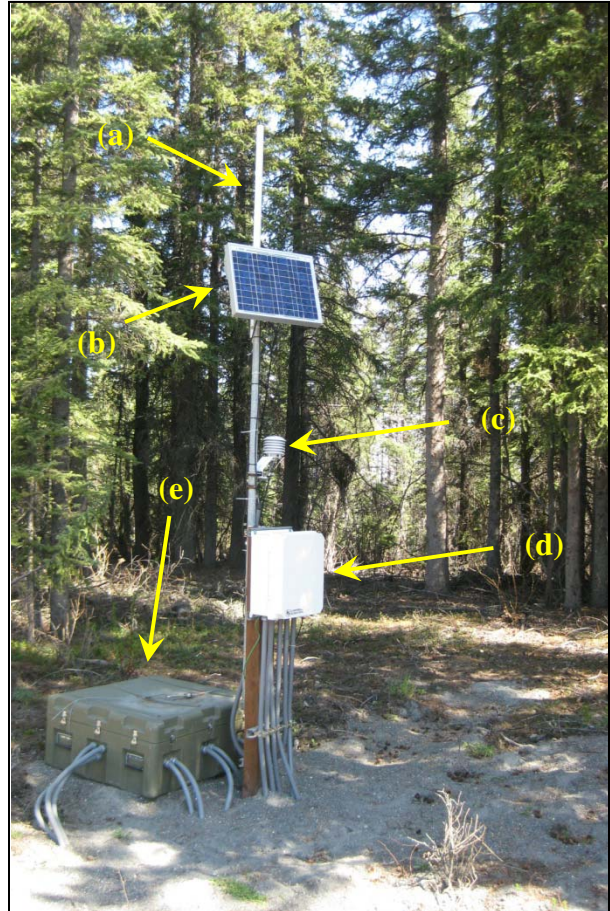
Figure 2.13. The complete ADAS installation: a) antenna; b) solar panel; c) air temperature sensors within radiation shield; d) instrumentation enclosure; e) battery enclosure.

and antenna are used to communicate to a base station at the Tazlina M&O station, as shown in Figure 2.15. The Tazlina M&O graciously allowed us to mount a second antenna to the outside of their building. The cable from the antenna is routed into the building to a second enclosure, which contains a second spread spectrum radio, a Moxa portserver to communicate to the internet, and a power supply. Using a DSL connection provided by a local communications company, we are able to communicate remotely with the Richardson Highway MP 113 site. A complete parts-list is included as Appendix C.

2.3 Specialized Laboratory Testing

Some of the samples obtained during the November 2008 field work were transported to a UAF laboratory for specialized testing. These tests are "specialized" in that they are not routinely performed by AK DOT&PF. The samples transported to UAF were in split-spoon liners in a frozen state, and were stored in a freezer until testing.
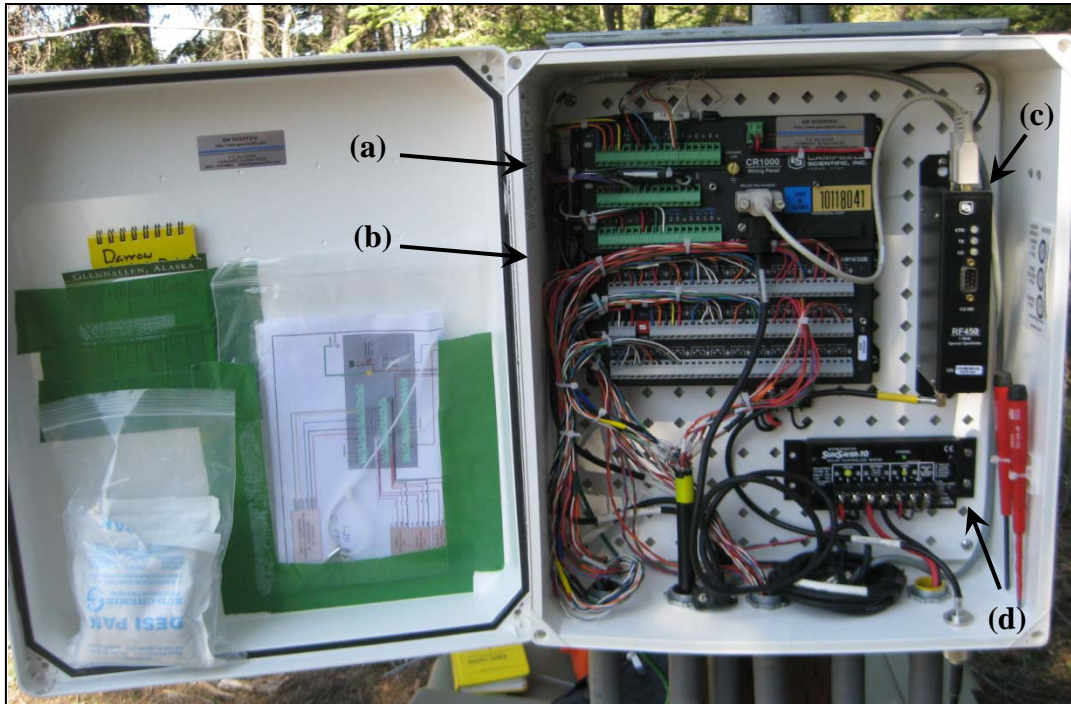
Figure 2.14. Data acquisition and telemetry components: a) CR1000 datalogger; b) AM16/32B multiplexer; c) RF450 900MHz 1W spread spectrum radio. Item (d) is a charge controller for the batteries and solar panel.

Figure 2.15. Telemetry components at the Tazlina M&O station: a) 900 MHz omni directional antenna mounted to the outside of the building; b) enclosure containing RF450 900MHz 1W spread spectrum radio, Moxa portserver, and 12 Vdc power supply with charging regulator and 7 Amp-Hr sealed rechargeable battery. The enclosure is mounted to a wall in the corner room on the second floor the building (the room contains the grate through which the antenna cable runs in (a).

14

2.3.1 Dry unit weight and volumetric water content

The moisture content of samples (often reported as "NM" for natural moisture on NRMS logs) is a standard test performed by the AK DOT&PF. This value is also called the gravimetric moisture content, as it is calculated as a percentage of the overall weight of the dry soil. The use of this number is rather nonsensical with ice-rich soils, however, as the gravimetric moisture content may be greater than 100%. A more appropriate measurement is volumetric moisture content (θ), which is calculated as a percentage of the total volume of the soil sample. This is calculated using the gravimetric moisture content and the dry unit weight.

We prepared portions of the frozen samples for dry unit weight and volumetric water content measurements. To determine dry unit weight (γ_d), the volume of each sample was measured by coating the soil sample in wax, submerging it into water, and reading the volume of displaced water. The weight of the sample was determined using standard oven drying techniques.

Table 2.2 is a summary of gravimetric and volumetric moisture contents, and dry unit weights, γ_d. The values for θ are reported as "VOL MC" on the test hole logs in Appendix A. Between 9.0 and 14.0 ft bgs, moisture content decreased with depth while the dry unit weight increased with depth.

Table 2.2. Moisture content and dry unit weight results.

Sample number	Depth (ft-ft)	Gravimetric moisture content (%)	Dry unit weight, γ_d (lb/ft^3)	Volumetric moisture content, θ (%)
4071A	9.0-9.4	27.9	108.2	48.2
4073A	12.5-13.0	20.3	114.8	37.3
4073B	13.0-13.5	16.2	119.9	31.0
4073C	13.5-14.0	15.6	121.2	24.4

2.3.2 Thermal conductivity

Thermal conductivity measurements were made using a Decagon KD2 Pro device, consisting of a single-needle probe and a handheld controller. The probe sends a heat pulse into the soil, then measures the temperature response. Thermal conductivity is calculated using a non-linear least squares procedure to minimize the difference between the measured response temperature and a modeled temperature (Decagon Devices, Inc. 2006). The modeled temperature assumes an infinite line heat source with a zero mass that applies a constant heat over a period of time, based on the work of Carslaw and Jaeger (1986).

Through trial and error, we discovered that the thermal conductivity readings varied depending on how many points of thermal contact the needle had with the soil grains. Thermal conductivity readings of the coarse-grained sandy gravel from the embankment were unsuccessful. We were successful obtaining readings from the frozen, fine-grained soil samples. We cut each frozen sample to the necessary length and drilled two holes in which we would later insert the probe and a temperature measurement device. The sample was thoroughly wrapped in plastic wrap and foil with one end exposed. It was placed into a temperature bath, exposed end up, and the fluid level

was raised until just below the top of the sample. We filled each pre-drilled hole with a thermal compound to ensure good thermal connections between the soil and the thermal conductivity probe and temperature measurement device, which were inserted into the holes. The soil sample and bath were covered to create a thermally stable environment, and the temperature of the bath was set to the desired value. We began the thermal conductivity readings at the lowest sub-freezing temperature, steadily raising the bath temperature through phase change, and then at two above-freezing temperatures. The bath was set to temperatures in degrees Celsius. These temperatures are listed here, followed by the equivalent temperature in degrees Fahrenheit: -20°C, (-4°F), -15°C (5°F), -10°C (14°F), -7.5°C (18.5°F), -5°C (23°F), -4°C (24.8°F), -3°C (26.6°F), -2°C (28.4°F), -1°C (30.2°F), -0.5°C (31.1°F), -0.2°C (31.6°F), 5°C (41°F), and 10°C (50°F).

Three thermal conductivity measurements were made at each temperature setting. Readings showed little variation for a given temperature; the average standard deviation for all temperatures was 0.008 Btu/ft·hr·°F. Because the needle probe sends a heat pulse into the soil, we measured the temperature of the soil sample before and after each set of thermal conductivity measurements. The temperature rise on average was 0.03°F. See Appendix D for the raw thermal conductivity data.

Figure 2.16 is a summary of the average thermal conductivity readings for each temperature for the Richardson Highway MP 113 samples. Each thermal conductivity value is plotted against the average of the recorded bath temperatures, rather than the bath set point since these values were slightly different. Generally, if a soil contains any amount of water, its frozen thermal conductivity (k_f) should be higher than unfrozen thermal conductivity (k_u), since the thermal conductivity of ice (1.27 Btu/ft·hr·°F) is higher than that of water (0.33 Btu/ft·hr·°F). This is true for each of the soil samples tested.

For three of the samples, as the temperature was raised from -4 °F and approached the phase change temperature, the k_f thermal conductivity rose steeply before falling to the k_u value. These spikes may be an artifact of the needle probe. Nearing the phase change temperature, the heat pulse that the probe gives off may melt some of the ice in the soil. This heat pulse results in a change of latent heat rather than sensible heat, giving an erroneously high reading for thermal conductivity (J. Zarling, pers. comm., June 2010). These spikes in thermal conductivity are still under investigation at this time.

These samples demonstrate a wide range in thermal conductivity, which is attributed to differences in soil composition and moisture content from sample to sample. The average k_u chosen from this range of data is 0.724 Btu/ft·hr·°F, and the average k_f is 0.992 Btu/ft·hr·°F. All of these samples demonstrated the change from k_u to k_f well below 32°F (as indicated by the red dashed line in Figure 2.16). This indicates that the soils are not "frozen," even though they are at sub-freezing temperatures, a phenomenon which can be explained by the presence of unfrozen water. Shur and Zhestkova (2003) also noted the presence of unfrozen clay at temperatures below 32°F in borings in the general area of the research site.
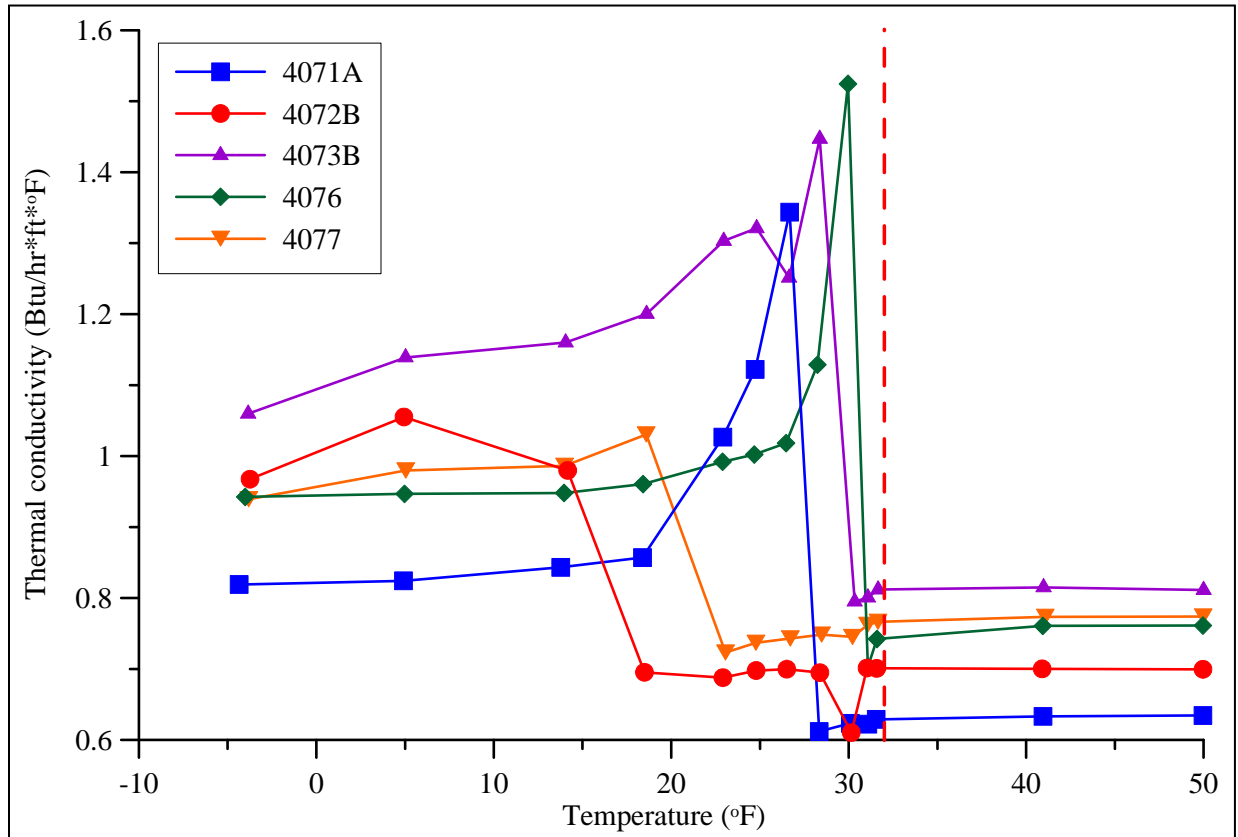
Figure 2.16. Summary of thermal conductivity measurements for the clayey soil samples, Richardson Highway MP 113 research site. The vertical dashed red line represents the 32°F isotherm.

3.1 Site Location, History, and Soil Characteristics

As with the first research site, we chose the Dalton Highway 9 Mile Hill location because of previous and ongoing work in the area, and fine-grained foundation soils that are ice-rich. This research site is located nine miles to the north of the start of the Dalton Highway from the Elliott Highway near Livengood (see Figure 3.1).

AK DOT&PF has been exploring realigning the section of the Dalton Highway between MP 8 and MP 12 for at least two decades. The current plans are to reconstruct this section of road, widening the surface and straightening the overall alignment. NRMS personnel have conducted exploration along proposed alignments in this area in 1990, 1991, 2008, and 2009. This site is also an active research site because of the nature of the permafrost in the area (Shur and Kanevskiy 2010). This large volume of data will not be summarized here. Instead, we direct the reader to the relevant reports (i.e., Schlichting and Darrow 2006, Rowland 2010).

3.2 2009 Fieldwork Program

The PI and the NRMS drill crew (J. Cline, C. Roach, J. Rowland, and J. Love from Anchorage) conducted a drilling program at the Dalton Highway 9 Mile Hill location from August 3 to August 7, 2009. C. McCabe, an undergraduate student working for this project, aided in the field work. We experienced dense smoke from wildfires in the area during drilling; this is the cause of the hazy appearance of the photographs from the field.

We drilled three borings with HS and two borings with SS with a track-mounted CME 850 Lite from Anchorage. Logs for each of these test holes are located in Appendix A and AK DOT&PF laboratory results are summarized in Appendix B.

3.2.1 Drilling and thermistor installation details, foundation soils, and AK DOT&PF laboratory results

During the morning of August 4, we first completed the boring for the post, TH09-1400, using HS. In this boring, the subsurface consisted of a 0.4-ft thick organic mat, underlain by saturated silt. We intercepted the permafrost table at 1.3 ft bgs. Where frozen, the silt contained as much as 50% visible ice.

Following the post installation, we completed the boring for the undisturbed location (TH09-1401), using HS. Both TH09-1400 and TH09-1401 were located in the black spruce to the west of the highway (see Figure 3.2). The subsurface consisted of a 0.4-ft thick organic mat, underlain by saturated silt. Again, we intercepted the permafrost table at 1.3 ft bgs. Where frozen, the silt contained 25-50% visible ice. We collected one ice-rich soil sample in a split-spoon liner from 2.5-4.5 ft bgs, which we placed into a freezer to transport back to the UAF laboratory. At 15 ft bgs, we intercepted massive ice to the BOH at 32.5 ft. The ice contained varying amounts of silt (see Figure 3.3). Using the process described in Section 2.2.2 of this report, we successfully installed a thermistor string to a depth of 30.0 ft bgs, and backfilled with commercially-available bagged sand. A CS107 temperature sensor was placed above the thermistor string, 0.17 ft below the surface. The upper portion of the boring was backfilled with
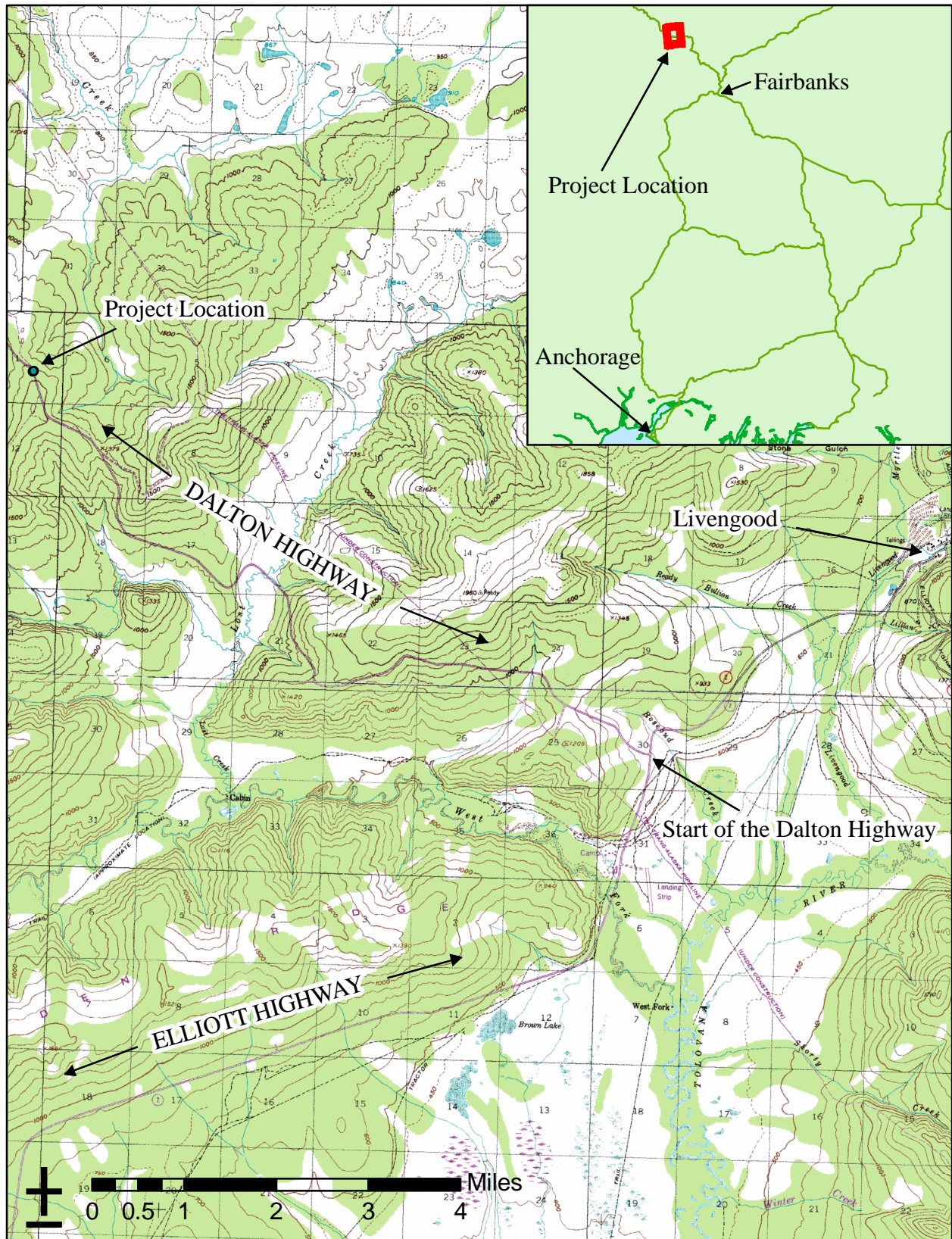
Figure 3.1. Location of the Dalton Highway 9 Mile Hill research location. Inset shows the project location relative to Fairbanks and Anchorage.

Figure 3.2. Drilling the boring for the undisturbed location, Dalton Highway 9 Mile Hill. Note the location of the post for the ADAS in the foreground.

Figure 3.3. Split-spoon samples of massive ice, TH09-1401: a) ice with silt from 15.5-17.5 ft bgs; b) ice from 23.0-25.0 ft bgs.

the wet silt. Once the thermistor cable was laid in a shallow trench to the ADAS, we replaced the organic mat as cover (see Figure 3.4).

On August 5, we drilled TH09-1402 and TH09-1403. TH09-1402, drilled with HS, was located in the shoulder of the Dalton Highway. We intercepted 11.2 ft of fill consisting of well-graded sand with clay and gravel. Immediately below the fill was 0.8 ft of organic silt, followed by massive ice to BOH at 28.0 ft. These transitions are clearly visible in Figure 3.5. At 28.0 ft, the pilot bit broke off of the auger and could not be retrieved. As a result, we abandoned this boring.

Moving three feet to the north of TH09-1402 along the shoulder, we began drilling TH09-1403 using SS (see Figure 3.6). We intercepted 10.0 ft of fill overlaying 0.7 ft of silt. Below the silt, we intercepted massive ice to BOH at 35.0 ft. When viewed from the ditch, the embankment appears to be roughly three-feet high (see Figure 3.7). In reality, it is 10.0-ft thick, which indicates the quantity of fill and tremendous amount of ongoing maintenance that this highway has experienced due to the melting of massive ice below it. After drilling, the bottom of the boring caved in. We were able to install the thermistor string only to a depth of 29.5 ft, requiring a 0.5 ft adjustment of all of the predetermined thermistor depths.

We excavated a small trench in the embankment by hand in which we placed the thermistor cable. The trench was between 0.5 ft to 1.0 ft deep to protect the cable from the effects of surface grading and general maintenance (see Figure 3.8). We backfilled the boring with commercially-available sand. The thermistor cable was bent over and placed into this small trench; as a result, the final position of the "0.5 ft" thermistor was roughly at 0.8 ft below the surface. We positioned a CS107 sensor directly above the thermistor string at approximately 0.4 ft below the surface. The CS107 cable was placed in flexible conduit. We backfilled the trench and around the CS107 sensor with soil from the embankment (see Figure 3.9). This location is referred to as the embankment location in what follows.

On August 6, we drilled the toe location, TH09-1404, with SS (see Figure 3.10). We intercepted 6.0 ft of fill consisting of well-graded sand with clay and gravel, which directly overlaid 2.0 ft of frozen ice-rich silt. At 8.0 ft bgs, we intercepted massive ice containing varying amounts of silt. From 36.0 to 39.0 ft (BOH), the ice was mixed with chips of schist, suggesting close proximity to the bedrock surface. We installed the thermistor string to 30.0 ft and backfilled with commercially-available sand. We also installed a CS107 sensor at 0.4 ft below the surface. As with the previous installation, the CS107 cable was placed in flexible conduit. We backfilled the upper portion of this boring with the fill material around the boring.

Once the drilling was complete, we concentrated our efforts on digging a shallow trench (~0.5-ft deep) from the embankment to the ADAS location. After positioning the thermistor cables, flexible conduit, and caution tape, we backfilled the trench.

A total of seven samples were transported to the AK DOT&PF NRMS laboratory for testing. Laboratory results are summarized on the test hole logs in Appendix A, as well as on summary sheets in Appendix B. Please refer to Table 2.1 for a listing of the laboratory testing performed by AK DOT&PF personnel for this project.

Figure 3.4. Replacement of the organic mat, covering TH09-1401.

Figure 3.5. Split-spoon sample (11.0-13.0 ft bgs) from TH09-1402, showing transition from fill (at far right) to silt (right of center) to massive ice (left of center).

3.2.2 ADAS set up

Using the first research location as an example, the PI, with the help of C. McCabe, installed the ADAS for the Dalton Highway 9 Mile Hill location. This ADAS is nearly identical to that for the Richardson Highway MP 113 location, with the exception of the radio telemetry (see Figures 3.11 and 3.12). Since this research location does not have line-of-sight radio communication with any AK DOT&PF facilities and since there is no cell phone service in the area, we are unable to communicate with the datalogger remotely. A complete parts-list for this site is included as Appendix C.

The ADAS was successfully logging temperature data on August 7, 2009. After all components were connected and powered up, we discovered that the thermistor bead at 23.0 ft at the undisturbed location had failed. Additionally, thermistor beads at 9.5 ft, 17.5 ft, and 29.5 ft at the shoulder location failed after installation.

Figure 3.6. Location of TH09-1403 on the Dalton Highway shoulder. View to the northwest.

Figure 3.7. Drilling TH09-1403 on the Dalton Highway shoulder. The apparent embankment height in this photograph is about three feet; the embankment thickness as drilled is approximately 10 feet.

Figure 3.8. Excavating a burial trench by hand through the embankment and side slope. In this photograph, the trench in the shoulder already was backfilled. The thermistor cable (black) and CS107 cable (in flexible conduit) were placed at the bottom of the trench below caution tape.

Figure 3.9. The backfilled location of TH09-1403 (to the right of the spade), and the backfilled trench.

Figure 3.10. Location of TH09-1404, at the toe of the embankment. Note the cables from TH09-1403 emerging from the side slope.
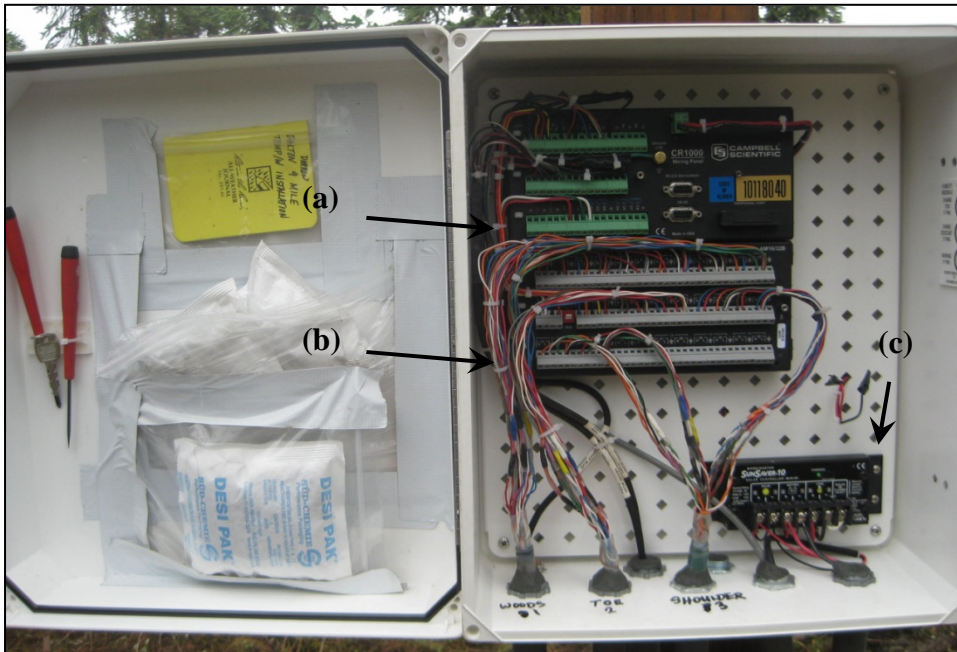
Figure 3.11. Data acquisition components: a) CR1000 datalogger; b) AM16/32B multiplexer. Item (c) is a charge controller for the batteries and solar panel.

25
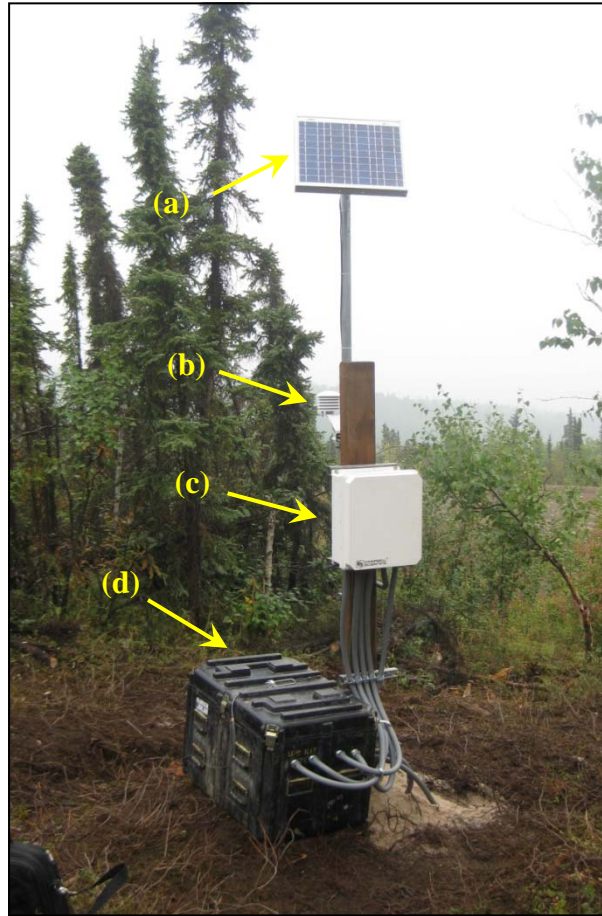
Figure 3.12. The complete ADAS installation: a) solar panel; b) air temperature sensors within radiation shield; c) instrumentation enclosure; and d) battery enclosure.

3.3 Specialized Laboratory Testing

Only one split-spoon liner was transported to a UAF laboratory for specialized testing. The intent was to collect more soil samples; however, we only intercepted suitable soil in the upper portion of the first boring. In the remaining test holes, we intercepted massive ice instead. In the field, we placed the sample into a freezer that was running in the back of a truck, powered by a generator. The freezer was transferred into the laboratory upon our return to Fairbanks.

3.3.1 Dry unit weight and volumetric water content

Only one portion of the frozen sample was prepared for the dry unit weight (γ_d) and volumetric water content (θ) measurements. We used the same techniques as outlined in Section 2.3.1 of this report. The soil sample tested was from a depth of 3.5-4.0 ft in TH09-1401. Its gravimetric moisture content was 146.1%, indicating ice content. We measured γ_d as 36.8 lb/ft^3. This low value for dry unit weight also indicates a high ice content. The calculated θ is 86.1%. This value indicates that out of this sample, only about 14% was soil solids while the rest of the volume was ice.

3.3.2 Thermal conductivity

Thermal conductivity measurements were made on three samples from the single split-spoon liner. The method is outlined in Section 2.3.2 of this report. For the Dalton Highway 9 Mile Hill samples, the average standard deviation for all temperatures was 0.012 Btu/ft·hr·°F. This value is higher than that reported in Section 2.3.2 due to the influence of one set of readings for sample 6600B at 50°F, where the standard deviation was 0.137 Btu/ft·hr·°F. Otherwise, the readings showed little variation for a given temperature. The average temperature rise in the soil sample for a set of readings was 0.02°F.

Figure 3.13 is a summary of the average thermal conductivity readings for each temperature for the Dalton Highway 9 Mile Hill samples; the raw thermal conductivity data is included in Appendix D. In Figure 3.13, each thermal conductivity value is plotted against the average of recorded bath temperatures, rather than the bath set point since these values were slightly different. As expected the frozen thermal conductivity (k_f) values are higher than unfrozen thermal conductivity (k_u) values.

As with the clayey soil samples from the Richardson Highway MP 113 site, these samples demonstrated a sharp peak in thermal conductivity as the phase change temperature was approached. Again, these spikes are attributed to the heat pulse given off by the needle probe. Unlike the clayey soil samples, however, the thermal conductivity curves for these three samples closely match each other. This is attributed to the uniform nature of the ice-rich silt. The average k_u chosen from this range of data is 0.5 Btu/ft·hr·°F, and the average k_f is 1.0 Btu/ft·hr·°F**.** All of these samples demonstrated the change from k_u to k_f well below 32°F (as indicated by the red dashed line in Figure 3.13). This indicates the presence of some unfrozen water in the frozen soil.
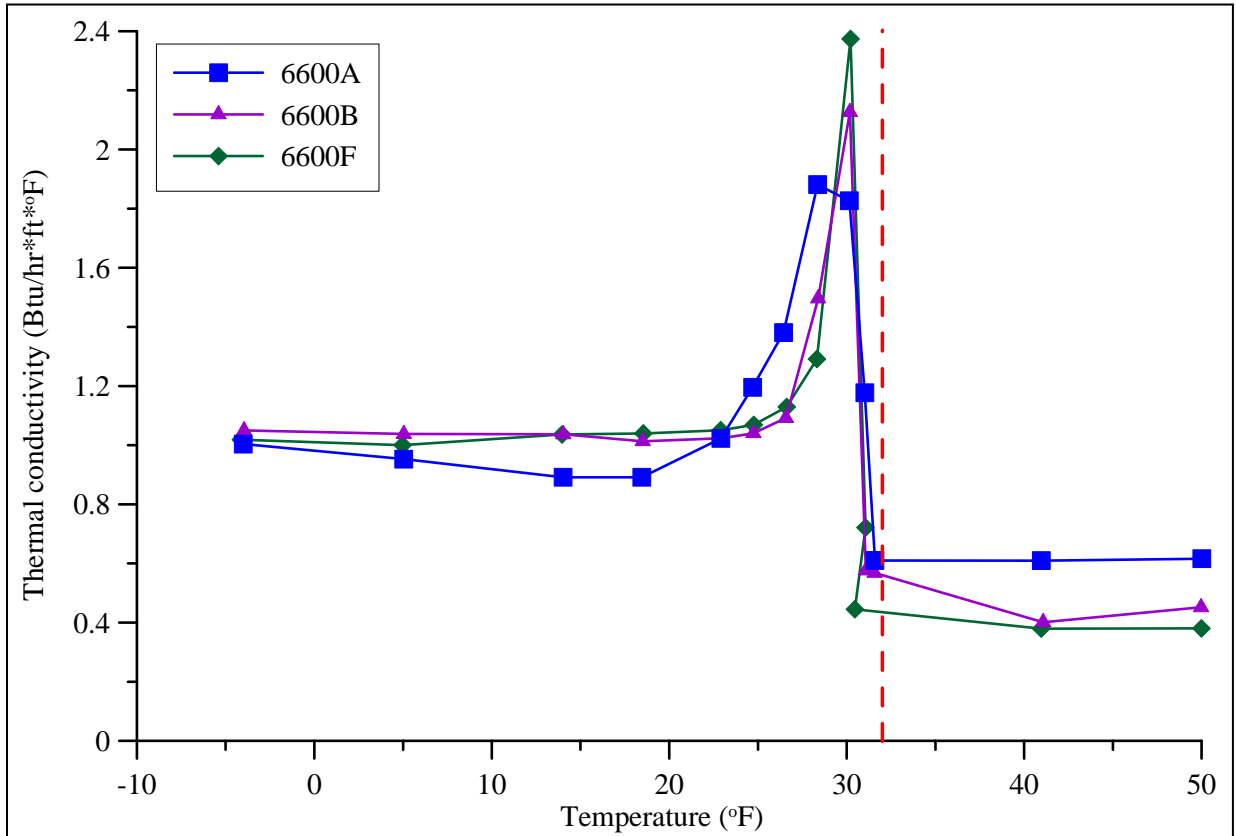
Figure 3.13. Summary of thermal conductivity measurements for the ice-rich silty soil samples, Dalton Highway 9 Mile Hill research site. The vertical dashed red line represents the 32°F isotherm.

4.1 Richardson Highway MP 113

We began recording temperatures at this site on November 11, 2008. Although we had radio telemetry devices installed both at the field site and at the Tazlina M&O building, we were unable to communicate with the site remotely for a variety of reasons, until early April 2010. Since April, the site data has been available over the internet. We will continue to collect data from the site; however, this report contains temperature data from November 11, 2008 to May 31, 2010.

Figures 4.1 through 4.3 are plots of soil temperatures at different depths with time for the embankment, toe, and undisturbed thermistor string locations, respectively. The temperatures for depths between 0.5 ft and 30 ft are those obtained from the thermistor strings. The "near surface" temperatures were recorded using the CS107 sensors; their depths varied between 0.25 and 0.3 ft below the surface, as detailed previously in Section 2.2.2. For each of the thermistor locations, temperatures measured within one foot of the surface closely match each other and show the effects of daily variations in air temperature (shown in light blue; see Figures 4.1-4.3). With greater depths, the amplitude of each temperature curve is reduced, or damped, and each peak shifts in time, or to the right in the figure. The damping of the amplitude and its phase shift are typical phenomena in soils, which depend on the soil properties (Hillel 1980). In other words, soils at increasingly greater depths are less affected by the daily air temperature, and take longer to demonstrate the effects of the seasonal temperatures. For the period of time shown in these figures, the maximum and minimum air temperatures were 72.0°F and -43.4°F, respectively.

While the temperatures measured in the upper one foot of the soil show the effects of air temperature, they do not match it exactly. Using the embankment thermistor string location as an example, in Figure 4.1 these upper soil temperatures are generally warmer than the air temperatures, both in the summer and in the winter. The warmer temperatures in the summer are attributed to the black surface of the asphalt pavement, whereas the warmer winter temperatures may be due to the limited snow cover left on the edge of the pavement and not removed during plowing activities. At the toe of the embankment, there is more of a difference in the air temperature and the soil temperatures in the upper one foot during the winter months. This is due to the insulating effects of the snow cover. Finally, these differences are quite pronounced for the undisturbed location, where the ground stays much warmer in the winter due to snow and cooler in the summer due to the natural vegetation cover.

It is difficult to measure true soil surface temperatures, since the temperature sensors must be placed so as to be protected from traffic, animal activity, and curious humans. Typically, soil surface temperatures are estimated from air temperatures using n-factors. The thaw n_t-factor is defined as:

$$n_t = \frac{I_{st}}{I_{at}}$$ 4.1

where I_{st} is the surface thawing index and I_{at} is the air thawing index (Andersland and Ladanyi 2004). The freeze n_f-factor is defined similarly as:
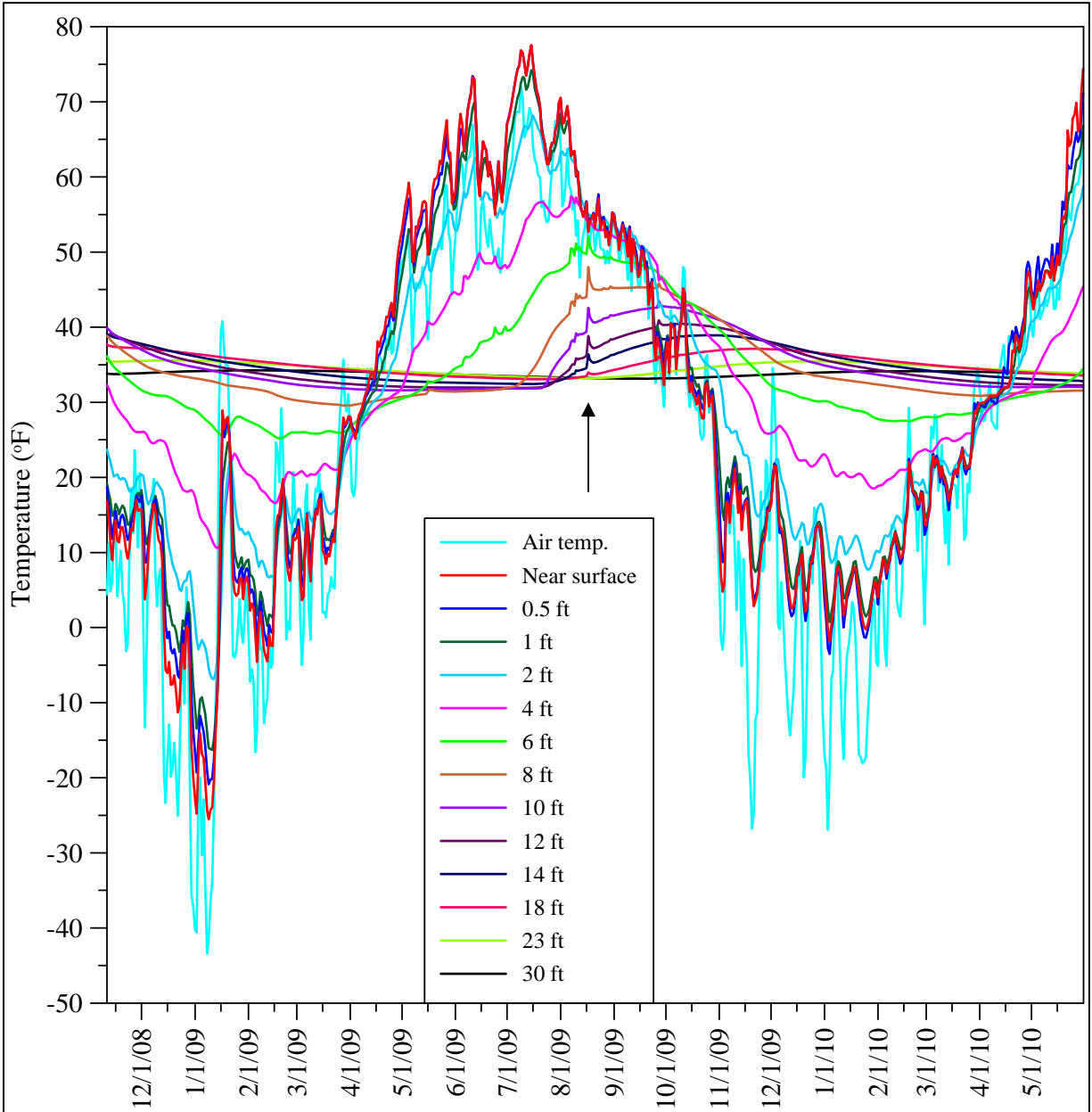
Figure 4.1. Measured temperatures from the embankment thermistor string, Richardson Highway MP 113 research location.
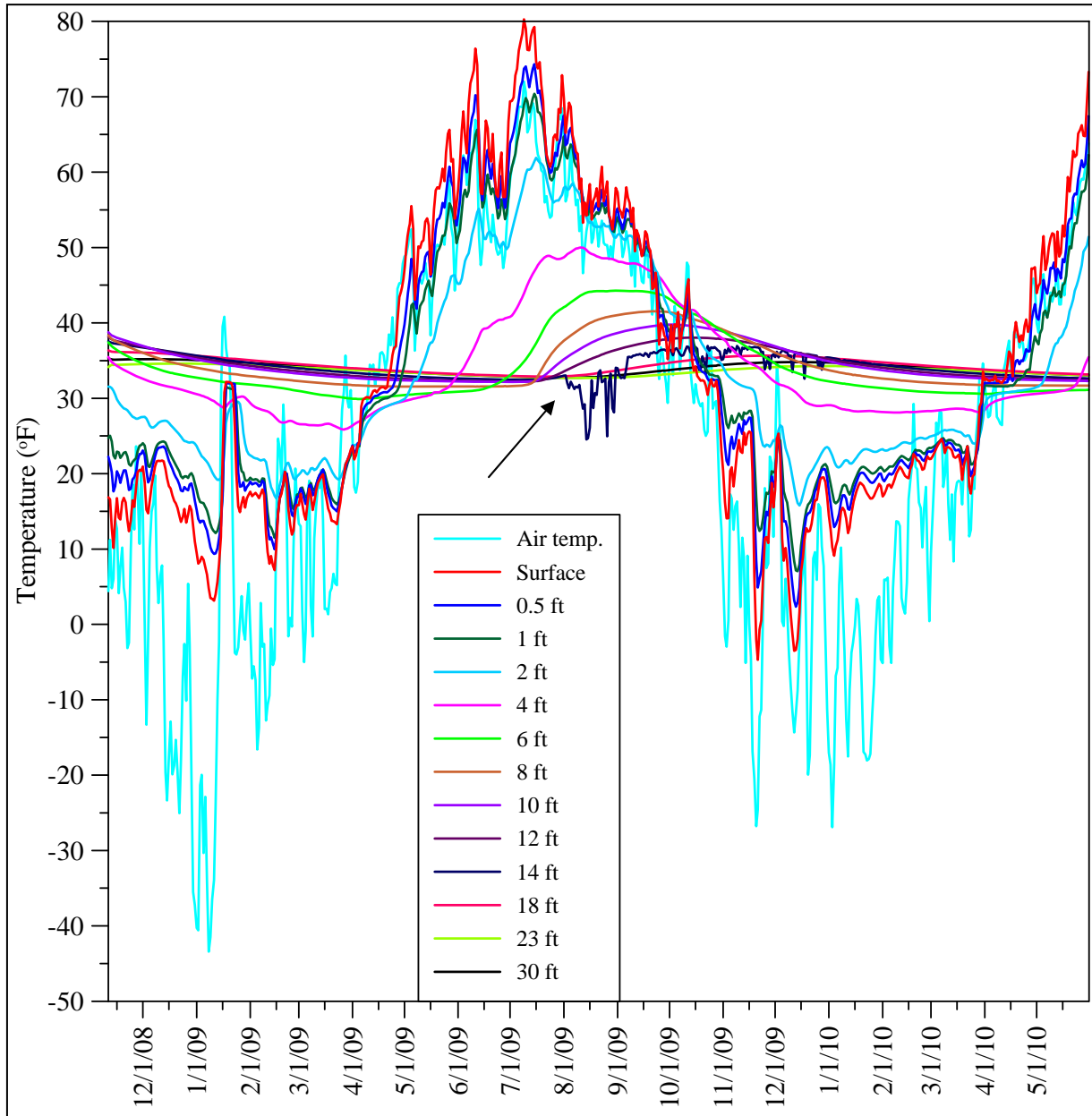
Figure 4.2. Measured temperatures from the toe thermistor string, Richardson Highway MP 113 research location.
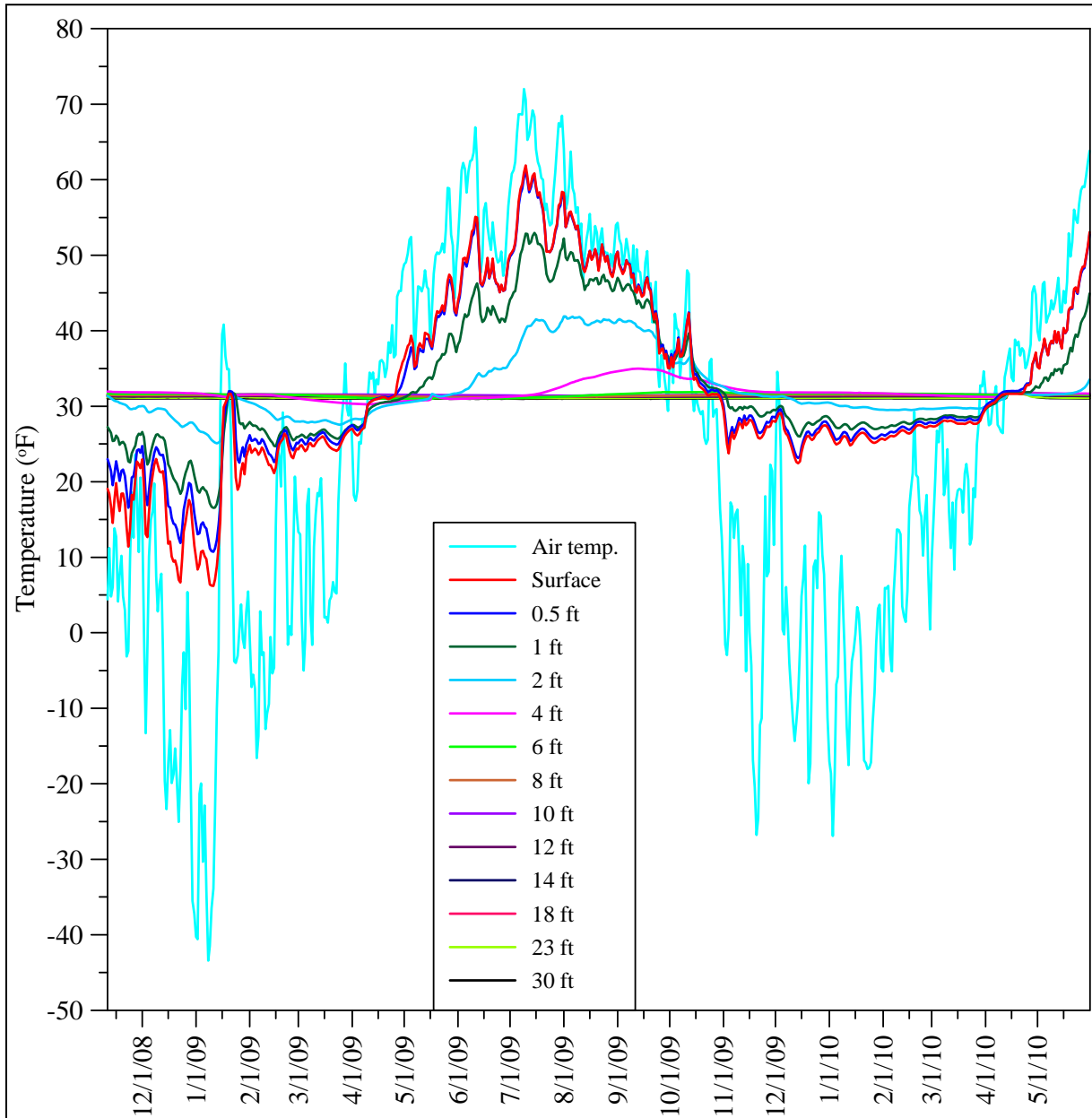
Figure 4.3. Measured temperatures from the undisturbed thermistor string, Richardson Highway MP 113 research location.

$$n_f = \frac{I_{sf}}{I_{af}} \qquad\qquad 4.2$$

where I_{sf} is the surface freezing index and I_{af} is the air freezing index. Table 4.1 contains "pseudo" n-factors calculated for the Richardson Highway MP 113 research site, using the air temperature data and the soil temperature data from the CS107 probes. These are "pseudo" n-factors since the CS107 probes were buried far too deeply to represent soil surface temperatures. While these values should not be used for seasonal freezing and thawing calculations, they do illustrate the insulative effects of the natural vegetation at the undisturbed location and of the winter snow cover at all locations. They also illustrate the increase in surface temperatures for areas covered with gravel or asphalt pavement.

Table 4.1 "Psuedo" n-factors for the Richardson Highway MP 113 research site.

Location	n_t	n_f
Embankment	1.3	0.8
Toe	1.3	0.6
Undisturbed	0.7	0.3

Generally, the temperatures in the upper few feet of the soil reflect spikes in the air temperature data. There are a few data anomalies, however, that are due to equipment and/or sensor malfunction. In Figure 4.1, there are spikes in measured temperatures at all depths on August 16, 2009 (as indicated by a black arrow). These spikes are not the result of an extremely warm day, as the air temperature was moderate. Additionally, the spikes are seen at all depths, which is atypical due to temperature damping in soils. These spikes are interpreted as a temporary malfunction in the datalogger/multiplexer system. In Figure 4.2, the black arrow indicates the beginning of a period of erroneous temperature readings in the thermistor at 14 ft from July 26 to December 24, 2009. After this time, the erroneous temperature spikes stopped. This is interpreted as a period of malfunction in that specific thermistor bead.

Drilling imparts a great deal of heat into the soil through friction. Hourly temperatures for the thermistors in the lower portion of each boring were analyzed to see how long it took for the drilling heat to dissipate. Plots of temperature versus time were visually examined to determine when temperature changes were negligible (see Figures 4.4 through 4.6). The ADAS was completely functional and data logging began at 7:00 pm on November 10, 2008. Drilling at the undisturbed location was completed at 11:15 am on November 7, 2008. Analysis of the data in Figure 4.4 indicates that there were no remaining temperature effects due to drilling heat when data logging began. In other words, the drilling heat dissipated in the 80 hours between the completion of drilling and the beginning of data logging. Drilling at the toe location was completed by 9:45 am on November 10, 2008. Analysis of Figure 4.5 indicates that temperatures at depth demonstrated negligible changes 40 hours after logging, or a total of 49 hours after drilling was completed. Drilling at the embankment location was completed at 12:00 pm on November 9, 2008. Analysis of Figure 4.6 indicates that temperatures at depth demonstrated negligible changes 32 hours after logging, or a total of 75 hours after drilling. In summary for these soils and temperature conditions, the drilling heat dissipated between 2 and 4 days after soil disturbance had ceased.

33
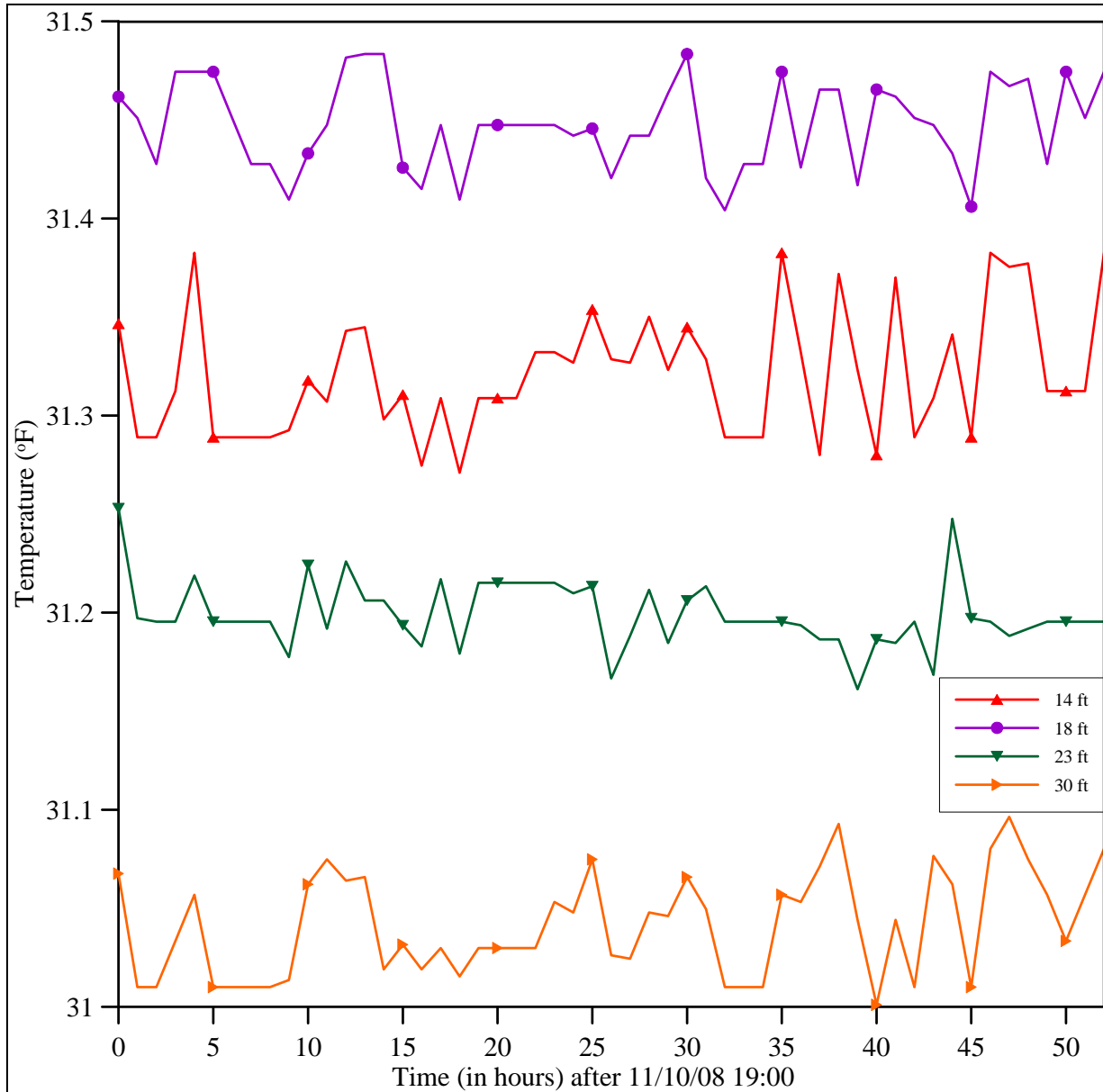
Figure 4.4. Hourly temperature measurements from the undisturbed thermistor string, Richardson Highway MP 113 research location. These are the first 52 hours of temperatures collected after the ADAS became operational on November 10, 2008 at 7:00 pm.
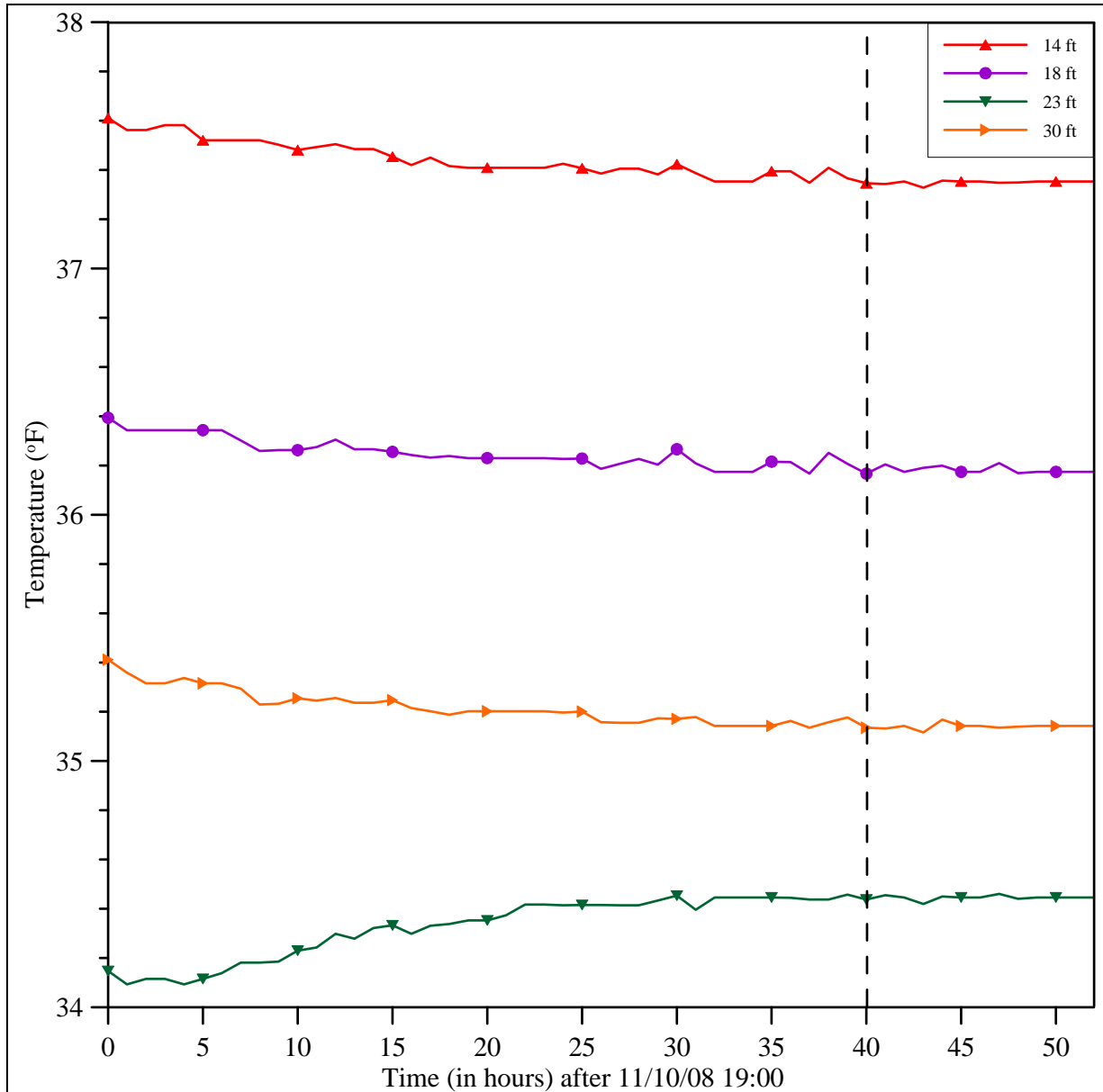
Figure 4.5. Hourly temperature measurements from the toe thermistor string, Richardson Highway MP 113 research location. These are the first 52 hours of temperatures collected after the ADAS became operational on November 10, 2008 at 7:00 pm. The dashed black line indicates the point at which temperature changes are negligible for all depths.
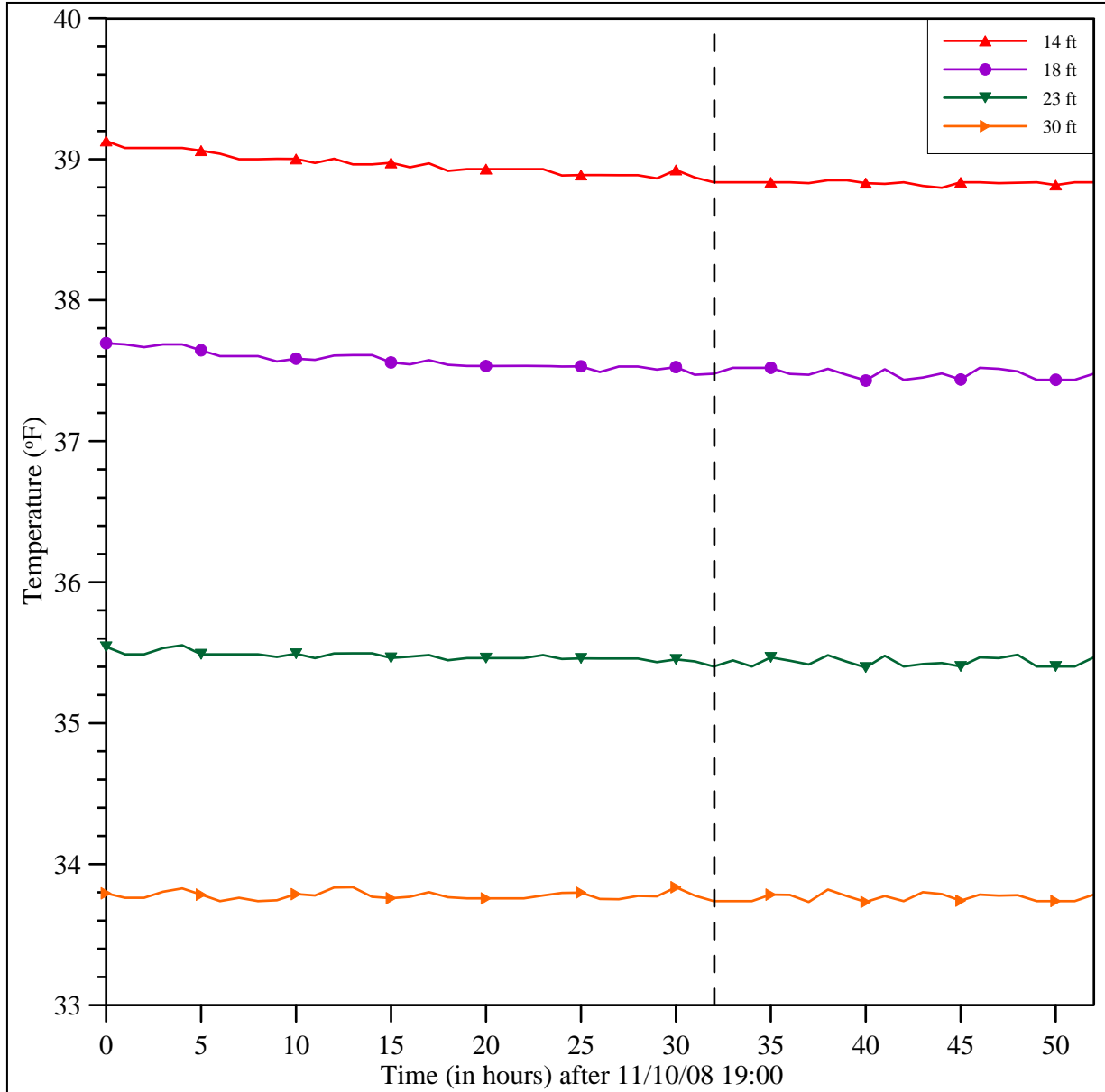
Figure 4.6. Hourly temperature measurements from the embankment thermistor string, Richardson Highway MP 113 research location. These are the first 52 hours of temperatures collected after the ADAS became operational on November 10, 2008 at 7:00 pm. The dashed black line indicates the point at which temperature changes are negligible for all depths.

Yet another way to examine the temperature data is to plot temperatures with depth on given days. Figures 4.7 through 4.9 are such plots, with temperature versus depth shown for the first of each month for 2009. These temperature profiles are commonly referred to as "trumpet curves" because of their shape.

The embankment temperature profile (see Figure 4.7) demonstrates a wide range of near surface temperatures. This plot also indicates that the active layer thickness is about 12 ft, and that there is no permafrost under the embankment to the depth drilled. The average temperature at 30 ft is 33.8°F; temperatures at 30 ft still demonstrate some effects due to surface temperatures, although these effects are small. At the toe thermistor location (see Figure 4.8), the near surface is warmer during the winter months, which is attributed to snow cover. The active layer depth is between 8 and 10 ft, and there is no permafrost to the depth drilled. The average temperature at 30 ft is 34.0°F; this depth is still affected by surface temperatures. The undisturbed temperature profile (see Figure 4.9) demonstrates the smallest range of near surface temperatures. Here the active layer thickness is about 6 ft with permafrost below this depth. The average temperature at 30 ft is 31.0°F, and the depth of negligible temperature amplitude is approximately 12 ft.
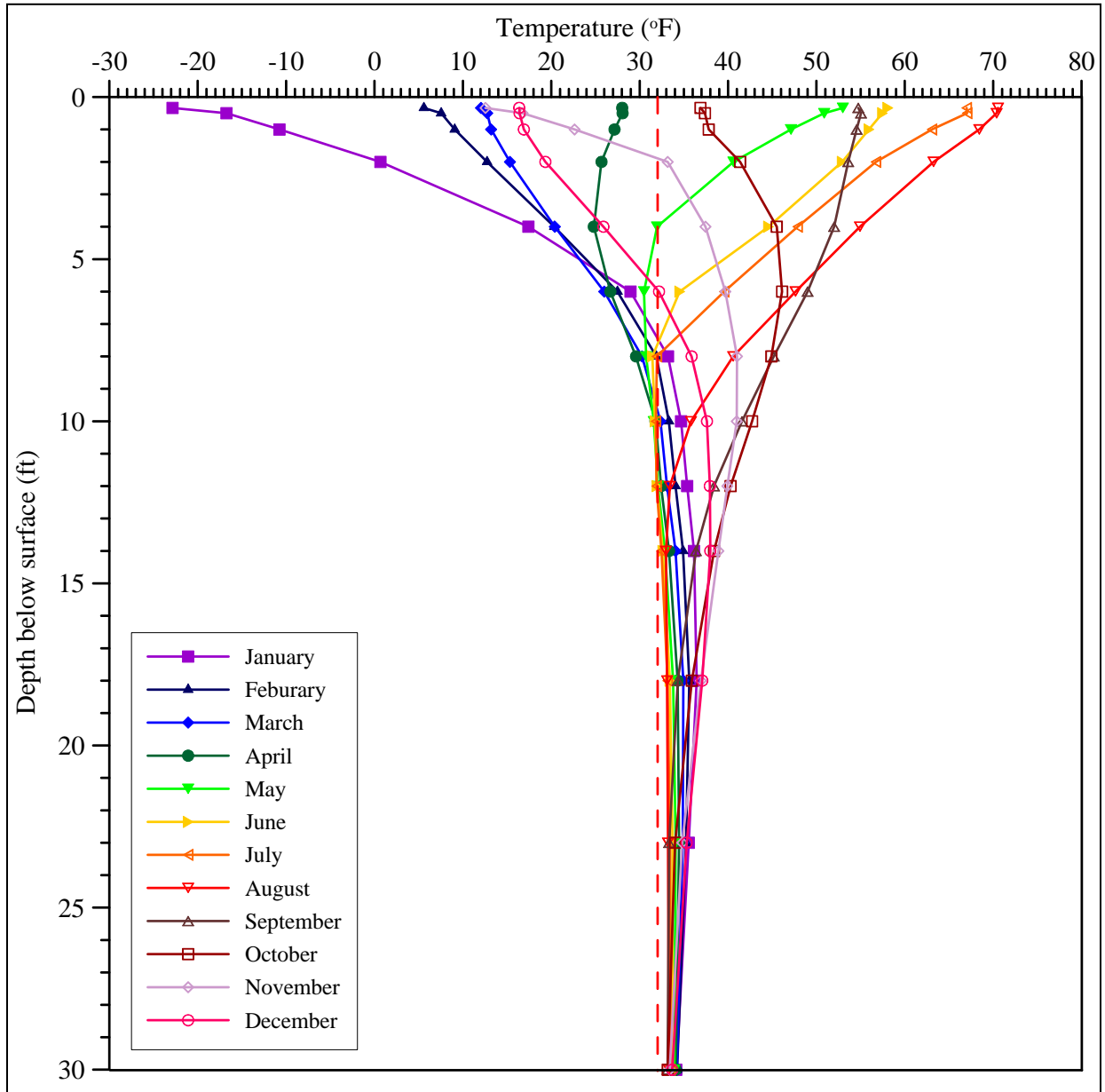
Figure 4.7. Temperature profile for the embankment thermistor string location, Richardson Highway MP 113 research location. Temperatures shown are from the first of each month during 2009. The 32°F isotherm is indicated by the red dashed line.
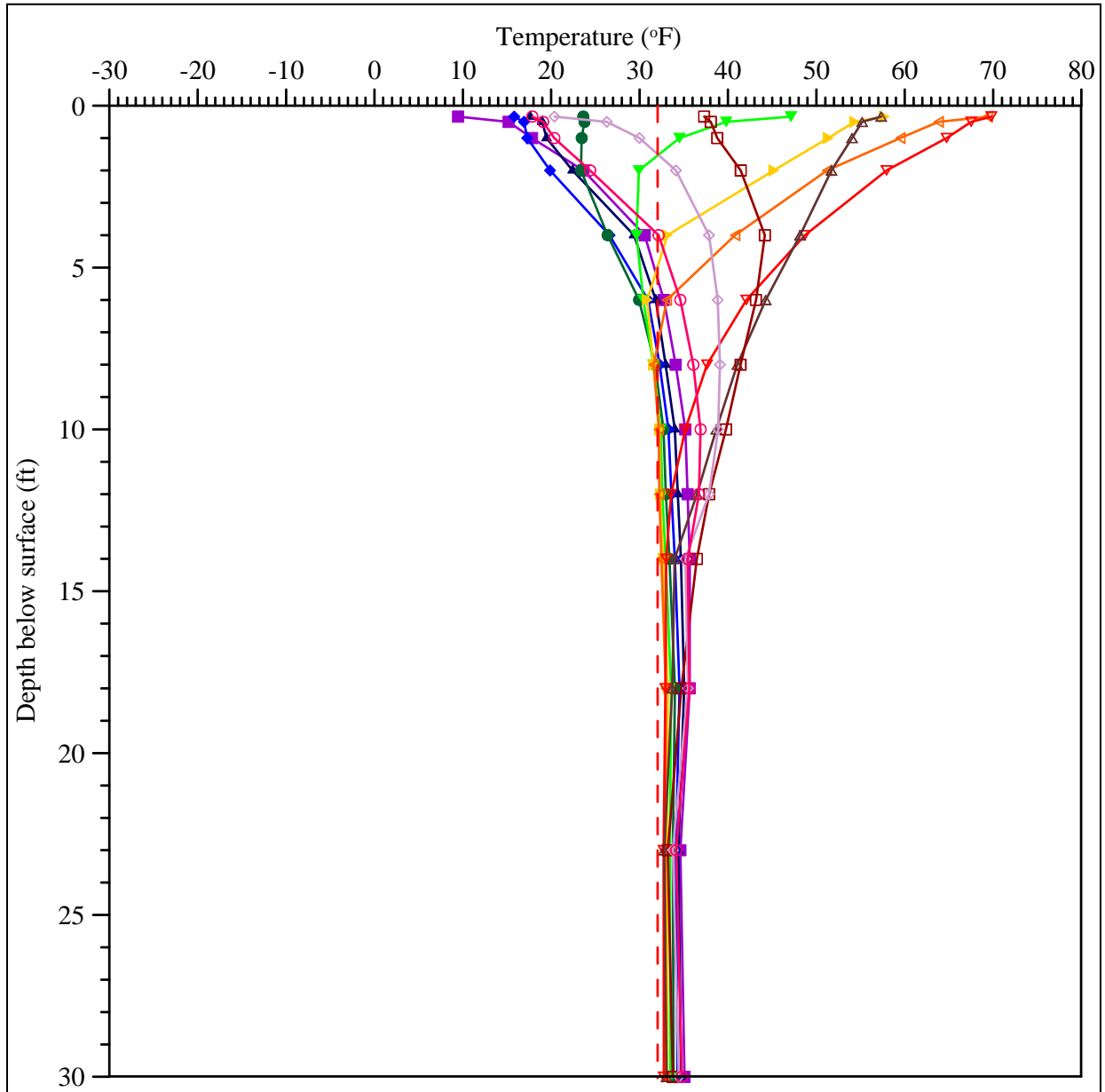
Figure 4.8. Temperature profile for the toe thermistor string location, Richardson Highway MP 113 research location. Temperatures shown are from the first of each month during 2009. The 32°F isotherm is indicated by the red dashed line.
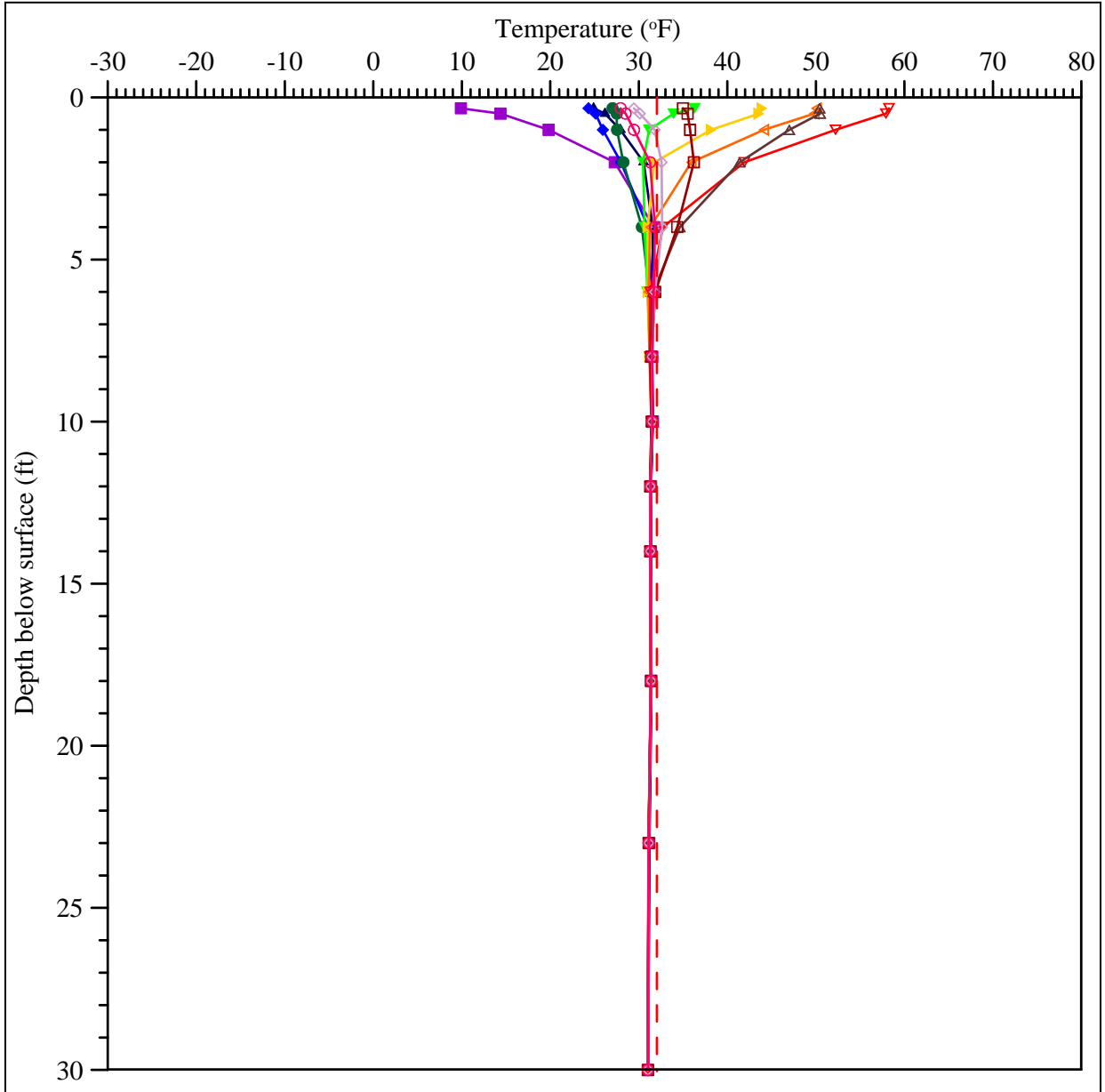
Figure 4.9. Temperature profile for the undisturbed thermistor string location, Richardson Highway MP 113 research location. Temperatures shown are from the first of each month during 2009. The 32°F isotherm is indicated by the red dashed line.

4.2 Dalton Highway 9 Mile Hill

We began recording temperatures at this site on August 8, 2009. Temperature data was collected several times through the rest of 2009 and into 2010. We will continue to collect data from this site; however, this report contains temperature data up to May 29, 2010. Unfortunately, due to delays in drilling at this site, we do not yet have a complete year of temperature data.

Figures 4.10 through 4.12 are plots of soil temperatures at different depths with time for the embankment, toe, and undisturbed thermistor string locations, respectively. The temperatures for depths between 0.5 ft and 30 ft are those obtained from the thermistor strings, with the exception of where thermistor beads were not functioning (see Section 3.2.2 for details). The "near surface" temperatures were recorded using the CS107 sensors; their depths varied between 0.17 and 0.4 ft below the surface, as detailed in Section 3.2.1.

Similar characteristics are present in these figures as in the temperature versus time plots for the Richardson Highway (e.g., damping with depth, lag with time). The measured near surface temperatures in the embankment typically are warmer than the measured air temperatures (see Figure 4.10). At the undisturbed location, the measured soil temperatures are much warmer in the winter and much cooler in the summer than the measured air temperatures (see Figure 4.12). The same is true for the toe location, to a lesser degree (see Figure 4.11). "Pseudo" *n*-factors are not presented for the Dalton Highway site, since a complete year of data is not available at the time of this report. Comparing the two research sites, the air and soil temperatures at the Dalton Highway site are cooler than those at the Richardson Highway site, with maximum and minimum air temperatures of 66.3°F and -35.6°F, respectively. The minimum air temperature at the Richardson Highway site in January 2009 was colder; however, this day occurred before data collection began at the Dalton Highway site.

Drilling heat dissipation also was analyzed for this location. Figures 4.13 through 4.15 are hourly temperatures from the first 400 hours of data collection, which began on August 7, 2009 at 10:00 am when the ADAS was fully operational. Drilling at the undisturbed location was completed at 5:30 pm on August 4, 2009. Analysis of Figure 4.13 indicates that temperatures equilibrated at 14 ft and at 18 ft by 140 hours after logging began, or about 205 hours after drilling. The temperature at 30 ft was still changing, albeit slightly, at 400 hours after logging began, or 465 hours after drilling. Drilling at the toe location was completed at 12:00 pm on August 6, 2009. Analysis of Figure 4.14 indicates that temperatures equilibrated at all depths by 368 hours after logging began, or 390 hours after drilling. Drilling at the shoulder location was completed at 4:00 pm on August 5, 2009. Figure 4.15 contains the measured temperatures at 23 ft, since this was the deepest thermistor that did not demonstrate surface temperature effects. Analysis of this data indicates that the measured temperatures had not yet reached equilibrium within 400 hours after logging began, or 442 hours after drilling, although the temperature was changing only slightly at this time. In summary for these soils and temperature conditions, it took around 19 days for the drilling heat to dissipate after soil disturbance had ceased.

Since this site is lacking a complete year's worth of temperature data, temperature profiles were constructed for the first of the month between August 2009 and May 2010. Temperatures recorded on May 29, 2010 were used to approximate June 1st conditions. The temperature profiles for embankment, toe, and undisturbed locations are shown in Figures 4.16 through 4.18, respectively.
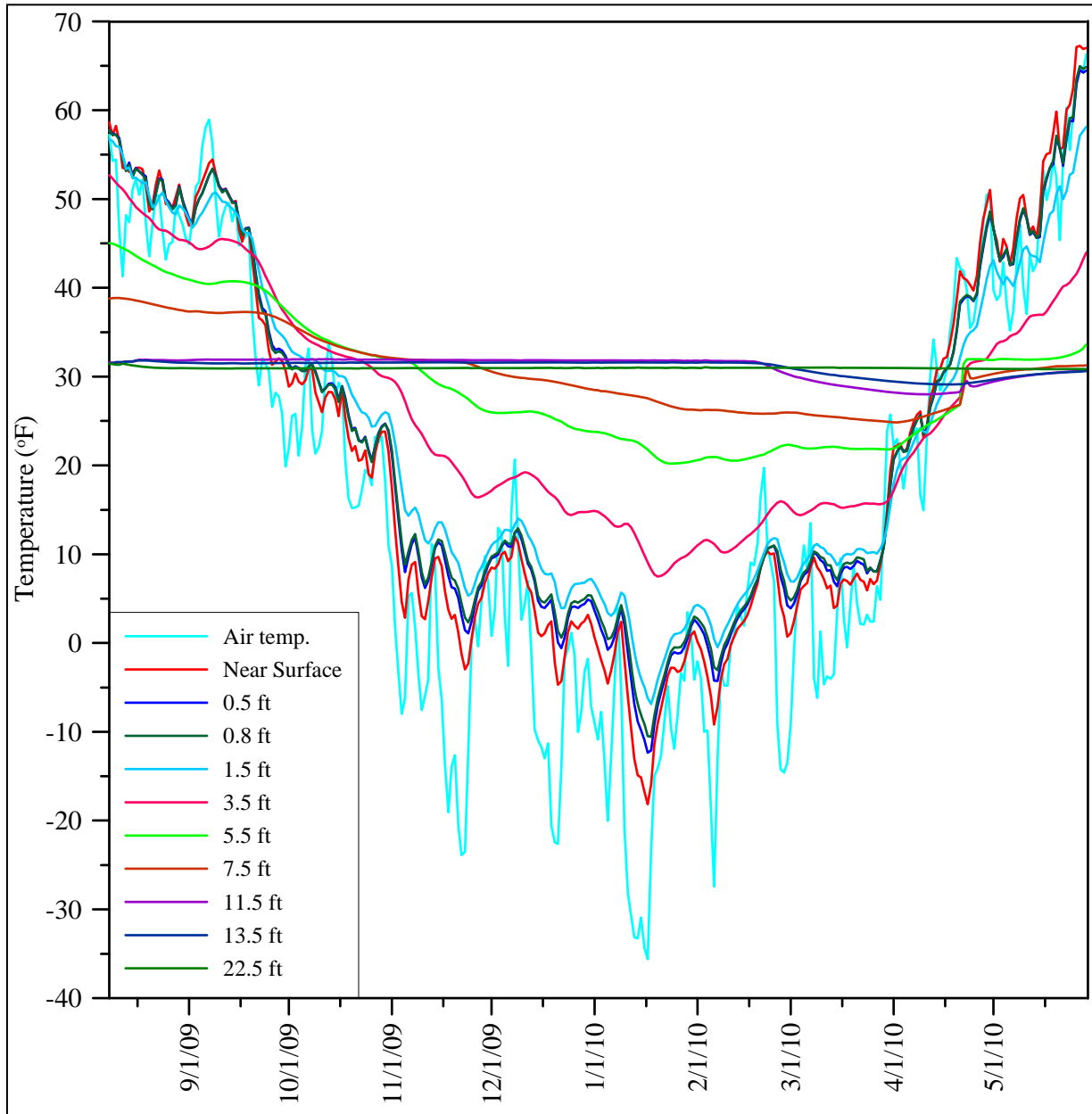
Figure 4.10. Measured temperatures from the embankment thermistor string, Dalton Highway 9 Mile Hill research location.
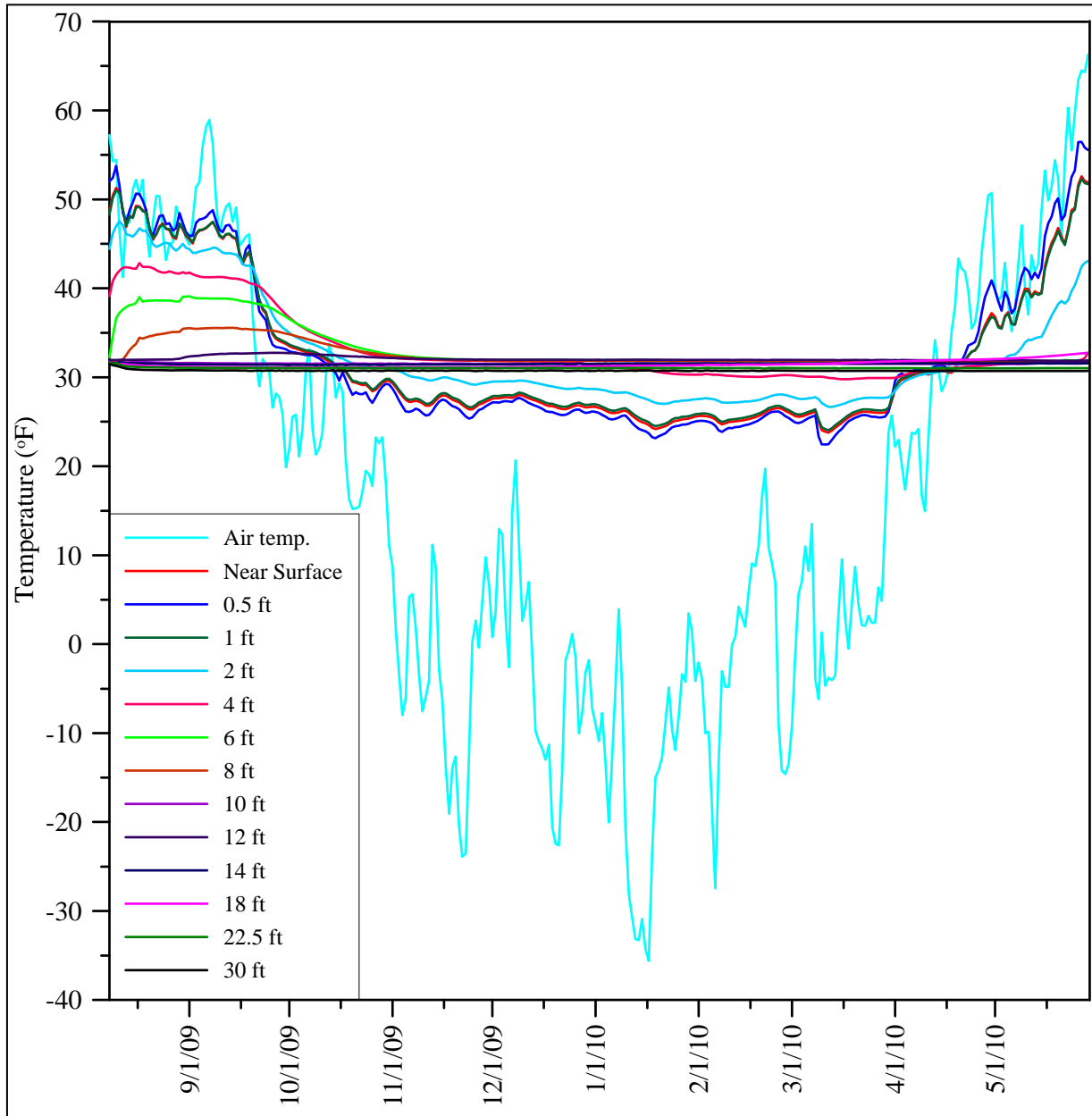
Figure 4.11. Measured temperatures from the toe thermistor string, Dalton Highway 9 Mile Hill research location.
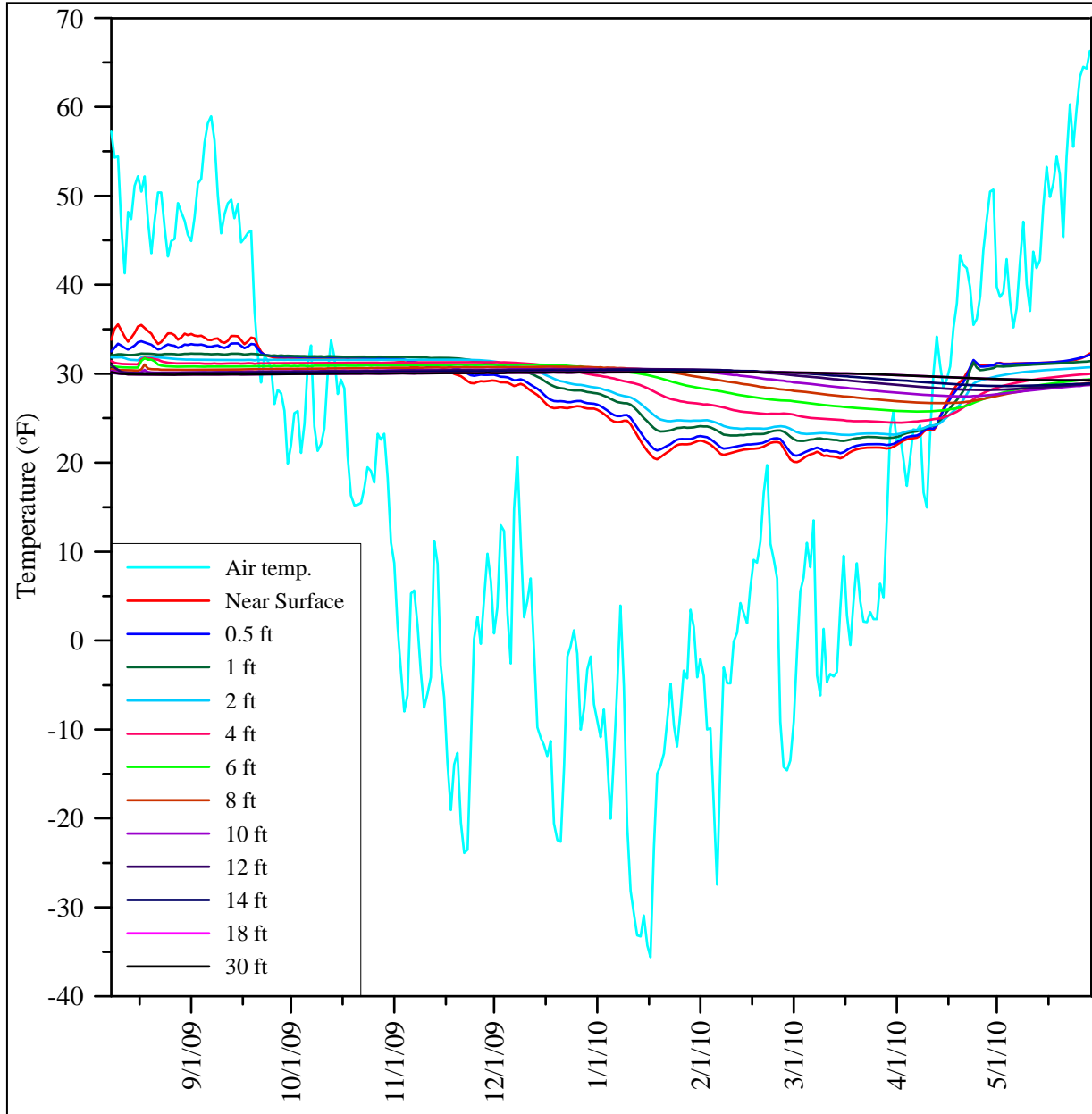
Figure 4.12. Measured temperatures from the undisturbed thermistor string, Dalton Highway 9 Mile Hill research location.
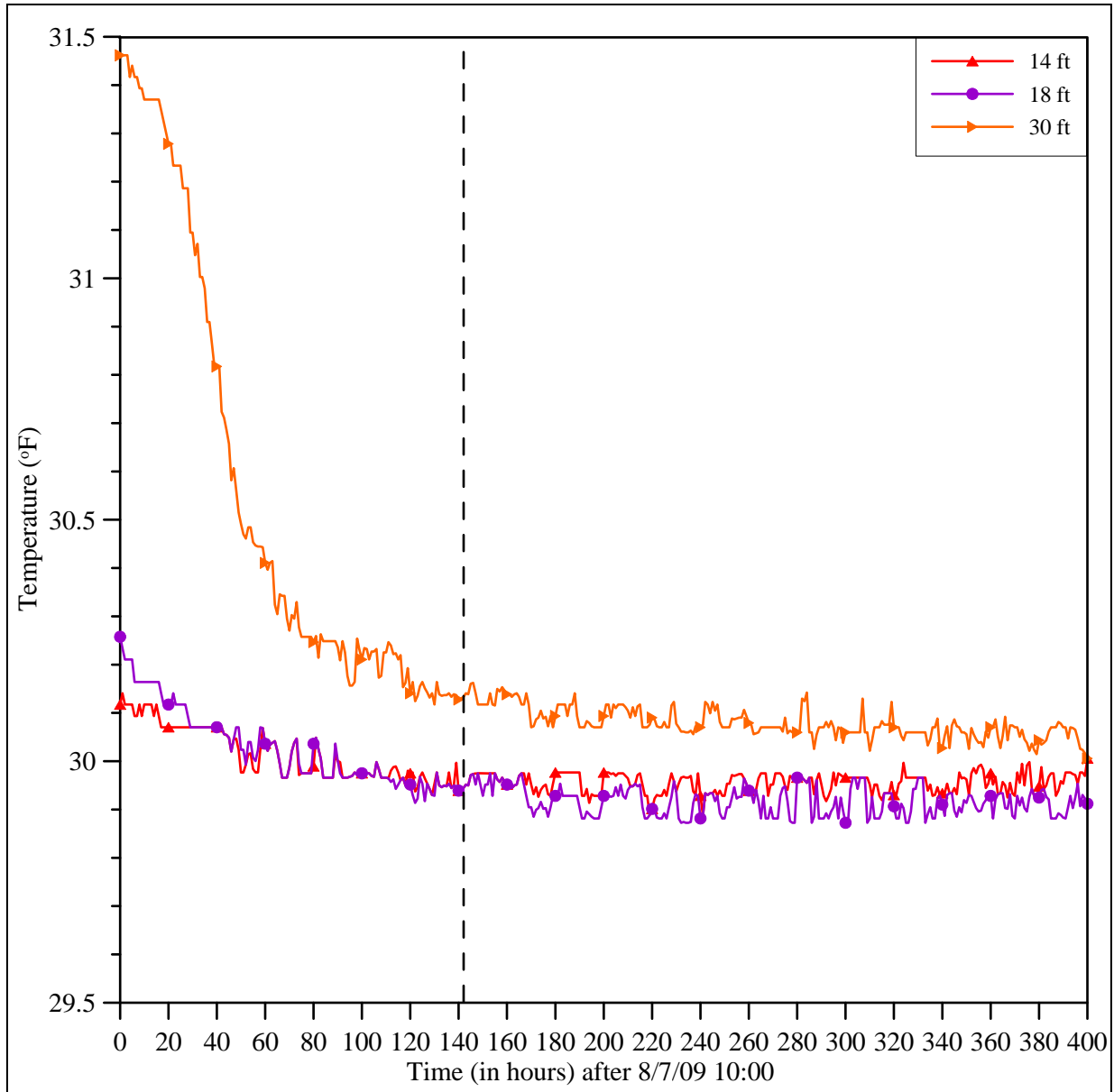
Figure 4.13. Hourly temperature measurements from the undisturbed thermistor string, Dalton Highway 9 Mile Hill research location. These are the first 400 hours of temperatures collected after the ADAS became operational on August 7, 2009 at 10:00 am. The dashed black line indicates the point at which temperature changes are negligible for all depths.
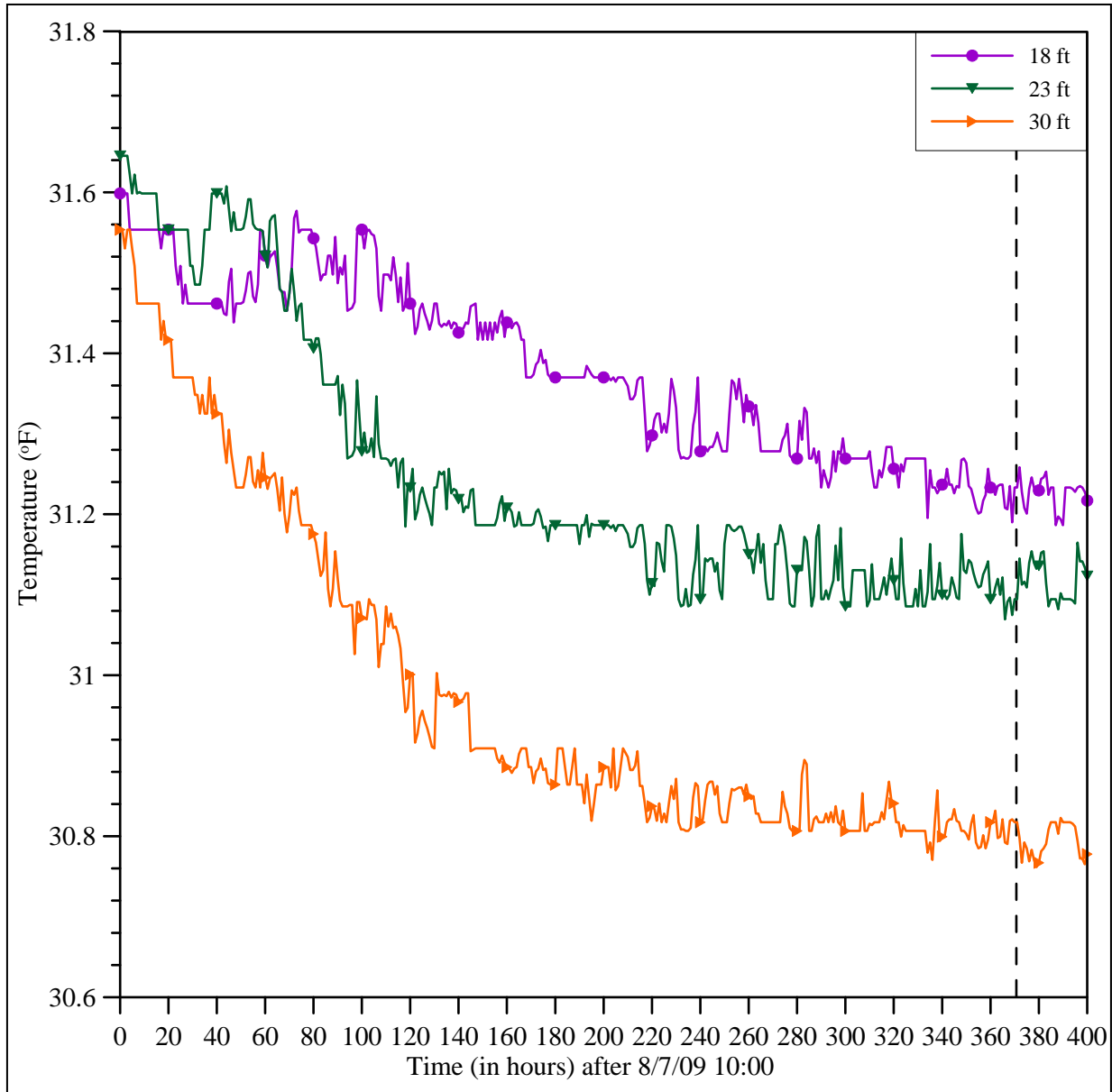
Figure 4.14. Hourly temperature measurements from the toe thermistor string, Dalton Highway 9 Mile Hill research location. These are the first 400 hours of temperatures collected after the ADAS became operational on August 7, 2009 at 10:00 am. The dashed black line indicates the point at which temperature changes are negligible for all depths.
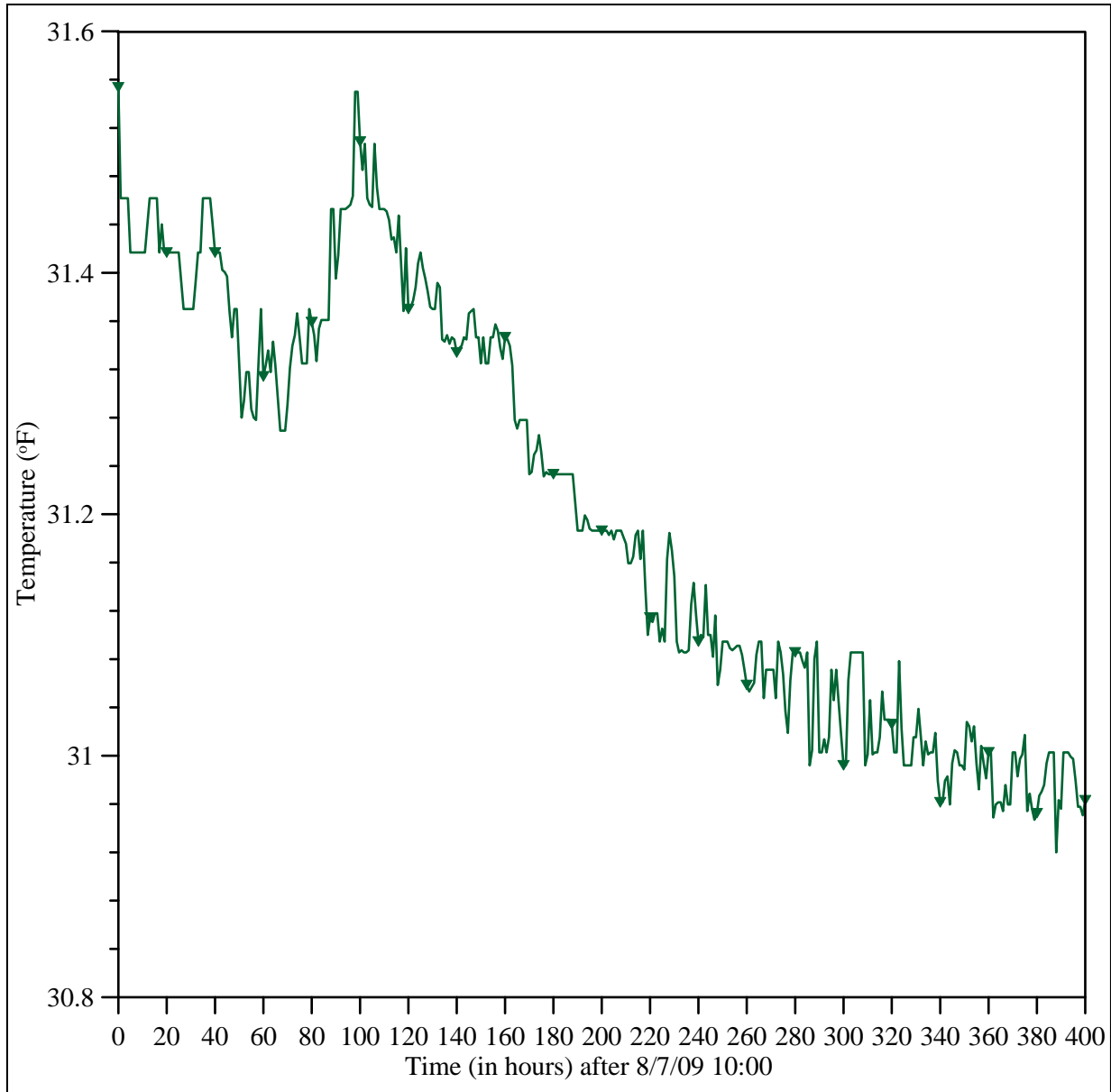
Figure 4.15. Hourly temperature measurements from the shoulder thermistor string at a depth of 22.5 ft, Dalton Highway 9 Mile Hill research location. These are the first 400 hours of temperatures collected after the ADAS became operational on August 7, 2009 at 10:00 am.
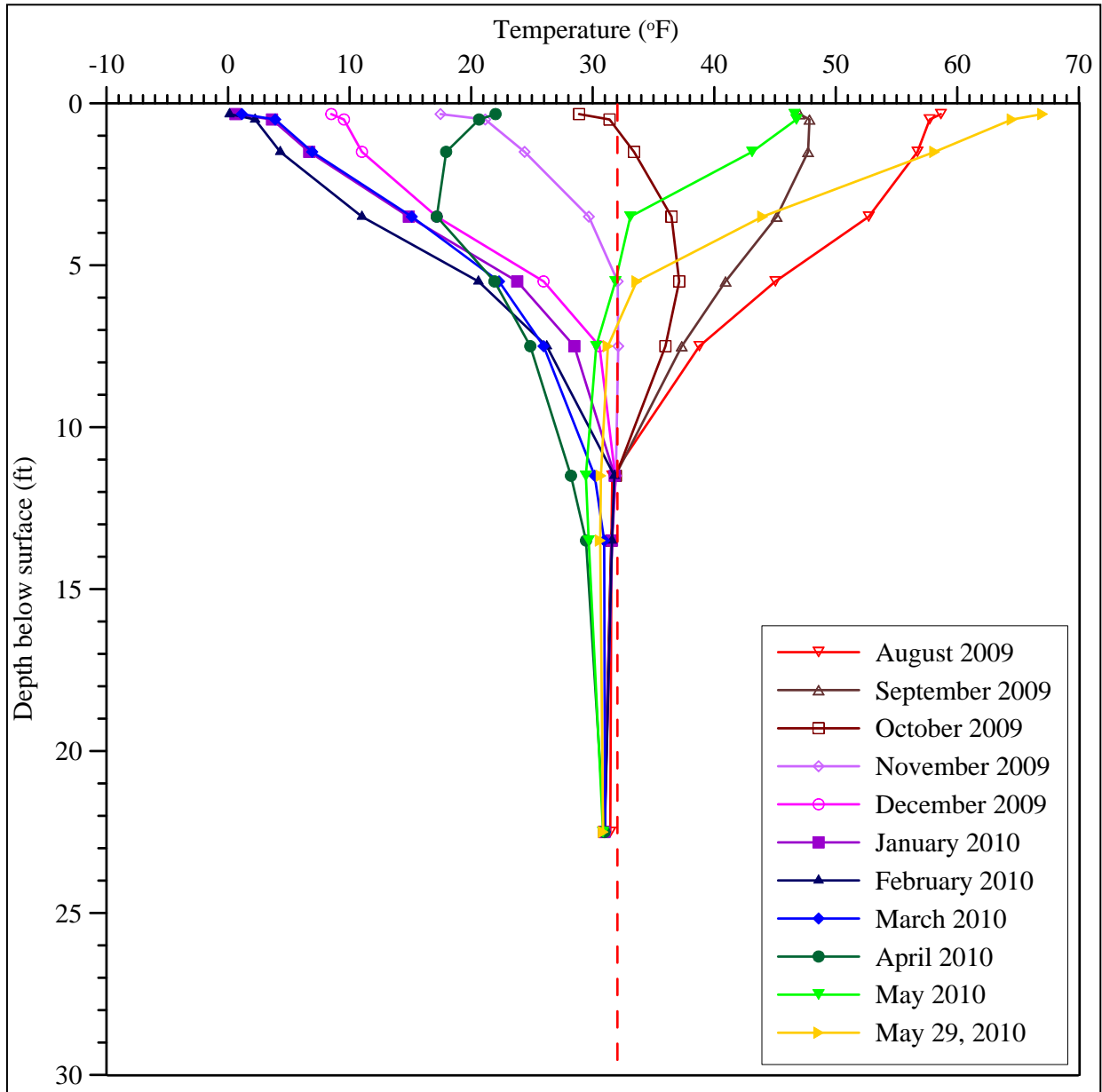
Figure 4.16. Temperature profile for the embankment thermistor string location, Dalton Highway 9 Mile Hill research location. Temperatures shown are from the first of each month between August 2009 and May 2010. The "June" curve are temperatures measured on May 29, 2010. The 32°F isotherm is indicated by the red dashed line.

48
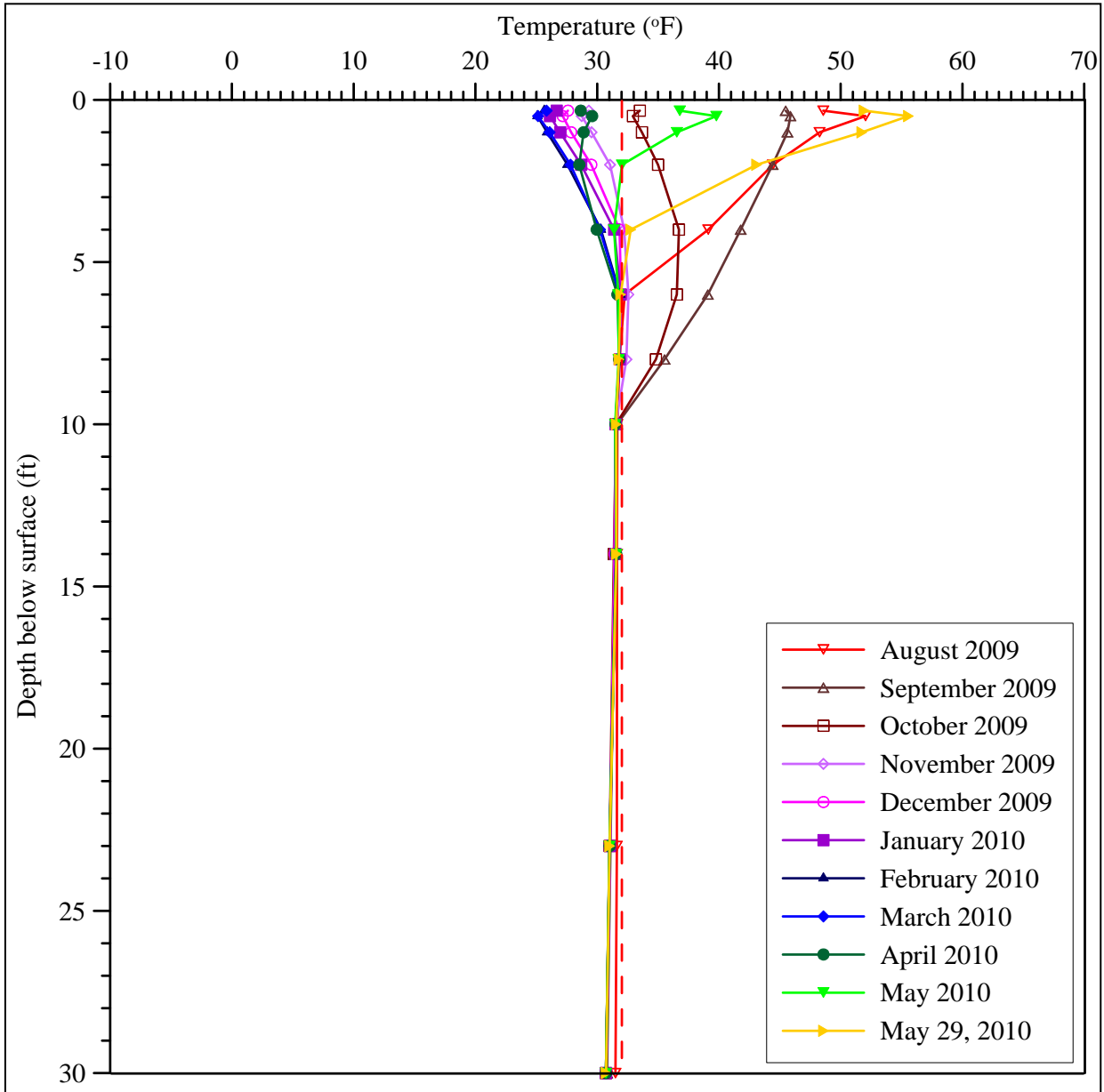
Figure 4.17. Temperature profile for the toe thermistor string location, Dalton Highway 9 Mile Hill research location. Temperatures shown are from the first of each month between August 2009 and May 2010. The "June" curve are temperatures measured on May 29, 2010. The 32°F isotherm is indicated by the red dashed line.
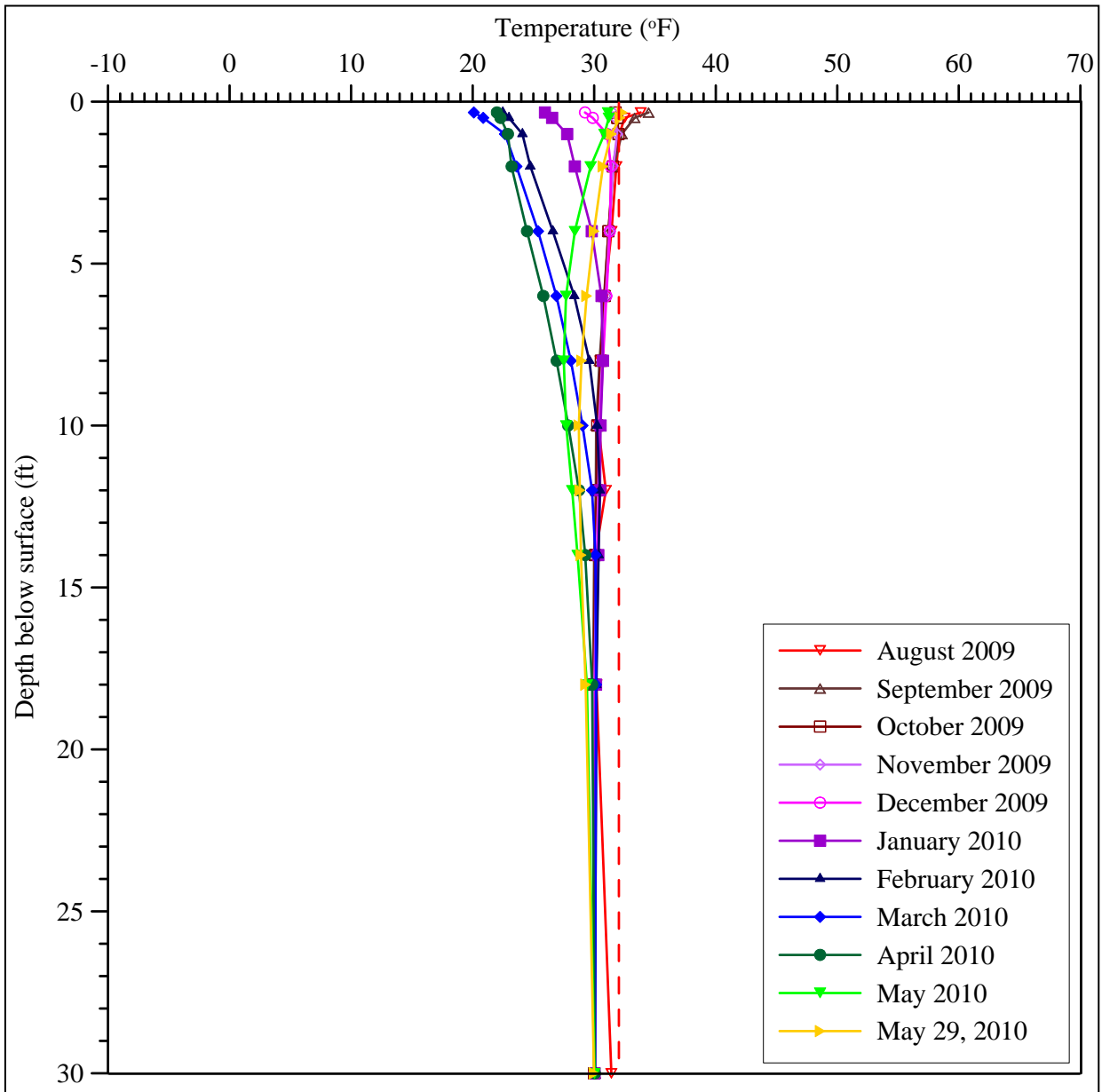
Figure 4.18. Temperature profile for the undisturbed thermistor string, Dalton Highway 9 Mile Hill research location. Temperatures shown are from the first of each month between August 2009 and May 2010. The "June" curve are temperatures measured on May 29, 2010. The 32°F isotherm is indicated by the red dashed line.

50

The embankment temperature profile (see Figure 4.16) demonstrates the widest range of near surface temperatures of the three thermistor locations. This plot indicates a seasonally thawed layer thickness of between 7.5 and 11.5 ft. This is in agreement with the drilling results, in which the permafrost table was intercepted at 10 ft below the surface. The average temperature at 22.5 ft is 31.0°F; this depth is still affected by surface temperatures. At the toe thermistor location (see Figure 4.17), the near surface is warmer during the winter months and cooler in the summer months than the near surface in the embankment. This is attributed to snow cover during the winter and the effects of shading from the nearby alders in the summer. The seasonally thawed layer thickness in August 2009 was 6 ft, which is in agreement with the drilling data. Figure 4.17 indicates that this layer deepened to between 8 and 10 ft during September and October. It is uncertain whether this is the true active layer thickness or due to the effects of drilling; collecting data for another year would answer this question. For example, the effects of drilling heat can be seen in the recorded August temperatures for 23 ft and 30 ft, which were warmer than all later temperatures. The average temperature at 30 ft is 30.8°F, and the depth of negligible temperature amplitude is approximately 10 ft.

The undisturbed temperature profile (see Figure 4.18) indicates an active layer thickness between 2 and 4 ft. Again, it is uncertain whether this is the true active layer thickness or due to drilling effects, as the measured seasonally thawed layer thickness in the field was 1.3 ft. As with the toe location, the effects of drilling heat can be seen in the recorded August temperature at 30 ft, which was warmer than all later temperatures. The average temperature at 30 ft is 30.1°F; this depth is also approximately the depth of negligible temperature amplitude. Further data collection may change these values slightly.

5.1 General Model Parameters and Configurations

This section covers the input parameters and analysis settings of the TEMP/W model, and the general modeling approach for both sites. The results from each research location are presented separately in the following sections. All modeling was done using TEMP/W Version 6.19, which is part of the GeoStudio 2004 program suite from GEO-SLOPE International.

For each site, a model was developed from the test hole data and measured surface topography. The first modeling attempt for each site will be referred to as the "traditional approach." In this approach, the input parameters either were chosen from among published values (such as *n*-factors and thermal conductivity), calculated based on other measured parameters (such as heat capacity), or collected from nearby stations (such as air temperature). Details of subsequent modeling iterations are described in Sections 5.2 and 5.3.

The TEMP/W program uses the following governing differential equation:

$$\frac{\partial}{\partial x}\left(k_x A \frac{\partial T}{\partial x}\right) + \frac{\partial}{\partial y}\left(k_y A \frac{\partial T}{\partial y}\right) + QA = A\left(C + L \cdot w_v \frac{\partial w_v}{\partial T}\right)\frac{\partial T}{\partial t} \qquad 5.1$$

where T is temperature, k_x and k_y are thermal conductivities in the x- and y-directions, respectively, A is the cross-sectional area, Q is an applied boundary flux, C is the volumetric heat capacity, L is the latent heat of water, w_v is the volumetric water content, w_u is the unfrozen water content, and t is time (Krahn 2004). When the system is in a transient state, as in the case of modeling roadway embankments, the right-hand term represents how well the soil stores heat (i.e., frozen or thawed heat capacity) and how much heat is stored or released by thawing or freezing (i.e., the latent heat term). Other than temperature, all of the other variables need to be determined by the user for a given analysis.

For each of the two research locations, one of the first preparatory steps in thermal modeling was to determine the cross-sectional geometry. At each site, a surface profile was created along the three borings using a hand level, stadia rod, and a tape. This profile was entered into the model as the ground surface and served as the horizontal extent of the model. Each mesh was extended to a depth of 100 ft. This was to ensure there was no interference between the upper and lower boundary conditions. Screen shots of the models for the two sites are shown in Figures 5.1 through 5.3. The configuration of the soil layers was interpreted from the test hole logs. Within each layer, the material was assumed to be homogeneous and isotropic.

The mesh developed for the Richardson Highway MP 113 area consisted of 1550 quadrilateral elements (see Figure 5.1). The medium blue area represents the relatively dry upper embankment. A 4-inch thick asphalt layer is present at the top of the embankment and shown in gray, although it is difficult to see at this scale. Drilling indicated that the lower portion of the embankment had a higher moisture content. This zone is represented as dark blue, and since its exact configuration is unknown, it is simply represented as a rectangle. The surficial silt is represented by the light green color. The clay is dark green and teal for frozen and unfrozen states, respectively. While the transitional nature of the silt and embankment materials was observed in the trench, the exact geometry of the thaw bulb under the highway was not
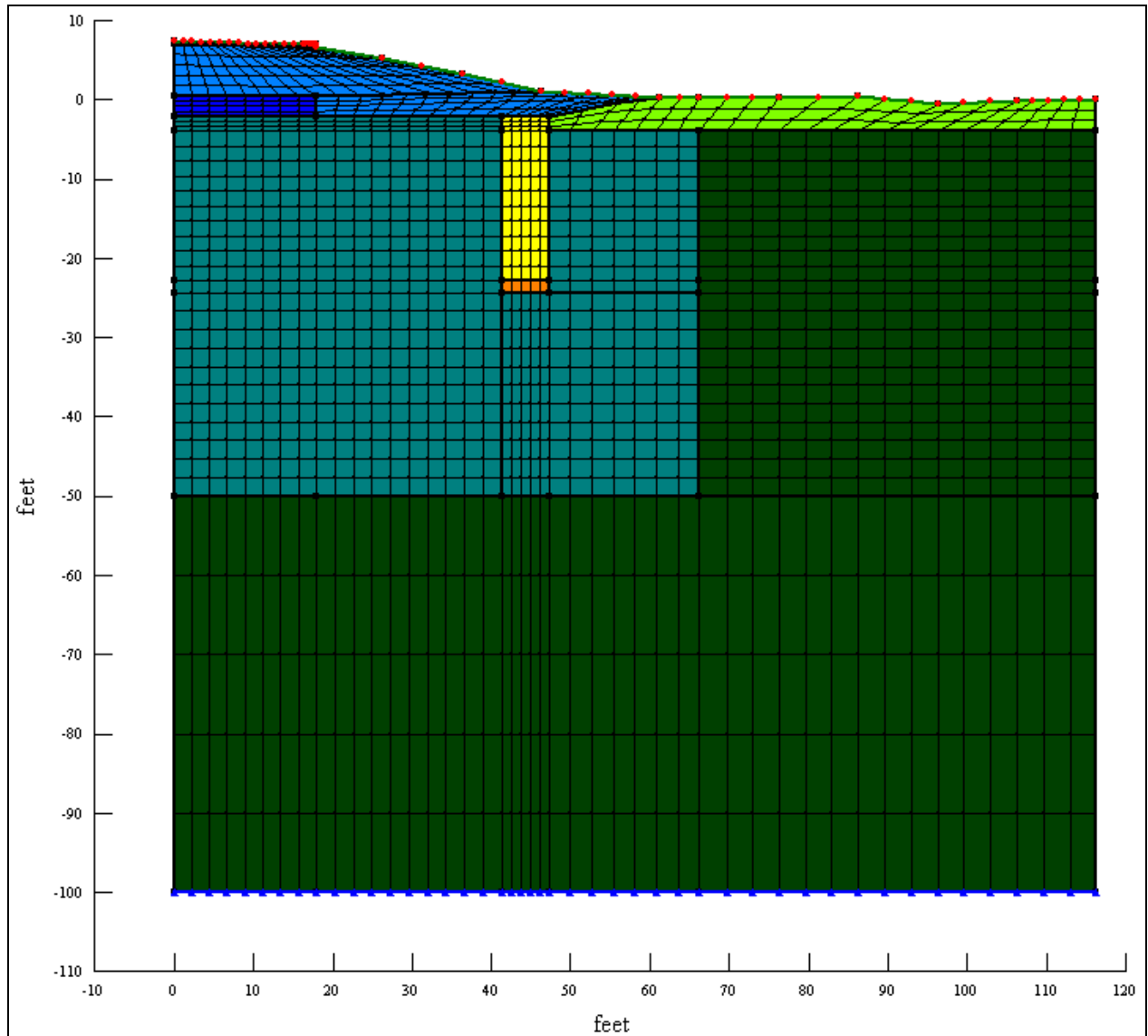
Figure 5.1. Mesh representing the Richardson Highway MP 113 research site. This mesh includes the underdrain. The vertical and horizontal scales are as viewed in TEMP/W.

determined from the three borings; thus the thawed clay is represented simply as a rectangle. Drilling indicated the presence of an underdrain, which was included in the initial traditional approach model. This is represented in Figure 5.1 as the yellow rectangle. The lower portion of the underdrain demonstrated a higher moisture content, and is represented as an orange rectangle. In another iteration of the modeling, the underdrain was not included, as shown in Figure 5.2.

The mesh for the Dalton Highway 9 Mile Hill research location consisted of 1495 quadrilateral elements (see Figure 5.3). The embankment is represented as medium blue, the *in situ* organic mat is represented as pink, and the ice-rich silt below is light green. The vegetation between the embankment and the organic mat was cleared at one point, possibly for improving visibility on this stretch of the highway. It was assumed that the silt underlying this area had thawed as a result of the clearing, and if refrozen, was no longer ice-rich. The foundation soils under the

53
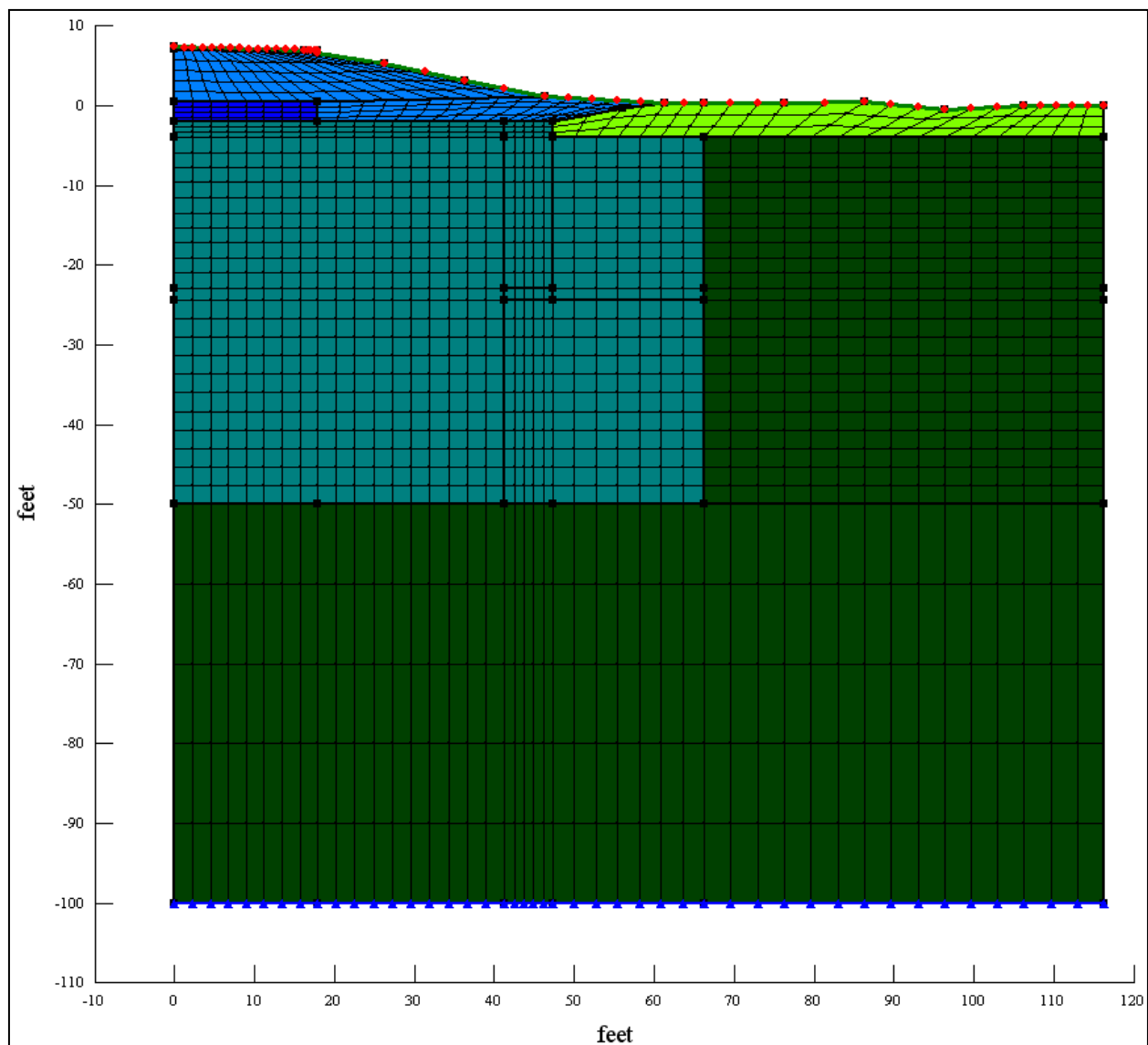
Figure 5.2. Mesh representing the Richardson Highway MP 113 research site, without the underdrain. The vertical and horizontal scales are as viewed in TEMP/W.

cleared area are represented as dark green. Each boring intercepted massive ice, which is represented as dark blue. Although there are most likely areas of silty soil within the ice, the massive ice was represented as a continuous layer for simplicity since its exact geometry is unknown. Below the massive ice is bedrock, which is represented by the purple area. Although the 2009 drilling did not intercept bedrock, other drilling in the area did. The depth to the bedrock surface is derived from those drilling results.

Table 5.1 summarizes the general units/input parameters used for all models. In TEMP/W, all other input parameters must be consistent with these units. The measured and/or calculated soil properties used for each of the traditional models are summarized in Table 5.2. The thermal properties for asphalt were taken from the FHWA "Pavements" webpage (http://www.fhwa.dot.gov/pavement/). The dry unit weight for each soil type was estimated

54
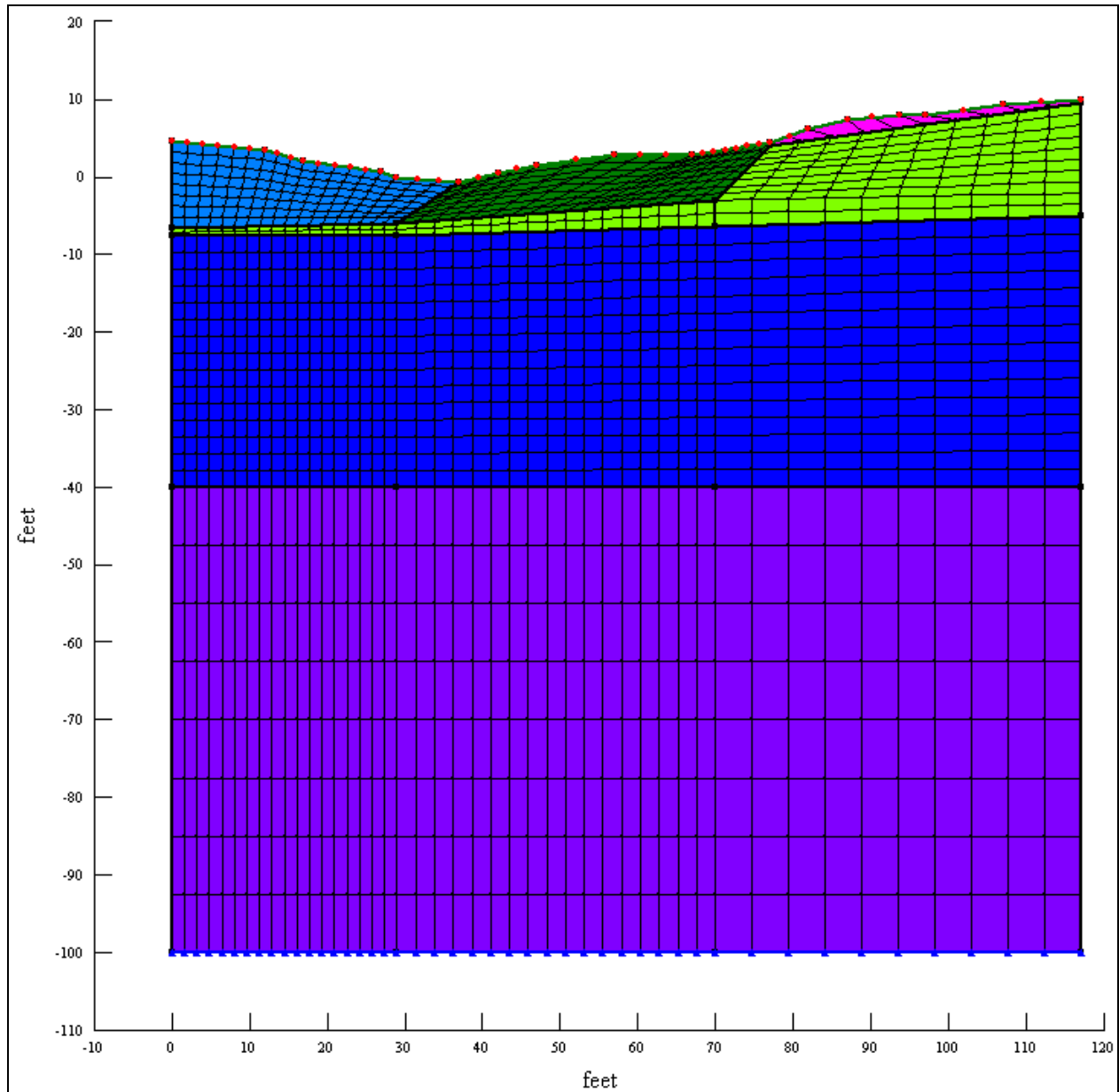
Figure 5.3. Mesh representing the Dalton Highway 9 Mile Hill research site. The vertical and horizontal scales are as viewed in TEMP/W.

Table 5.1. Summary of general units/input parameters used for all models.

Item	Value or Unit
Time step	24 hours
Temperature	°F
Phase change temperature	32°F
Heat energy	Btu
Latent heat of water	8,986 Btu/ft^3

55

Table 5.2. Summary of soil properties used as input parameters.

	Material (color in model shown to the right)	Dry unit weight (lb/ft^3)	Moisture content (%)		Thermal conductivity Btu/ft·day·°F		Heat capacity Btu/ft^3·°F	
			gravimetric	volumetric	k_f	k_u	c_f	c_u
RICHARDSON	Asphalt	---	---	0.1	16.1	16.1	34.0	34.0
	Embankment (dry)	120	2.4	4.6	14.4	21.6	21.8	23.3
	Embankment (wet)	120	14.7	28.3	57.6	38.4	29.2	38.0
	Underdrain (dry)	100	5.0	8.0	12.0	17.3	19.5	22.0
	Underdrain (wet)	100	11.3	18.1	21.6	22.1	22.7	34.0
	Silt	90	19.0	27.4	19.2	15.4	23.9	32.4
	Clay (unfrozen)	110	13.7	24.2	21.6	20.4	26.2	33.8
	Clay (frozen)	110	21.0	37.0	28.8	24.0	30.3	41.8
DALTON	Embankment	120	2.6	5.0	14.4	21.6	23.4	26.4
	Organic mat	---	---	5.0	13.9	16.6	25.4	22.4
	Thawed silt	90	24.0	34.6	24.0	16.8	26.1	15.5
	Ice-rich silt	---	---	70.0	31.2	12.6	28.9	52.9
	Massive ice	---	---	100.0	33.6	7.2	29.0	63.4
	Bedrock	---	---	1.0	30.5	30.5	33.0	33.0

from experience with similar soils and checked against published references, such as Coduto (1999) and Das (1998). The gravimetric moisture contents were averaged for each soil type from the drilling data, and the volumetric moisture contents, θ, were calculated using:

$$\theta = w \frac{\gamma_d}{\gamma_w} \qquad\qquad 5.2$$

where w is the gravimetric moisture content, γ_d is the dry unit weight, and γ_w is the unit weight of water.

Frozen and unfrozen thermal conductivities (k_f and k_u, respectively) were estimated using the charts developed by Kersten (1949). Frozen and unfrozen heat capacities (c_f and c_u, respectively) were calculated using the data in Table 5.2, and the following equations:

$$c_f = \gamma_d [0.17 + 0.5 \cdot (^w/_{100})] \qquad\qquad 5.3$$

$$c_u = \gamma_d [0.17 + (^w/_{100})] \qquad\qquad 5.4$$

where γ_d is the dry unit weight of the soil, and w is the gravimetric water content. Equations 5.3 and 5.4 have been simplified to include the specific heat of dry soil and the specific heat of water or ice, and values for c_f and c_u are in units of Btu/ft^3·°F. These equations can be modified to include the unfrozen water content of the soil. For the traditional approach, this step was not performed.

Unfrozen water content versus temperature can be incorporated into the TEMP/W model as a thermal function. For the traditional approach, the volumetric unfrozen water content data for Fairbanks silt as reported by Huang et al. (2004) was used for all of the foundation soils (i.e., silt and clay at the Richardson Highway site and silt at the Dalton Highway site). The embankment and underdrain at the Richardson Highway site, and the embankment, massive ice, and bedrock at the Dalton Highway site, were designated as not having an unfrozen water content for any below freezing temperature.

The nodes along the bottom of each mesh (represented by blue triangles in Figures 5.1 through 5.3) were given a flux boundary condition of 0.24 Btu/ft^2·day to simulate the geothermal gradient. Air temperature was applied as a function boundary condition at the nodes along the top of each mesh (represented by red circles in Figures 5.1 through 5.3). For the traditional approach, air temperature data was collected from the Western Regional Climate Center webpage (http://www.wrcc.dri.edu/index.html). For the Richardson Highway location, the average daily air temperature data used was from the Gulkana FAA/AMOS site (503465), averaged over the period from 1971 to 2000. This is a complete set of data, with between 28 and 30 years of data for each day summarized. For the Dalton Highway location, the closest air temperature data was from the Livengood site (505534), averaged over the period from 1971 to 2000. It is unclear from this website for which years data was collected, but the webpage indicates that it was spotty, with between 0 to 4 readings per day for this period.

The air temperature boundary condition was modified using n-factors to simulate surface temperatures. The n-factors used for the various surfaces were taken from the literature (e.g., Andersland and Ladanyi 2004) and are summarized in Table 5.3. It was assumed that the asphalt surface and the surface of the gravel roadway would remain mostly cleared of snow during the

Table 5.3. Original *n*-factors used in the thermal modeling.

Location	Surface	n_t	n_f
RICHARDSON	Asphalt	1.8	0.9
	Gravel slope/disturbed gravel surface	1.5	0.6
	Spruce forest	0.37	0.29
DALTON	Gravel road	1.5	0.9
	Gravel slope	1.5	0.6
	Cleared area	1.2	0.4
	Spruce forest	0.37	0.29

winter months; however, it also was assumed that the gravel side slopes at both research locations would remain snow covered. Typical *n*-factors for spruce trees, brush, and moss over peat soil were chosen for the undisturbed areas, and the *n*-factors used for the previously cleared area at the Dalton Highway location were chosen to simulate a mostly bare soil surface.

Each node was given an initial condition very roughly approximating soil temperatures on January 1st for the first time step of each traditional approach model. Setting initial conditions reduces the number of iterations that the model must go through before reaching a solution for each time step. For the Richardson Highway MP 113 location, the embankment and silt areas were given an initial condition of 28°F. The area below the embankment to the bottom of the underdrain and including the underdrain was set at 33°F, and the remaining foundation soils were set at 31°F. For the Dalton Highway location, the entire mesh was set at 30°F.

For the traditional approach for each location, the model was run for 50 years (a total of 18,250 time steps), with model results saved every year (or every 365 time steps). The model was then run for an additional five years (a total of 1,825 time steps), with model results saved every 5 days.

5.2 Modeling Results for Richardson Highway MP 113

Table 5.4 summarizes the model iterations that were analyzed for the Richardson Highway location. In the following discussion, each iteration will be referred to as the corresponding run number. The traditional approach was split into two runs, with Run 1a representing the 50 year model results, and Run 1b representing the results of the 5 year model.

The first model was run for 50 years to check for the thermal equilibrium of the thaw bulb. Figure 5.4 is a portion of the mesh, with phase change isotherms on January 1st for multiple years shown for comparison. At the start of the model, it was assumed that a thaw bulb existed under the highway. The phase change isotherm at the end of the first model year demonstrates some of the rectangular nature of the assumed thaw bulb. Through the 50 years, the upper configuration of the thaw bulb remained consistent. The thaw bulb extended away from the highway centerline below the disturbed area with a gravel surface. The presence of the underdrain is obvious with the deeper freezing front at its location. The lower configuration of the thaw bulb changed throughout the 50 years, with the lateral portion freezing back towards the center of the embankment and the bottom portion continuing to deepen. Along the highway centerline, the

Table 5.4. Summary of model iterations for the Richardson Highway MP 113 research site

Run number	Comments
1a	Traditional approach, 50 year model
1b	Traditional approach, 5 year model
2	Modified traditional approach: elimination of underdrain; larger initial thaw bulb, 55 year model, initial conditions derived from Run 1
3	Revised Run 1b using measured k_f and k_u (i.e., k_f = 23.8 Btu/ft·day·°F, k_u = 17.4 Btu/ft·day·°F)
4	Revised Run 1b using measured site air temperatures and measured k_f and k_u
5	Revised Run 4 using measured w_U
6	Revised Run 5 using adjusted n-factors

position of the phase change isotherm was compared over 10-year intervals; the rate of thaw progression as suggested by the model over the 50 years is presented in Table 5.5. The high rate of change over the first 10 years suggests that the model was rapidly adjusting to the surface boundary condition. For the next 40 years, the rate of thaw bulb progression slowly attenuates, but is still advancing at the end of 50 years with a thaw bulb 45.6-ft deep below the highway centerline. Although the drilling for this project did not advance this deeply, results from other drilling conducted by AK DOT&PF in the general area indicate similar thaw bulb depths beneath the highways (Darrow 2006).

Figures 5.5 through 5.16 are some of the model results from Run 1b. The figures contain model results for the first day of each month from the last year of the 5-year period. Model temperatures are presented with a 2°F contour interval, and the phase change isotherm is represented as a dashed blue line. On each figure, the measured thermistor temperatures from the selected depths of 0.5 ft, 2 ft, 6 ft, 10 ft, 14 ft, 18 ft, 23 ft, and 30 ft are superimposed over the contours in black text. These depths were chosen for the best readability of the results. For each figure, the measured temperatures shown are from the first of the month in 2009. The phase change isotherm approximated from the measured temperatures is shown as a dashed yellow line. As the dashed yellow line is only a rough approximation given the temperature measurement interval (i.e. typically 2 ft), it should not be used to validate the accuracy of the model results. The measured and modeled temperatures for each of the selected depths were compared, and these comparisons are tabulated in Appendix E.

Overall, the modeled temperatures are colder than the measured temperatures. At a depth of 30 ft at the undisturbed location, the modeled temperatures are colder typically by 2°F; however, there is good agreement in measured and modeled temperatures at this depth for the months of October through December. Moving towards the surface, the difference between modeled and measured temperatures becomes greater, differing by as much as 16.9°F at 0.5 ft in August.

For the toe location, the modeled temperatures are colder than the measured temperatures by an average of 3.8°F at 30 ft. Moving towards the surface, this difference becomes greater, differing by as much as 20°F at 0.5 ft in February; however, in some cases the modeled temperatures are warmer than the measured temperatures in the upper two feet. For the shoulder location, the modeled temperatures are roughly 1°F colder than the measured temperatures at depths between 10 ft and 30 ft. Moving towards the surface, the modeled temperatures become increasingly colder than the measured temperatures, although for some months, the opposite is true.
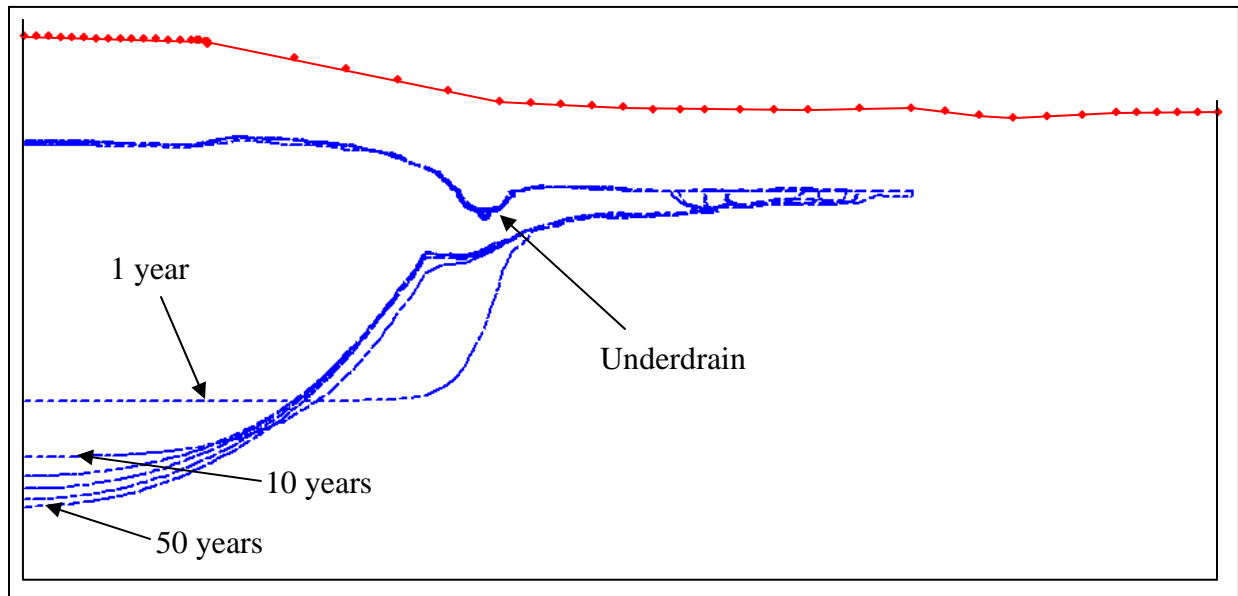
Figure 5.4. A portion of the model results from Run 1a: 50 year model, Richardson Highway MP 113. The ground surface is represented by the red line and circles. The phase change isotherms, or freeze-thaw lines, are represented by blue dashed lines. The thaw bulb positions at the end of 1 year, 10 years, and 50 years are indicated. The remaining phase change isotherms are for 20, 30 and 40 years. Each phase change isotherm represents the thermal state as of January 1st.

Table 5.5. Thaw bulb progression below highway centerline, Richardson Highway MP 113 research site.

Time interval (number of years)	Vertical change in phase change isotherm (ft)
10	5.46
20	1.85
30	1.16
40	1.22
50	0.63

Figure 5.5. Thermal modeling results for January 1st, Run 1b, Richardson Highway MP 113 research site. The phase change isotherm is represented as the dashed blue line and the temperature results are shown with a 2°F contour interval. Some of the measured temperatures along each thermistor string are shown in black text superimposed on the contours. The phase change isotherm approximated from the measured data is shown as a yellow dashed line.

Figure 5.6. Thermal modeling results for February 1st, Run 1b, Richardson Highway MP 113 research site. The phase change isotherm is represented as the dashed blue line and the temperature results are shown with a 2°F contour interval. Some of the measured temperatures along each thermistor string are shown in black text superimposed on the contours. The phase change isotherm approximated from the measured data is shown as a yellow dashed line.

Figure 5.7. Thermal modeling results for March 1st, Run 1b, Richardson Highway MP 113 research site. The phase change isotherm is represented as the dashed blue line and the temperature results are shown with a 2°F contour interval. Some of the measured temperatures along each thermistor string are shown in black text superimposed on the contours. The phase change isotherm approximated from the measured data is shown as a yellow dashed line.

Figure 5.8. Thermal modeling results for April 1st, Run 1b, Richardson Highway MP 113 research site. The phase change isotherm is represented as the dashed blue line and the temperature results are shown with a 2°F contour interval. Some of the measured temperatures along each thermistor string are shown in black text superimposed on the contours. The phase change isotherm approximated from the measured data is shown as a yellow dashed line.

Figure 5.9. Thermal modeling results for May 1st, Run 1b, Richardson Highway MP 113 research site. The phase change isotherm is represented as the dashed blue line and the temperature results are shown with a 2°F contour interval. Some of the measured temperatures along each thermistor string are shown in black text superimposed on the contours. The phase change isotherm approximated from the measured data is shown as a yellow dashed line.

Figure 5.10. Thermal modeling results for June 1st, Run 1b, Richardson Highway MP 113 research site. The phase change isotherm is represented as the dashed blue line and the temperature results are shown with a 2°F contour interval. Some of the measured temperatures along each thermistor string are shown in black text superimposed on the contours. The phase change isotherm approximated from the measured data is shown as a yellow dashed line.

Figure 5.11. Thermal modeling results for July 1st, Run 1b, Richardson Highway MP 113 research site. The phase change isotherm is represented as the dashed blue line and the temperature results are shown with a 2°F contour interval. Some of the measured temperatures along each thermistor string are shown in black text superimposed on the contours. The phase change isotherm approximated from the measured data is shown as a yellow dashed line.

Figure 5.12. Thermal modeling results for August 1st, Run 1b, Richardson Highway MP 113 research site. The phase change isotherm is represented as the dashed blue line and the temperature results are shown with a 2°F contour interval. Some of the measured temperatures along each thermistor string are shown in black text superimposed on the contours. The phase change isotherm approximated from the measured data is shown as a yellow dashed line.

Figure 5.13. Thermal modeling results for September 1st, Run 1b, Richardson Highway MP 113 research site. The phase change isotherm is represented as the dashed blue line and the temperature results are shown with a 2°F contour interval. Some of the measured temperatures along each thermistor string are shown in black text superimposed on the contours. The phase change isotherm approximated from the measured data is shown as a yellow dashed line.

69

Figure 5.14. Thermal modeling results for October 1st, Run 1b, Richardson Highway MP 113 research site. The phase change isotherm is represented as the dashed blue line and the temperature results are shown with a 2°F contour interval. Some of the measured temperatures along each thermistor string are shown in black text superimposed on the contours. The phase change isotherm approximated from the measured data is shown as a yellow dashed line.

Figure 5.15. Thermal modeling results for November 1st, Run 1b, Richardson Highway MP 113 research site. The phase change isotherm is represented as the dashed blue line and the temperature results are shown with a 2°F contour interval. Some of the measured temperatures along each thermistor string are shown in black text superimposed on the contours. The phase change isotherm approximated from the measured data is shown as a yellow dashed line.

Figure 5.16. Thermal modeling results for December 1st, Run 1b, Richardson Highway MP 113 research site. The phase change isotherm is represented as the dashed blue line and the temperature results are shown with a 2°F contour interval. Some of the measured temperatures along each thermistor string are shown in black text superimposed on the contours. The phase change isotherm approximated from the measured data is shown as a yellow dashed line.

Comparing modeled thaw or freeze depths to those approximated from the measured data is complicated for several reasons. First of all, the comparison must be done graphically due to the nature of the TEMP/W output. For some months there are multiple phase change isotherms for a given location, and for other months a phase change isotherm may be present in either the measured or modeled data but not in the other. Additionally, the rates of freezing or thawing may differ slightly between the model results and the measured temperatures. For all of these reasons, the modeled phase change isotherms were evaluated only against the active layer depths indicated by the analysis in Chapter 4.

Table 5.6 contains a summary of the modeled phase change isotherm depths for Runs 1b, 4, and 6; Runs 4 and 6 will be discussed separately. Focusing on Run 1b, the data in Table 5.6 indicates that the active layer depth in the embankment (i.e., depth of freeze) is approximately 11 ft in April, and the active layer depth at the undisturbed location (i.e., depth of thaw) is 5 ft in December. These values are in agreement with the active layer depths obtained from the measured data (i.e., 12 ft for the embankment, and 6 ft for the undisturbed location).

A major difference in the active layer/thaw bulb shape occurs at the toe location. The measured temperatures indicate that the thaw bulb is much wider and includes the thermistor string at this location. One possible reason for this difference may be that the underdrain has a greater cooling effect in the model than in reality.

Based on this analysis, the model was run again, replacing the underdrain material and thermal properties with those of thawed clay (see Figure 5.2). The initial temperatures assigned simulated a wider thaw bulb; otherwise, the model results from Run 1b on January 1st were used as the initial conditions. The model was run for a total of 55 years. This model iteration will be referred to as Run 2, and the results for each month are presented in Appendix F. A different color scheme was necessary in Figures F.1 through F.12 for the shaded contours in order to see the phase change isotherm. In Run 2, the thaw bulb deepened to 93.7 ft below the highway centerline, and thawing was beginning from the bottom of the mesh. The upper configuration of the thaw bulb remained very similar to that in Runs 1a and 1b, however. The thawed soils in the simulated wider thaw bulb froze back towards the embankment, resulting in a similar shape in the upper portion of the thaw bulb. Visual comparison of the temperature contour plots indicates that the modeled temperatures in these two iterations are unremarkable in their differences with the exception of the lower portion of the thaw bulb configuration.

For the third model iteration, the approximated values for k_f and k_u for the clay were replaced with the measured values from the site (i.e., k_f = 23.8 Btu/ft·day·°F, k_u = 17.4 Btu/ft·day·°F). This model, Run 3, was otherwise similar to Run 1b, including the presence of the underdrain and the smaller initial thaw bulb. The model results are presented in Figures F.13 through F.24 in Appendix F, and can be compared with the Run 1b results presented in Figures 5.5 through 5.16. With the measured thermal conductivity values, the modeled temperatures are slightly colder in some areas of the model. Otherwise, the temperatures and thaw bulb configurations are unremarkable in their differences between Runs 1b and 3.

For Run 4, the air temperatures measured at the site were used as the upper boundary condition. To eliminate some of the daily fluctuation, all of the available data were averaged for each calendar day. Only one set of air temperatures was available for the dates between May 25th and

Table 5.6. Summary of modeled phase change isotherm depths, Richardson Highway MP 113 research site. Where relevant, 'U' and 'L' indicate upper and lower phase change isotherms, respectively. For months when no phase change isotherm was present, '---' is shown. For means of comparison, measured data included in Chapter 4 indicates the following active layer depths: shoulder – 12 ft; toe – between 8 and 10 ft; undisturbed – 6 ft.

Month		Run 1b			Run 4			Run 6		
		Shoulder	Toe	Undisturbed	Shoulder	Toe	Undisturbed	Shoulder	Toe	Undisturbed
January	U	9.9	8.0	---	9.4	7.9	6.0	10.7	8.1	---
	L		11.0			11.8	6.7		17.4	
February	U	10.3	---	---	9.9	9.9	---	12.7	11.7	---
	L					12.7			18.2	
March	U	10.7	---	---	10.8	---	---	13.8	15.4	---
	L								18.5	
April	U	11.3	---	---	0.5	0.3	0.5	0.4	0.2	0.3
	L				10.2	---	---	14.9	17.2	---
May	U	4.6	1.5	1.2	8.8	2.5	1.5	5.2	2.2	1.5
	L	11.2			9.9	---	---	16.4		---
June	U	10.4	4.3	1.7	---	5.5	2.9	10.4	4.2	3.0
	L							17.2		---
July	U	---	5.9	2.9	---	7.8	3.9	13.6	7.3	3.8
	L							17.6		
August		---	7.0	3.7	---	8.8	4.5	---	9.3	5.4
September		---	8.0	4.0	---	10.0	5.4	---	11.3	6.1
October		---	8.6	4.4	---	10.5	5.6	---	13.0	7.0
November	U	4.9	2.9	1.9	3.2	2.0	1.4	3.2	1.8	1.7
	L		9.8	4.7	---	11.2	5.8		15.0	-5.4
December	U	8.8	5.8	4.2	7.2	5.3	3.7	8.1	4.3	3.8
	L		10.1	5.0		11.6	6.0		15.7	7.7

November 10th. The measured values for k_f and k_u for the clay also were used in this iteration, and the underdrain properties were replaced with those of clay. The model results are presented in Figures 5.17 through 5.28. The measured and modeled temperatures for each of the selected depths were compared, and these comparisons are tabulated in Appendix E. Additionally, Table 5.6 contains a summary of the phase change isotherm depths for this model iteration.

For the undisturbed location, the modeled temperatures match the measured temperatures at 30 ft, and are within 1°F on average of the measured temperatures below 10 ft. There is up to 12.5°F variation between modeled and measured temperatures at 0.5 ft in September. For the toe location, the modeled temperatures are colder than the measured temperatures by an average of 2.3°F at 30 ft. Between 10 ft and 30 ft, the modeled temperatures are 2.8°F colder on average than the measured temperatures. This indicates that the modeled thaw bulb is still too narrow, having not progressed wide enough to contain the thermistor string location. Between the surface and 10 ft, the modeled temperatures deviate more from the measured temperatures, being both warmer and colder. For the shoulder location, at 30 ft the modeled temperatures are 1.2°F warmer on average than the measured temperatures. Moving towards the surface, the modeled temperatures are increasingly warmer than the measured temperatures. Between the surface and 10 ft, the modeled temperatures deviate more from the measured temperatures, being both warmer and colder.

For Run 4, the active layer depth in the embankment (i.e., maximum depth of freeze) is approximately 10 ft in April, which is in agreement with the measured data (i.e., 12 ft maximum depth). The active layer depth at the undisturbed location (i.e., depth of thaw) is approximately 7 ft in January, which is deeper than that measured (i.e., 6 ft depth). As with previous model iterations, the thaw bulb configuration at the toe thermistor string location continues to be a difficult area to assess. In Run 4, the model again produces a thaw bulb that is narrower than what was measured, failing to include the toe thermistor string location.

For the next model iteration (i.e., Run 5), the silt unfrozen water content (w_U) function initially used for the clayey soil was replaced with a soil-specific function based on laboratory data. The w_U function for the clay was taken from Darrow et al. (2009); this data was obtained from clayey soil a few hundred feet from the research site, and is representative of the clayey soil in the Richardson Highway MP 113 research area. Other than this change, Run 5 was identical to Run 4. The model results are presented in Figures 5.29 through 5.40. Comparisons of the measured and modeled temperature for each of the selected depths are tabulated in Appendix E.

For the undisturbed location, the modeled temperatures match the measured temperatures at 30 ft and are within 0.5°F on average of the measured temperatures below 10 ft. There is up to 11.5°F variation between modeled and measured temperatures at 0.5 ft in September. For the toe location, the modeled temperatures are colder than the measured temperatures by an average of 2.0°F at 30 ft. Between 10 ft and 30 ft, the modeled temperatures are 2.2°F colder on average than the measured temperatures. As with Run 4, between the surface and 10 ft, the modeled temperatures deviate more from the measured temperatures. For the shoulder location, at 30 ft the modeled temperatures are 0.9°F warmer on average than the measured temperatures, and deviate more from the measured temperatures towards the surface, being both warmer and colder.
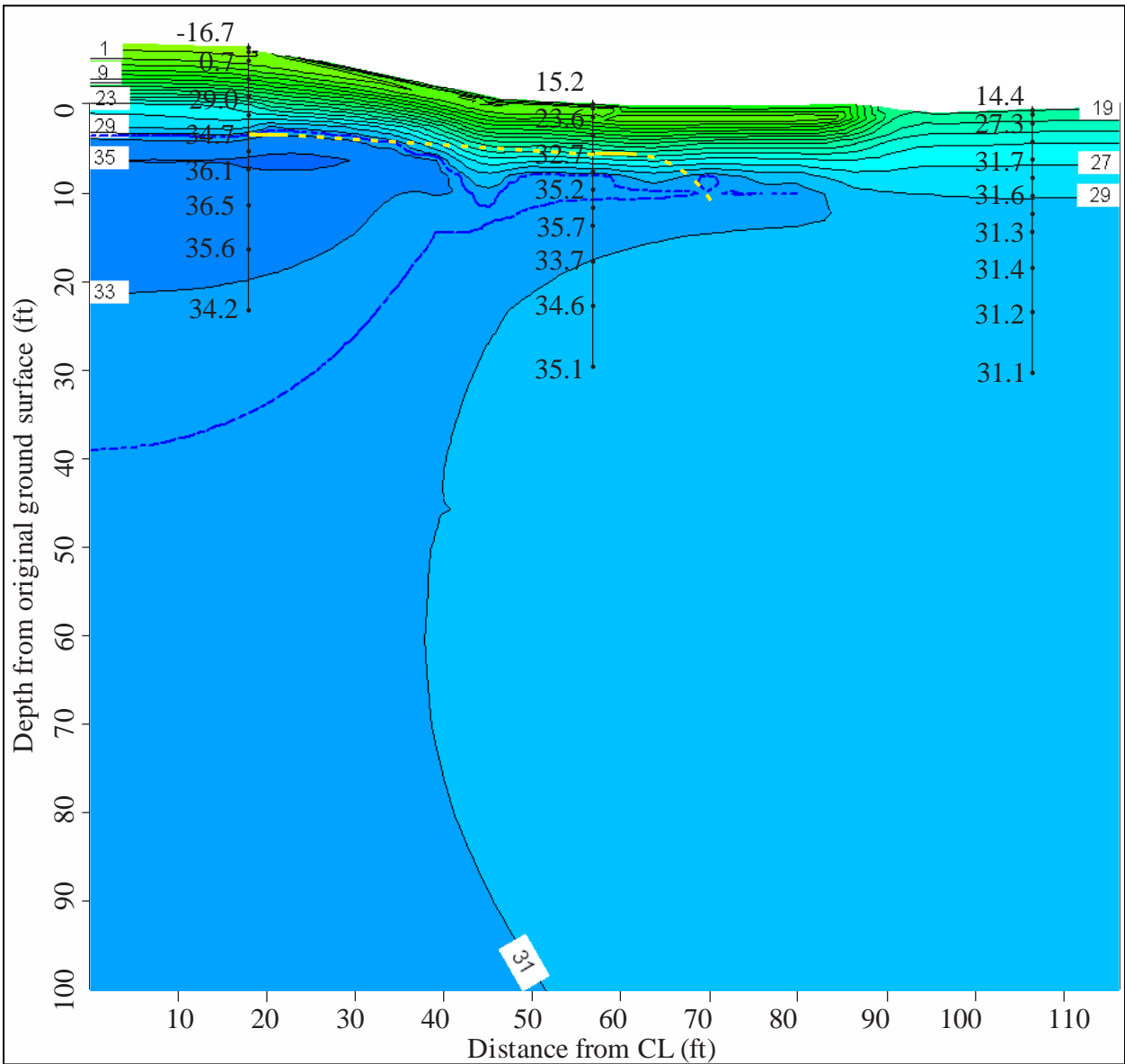
Figure 5.17. Thermal modeling results for January 1st, Run 4, Richardson Highway MP 113 research site. The phase change isotherm is represented as the dashed blue line and the temperature results are shown with a 2°F contour interval. Some of the measured temperatures along each thermistor string are shown in black text superimposed on the contours. The phase change isotherm approximated from the measured data is shown as a yellow dashed line.
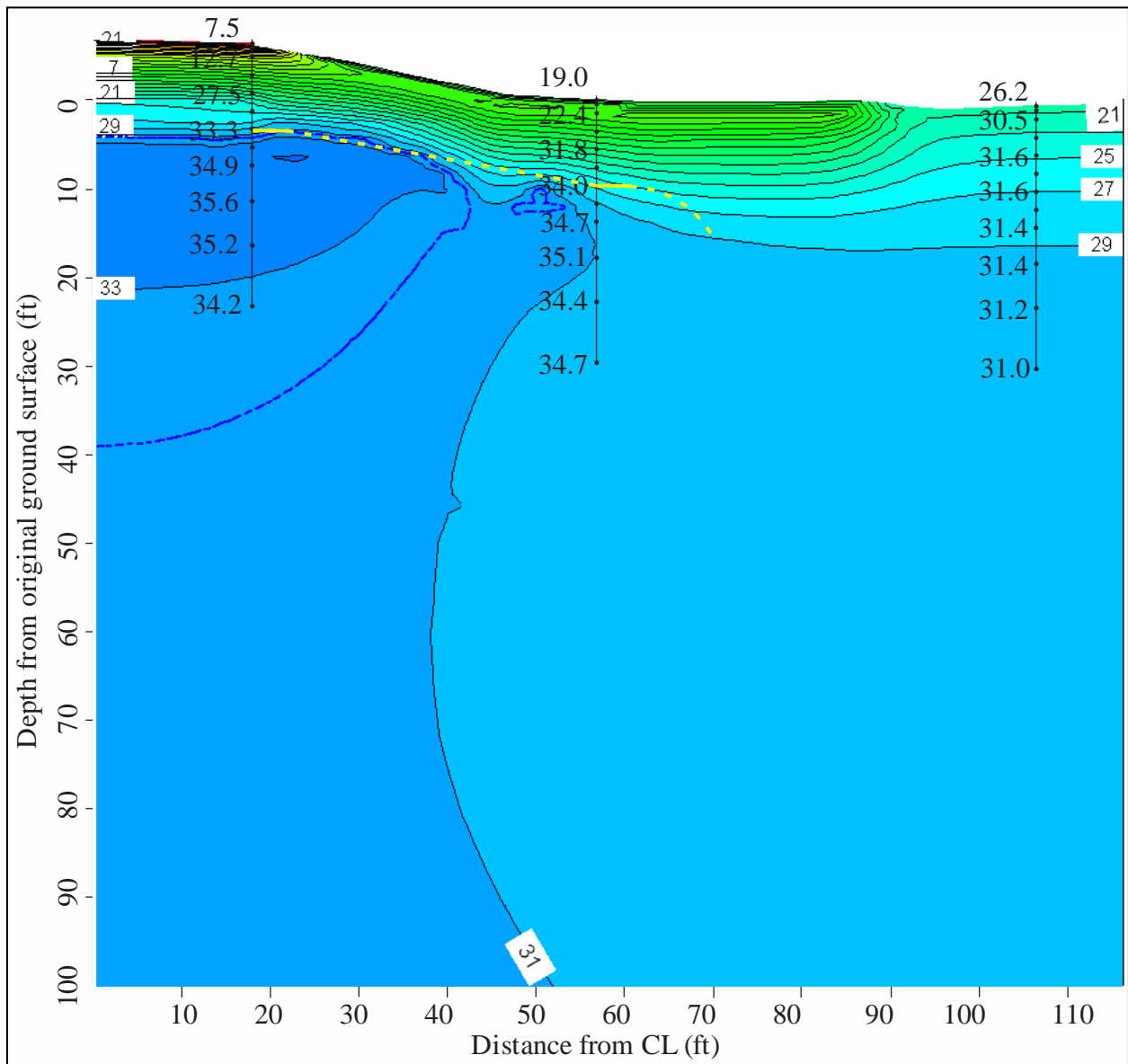
Figure 5.18. Thermal modeling results for February 1st, Run 4, Richardson Highway MP 113 research site. The phase change isotherm is represented as the dashed blue line and the temperature results are shown with a 2°F contour interval. Some of the measured temperatures along each thermistor string are shown in black text superimposed on the contours. The phase change isotherm approximated from the measured data is shown as a yellow dashed line.
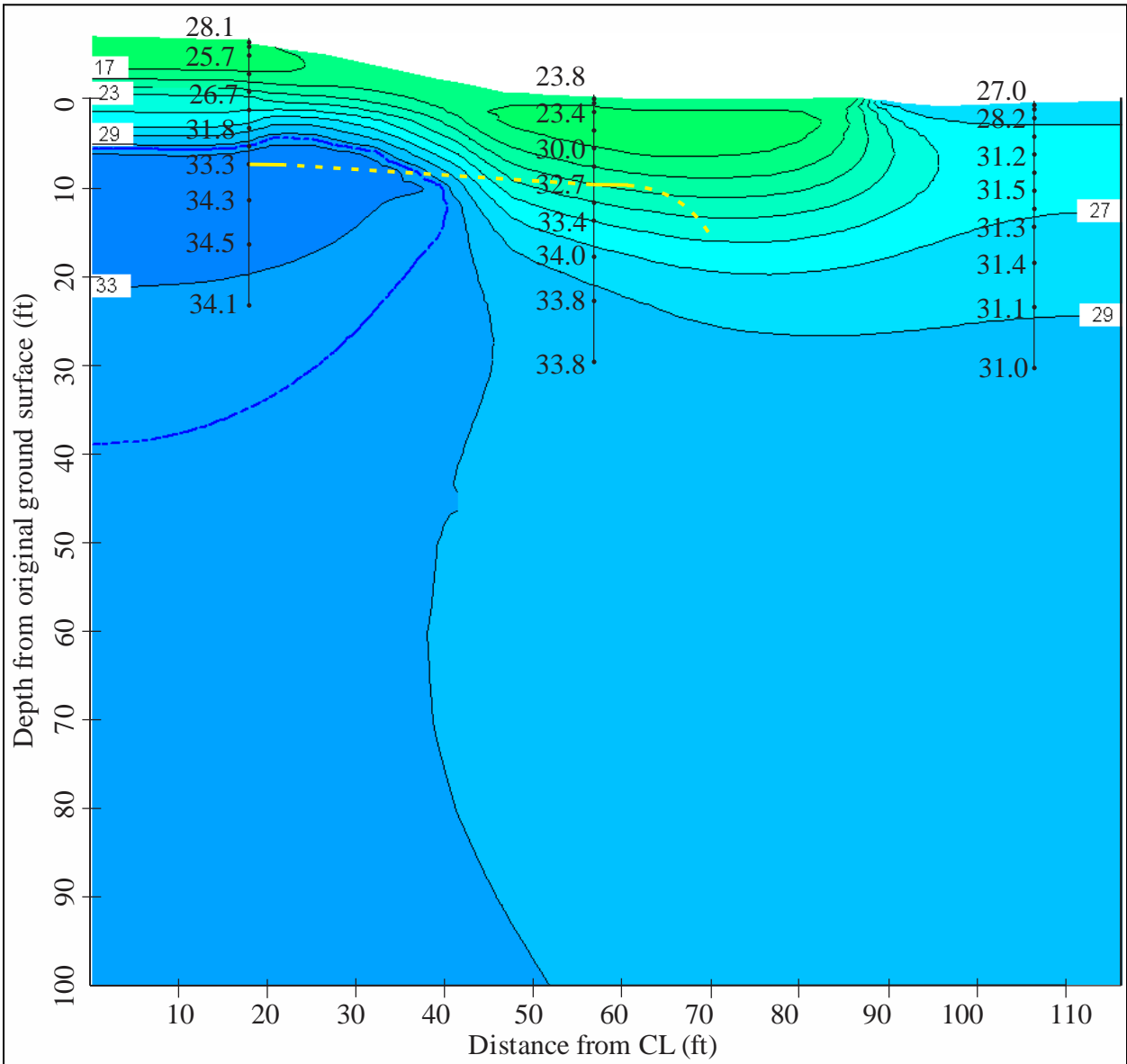
Figure 5.19. Thermal modeling results for March 1ˢᵗ, Run 4, Richardson Highway MP 113 research site. The phase change isotherm is represented as the dashed blue line and the temperature results are shown with a 2°F contour interval. Some of the measured temperatures along each thermistor string are shown in black text superimposed on the contours. The phase change isotherm approximated from the measured data is shown as a yellow dashed line.
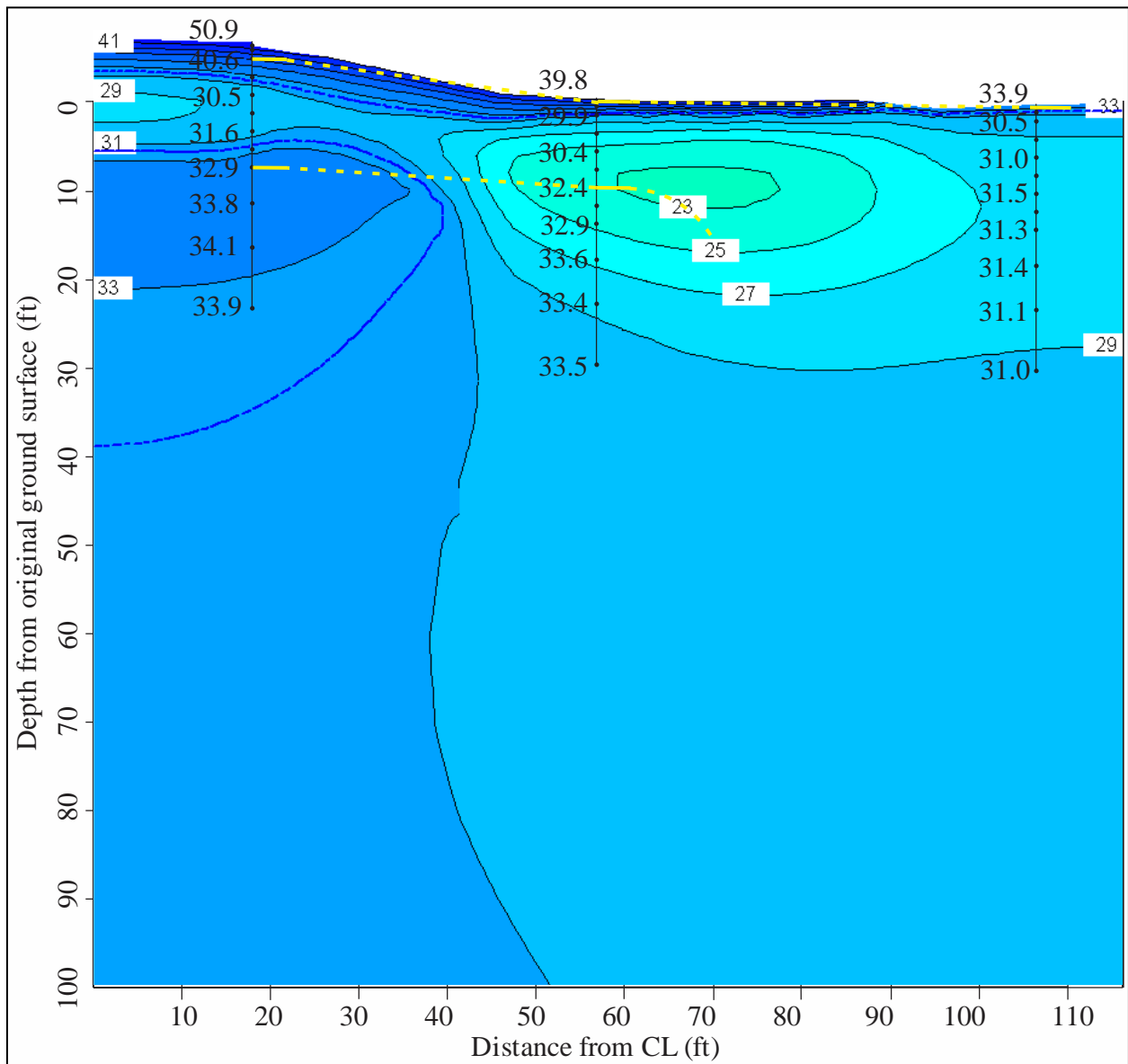
Figure 5.20. Thermal modeling results for April 1st, Run 4, Richardson Highway MP 113 research site. The phase change isotherm is represented as the dashed blue line and the temperature results are shown with a 2°F contour interval. Some of the measured temperatures along each thermistor string are shown in black text superimposed on the contours. The phase change isotherm approximated from the measured data is shown as a yellow dashed line.

Figure 5.21. Thermal modeling results for May 1st, Run 4, Richardson Highway MP 113 research site. The phase change isotherm is represented as the dashed blue line and the temperature results are shown with a 2°F contour interval. Some of the measured temperatures along each thermistor string are shown in black text superimposed on the contours. The phase change isotherm approximated from the measured data is shown as a yellow dashed line.
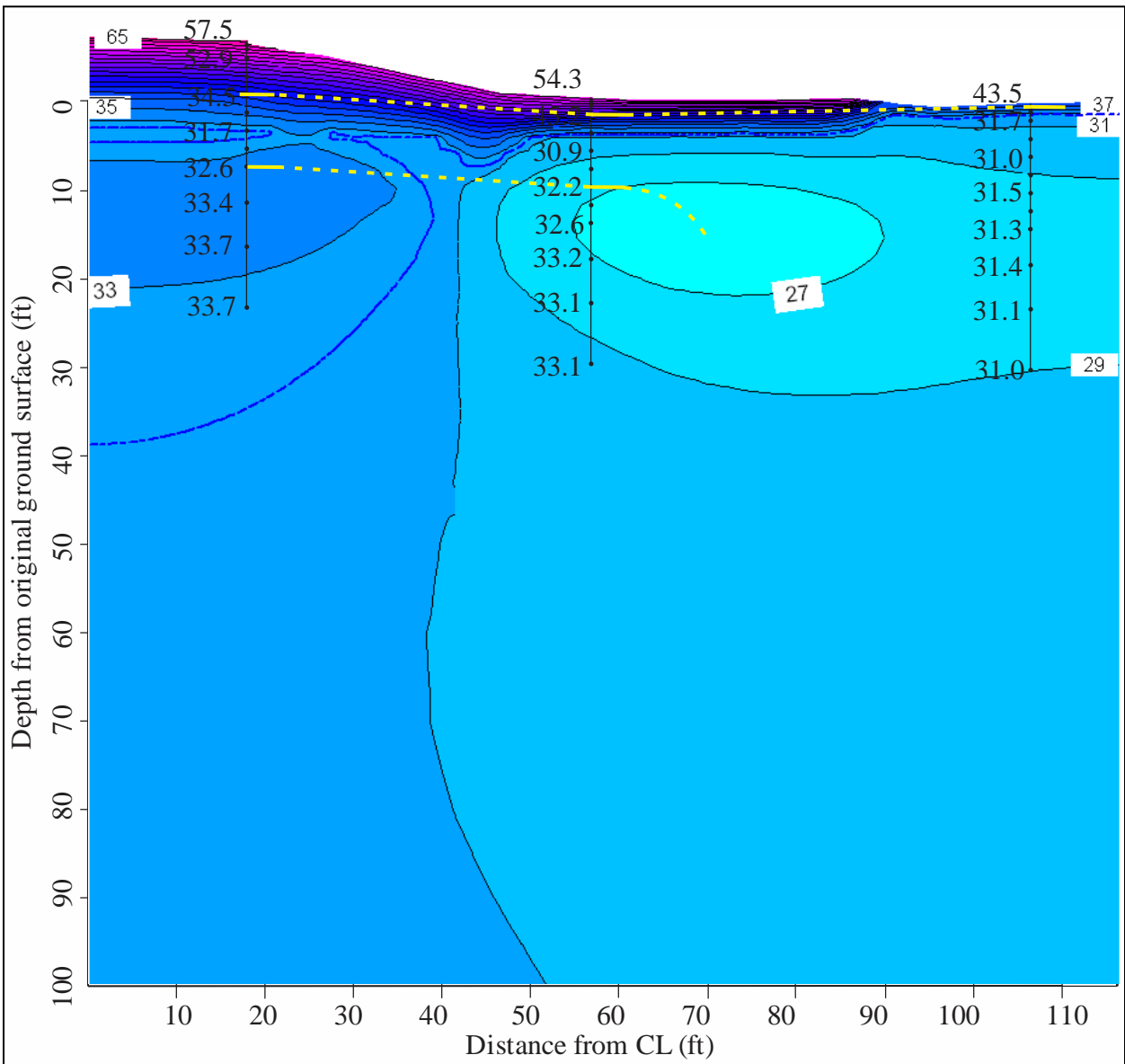
Figure 5.22. Thermal modeling results for June 1st, Run 4, Richardson Highway MP 113 research site. The phase change isotherm is represented as the dashed blue line and the temperature results are shown with a 2°F contour interval. Some of the measured temperatures along each thermistor string are shown in black text superimposed on the contours. The phase change isotherm approximated from the measured data is shown as a yellow dashed line.
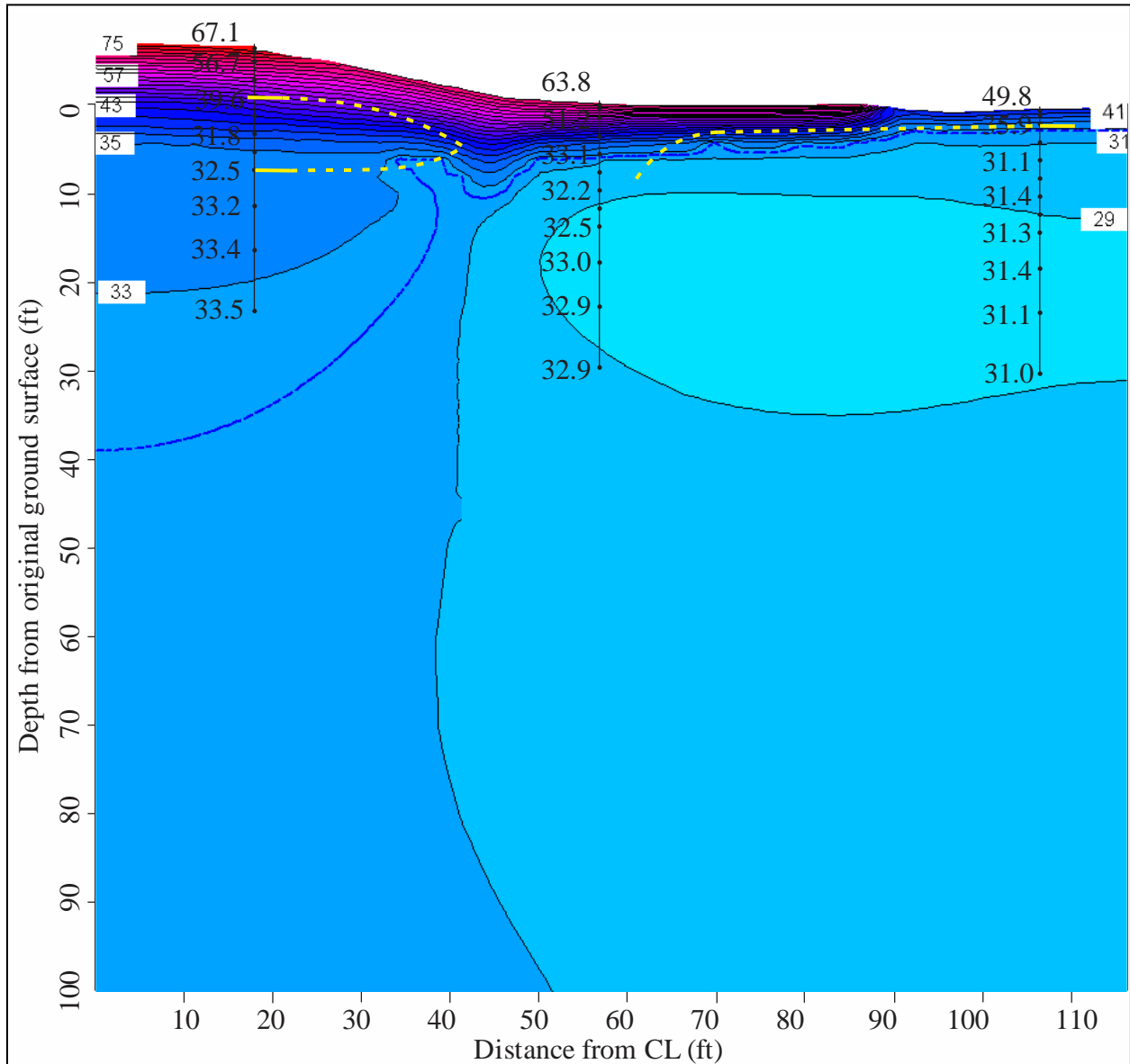
Figure 5.23. Thermal modeling results for July 1st, Run 4, Richardson Highway MP 113 research site. The phase change isotherm is represented as the dashed blue line and the temperature results are shown with a 2°F contour interval. Some of the measured temperatures along each thermistor string are shown in black text superimposed on the contours. The phase change isotherm approximated from the measured data is shown as a yellow dashed line.
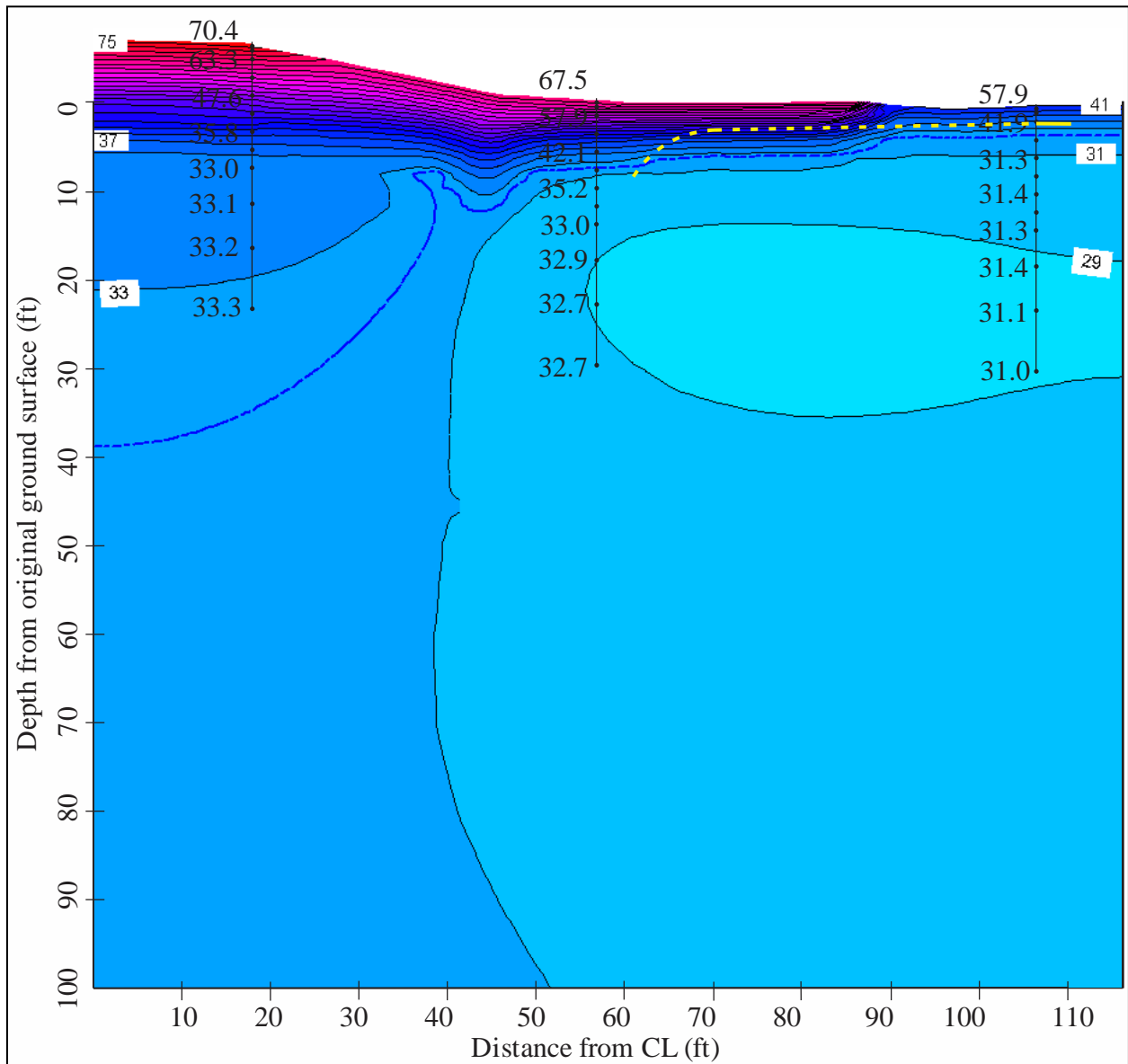
Figure 5.24. Thermal modeling results for August 1st, Run 4, Richardson Highway MP 113 research site. The phase change isotherm is represented as the dashed blue line and the temperature results are shown with a 2°F contour interval. Some of the measured temperatures along each thermistor string are shown in black text superimposed on the contours. The phase change isotherm approximated from the measured data is shown as a yellow dashed line.

Figure 5.25. Thermal modeling results for September 1st, Run 4, Richardson Highway MP 113 research site. The phase change isotherm is represented as the dashed blue line and the temperature results are shown with a 2°F contour interval. Some of the measured temperatures along each thermistor string are shown in black text superimposed on the contours. The phase change isotherm approximated from the measured data is shown as a yellow dashed line.
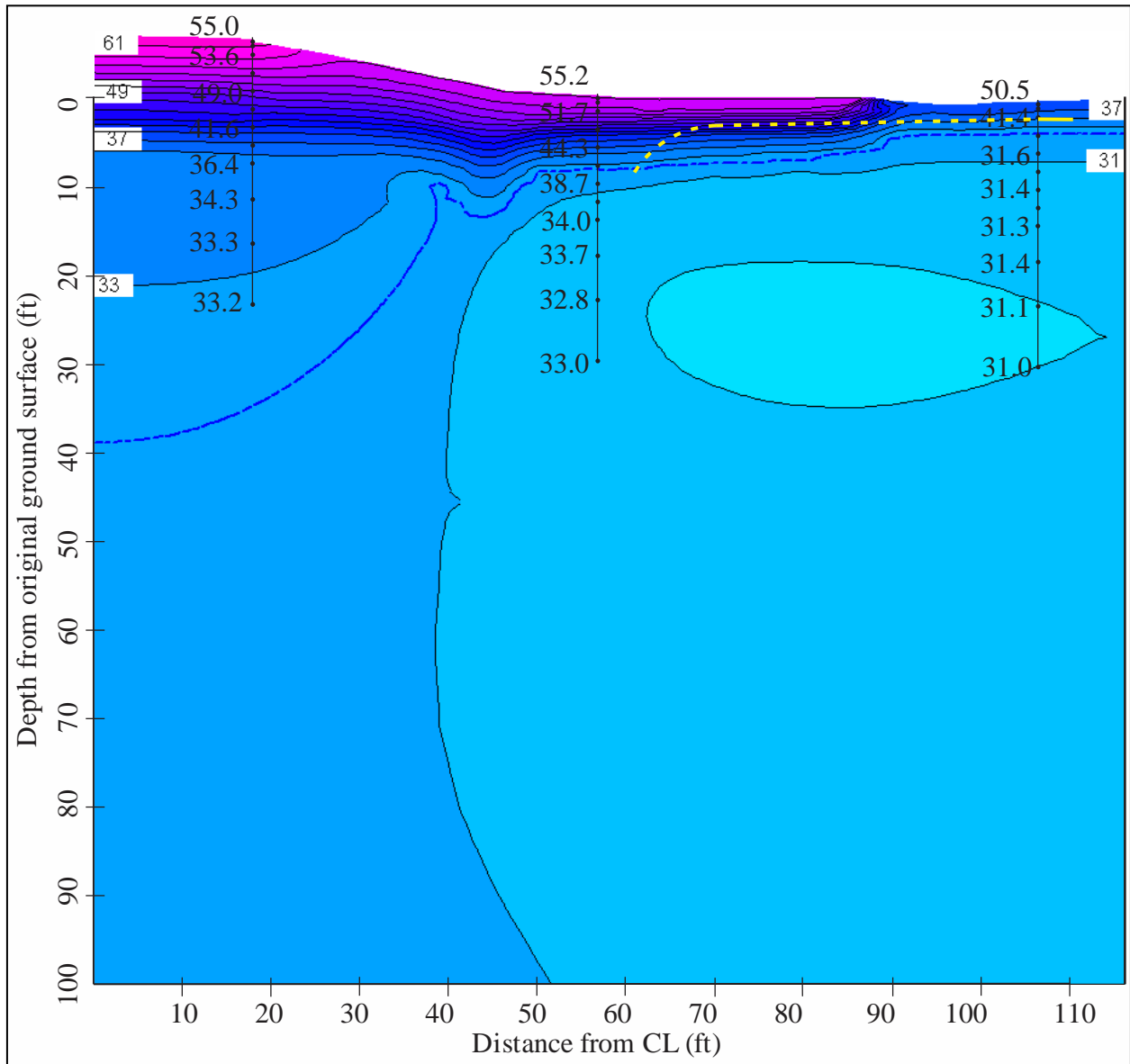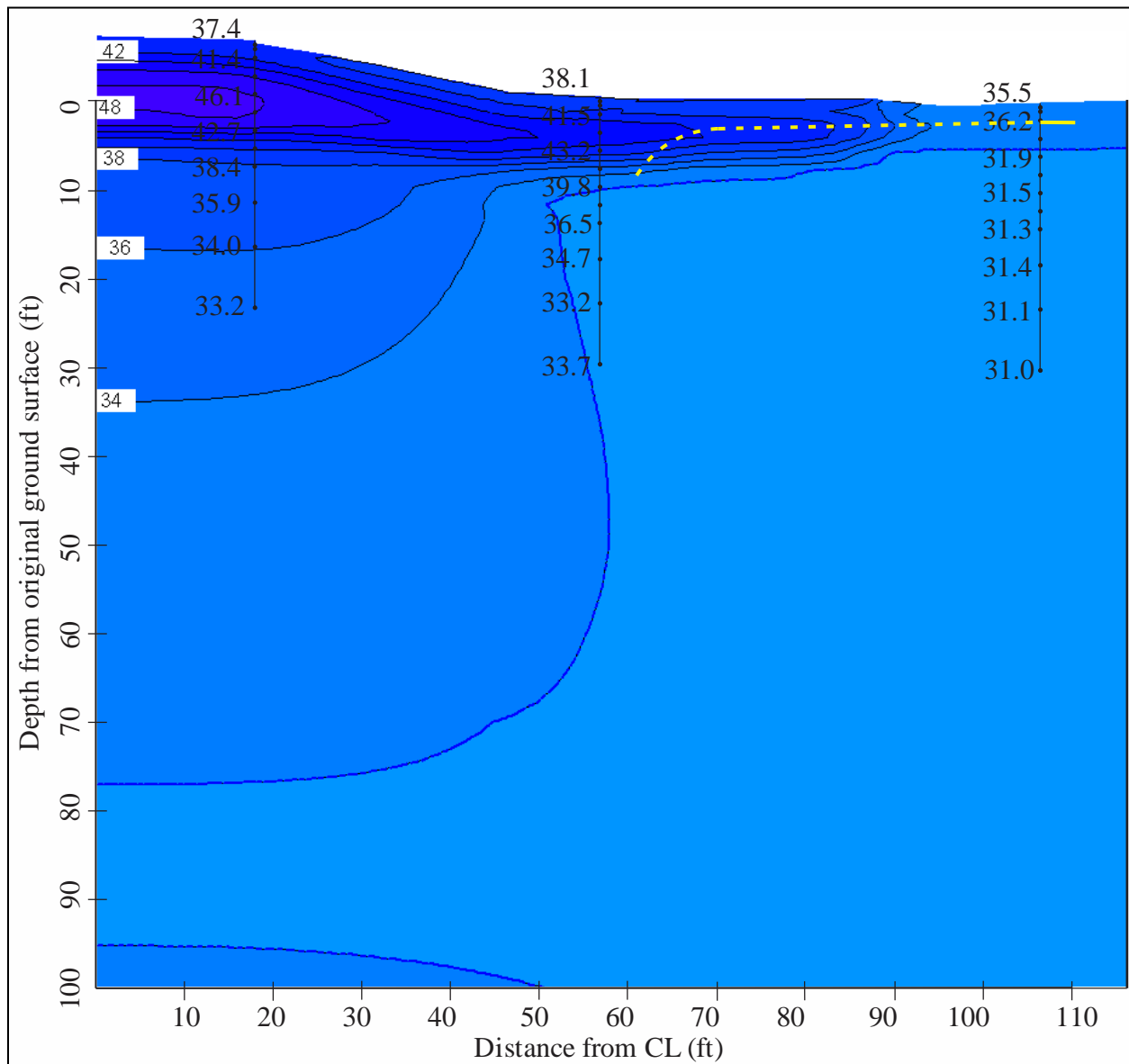
Figure 5.26. Thermal modeling results for October 1ˢᵗ, Run 4, Richardson Highway MP 113 research site. The phase change isotherm is represented as the dashed blue line and the temperature results are shown with a 2°F contour interval. Some of the measured temperatures along each thermistor string are shown in black text superimposed on the contours. The phase change isotherm approximated from the measured data is shown as a yellow dashed line.
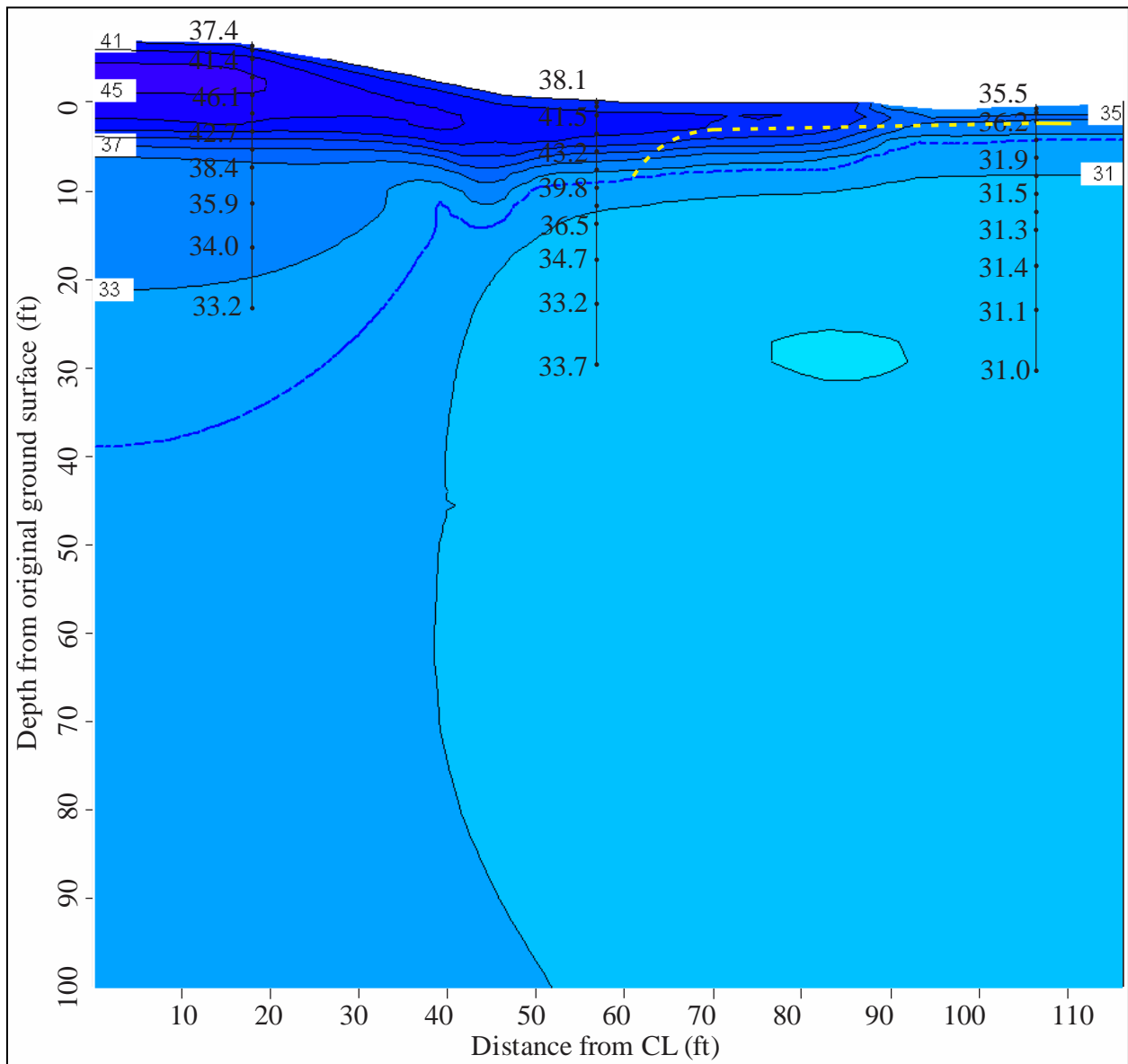
85
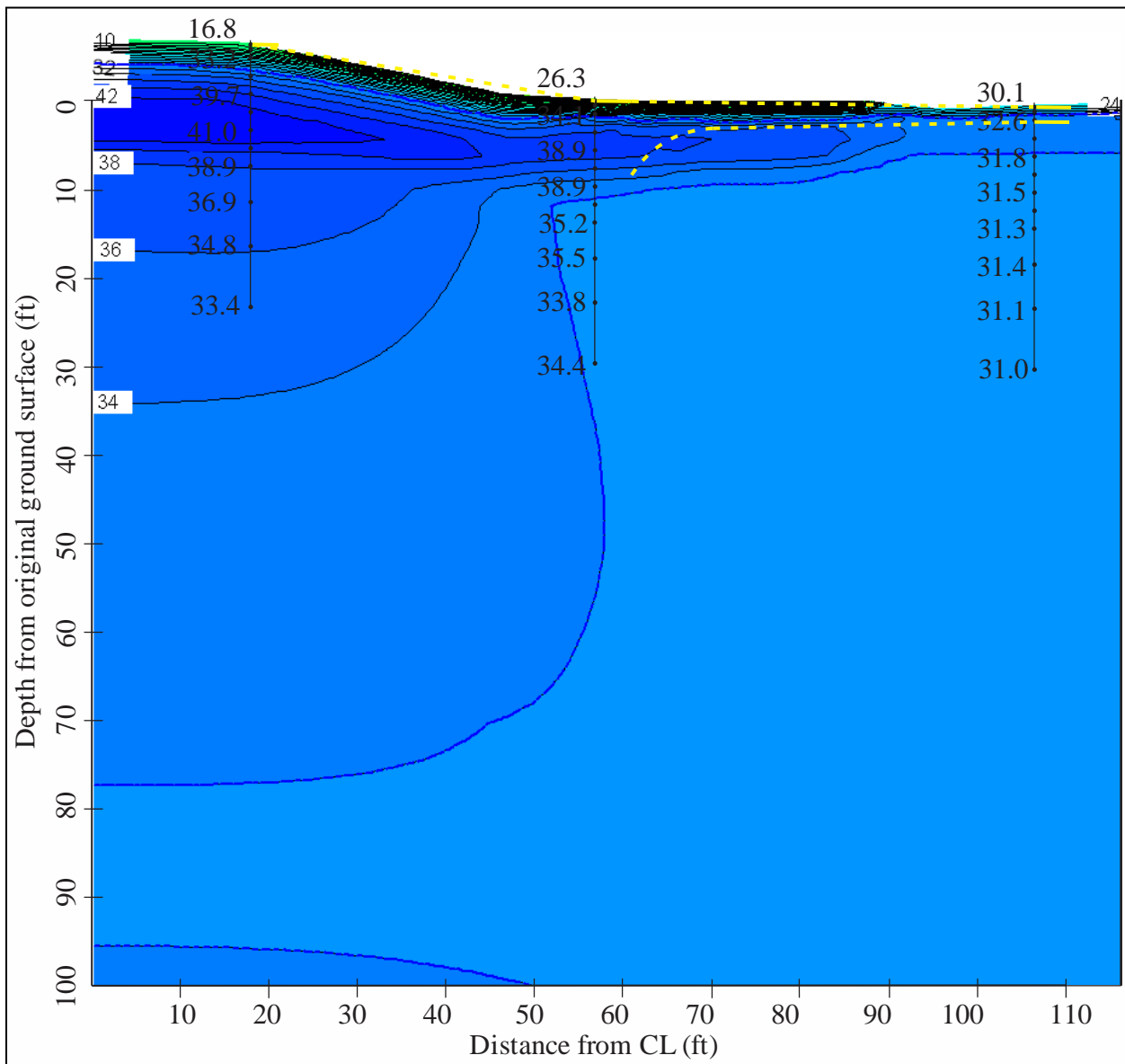
Figure 5.27. Thermal modeling results for November 1st, Run 4, Richardson Highway MP 113 research site. The phase change isotherm is represented as the dashed blue line and the temperature results are shown with a 2°F contour interval. Some of the measured temperatures along each thermistor string are shown in black text superimposed on the contours. The phase change isotherm approximated from the measured data is shown as a yellow dashed line.
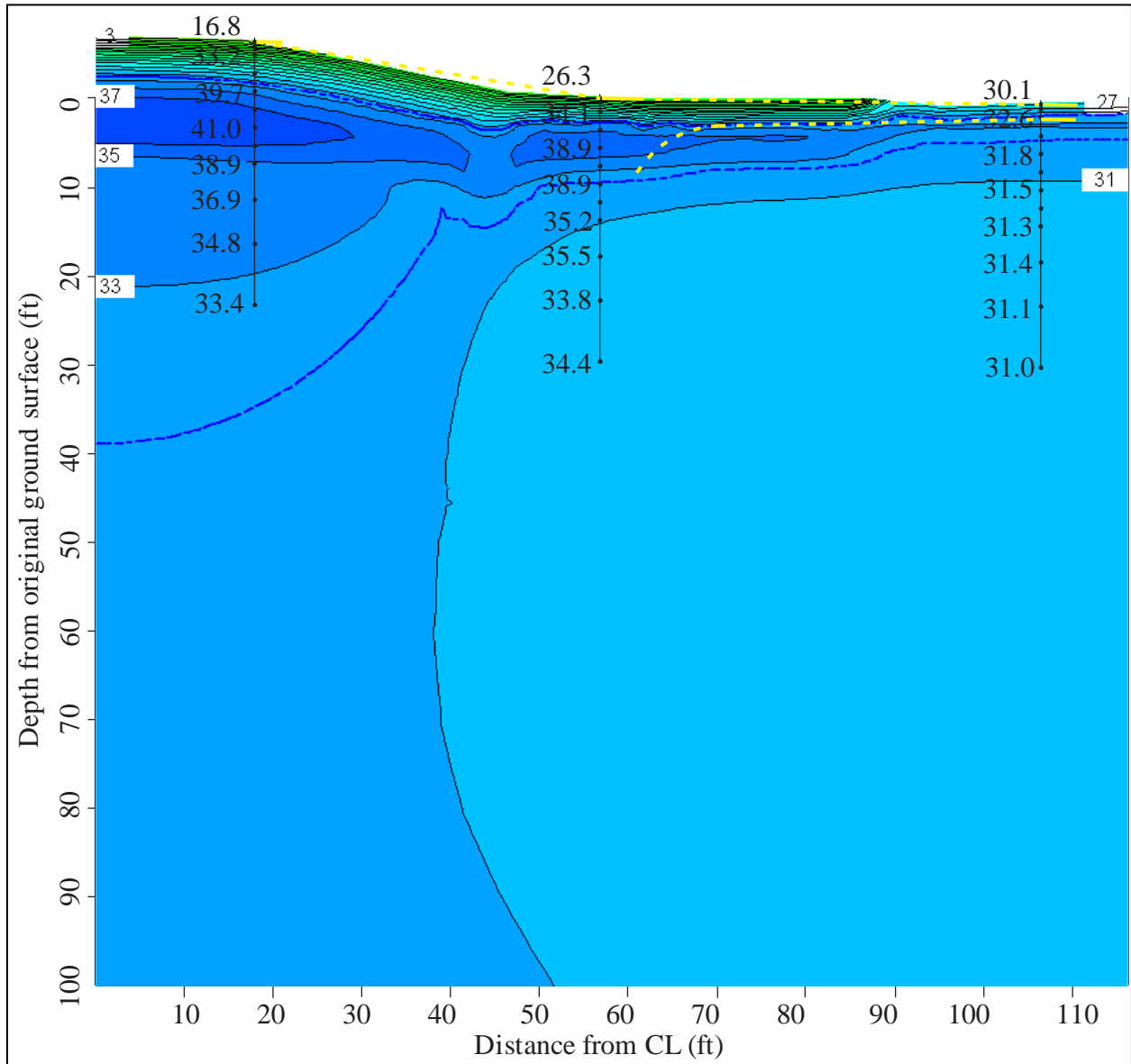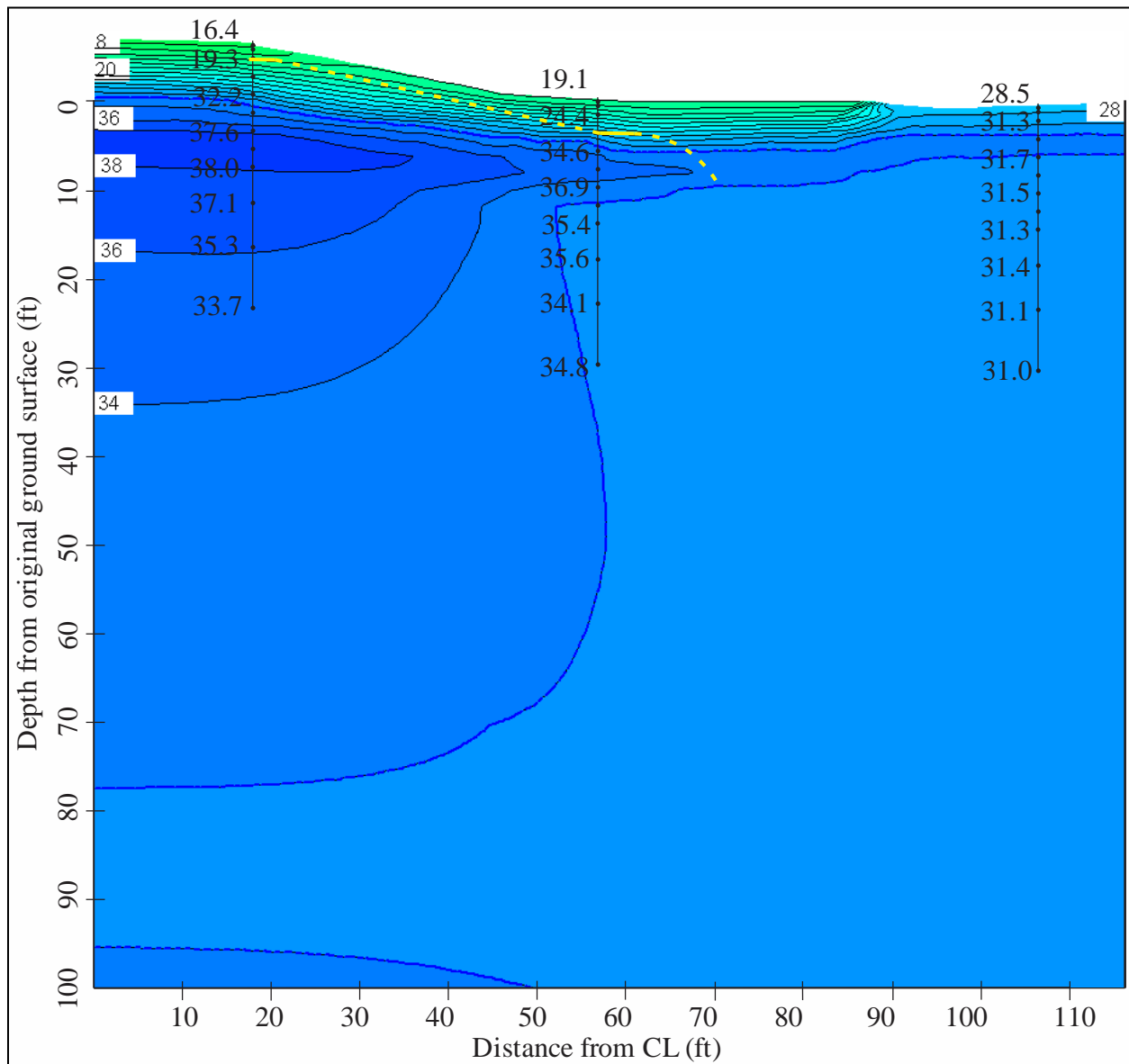
Figure 5.28. Thermal modeling results for December 1st, Run 4, Richardson Highway MP 113 research site. The phase change isotherm is represented as the dashed blue line and the temperature results are shown with a 2°F contour interval. Some of the measured temperatures along each thermistor string are shown in black text superimposed on the contours. The phase change isotherm approximated from the measured data is shown as a yellow dashed line.
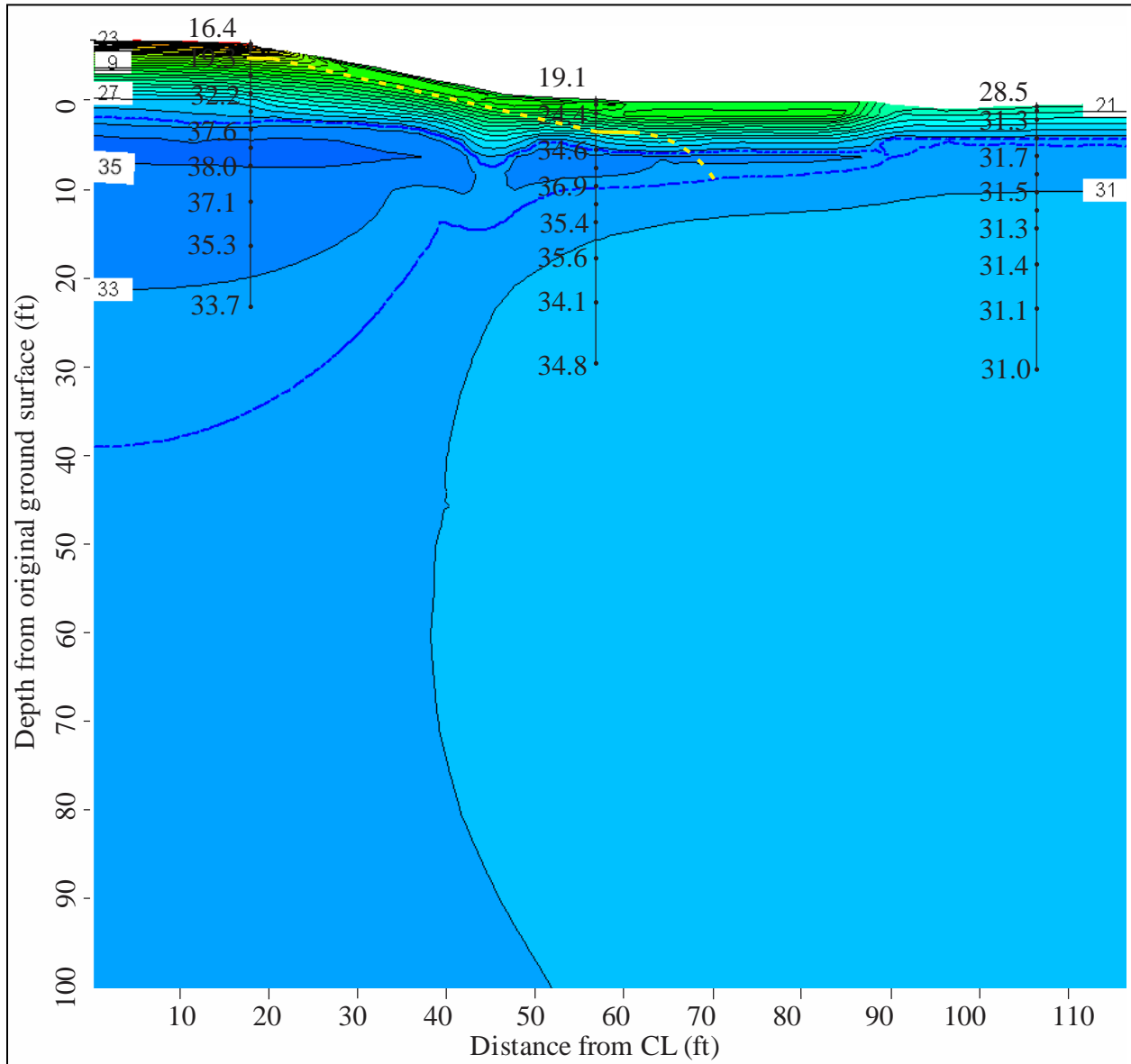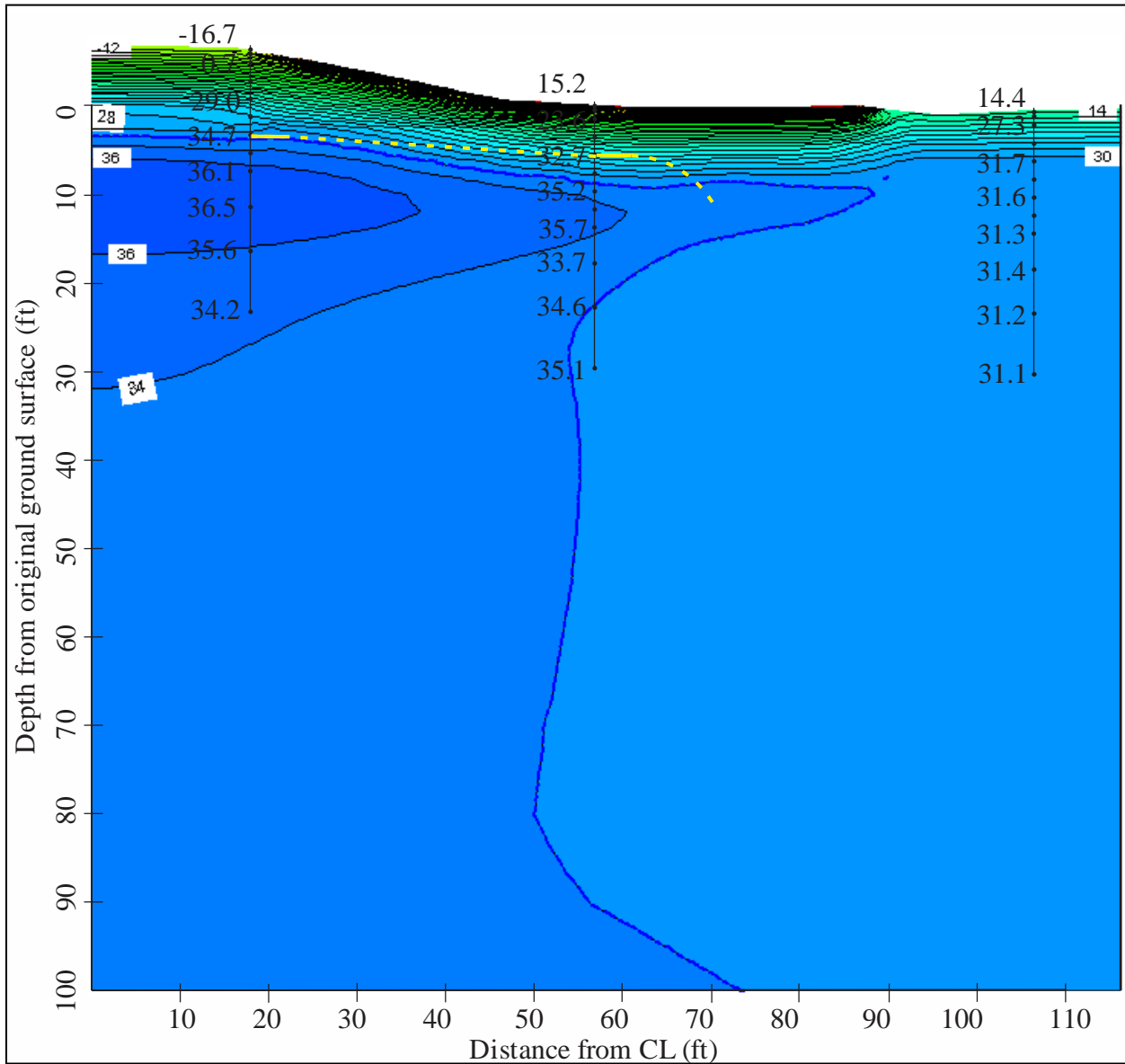
Figure 5.29. Thermal modeling results for January 1st, Run 5, Richardson Highway MP 113 research site. The phase change isotherm is represented as the dashed blue line and the temperature results are shown with a 2°F contour interval. Some of the measured temperatures along each thermistor string are shown in black text superimposed on the contours. The phase change isotherm approximated from the measured data is shown as a yellow dashed line.
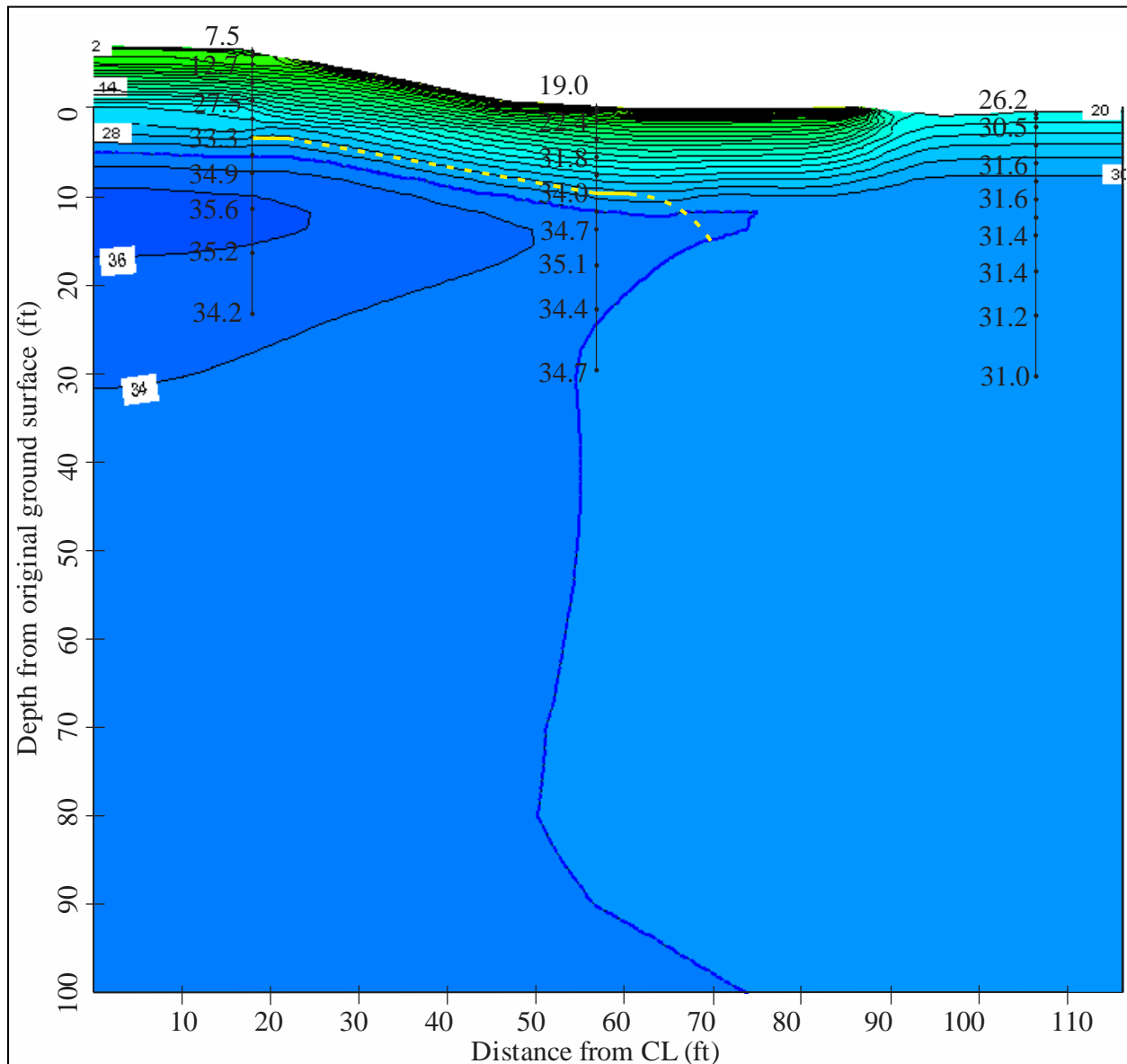
Figure 5.30. Thermal modeling results for February 1st, Run 5, Richardson Highway MP 113 research site. The phase change isotherm is represented as the dashed blue line and the temperature results are shown with a 2°F contour interval. Some of the measured temperatures along each thermistor string are shown in black text superimposed on the contours. The phase change isotherm approximated from the measured data is shown as a yellow dashed line.
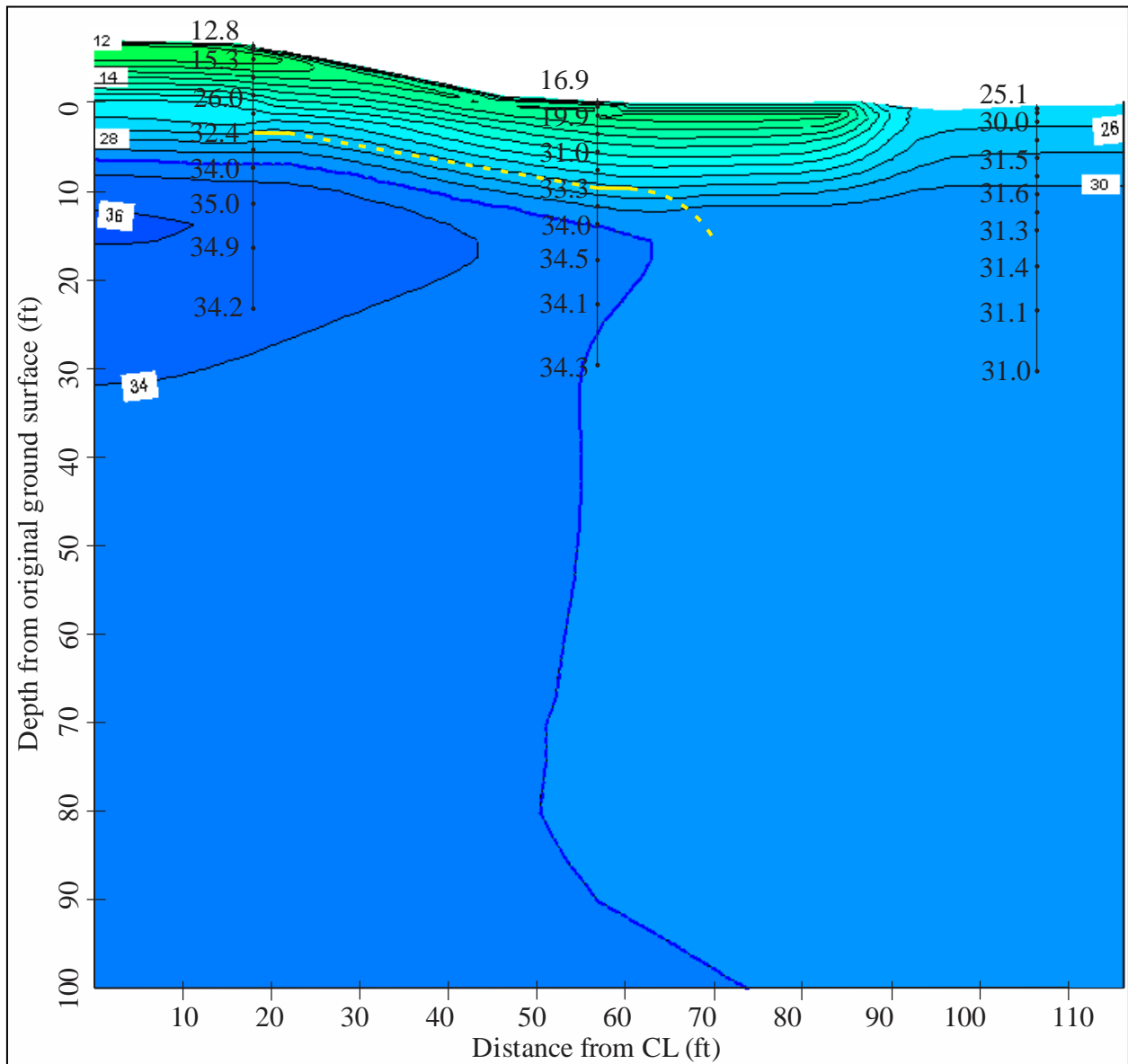
Figure 5.31. Thermal modeling results for March 1st, Run 5, Richardson Highway MP 113 research site. The phase change isotherm is represented as the dashed blue line and the temperature results are shown with a 2°F contour interval. Some of the measured temperatures along each thermistor string are shown in black text superimposed on the contours. The phase change isotherm approximated from the measured data is shown as a yellow dashed line.
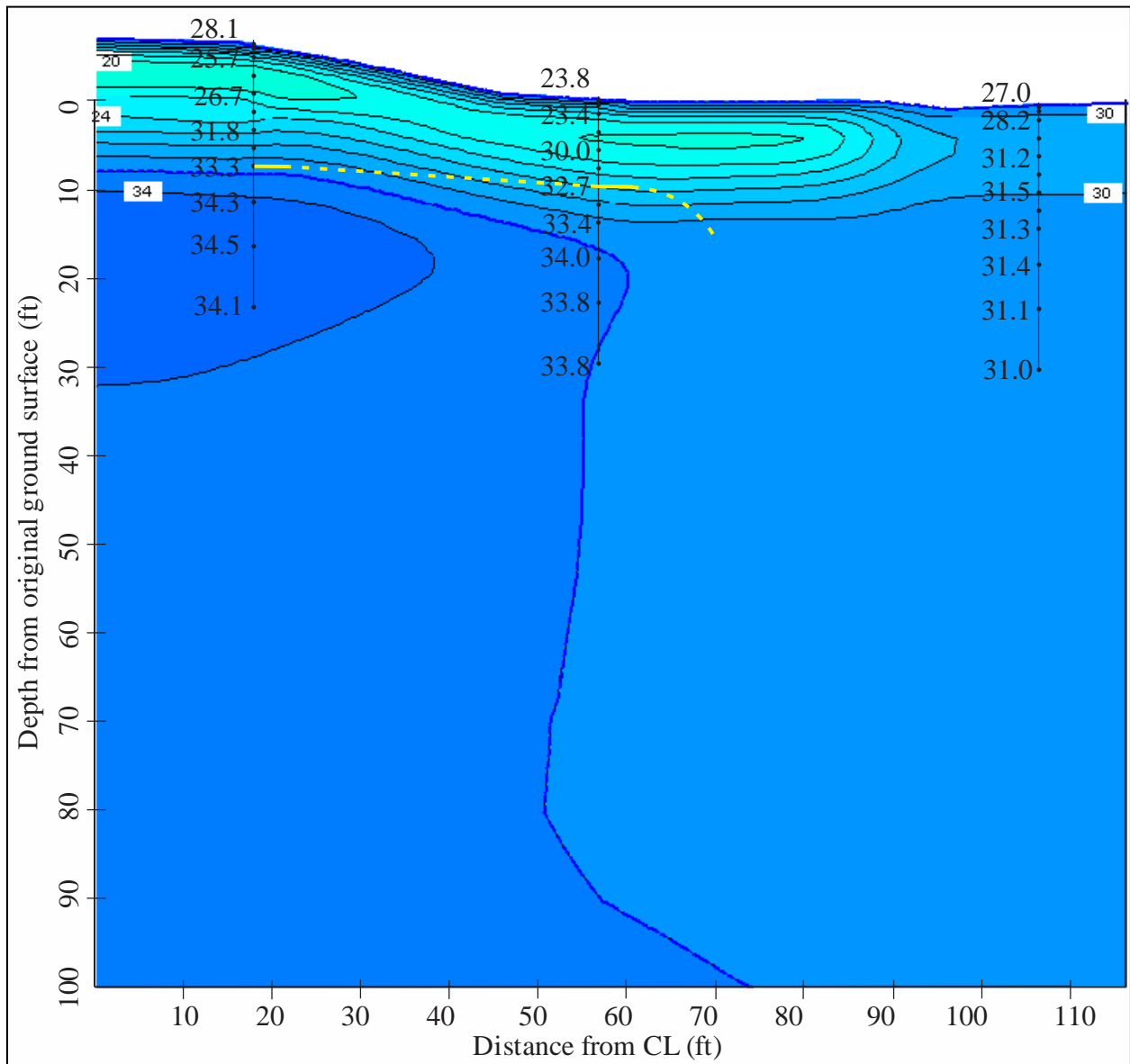
Figure 5.32. Thermal modeling results for April 1st, Run 5, Richardson Highway MP 113 research site. The phase change isotherm is represented as the dashed blue line and the temperature results are shown with a 2°F contour interval. Some of the measured temperatures along each thermistor string are shown in black text superimposed on the contours. The phase change isotherm approximated from the measured data is shown as a yellow dashed line.

Figure 5.33. Thermal modeling results for May 1st, Run 5, Richardson Highway MP 113 research site. The phase change isotherm is represented as the dashed blue line and the temperature results are shown with a 2°F contour interval. Some of the measured temperatures along each thermistor string are shown in black text superimposed on the contours. The phase change isotherm approximated from the measured data is shown as a yellow dashed line.

Figure 5.34. Thermal modeling results for June 1st, Run 5, Richardson Highway MP 113 research site. The phase change isotherm is represented as the dashed blue line and the temperature results are shown with a 2°F contour interval. Some of the measured temperatures along each thermistor string are shown in black text superimposed on the contours. The phase change isotherm approximated from the measured data is shown as a yellow dashed line.

Figure 5.35. Thermal modeling results for July 1st, Run 5, Richardson Highway MP 113 research site. The phase change isotherm is represented as the dashed blue line and the temperature results are shown with a 2°F contour interval. Some of the measured temperatures along each thermistor string are shown in black text superimposed on the contours. The phase change isotherm approximated from the measured data is shown as a yellow dashed line.

94
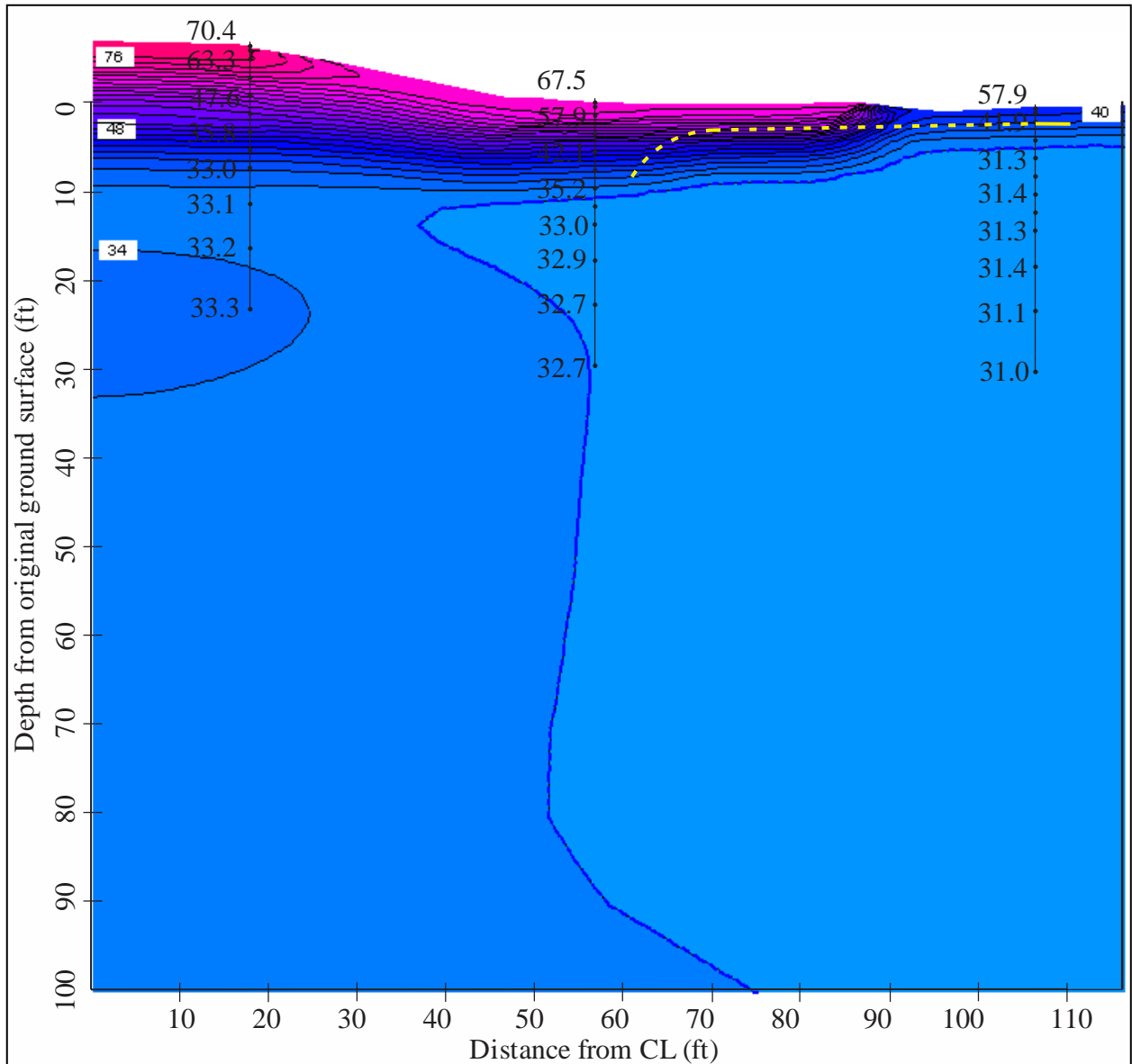
Figure 5.36. Thermal modeling results for August 1st, Run 5, Richardson Highway MP 113 research site. The phase change isotherm is represented as the dashed blue line and the temperature results are shown with a 2°F contour interval. Some of the measured temperatures along each thermistor string are shown in black text superimposed on the contours. The phase change isotherm approximated from the measured data is shown as a yellow dashed line.

Figure 5.37. Thermal modeling results for September 1st, Run 5, Richardson Highway MP 113 research site. The phase change isotherm is represented as the dashed blue line and the temperature results are shown with a 2°F contour interval. Some of the measured temperatures along each thermistor string are shown in black text superimposed on the contours. The phase change isotherm approximated from the measured data is shown as a yellow dashed line.

Figure 5.38. Thermal modeling results for October 1st, Run 5, Richardson Highway MP 113 research site. The phase change isotherm is represented as the dashed blue line and the temperature results are shown with a 2°F contour interval. Some of the measured temperatures along each thermistor string are shown in black text superimposed on the contours. The phase change isotherm approximated from the measured data is shown as a yellow dashed line.

97

Figure 5.39. Thermal modeling results for November 1st, Run 5, Richardson Highway MP 113 research site. The phase change isotherm is represented as the dashed blue line and the temperature results are shown with a 2°F contour interval. Some of the measured temperatures along each thermistor string are shown in black text superimposed on the contours. The phase change isotherm approximated from the measured data is shown as a yellow dashed line.

98

Figure 5.40. Thermal modeling results for December 1st, Run 5, Richardson Highway MP 113 research site. The phase change isotherm is represented as the dashed blue line and the temperature results are shown with a 2°F contour interval. Some of the measured temperatures along each thermistor string are shown in black text superimposed on the contours. The phase change isotherm approximated from the measured data is shown as a yellow dashed line.

Generally, the results from Run 5 are a better fit to the measured temperatures than Run 4 by about 0.5°F. The most notable difference between these two model iterations is the shape of the thaw bulb. While the upper surface changes little between the two iterations, the bottom thaw bulb boundary progresses beyond the mesh extent in Run 5. Also, the thaw bulb progresses farther away from the highway centerline to include the position of the thermistor string at the toe. Overall, Run 5 is a better fit to the measured data, although differences still remain.

For the final model iteration (i.e., Run 6), the *n*-factors were adjusted to see what effect this had on the modeled temperatures and phase change isotherm depths. While in all preceding model iterations an estimated input parameter was replaced with that either measured at the site or from soils obtained at the site, this model iteration is the first where an estimated parameter was replaced with another estimated parameter in an effort to fine-tune the model. The adjusted *n*-factors used in Run 6 are listed in Table 5.7. These values were chosen based on analysis of the surface temperatures in the previous model results. With the exception of the adjusted *n*-factors, Run 6 was similar to Run 5. The model results are presented in Figures 5.41 through 5.52. The measured and modeled temperatures for each of the selected depths were compared, and these comparisons are tabulated in Appendix E. Additionally, Table 5.6 contains a summary of the phase change isotherm depths for this model iteration.

Table 5.7. Adjusted *n*-factors used in Run 6, Richardson Highway MP 113 research site

Surface	Original *n*-factors		Adjusted *n*-factors	
	n_t	n_f	n_t	n_f
Asphalt	1.8	0.9	1.4	0.8
Gravel slope/disturbed gravel surface	1.5	0.6	1.0	0.3
Spruce forest	0.37	0.29	0.45	0.2

For the shoulder location, the modeled temperatures from Run 6 are a better fit to the measured temperatures. At 30 ft, the modeled temperatures are 0.5°F colder on average than the measured temperatures, and on average the modeled temperatures between 10 and 30 ft are 0.6°F colder than the measured temperatures. Although the deviation in near-surface temperatures between those measured and modeled continues to exist, the magnitude of this deviation is less in Run 6.

For the toe location, the modeled temperatures in Run 6 generally are colder than those of Run 5. At 30 ft, the modeled temperatures are 2.3°F colder on average than the measured temperatures, and on average the modeled temperatures between 10 and 30 ft are 2.5°F colder than the measured temperatures. As with the shoulder location, the deviation in near-surface temperatures between measured and modeled is reduced in Run 6.

For the undisturbed location, there is excellent agreement between the measured and modeled temperatures below 10 ft, differing by less than 0.4°F on average. At the surface, the measured and modeled temperatures are within 3°F of each other on average.

Table 5.6 contains a summary of the modeled phase change isotherm depths for Run 6. This data indicates that the active layer depth in the embankment (i.e., maximum depth of freeze) is approximately 18 ft in July, which is deeper than that measured by 6 ft. The active
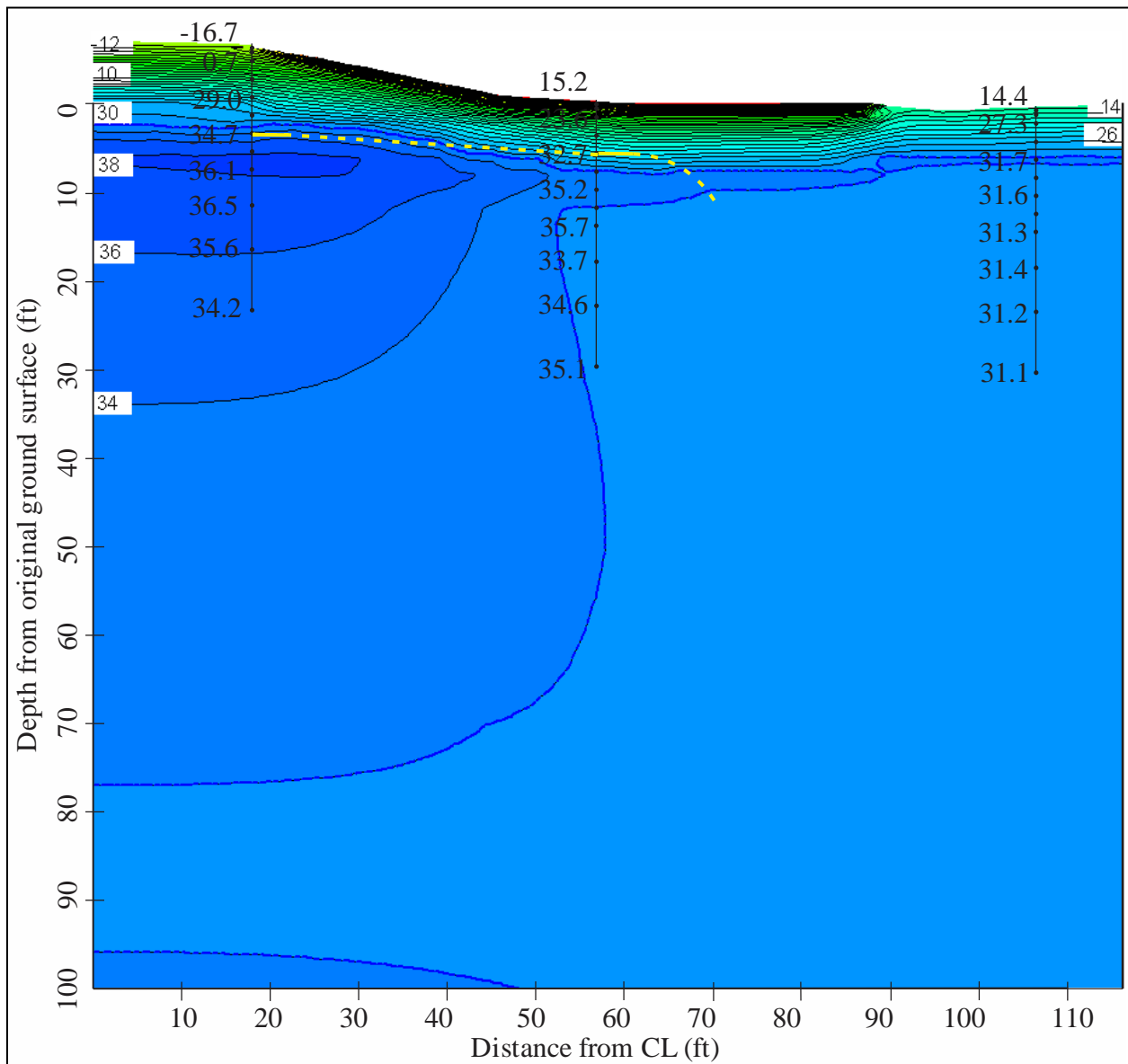
Figure 5.41. Thermal modeling results for January 1st, Run 6, Richardson Highway MP 113 research site. The phase change isotherm is represented as the dashed blue line and the temperature results are shown with a 2°F contour interval. Some of the measured temperatures along each thermistor string are shown in black text superimposed on the contours. The phase change isotherm approximated from the measured data is shown as a yellow dashed line.
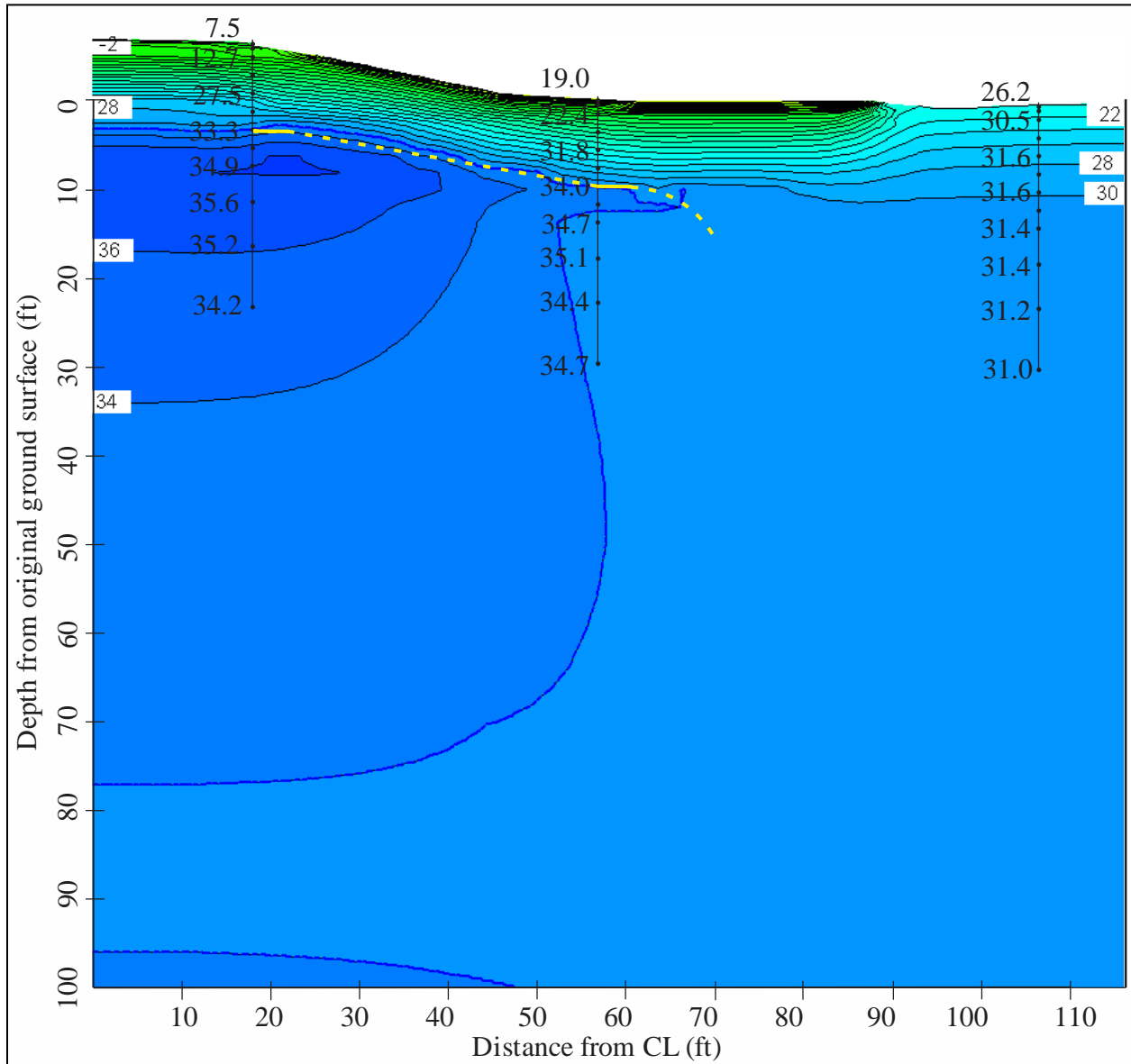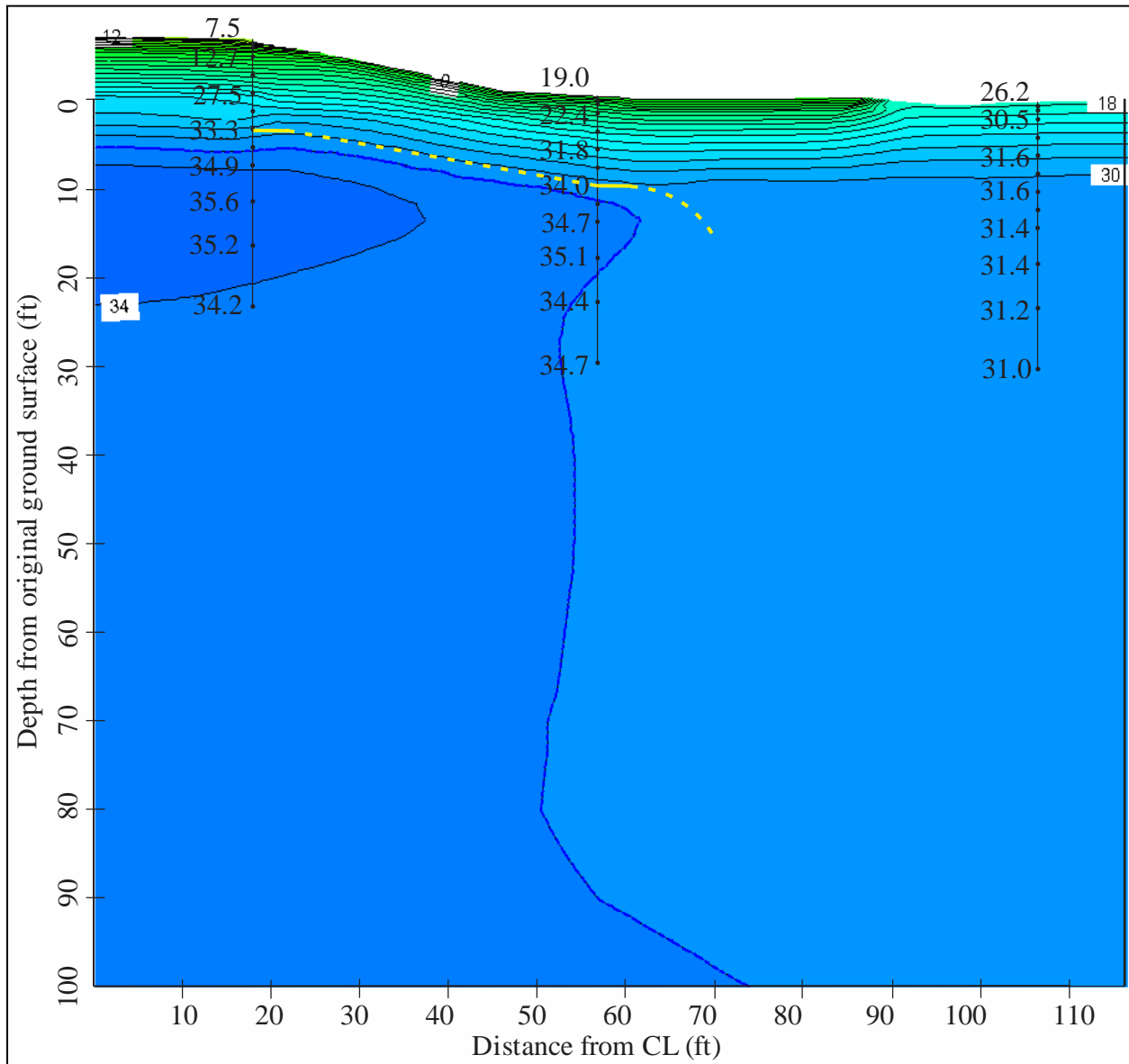
Figure 5.42. Thermal modeling results for February 1st, Run 6, Richardson Highway MP 113 research site. The phase change isotherm is represented as the dashed blue line and the temperature results are shown with a 2°F contour interval. Some of the measured temperatures along each thermistor string are shown in black text superimposed on the contours. The phase change isotherm approximated from the measured data is shown as a yellow dashed line.
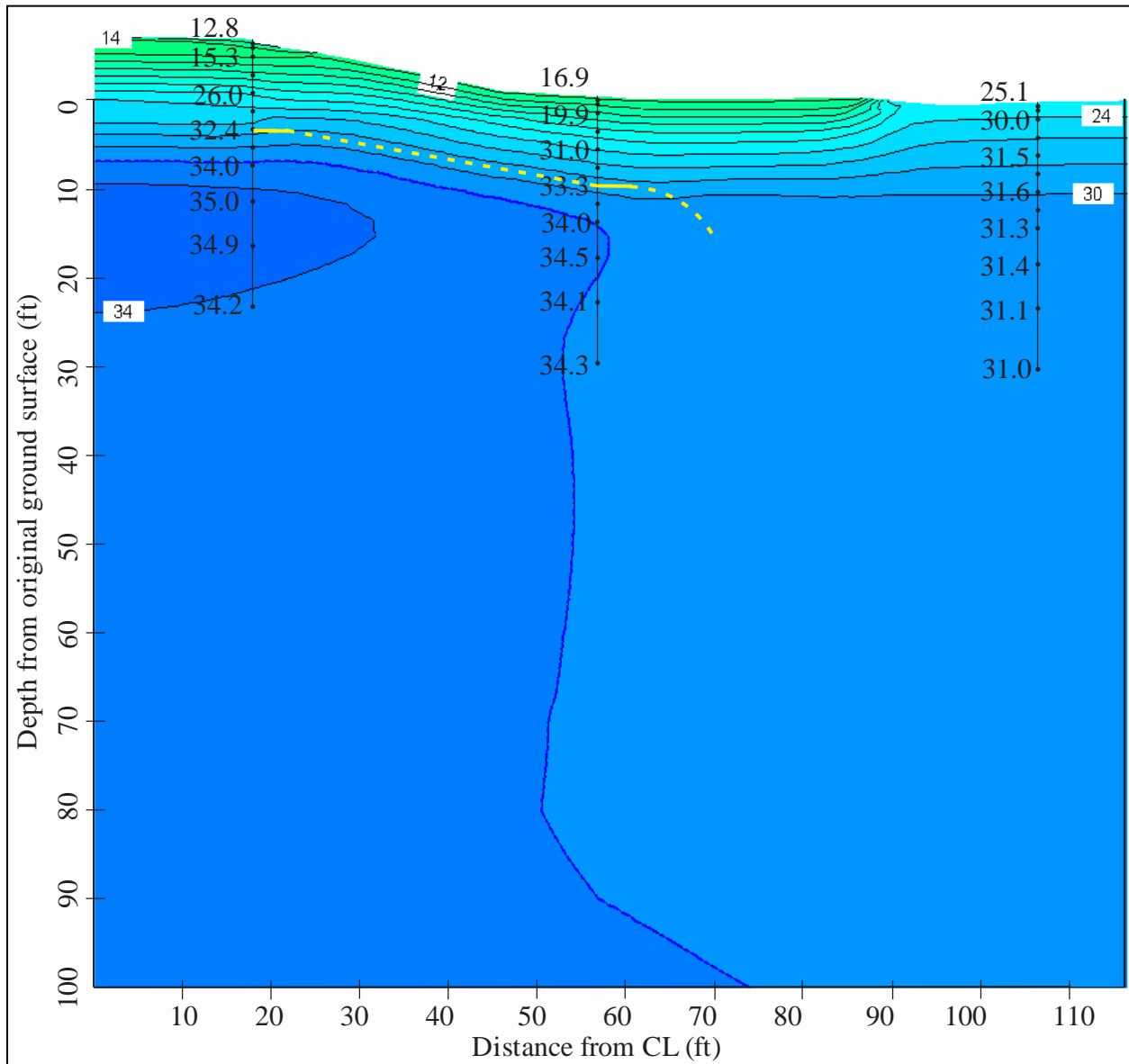
Figure 5.43. Thermal modeling results for March 1st, Run 6, Richardson Highway MP 113 research site. The phase change isotherm is represented as the dashed blue line and the temperature results are shown with a 2°F contour interval. Some of the measured temperatures along each thermistor string are shown in black text superimposed on the contours. The phase change isotherm approximated from the measured data is shown as a yellow dashed line.
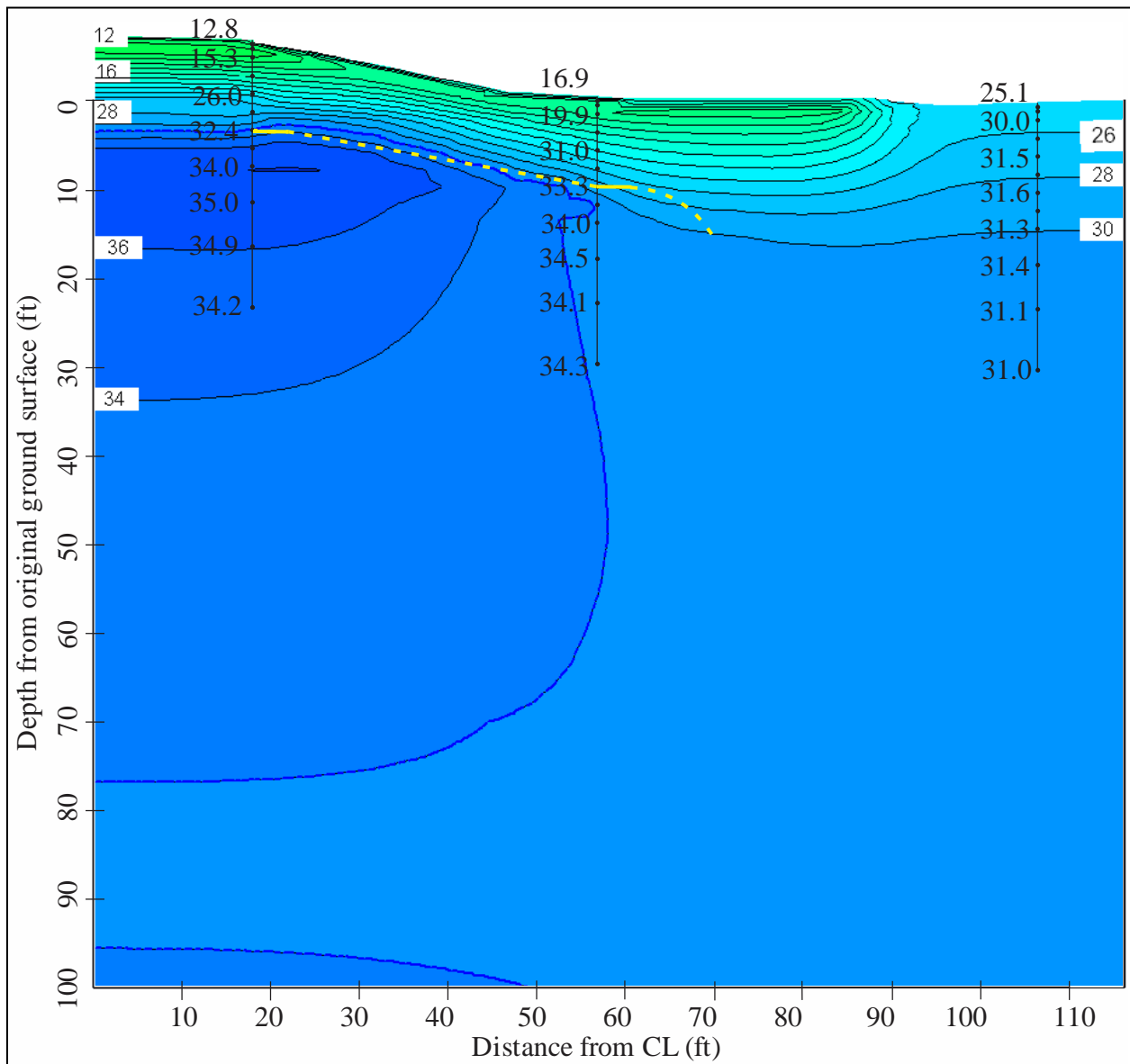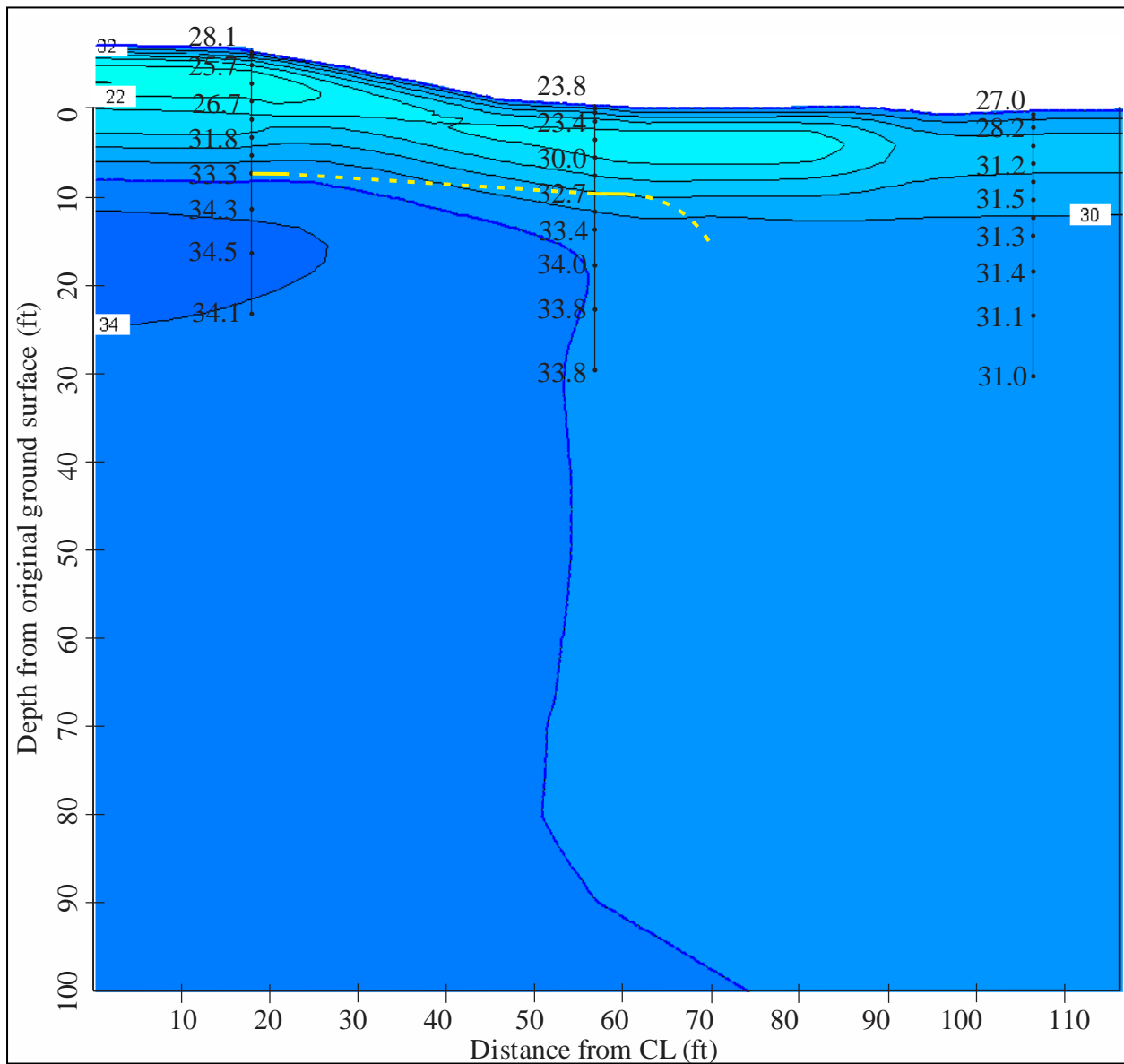
Figure 5.44. Thermal modeling results for April 1ˢᵗ, Run 6, Richardson Highway MP 113 research site. The phase change isotherm is represented as the dashed blue line and the temperature results are shown with a 2°F contour interval. Some of the measured temperatures along each thermistor string are shown in black text superimposed on the contours. The phase change isotherm approximated from the measured data is shown as a yellow dashed line.
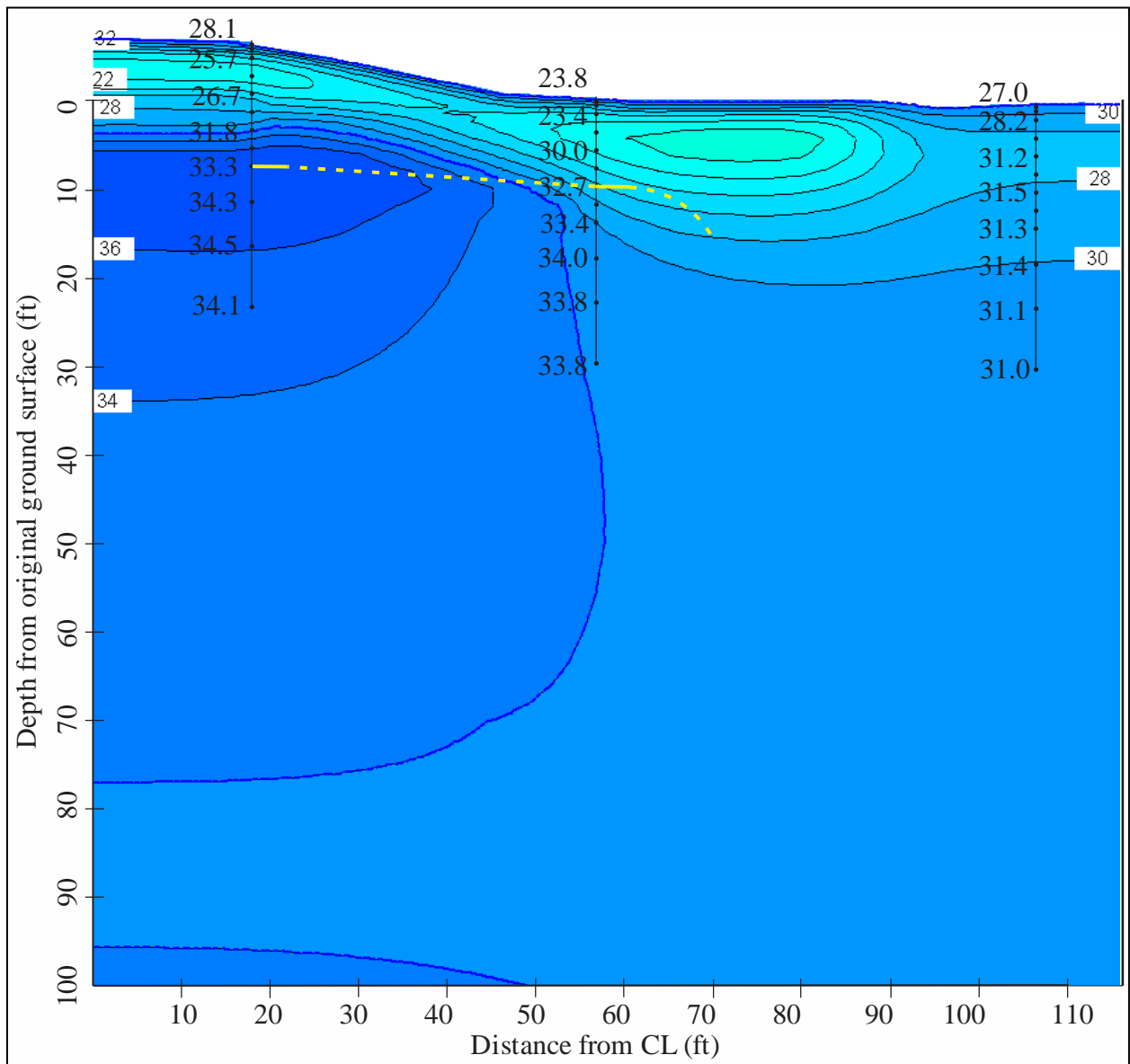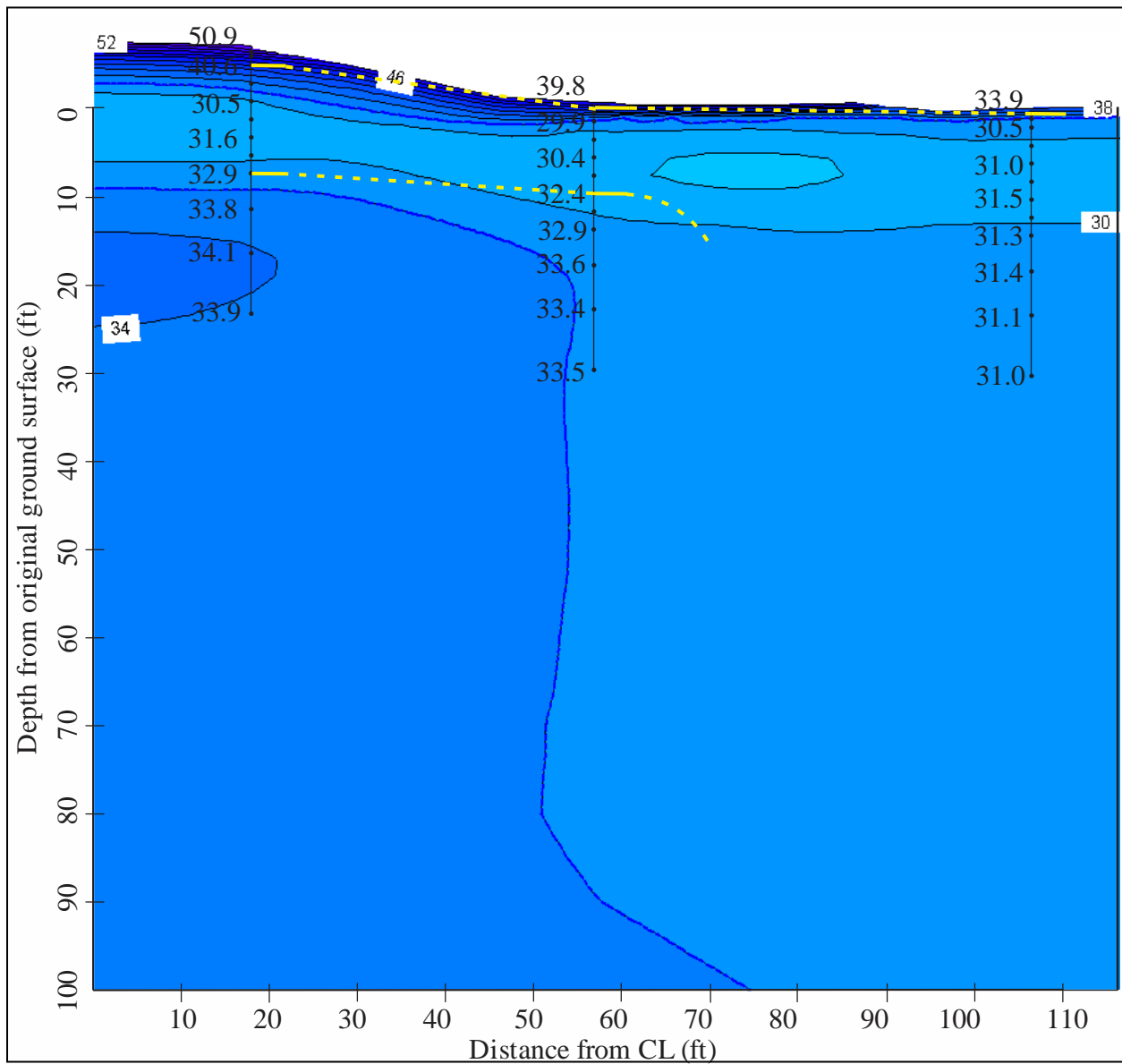
Figure 5.45. Thermal modeling results for May 1st, Run 6, Richardson Highway MP 113 research site. The phase change isotherm is represented as the dashed blue line and the temperature results are shown with a 2°F contour interval. Some of the measured temperatures along each thermistor string are shown in black text superimposed on the contours. The phase change isotherm approximated from the measured data is shown as a yellow dashed line.
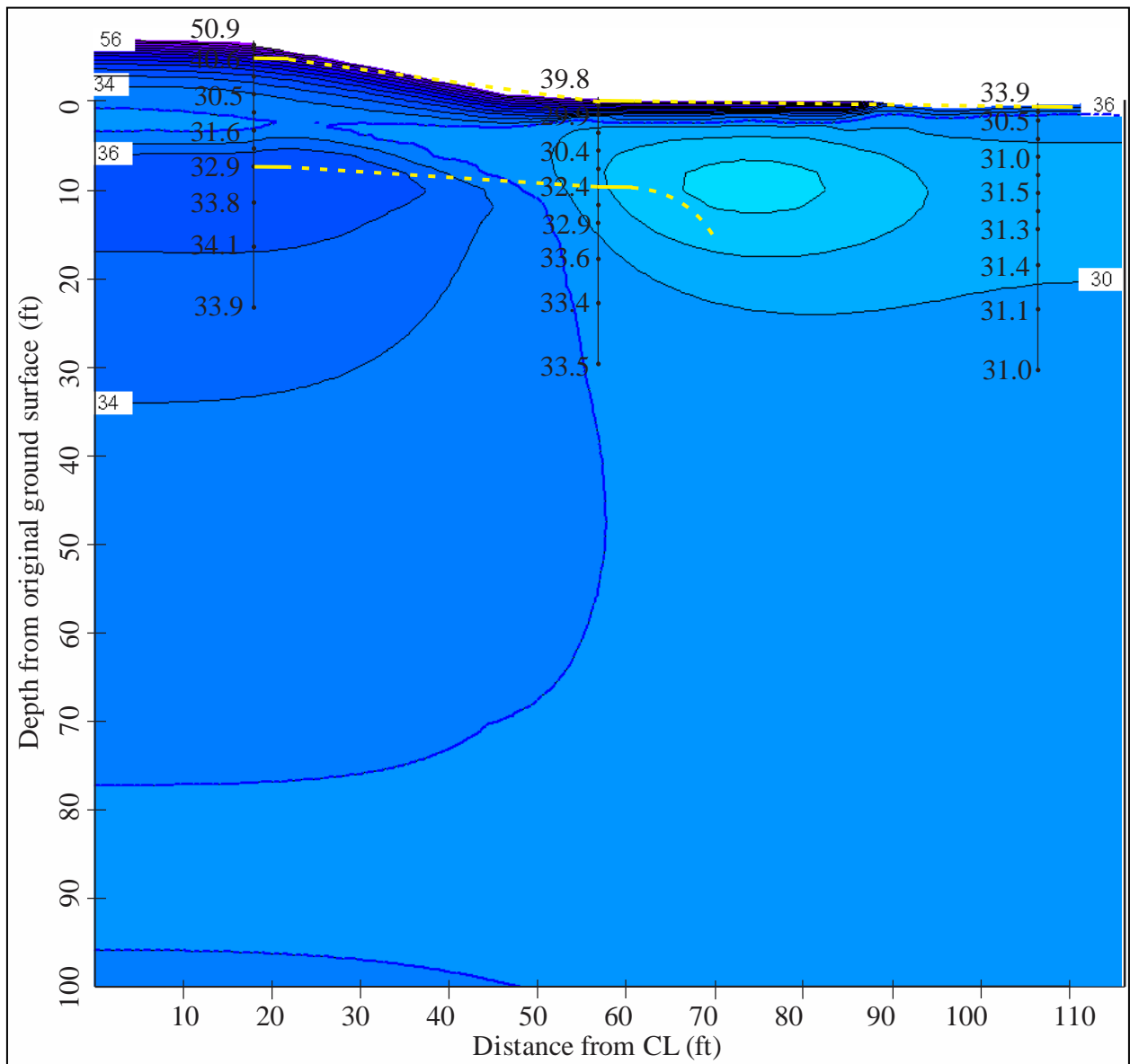
Figure 5.46. Thermal modeling results for June 1st, Run 6, Richardson Highway MP 113 research site. The phase change isotherm is represented as the dashed blue line and the temperature results are shown with a 2°F contour interval. Some of the measured temperatures along each thermistor string are shown in black text superimposed on the contours. The phase change isotherm approximated from the measured data is shown as a yellow dashed line.
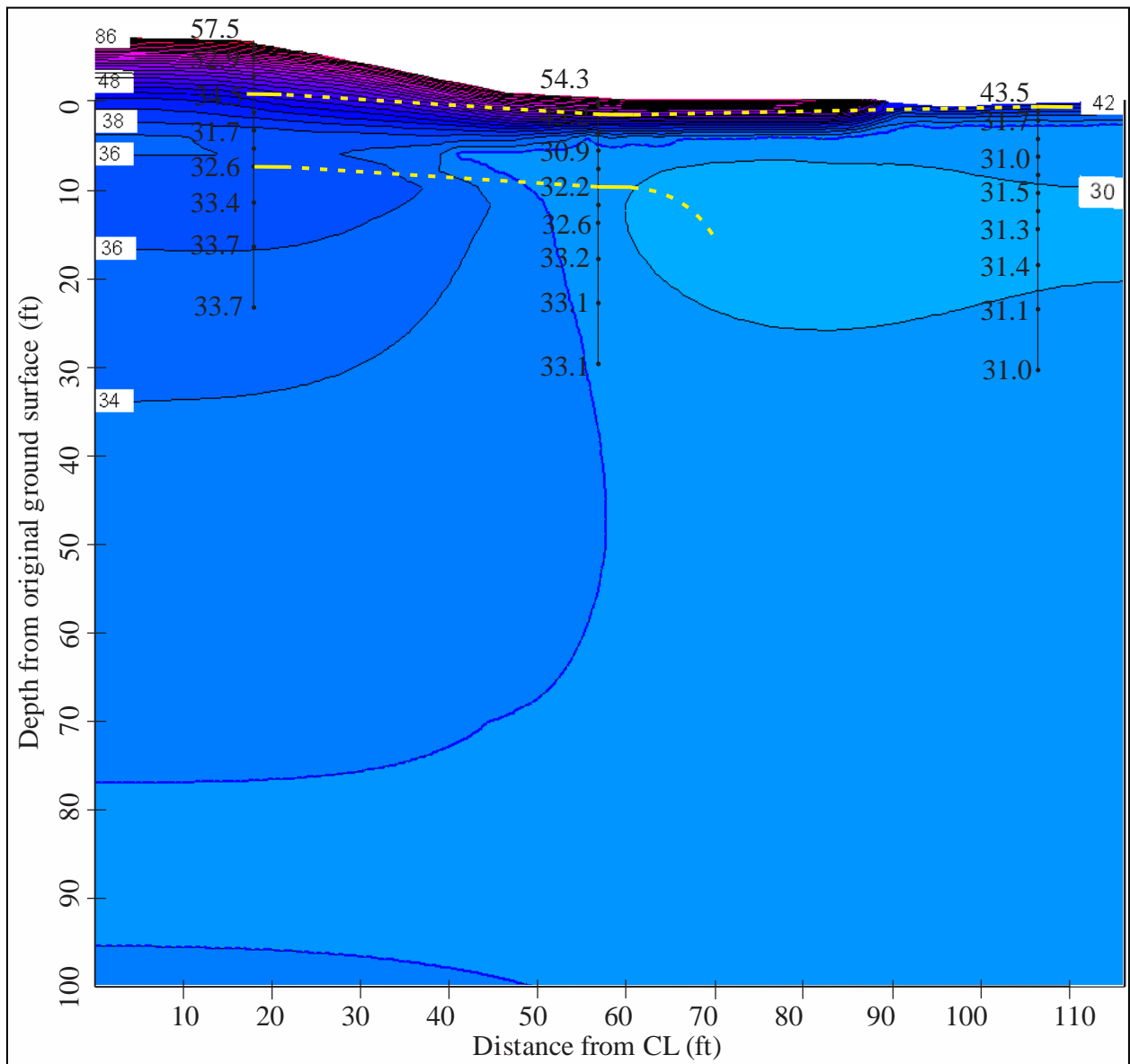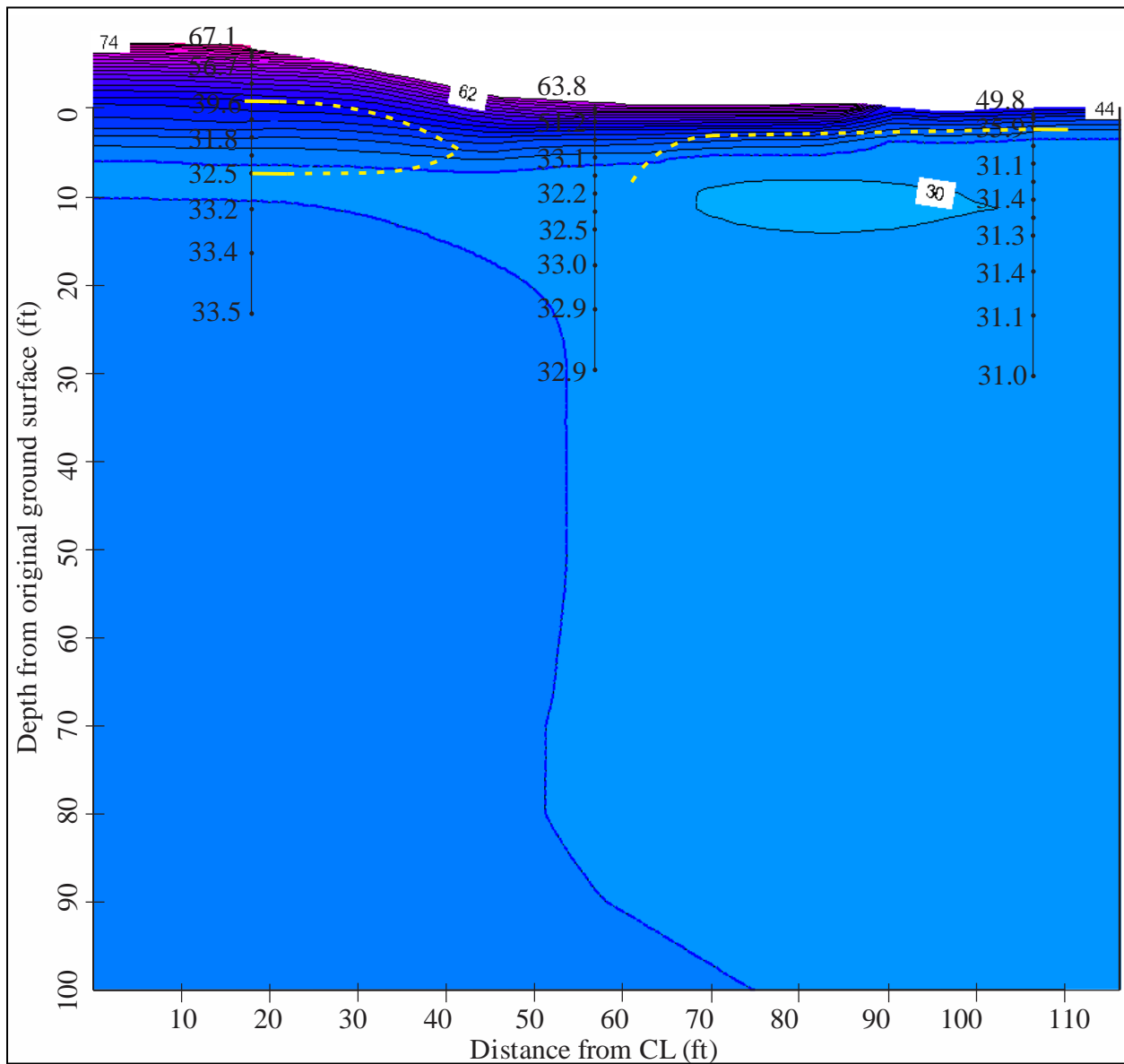
Figure 5.47. Thermal modeling results for July 1st, Run 6, Richardson Highway MP 113 research site. The phase change isotherm is represented as the dashed blue line and the temperature results are shown with a 2°F contour interval. Some of the measured temperatures along each thermistor string are shown in black text superimposed on the contours. The phase change isotherm approximated from the measured data is shown as a yellow dashed line.

Figure 5.48. Thermal modeling results for August 1st, Run 6, Richardson Highway MP 113 research site. The phase change isotherm is represented as the dashed blue line and the temperature results are shown with a 2°F contour interval. Some of the measured temperatures along each thermistor string are shown in black text superimposed on the contours. The phase change isotherm approximated from the measured data is shown as a yellow dashed line.
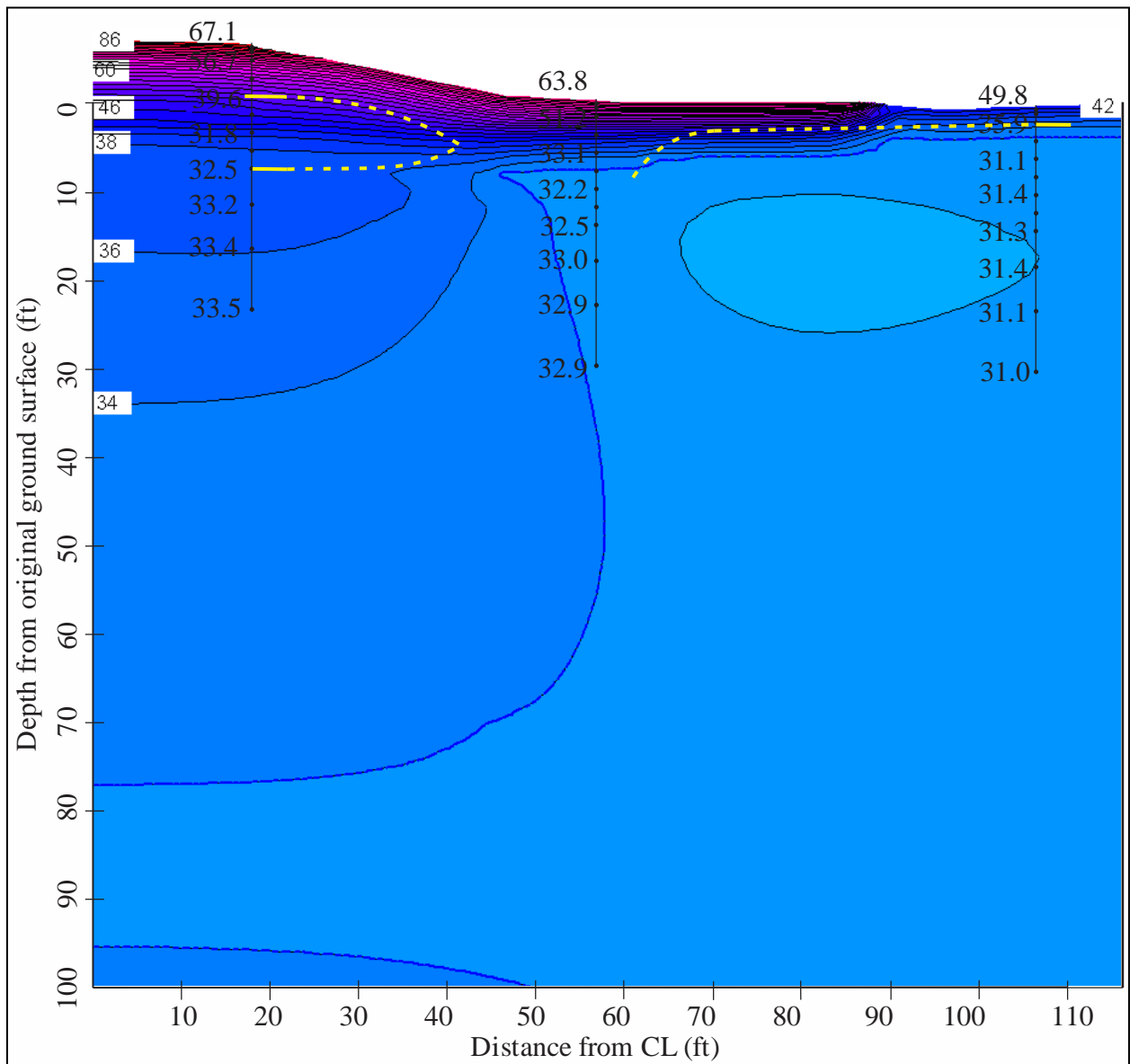
Figure 5.49. Thermal modeling results for September 1ˢᵗ, Run 6, Richardson Highway MP 113 research site. The phase change isotherm is represented as the dashed blue line and the temperature results are shown with a 2°F contour interval. Some of the measured temperatures along each thermistor string are shown in black text superimposed on the contours. The phase change isotherm approximated from the measured data is shown as a yellow dashed line.
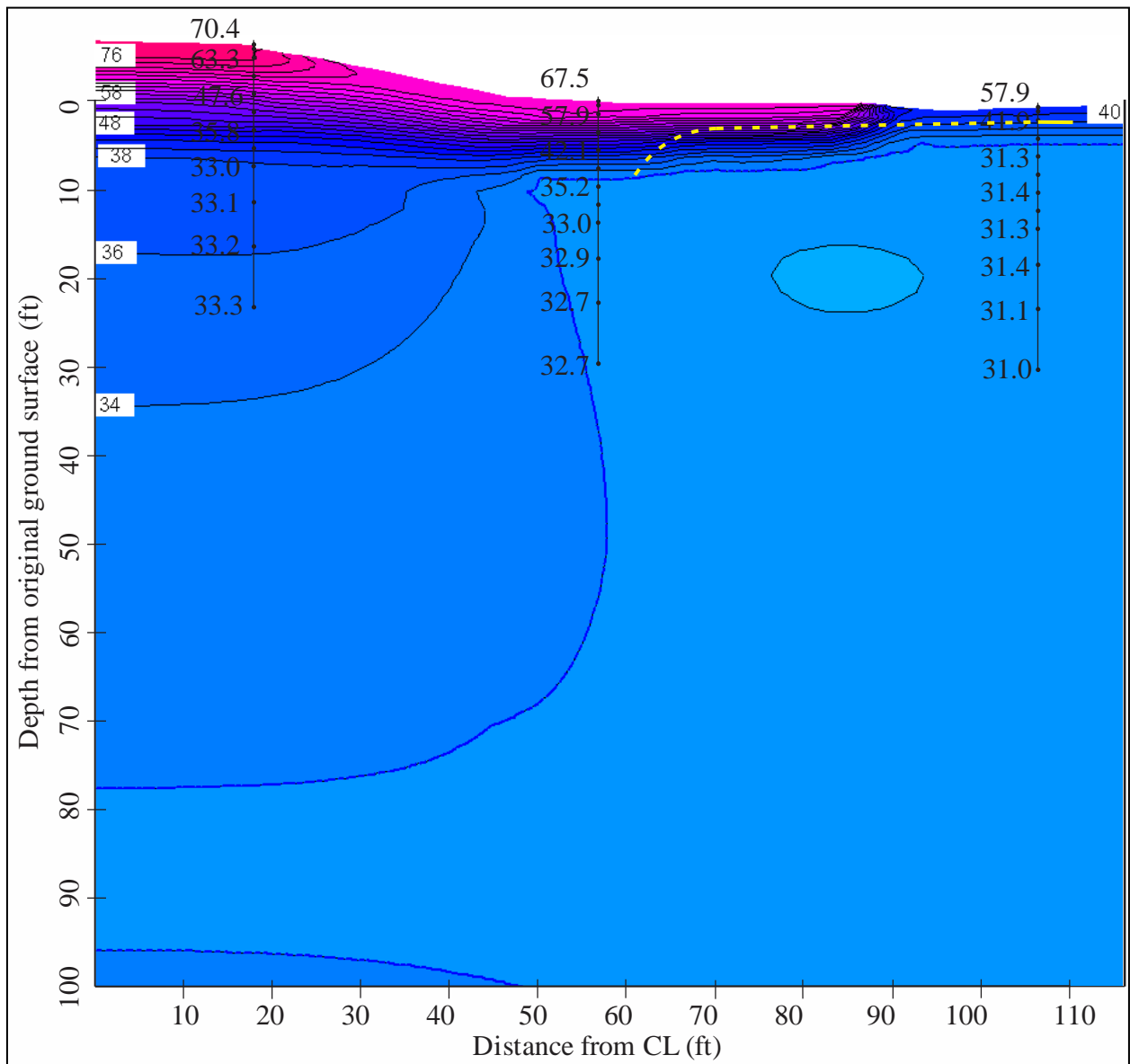
Figure 5.50. Thermal modeling results for October 1st, Run 6, Richardson Highway MP 113 research site. The phase change isotherm is represented as the dashed blue line and the temperature results are shown with a 2°F contour interval. Some of the measured temperatures along each thermistor string are shown in black text superimposed on the contours. The phase change isotherm approximated from the measured data is shown as a yellow dashed line.
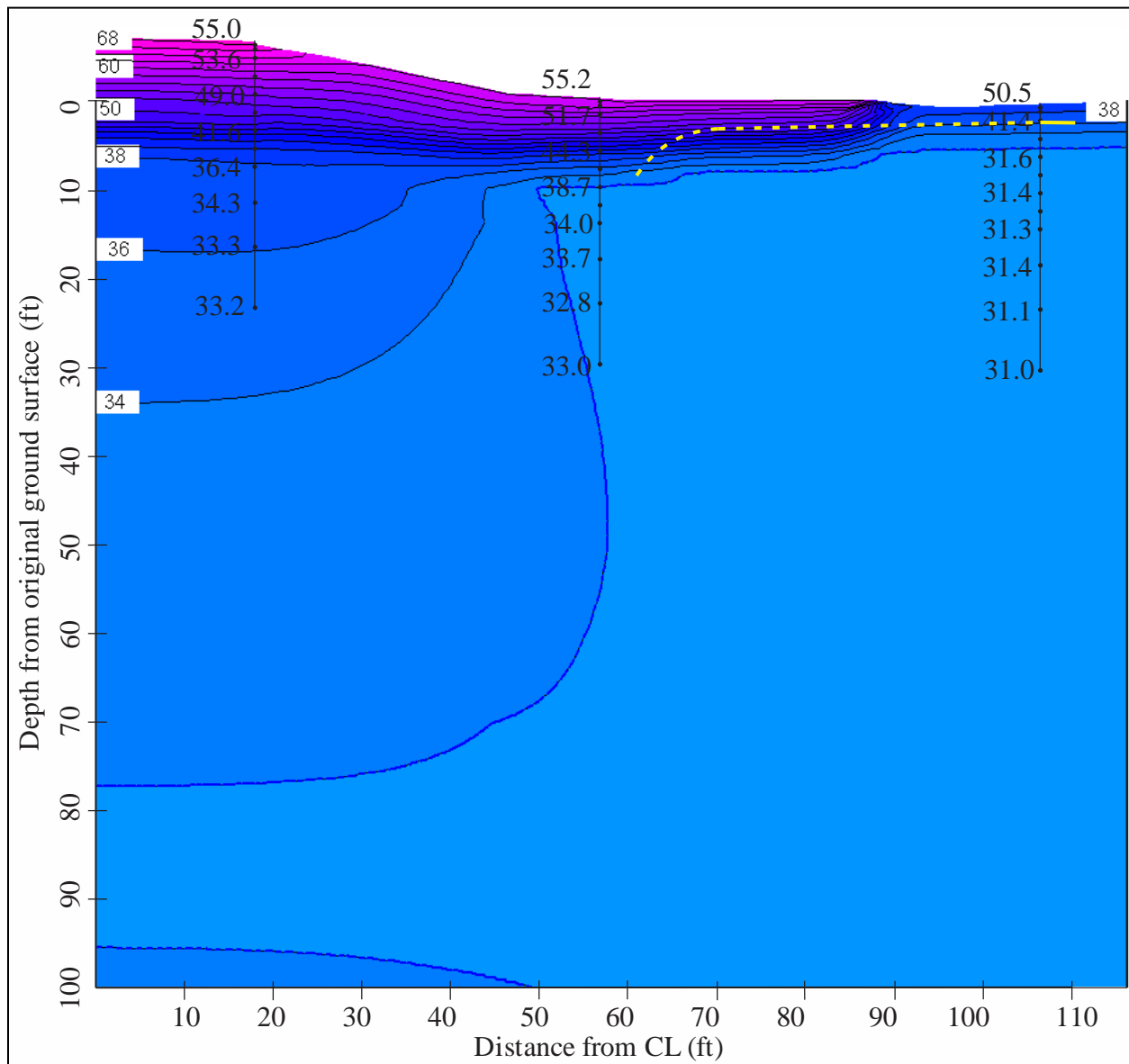
Figure 5.51. Thermal modeling results for November 1st, Run 6, Richardson Highway MP 113 research site. The phase change isotherm is represented as the dashed blue line and the temperature results are shown with a 2°F contour interval. Some of the measured temperatures along each thermistor string are shown in black text superimposed on the contours. The phase change isotherm approximated from the measured data is shown as a yellow dashed line.

Figure 5.52. Thermal modeling results for December 1ˢᵗ, Run 6, Richardson Highway MP 113 research site. The phase change isotherm is represented as the dashed blue line and the temperature results are shown with a 2°F contour interval. Some of the measured temperatures along each thermistor string are shown in black text superimposed on the contours. The phase change isotherm approximated from the measured data is shown as a yellow dashed line.

layer depth at the undisturbed location (i.e., maximum depth of thaw) is approximately 8 ft in December, which is deeper than that measured by 2 ft. As with Run 5, the shape of the thaw bulb at the toe thermistor string location in Run 6 is a closer fit to the measured data; however, due to the colder temperatures at the toe, the thaw bulb configuration narrowed again in this model iteration to exclude the lower portion of the toe thermistor string.

5.3 Modeling Results for Dalton Highway 9 Mile Hill

Table 5.8 summarizes the model iterations that were analyzed for the Dalton Highway location. In the following discussion, each iteration will be referred to as the corresponding run number. Initially, the model was run for 55 years to check the thermal equilibrium of the model and to check for the development of a thaw bulb. Since no thaw bulb developed under the highway in this model iteration, only the monthly temperatures from the last year of Run 1 will be discussed.

Table 5.8. Summary of model iterations for the Dalton Highway 9 Mile Hill research site

Run number	Comments
1	Traditional approach, 55 year model
2	Revised Run 1 using measured k_f and k_u (i.e., k_f = 24.0 Btu/ft·day·°F, k_u = 12.0 Btu/ft·day·°F)
3	10 year model using measured site air temperatures and measured k_f and k_u
4	Revised Run 3 using adjusted *n*-factors

Figures 5.53 through 5.64 are some of the model results from the last year of Run 1. The figures contain model results from the first day of each month. Model temperatures are presented with a 2°F contour interval, and the phase change isotherm is represented as a dashed blue line. On each figure, measured thermistor temperatures are superimposed over the contours in black text. The depths reported were chosen for the best readability of the results and to show as much data as possible, considering the malfunction of several thermistor beads. For the toe location, the temperatures are reported at depths of 0.5 ft, 2 ft, 6 ft, 10 ft, 14 ft, 18 ft, 23 ft, and 30 ft. The depths for the undisturbed location are the same with the exception of the absence of the thermistor at 23 ft, which malfunctioned. The temperatures reported for the shoulder location are at the depths of 0.5 ft, 1.5 ft, 5.5 ft, 11.5 ft, 13.5 ft, and 23.5 ft. The measured temperatures shown are from the first of the month for September through December 2009, and January through May 2010. The measured temperatures superimposed on the June 1st model results (see Figure 5.58) are from May 29, 2010, the last day data was collected. As of the writing of this report, temperatures have not been measured at the site for July 1st or August 1st. In Figures 5.59 and 5.60, these missing temperatures are represented as dashes. The measured and modeled temperatures for each of these selected depths for January through June and for September through December were compared, and these comparisons are tabulated in Appendix E. Additionally, Table 5.9 contains a summary of the phase change isotherm depths for this model iteration.

Generally for Run 1, the modeled temperatures are several degrees colder than the measured temperatures. In the undisturbed location, the modeled temperatures are 3.0°F colder on average than the measured temperatures, and up to 3.5°F colder at 30 ft. At the toe location, the modeled

Figure 5.53. Thermal modeling results for January 1st, Run 1, Dalton Highway 9 Mile Hill research site. The phase change isotherm is represented as the dashed blue line and the temperature results are shown with a 2°F contour interval. Some of the measured temperatures along each thermistor string are shown in black text superimposed on the contours.
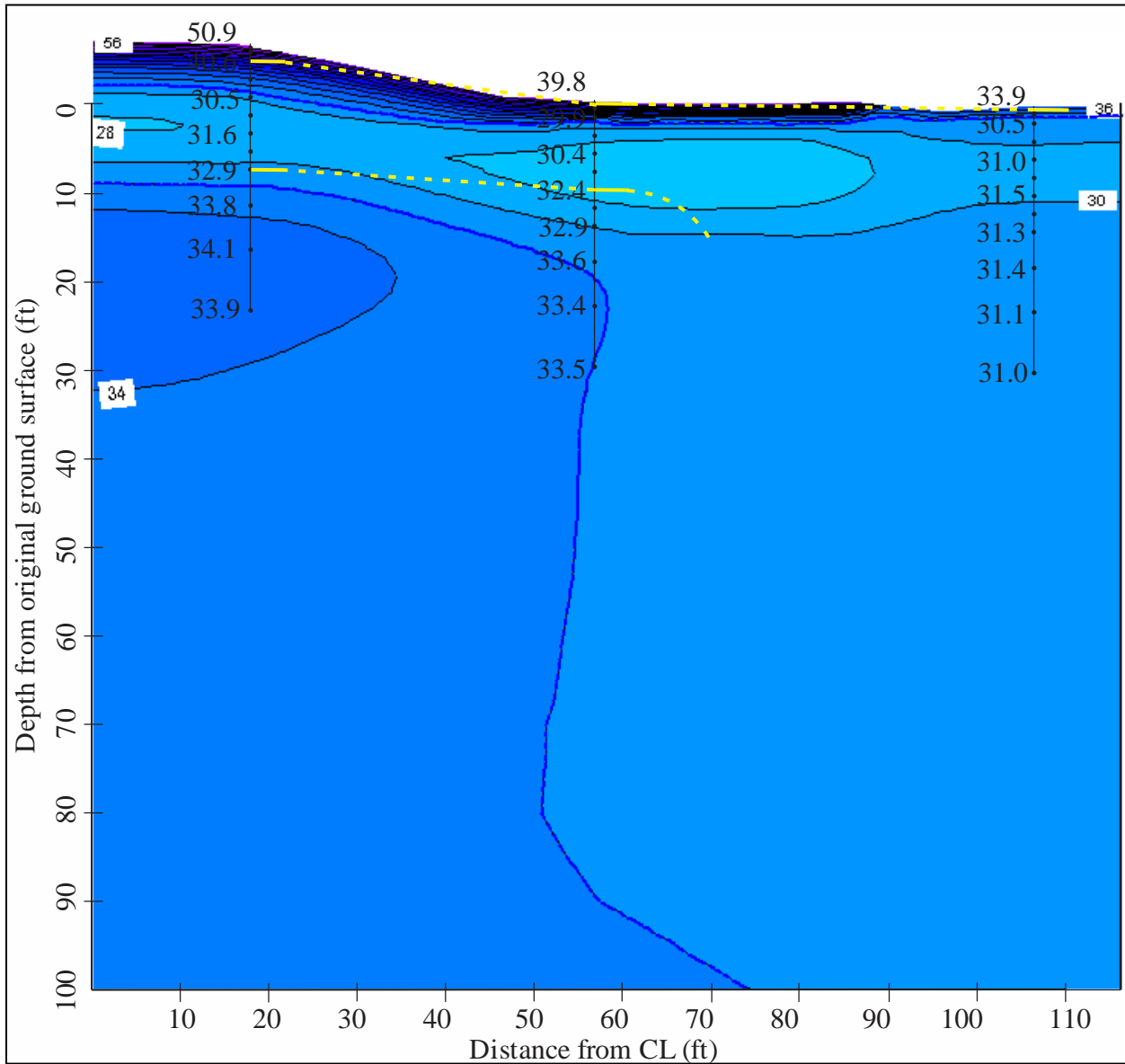
114

Figure 5.54. Thermal modeling results for February 1st, Run 1, Dalton Highway 9 Mile Hill research site. The phase change isotherm is represented as the dashed blue line and the temperature results are shown with a 2°F contour interval. Some of the measured temperatures along each thermistor string are shown in black text superimposed on the contours.
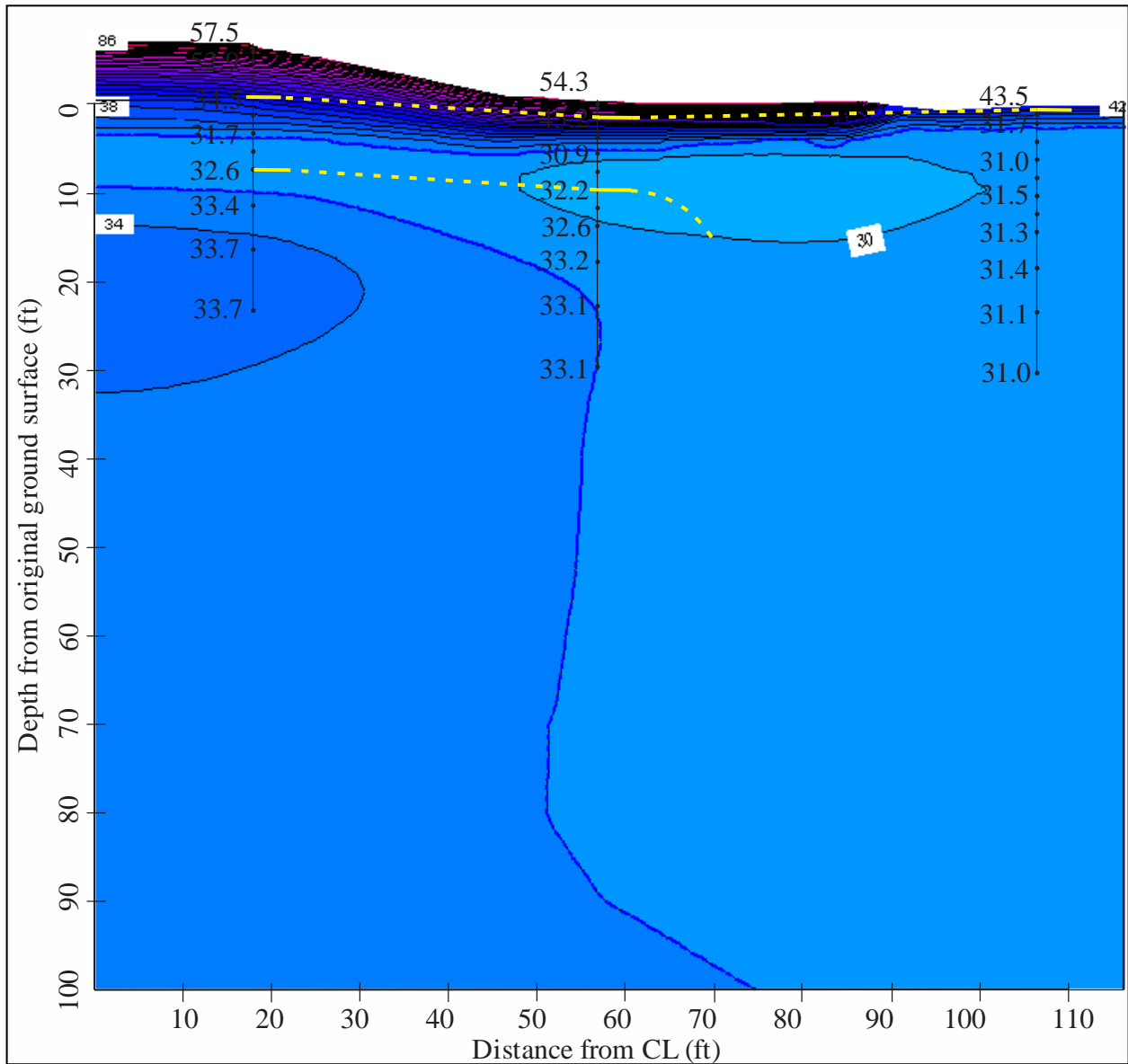
Figure 5.55. Thermal modeling results for March 1st, Run 1, Dalton Highway 9 Mile Hill research site. The phase change isotherm is represented as the dashed blue line and the temperature results are shown with a 2°F contour interval. Some of the measured temperatures along each thermistor string are shown in black text superimposed on the contours.

Figure 5.56. Thermal modeling results for April 1st, Run 1, Dalton Highway 9 Mile Hill research site. The phase change isotherm is represented as the dashed blue line and the temperature results are shown with a 2°F contour interval. Some of the measured temperatures along each thermistor string are shown in black text superimposed on the contours.
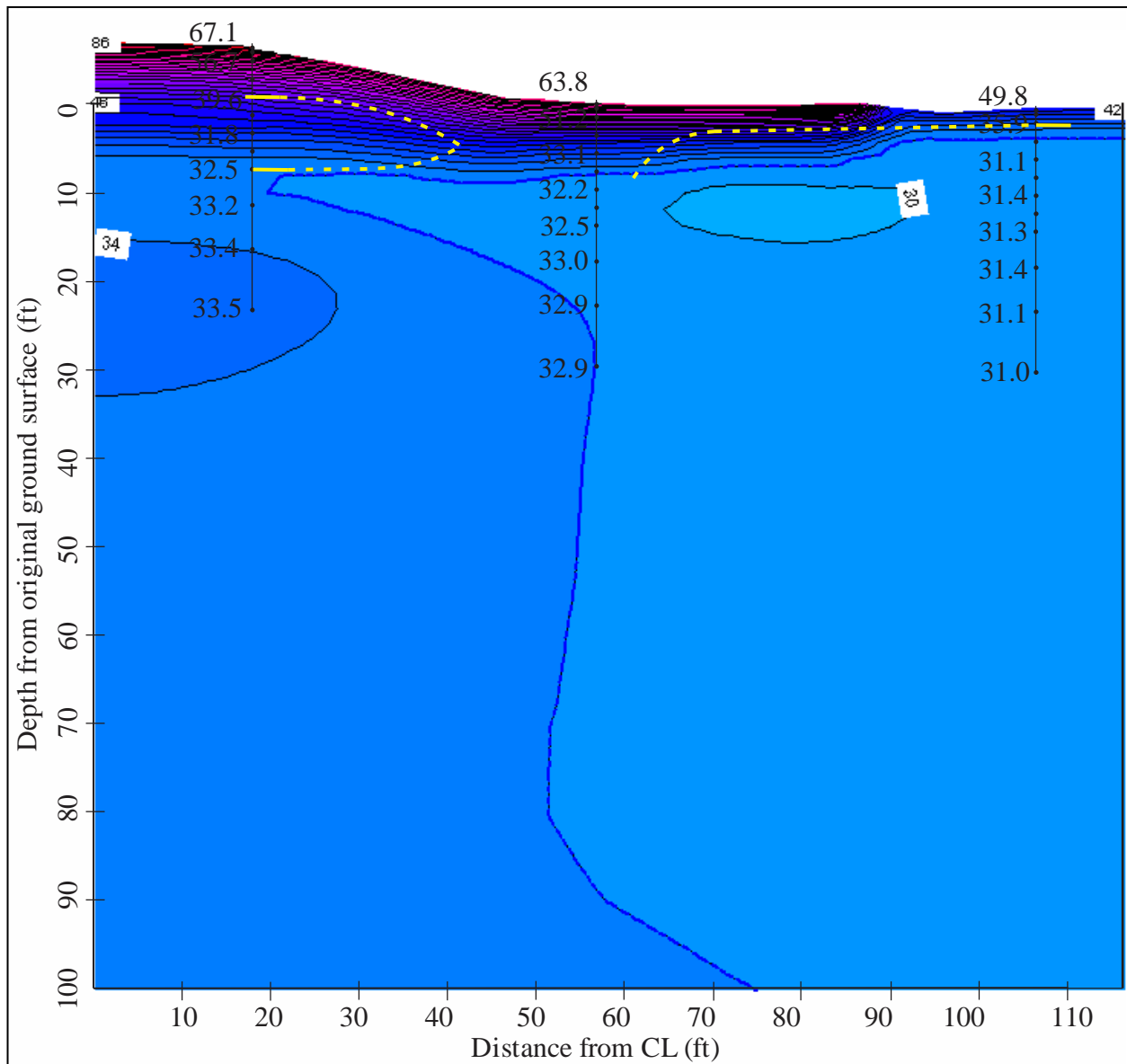
117

Figure 5.57. Thermal modeling results for May 1st, Run 1, Dalton Highway 9 Mile Hill research site. The phase change isotherm is represented as the dashed blue line and the temperature results are shown with a 2°F contour interval. Some of the measured temperatures along each thermistor string are shown in black text superimposed on the contours.

Figure 5.58. Thermal modeling results for June 1st, Run 1, Dalton Highway 9 Mile Hill research site. The phase change isotherm is represented as the dashed blue line and the temperature results are shown with a 2°F contour interval. Some of the measured temperatures along each thermistor string from May 29, 2010 are shown in black text superimposed on the contours.

Figure 5.59. Thermal modeling results for July 1st, Run 1, Dalton Highway 9 Mile Hill research site. The phase change isotherm is represented as the dashed blue line and the temperature results are shown with a 2°F contour interval. Temperatures at the site were not yet measured for July 1st.

Figure 5.60. Thermal modeling results for August 1st, Run 1, Dalton Highway 9 Mile Hill research site. The phase change isotherm is represented as the dashed blue line and the temperature results are shown with a 2°F contour interval. Temperatures at the site were not yet measured for August 1st.
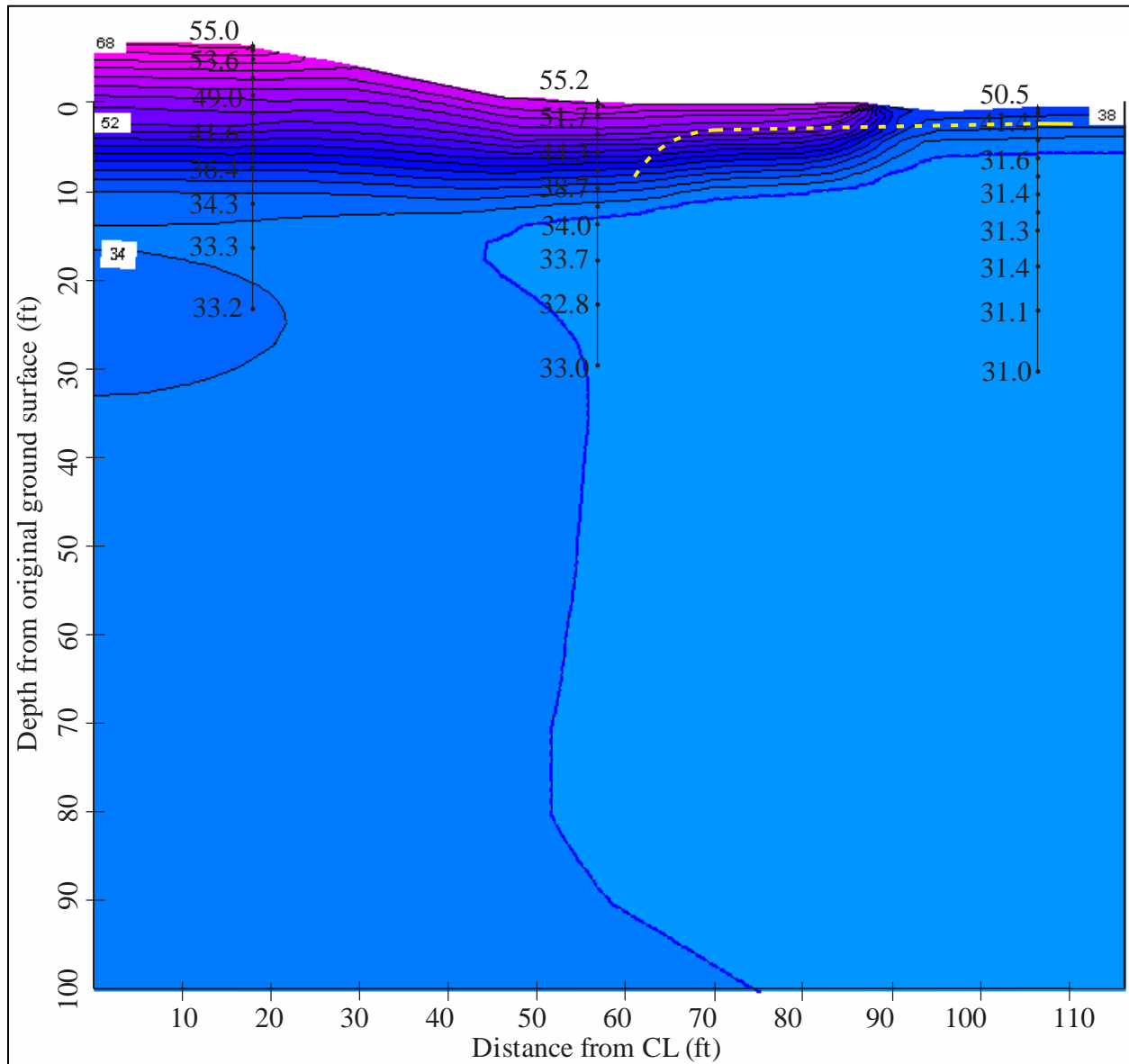
121

Figure 5.61. Thermal modeling results for September 1st, Run 1, Dalton Highway 9 Mile Hill research site. The phase change isotherm is represented as the dashed blue line and the temperature results are shown with a 2°F contour interval. Some of the measured temperatures along each thermistor string are shown in black text superimposed on the contours.
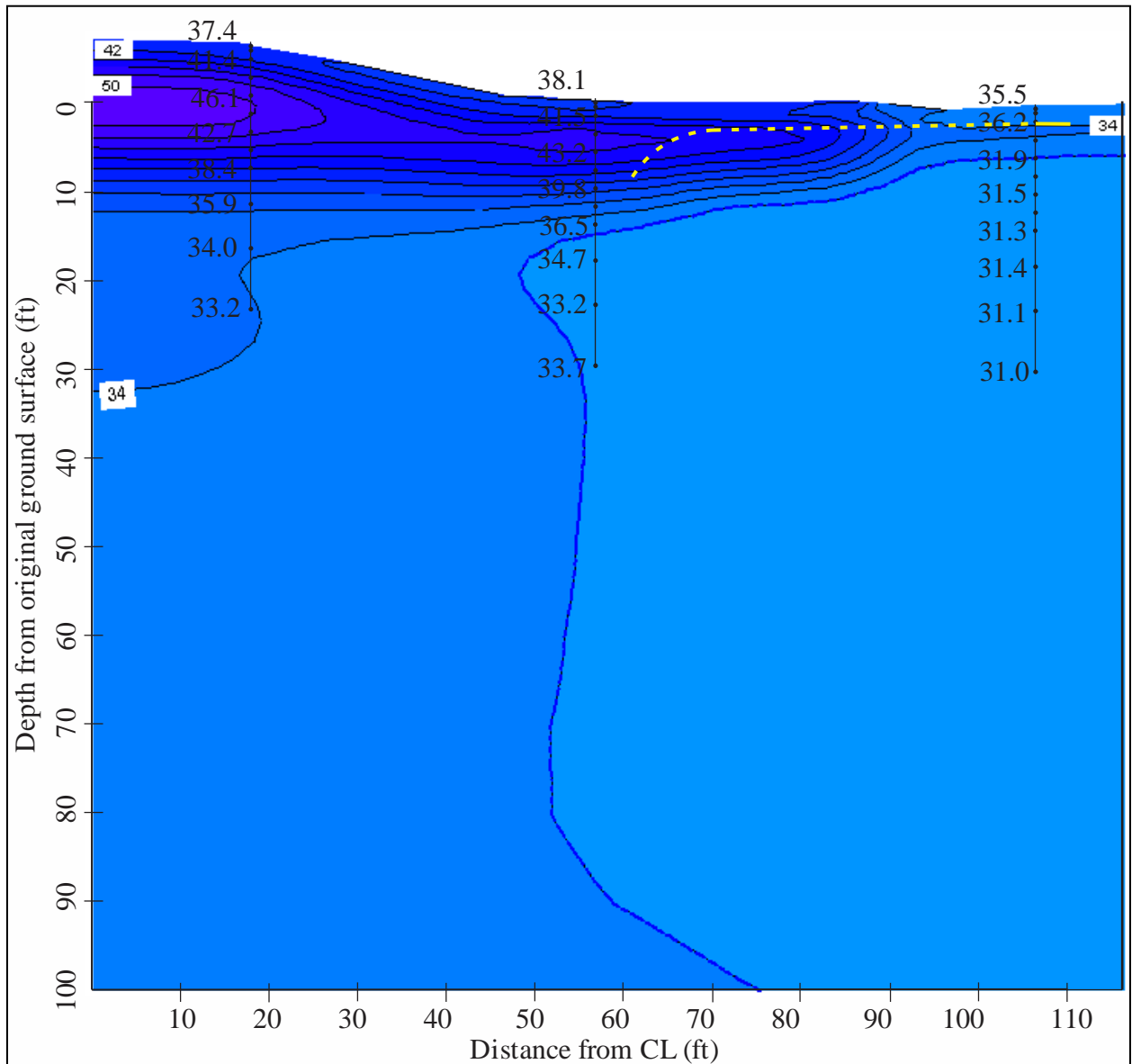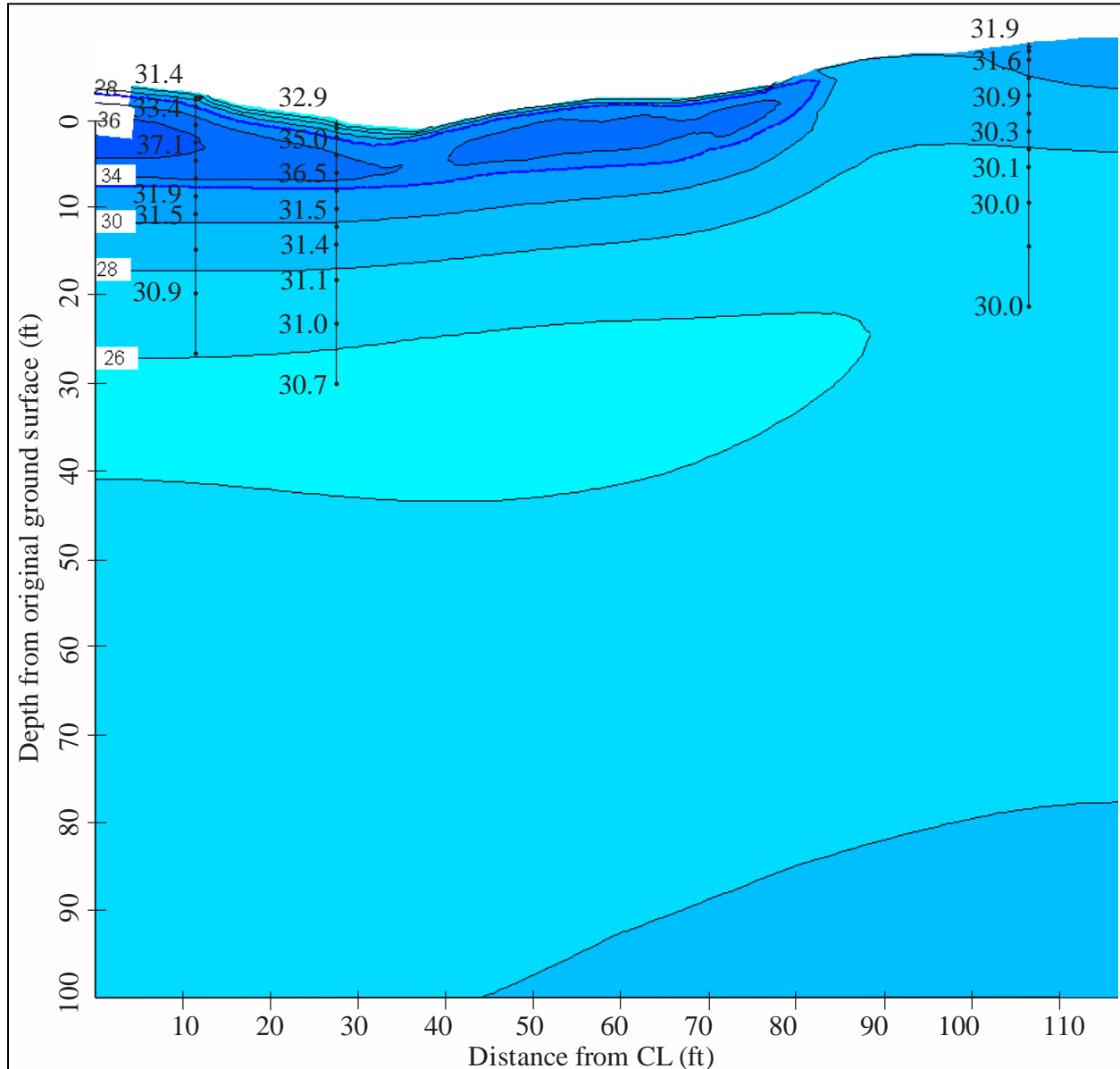
Figure 5.62. Thermal modeling results for October 1st, Run 1, Dalton Highway 9 Mile Hill research site. The phase change isotherm is represented as the dashed blue line and the temperature results are shown with a 2°F contour interval. Some of the measured temperatures along each thermistor string are shown in black text superimposed on the contours.
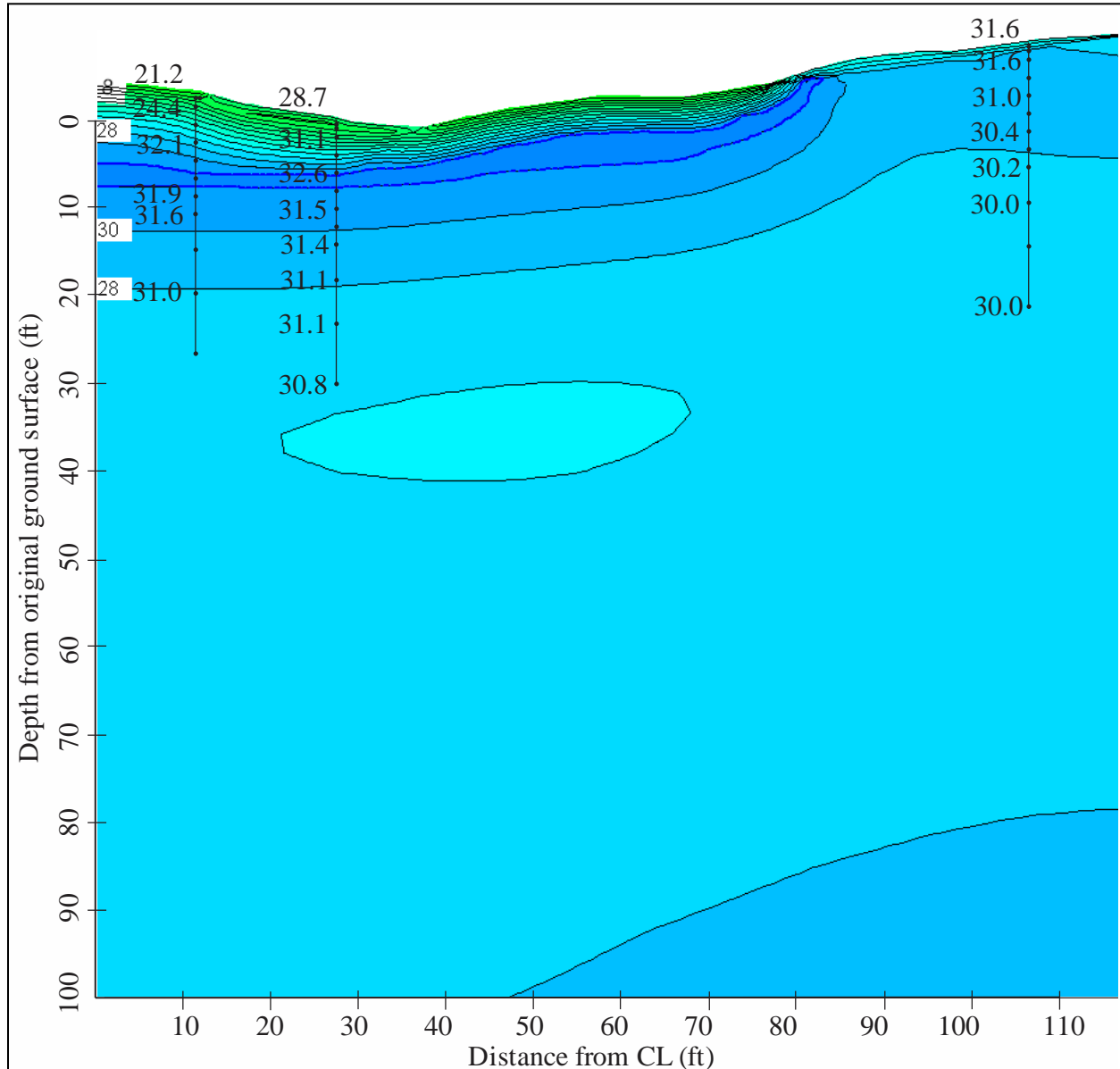
Figure 5.63. Thermal modeling results for November 1st, Run 1, Dalton Highway 9 Mile Hill research site. The phase change isotherm is represented as the dashed blue line and the temperature results are shown with a 2°F contour interval. Some of the measured temperatures along each thermistor string are shown in black text superimposed on the contours.
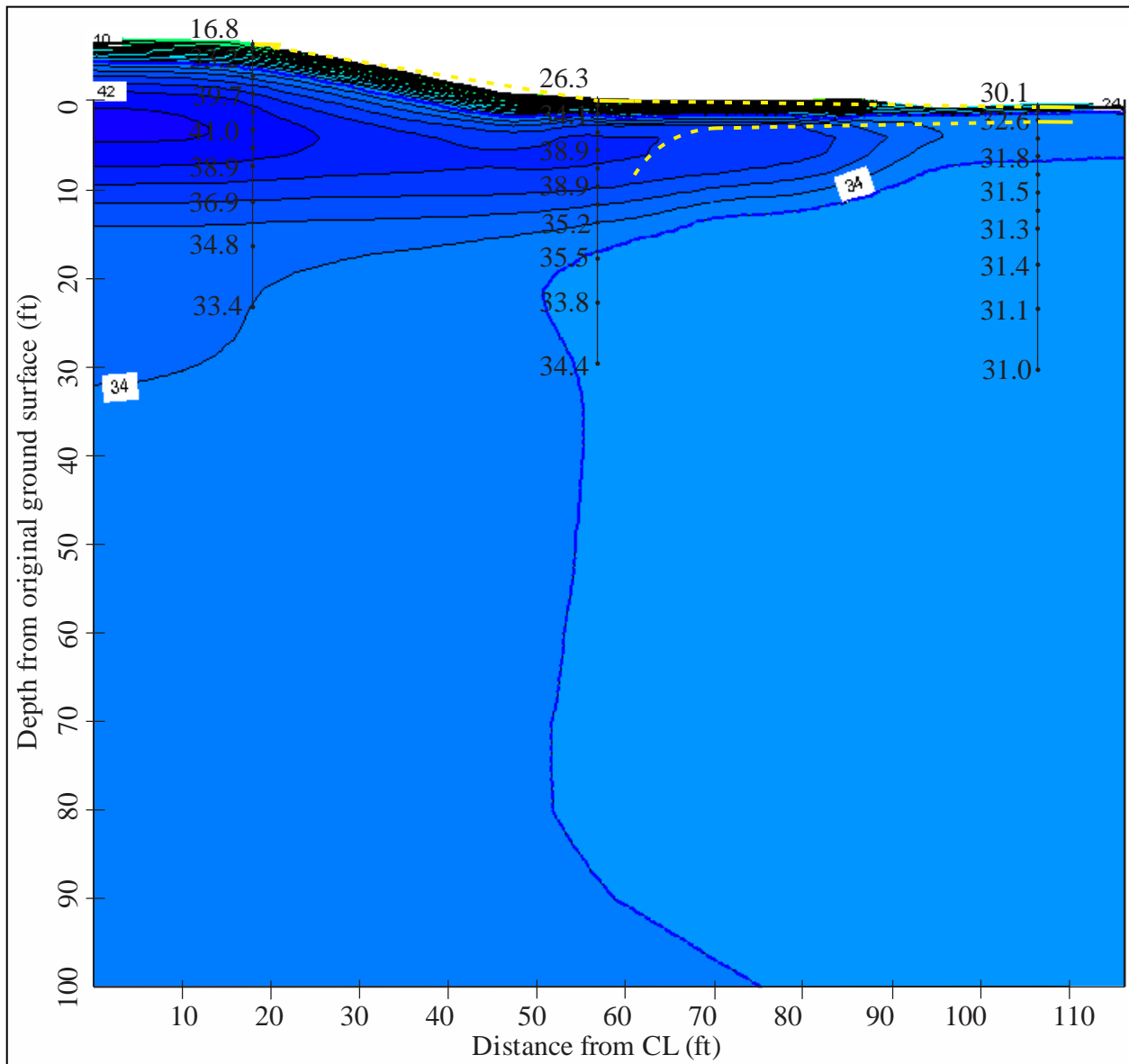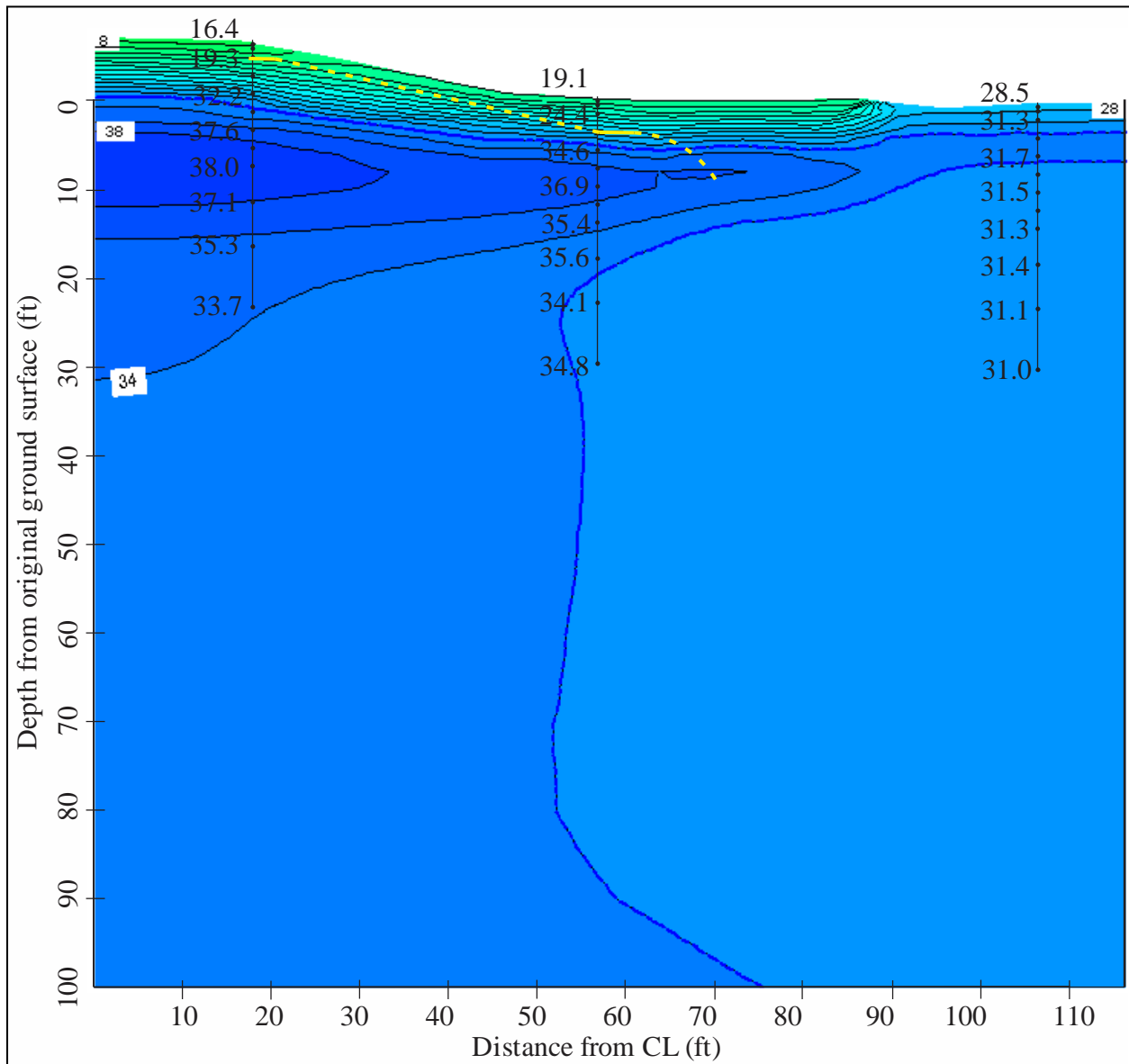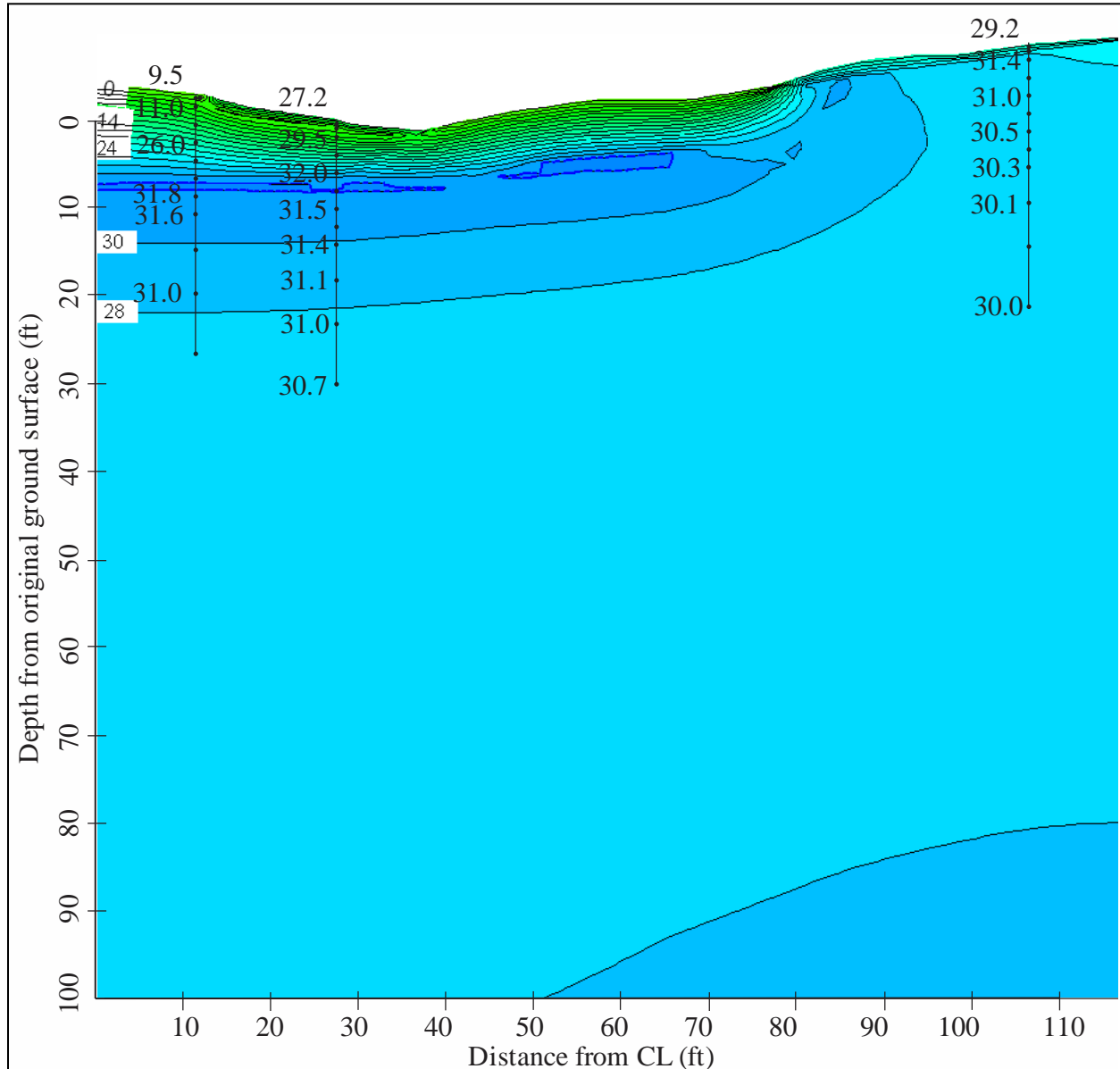
Figure 5.64. Thermal modeling results for December 1st, Run 1, Dalton Highway 9 Mile Hill research site. The phase change isotherm is represented as the dashed blue line and the temperature results are shown with a 2°F contour interval. Some of the measured temperatures along each thermistor string are shown in black text superimposed on the contours.

Table 5.9. Summary of modeled phase change isotherm depths, Dalton Highway 9 Mile Hill research site. Where relevant, 'U,' 'M,' and 'L' indicate upper, middle, and lower phase change isotherms, respectively. For months when no phase change isotherm was present, '---' is shown. For means of comparison, measured data included in Chapter 4 indicates the following active layer depths: shoulder – between 7.5 and 11.5 ft; toe – between 8 and 10 ft; undisturbed – between 2 and 4 ft.

Month		Run 1			Run 3			Run 4		
		Shoulder	Toe	Undisturbed	Shoulder	Toe	Undisturbed	Shoulder	Toe	Undisturbed
January	U	---	---	---	10.0	7.4	---	10.6	8.0	---
	L	---	---	---	15.2	10.6	---	11.4	8.8	---
February	U	---	---	---	10.1	7.9	---	---	---	---
	L	---	---	---	15.3	11.2	---	---	---	---
March	U	---	---	---	10.5	8.1	---	---	---	---
	L	---	---	---	15.3	11.2	---	---	---	---
April	U	---	---	---	10.5	8.1	---	---	---	---
	L	---	---	---	15.3	11.3	---	---	---	---
May	U	---	---	---	5.3	6.4	1.1	3.7	3.5	1.1
	M	---	---	---	10.6	9.2	---	---	---	---
	L	---	---	---	15.2	11.7	---	---	---	---
June	U	4.0	3.7	0.9	15.3	7.4	1.4	8.1	6.7	1.2
	L	---	---	---	---	9.0	---	---	---	---
July	U	9.1	6.8	1.3	15.4	8.2	1.6	10.3	7.4	1.3
	L	---	---	---	---	9.3	---	---	---	---
August		10.3	7.5	1.3	15.9	9.6	1.6	10.6	8.0	1.4
September		10.6	8.0	1.5	16.0	10.2	1.6	11.0	8.2	1.4
October	U	1.9	2.3	---	1.9	2.2	---	2.4	2.6	---
	L	11.1	8.0	---	16.0	10.2	---	11.1	8.3	---
November	U	9.7	6.8	---	5.0	5.2	---	7.4	6.3	---
	L	11.2	8.3	---	15.9	10.2	---	11.2	8.5	---
December	U	10.3	8.2	---	8.8	6.8	---	9.9	7.1	---
	L	11.1	---	---	15.4	10.4	---	11.2	8.7	---

temperatures are 4.7°F colder than the measured temperatures at 30 ft. This discrepancy increases in magnitude closer to the surface, with the greatest difference occurring in January when the modeled temperature near the surface was 46.1°F colder than the measured temperature. At the shoulder location, the modeled temperatures at 30 ft were 4.9°F colder on average than the measured temperatures, with this discrepancy increasing towards the surface.

Analysis of the measured temperature data summarized in Chapter 4 indicates the following active layer depths: for the shoulder location, between 7.5 and 11.5 ft; for the toe location, between 8 and 10 ft; and for the undisturbed location, between 2 and 4 ft. These depths are listed as ranges due to malfunctioning thermistor beads or due to remaining influences from drilling heat. Analysis of the data in Table 5.9 indicates that the modeled active layer depth at the shoulder location reaches a maximum in November of approximately 11 ft. At the shoulder location, the modeled active layer depth is approximately 8 ft in November. Finally, the modeled active layer depth at the undisturbed location reaches a maximum of 1.5 ft in September. Each of these values agrees with its measured counterpart.

For the second model iteration, the approximated values for k_f and k_u for the ice-rich silt were replaced with the measured values from the site (i.e., k_f = 24.0 Btu/ft·day·°F, k_u = 12.0 Btu/ft·day·°F). This model, Run 2, was otherwise similar to Run 1. The model results are presented in Figures G.1 through G.12 in Appendix G, and can be compared to Figures 5.53 through 5.64. With the measured thermal conductivity values, the modeled temperatures are slightly warmer in some areas of the model. Otherwise, the temperatures and active layer configurations are unremarkable in their differences between Runs 1 and 2.

For Run 3, the air temperatures measured at the site were used as the upper boundary condition. Since this site does not yet have a complete year's worth of data, the missing data were estimated to complete the sinusoidal function for air temperature. The measured values for k_f and k_u for the ice-rich silt also were used in this iteration. This run was reduced to 10 years (a total of 3,650 time steps), with model results saved every 5 days. Figures 5.65 through 5.76 are some of the model results from the last year of Run 3. Comparisons of the measured and modeled temperatures are tabulated in Appendix E. Additionally, Table 5.9 contains a summary of the phase change isotherm depths for this model iteration.

For Run 3, the modeled temperatures are typically within 5°F of the measured temperatures throughout the cross section. For example, at a depth of 30 ft at the undisturbed location, the modeled temperatures are between 0.5°F and 1°F colder than the measured temperatures. Between the depths of 10 ft and 30 ft, the model is typically within 0.5°F of the measured temperatures, and within 5°F of the measured temperatures at the surface.

For the toe location, the modeled temperatures are typically 0.3°F warmer than the measured temperatures at 30 ft. Between 10 ft and 30 ft, the model is excellent agreement with the measured temperatures, on average being 0.1°F warmer than the measured temperatures. There are, however, tremendous differences in the surface temperatures, with the modeled temperatures being nearly 40°F too cold in the winter and nearly 30°F too warm in the summer.

For the shoulder location, the modeled temperatures at 30 ft are in excellent agreement with the measured temperatures for the months of January through March, and are within 1°F of each
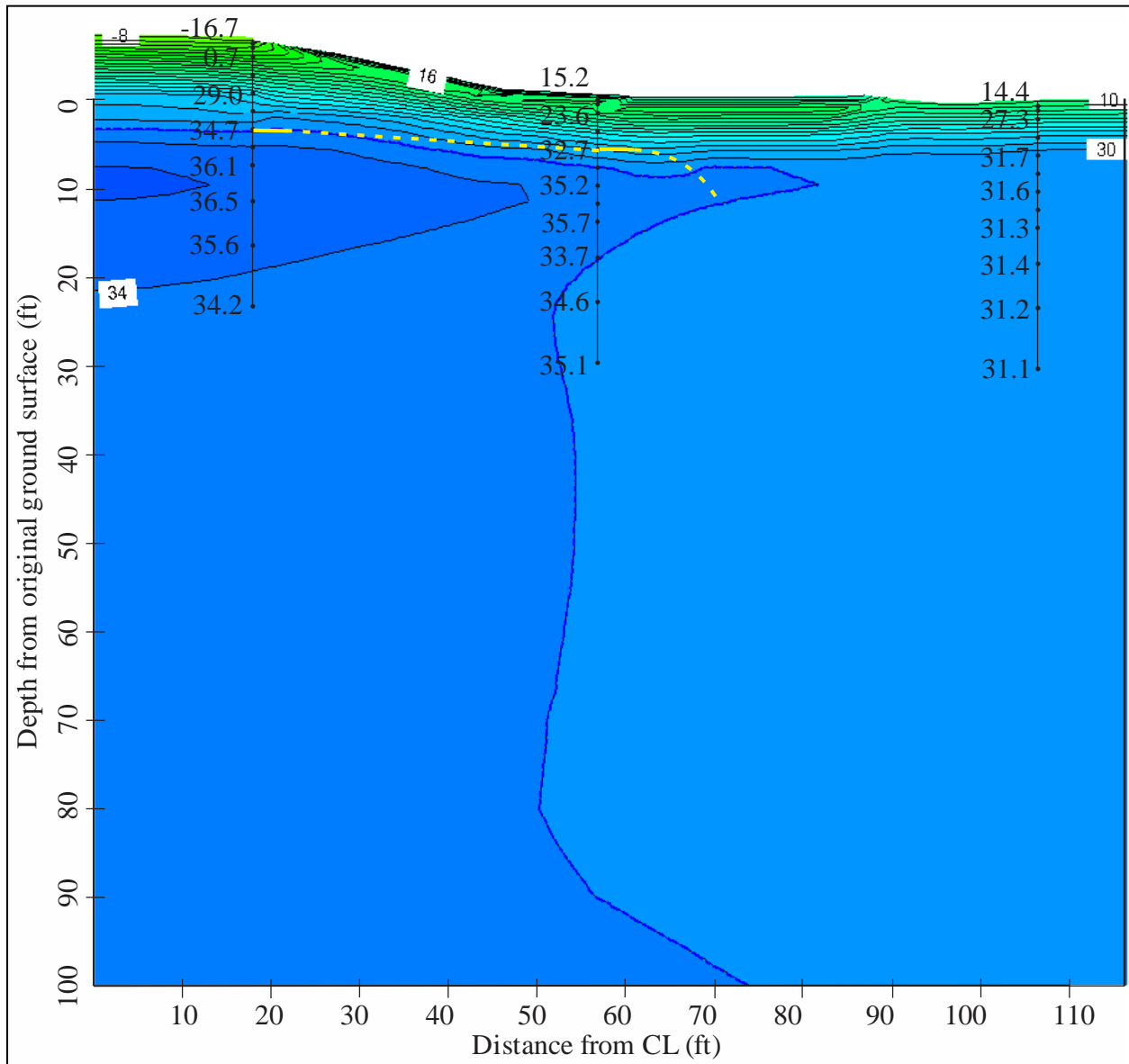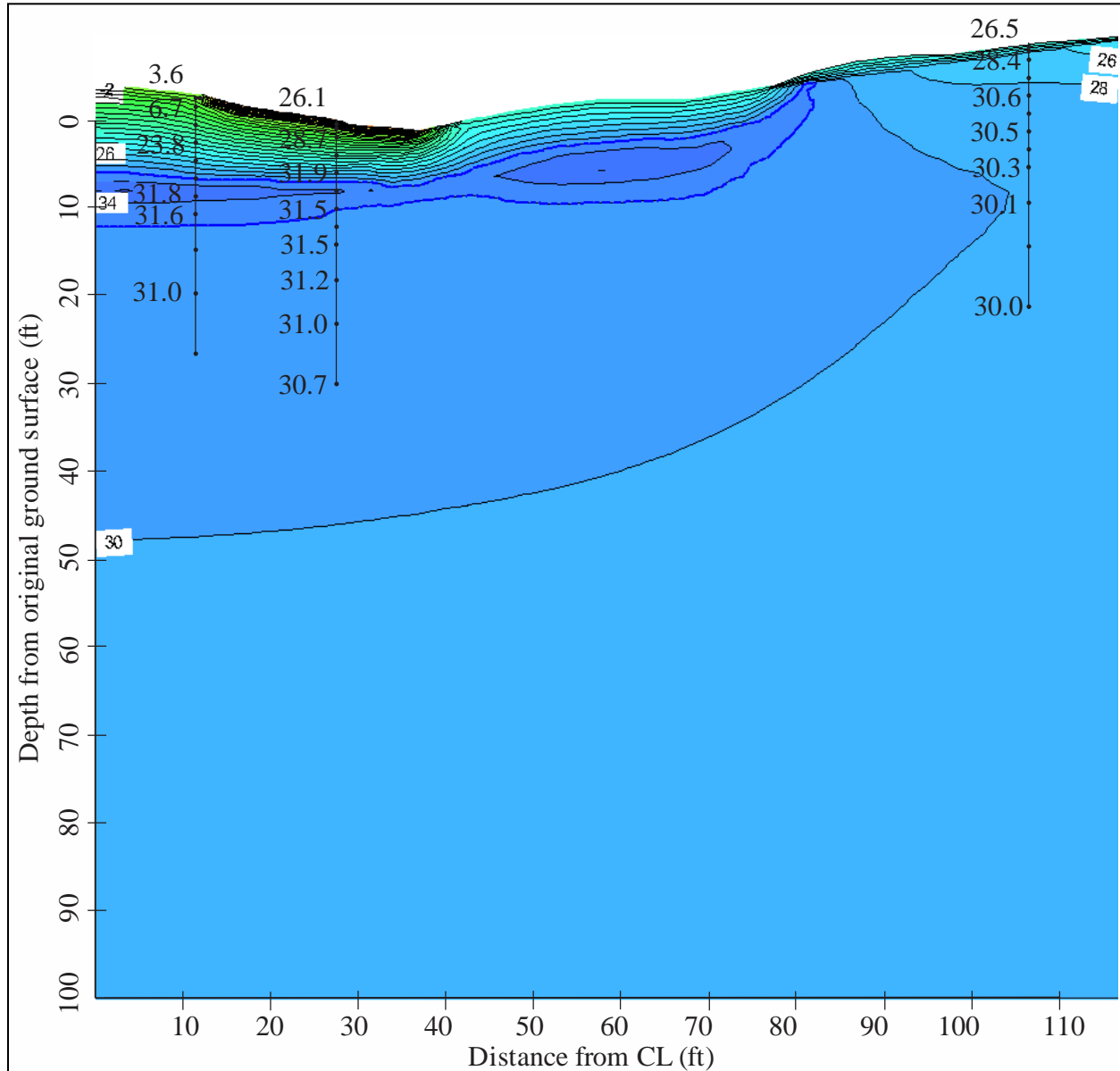
Figure 5.65. Thermal modeling results for January 1st, Run 3, Dalton Highway 9 Mile Hill research site. The phase change isotherm is represented as the dashed blue line and the temperature results are shown with a 2°F contour interval. Some of the measured temperatures along each thermistor string are shown in black text superimposed on the contours.
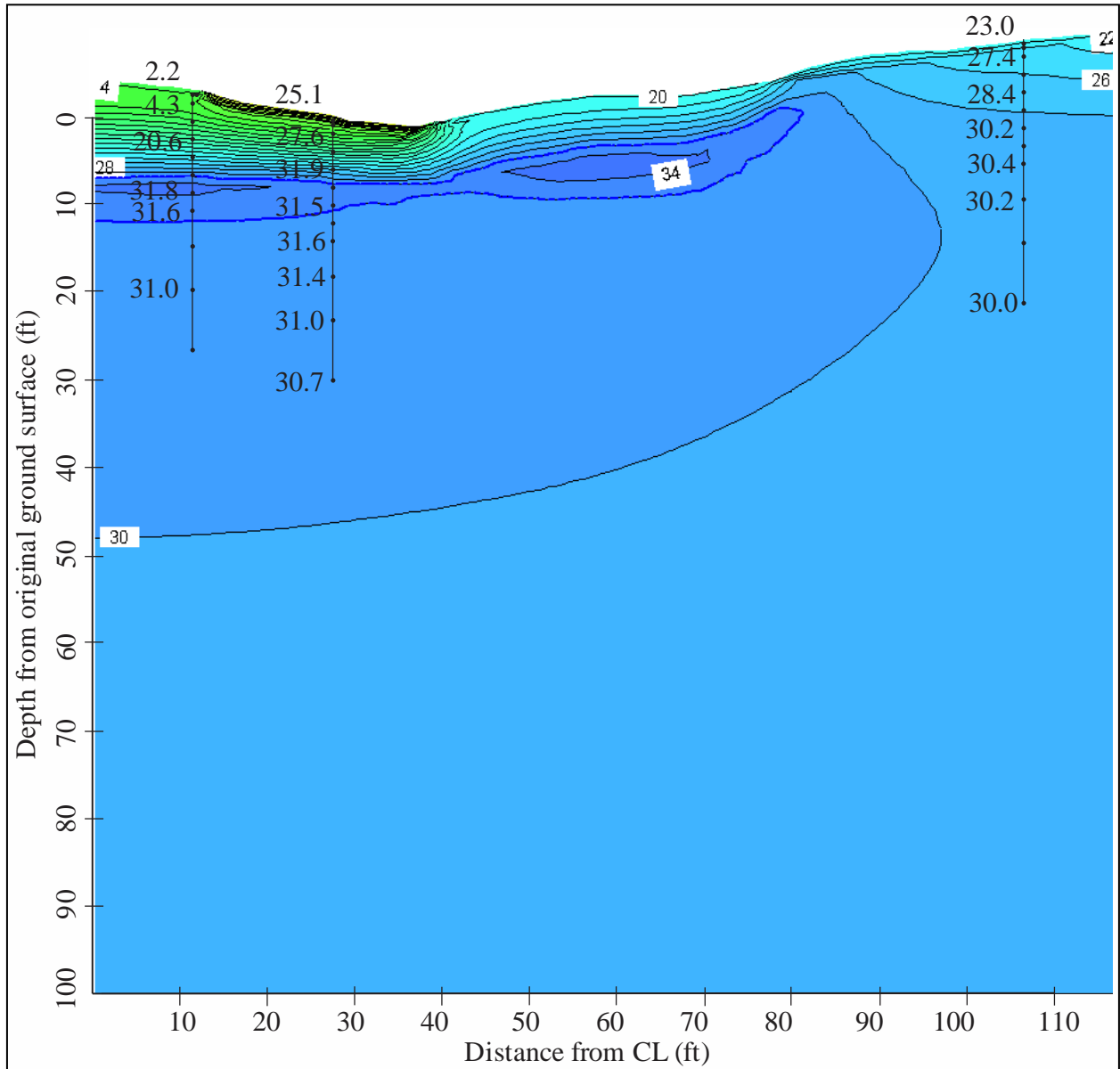
Figure 5.66. Thermal modeling results for February 1st, Run 3, Dalton Highway 9 Mile Hill research site. The phase change isotherm is represented as the dashed blue line and the temperature results are shown with a 2°F contour interval. Some of the measured temperatures along each thermistor string are shown in black text superimposed on the contours.
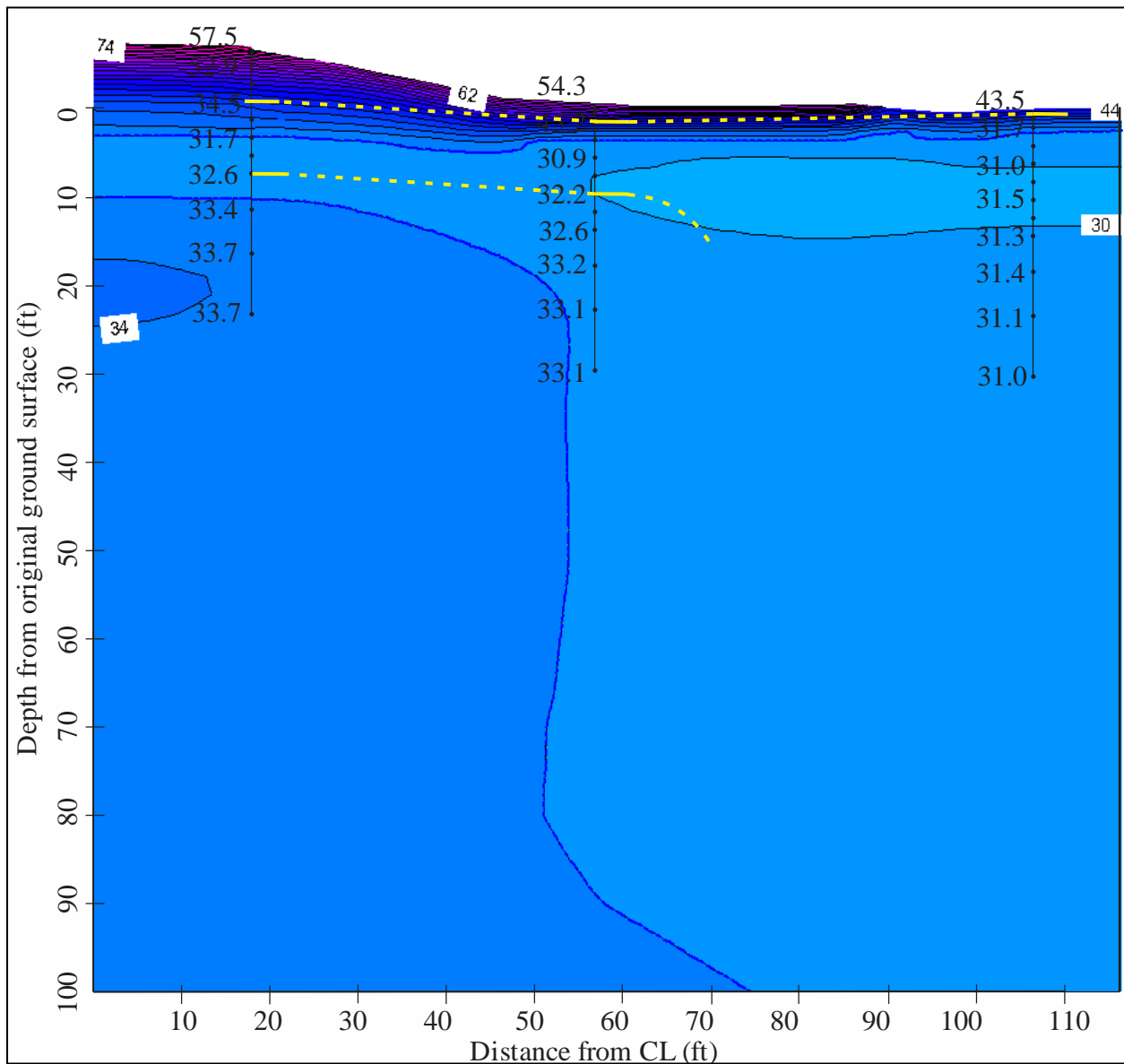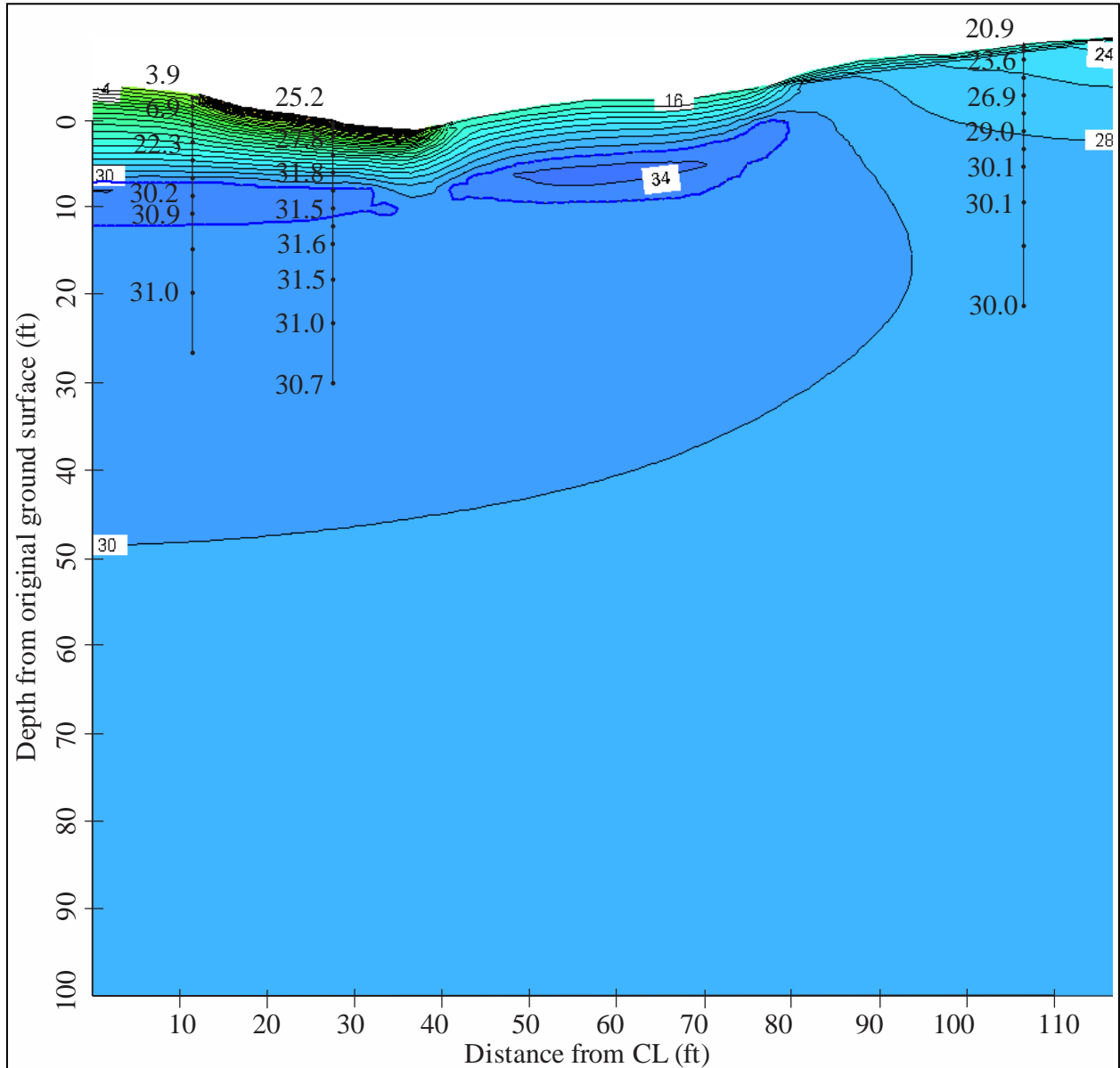
Figure 5.67. Thermal modeling results for March 1st, Run 3, Dalton Highway 9 Mile Hill research site. The phase change isotherm is represented as the dashed blue line and the temperature results are shown with a 2°F contour interval. Some of the measured temperatures along each thermistor string are shown in black text superimposed on the contours.
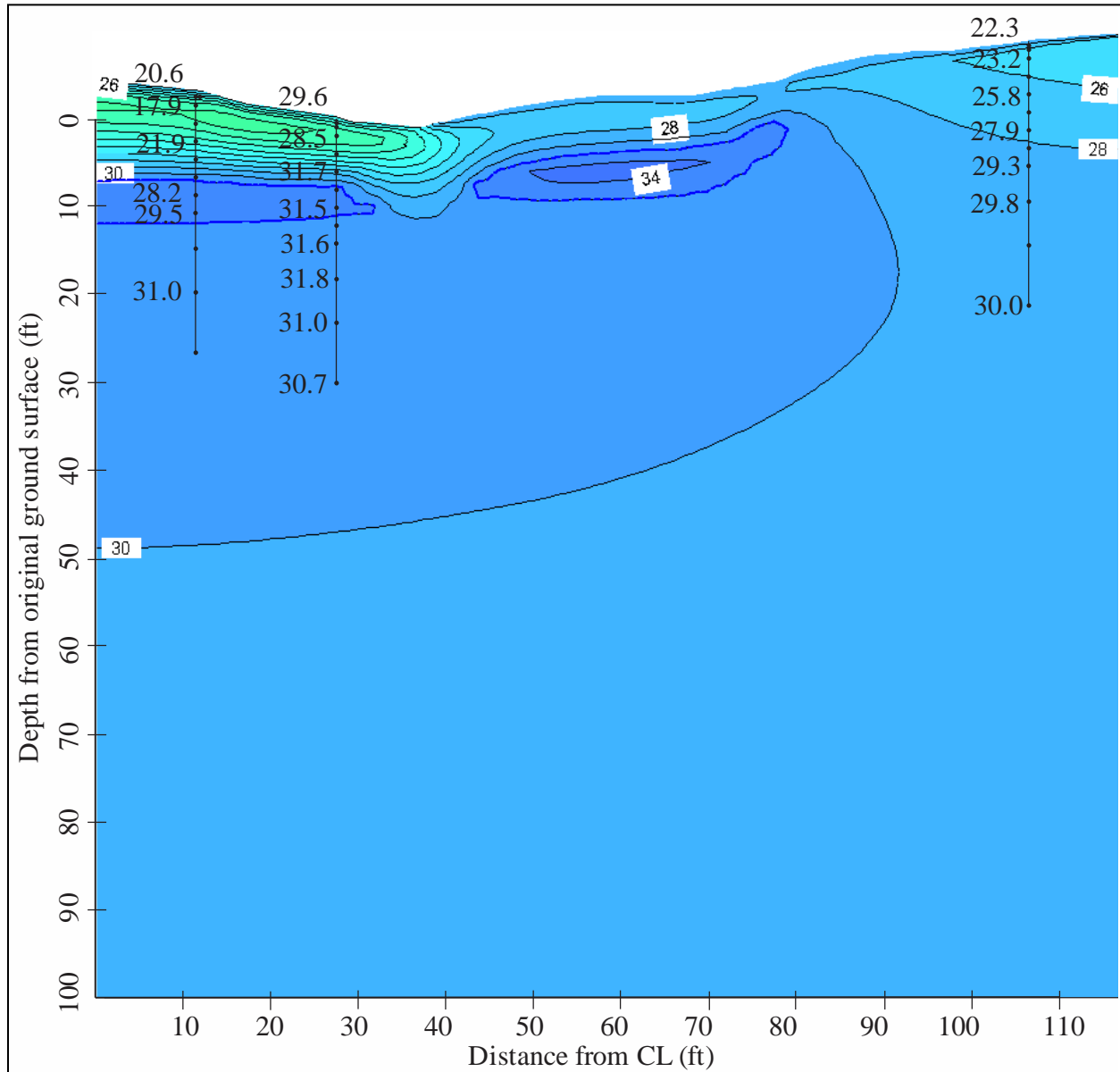
Figure 5.68. Thermal modeling results for April 1st, Run 3, Dalton Highway 9 Mile Hill research site. The phase change isotherm is represented as the dashed blue line and the temperature results are shown with a 2°F contour interval. Some of the measured temperatures along each thermistor string are shown in black text superimposed on the contours.
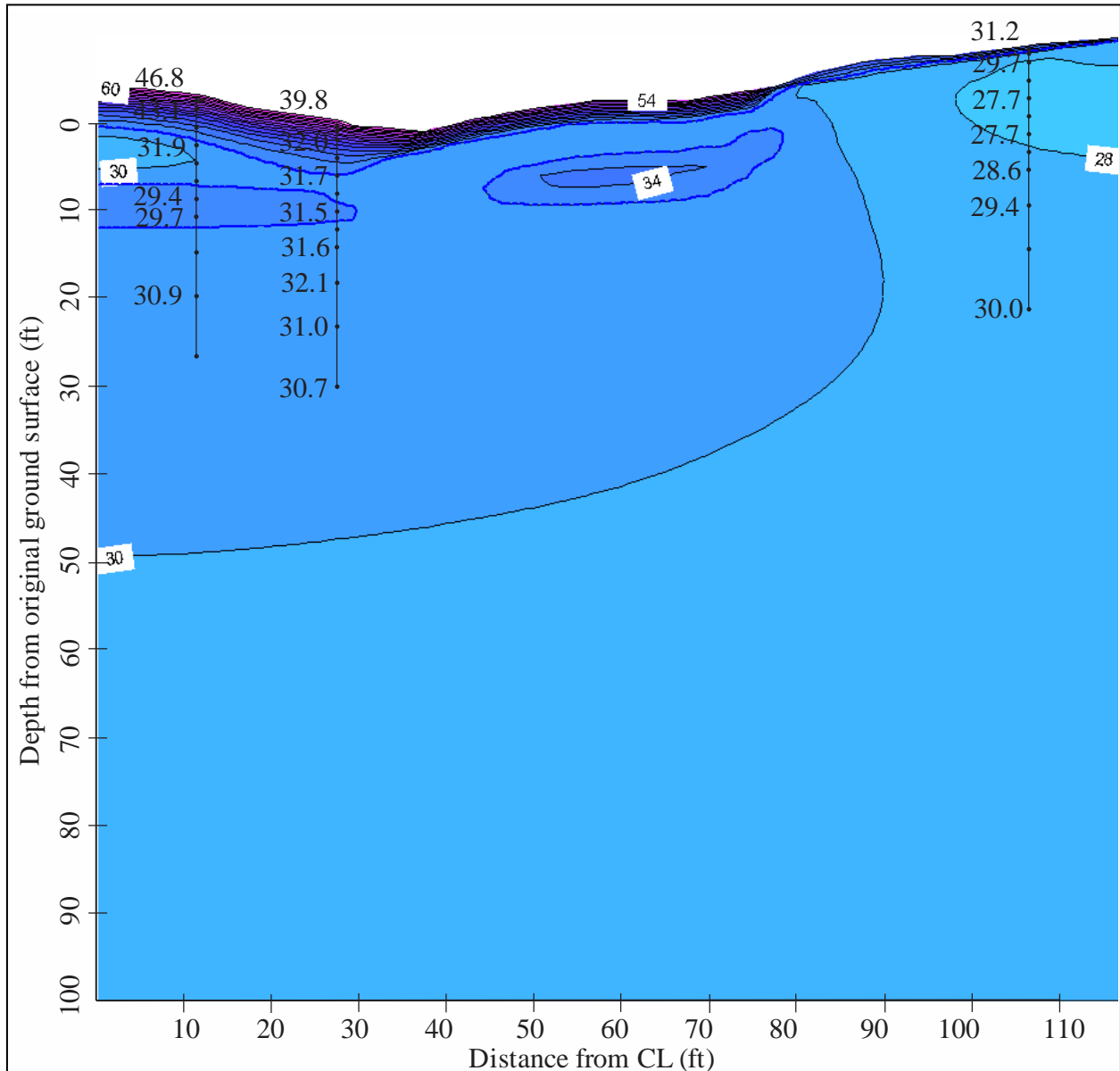
Figure 5.69. Thermal modeling results for May 1st, Run 3, Dalton Highway 9 Mile Hill research site. The phase change isotherm is represented as the dashed blue line and the temperature results are shown with a 2°F contour interval. Some of the measured temperatures along each thermistor string are shown in black text superimposed on the contours.
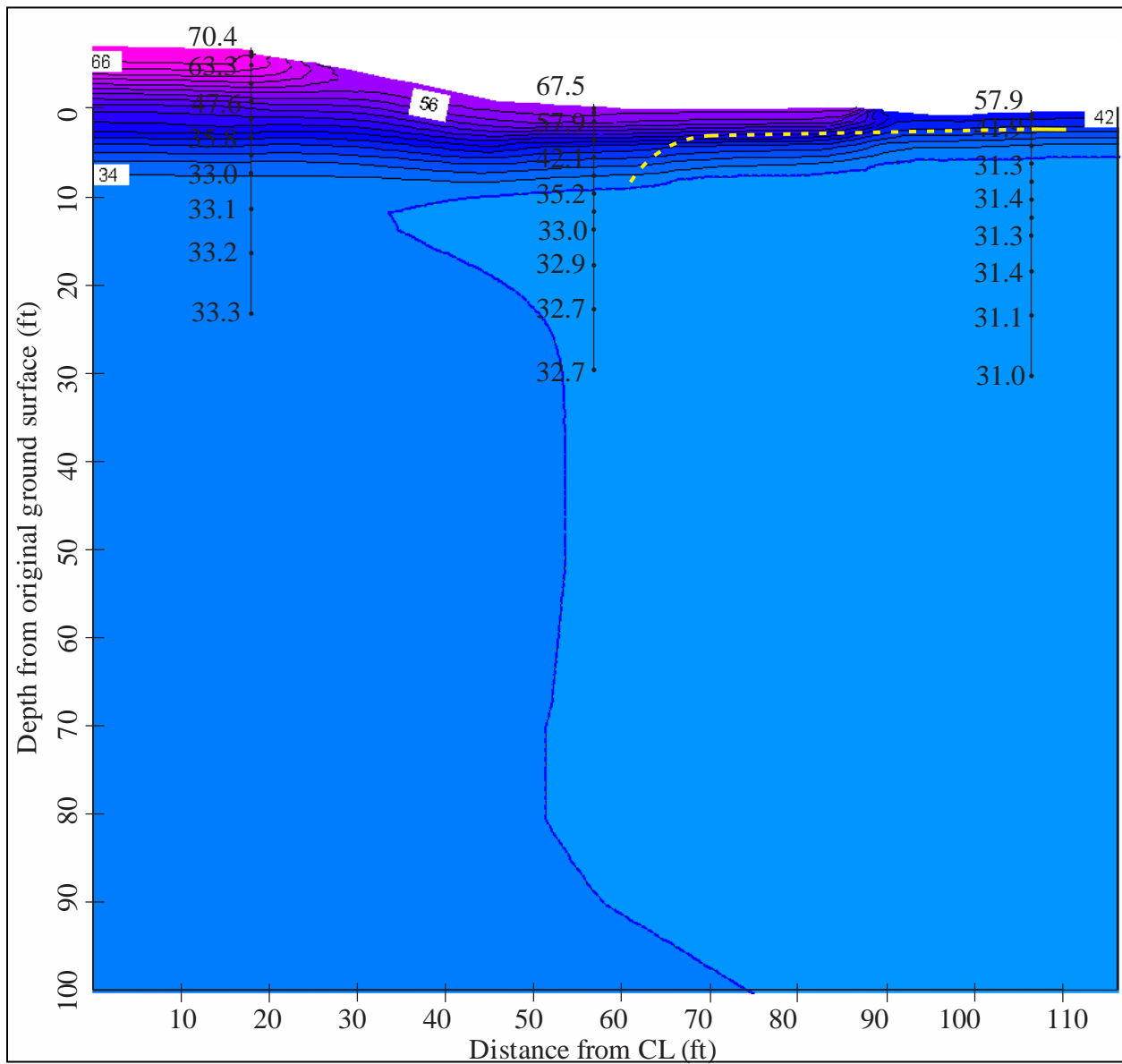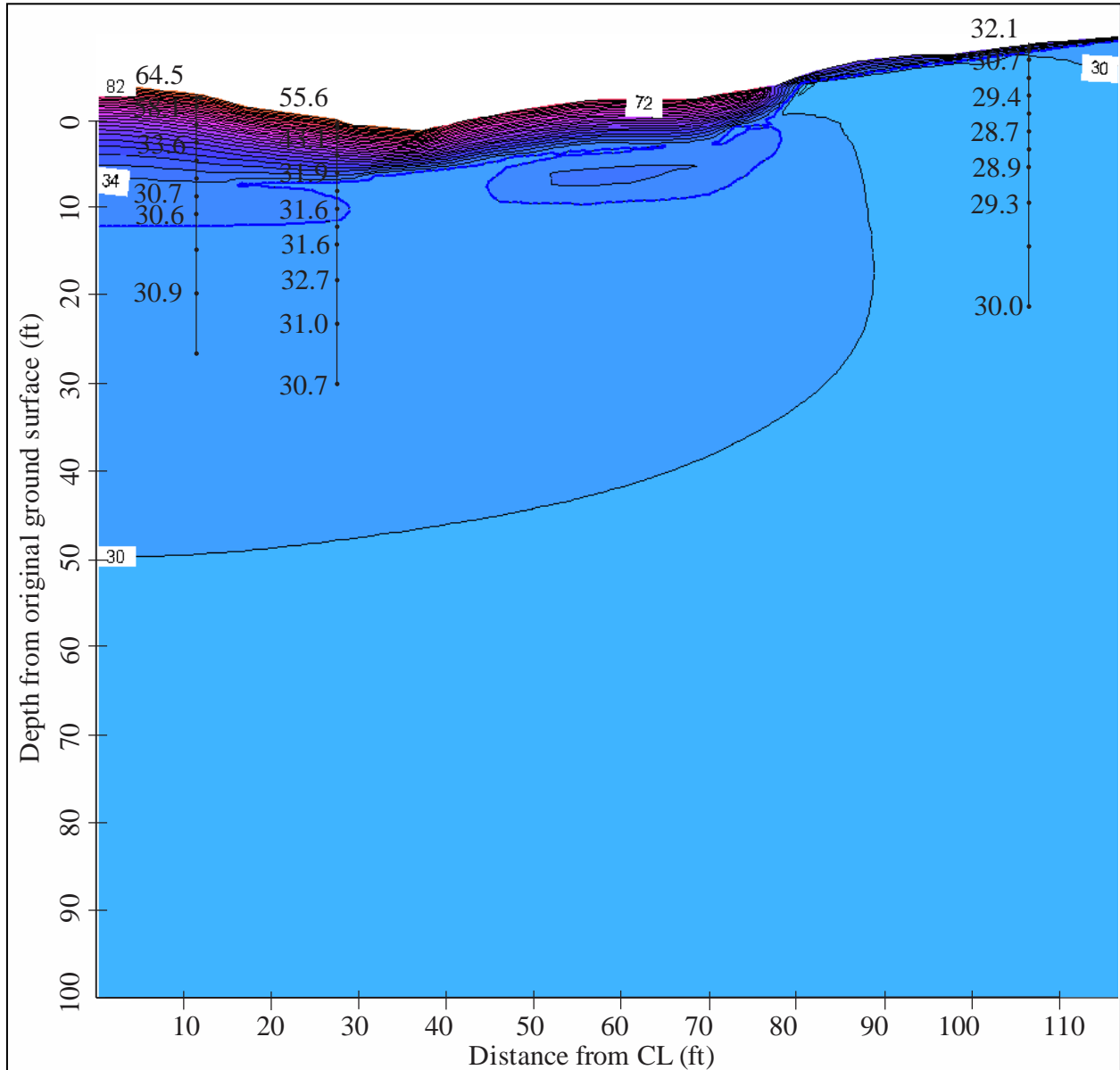
Figure 5.70. Thermal modeling results for June 1st, Run 3, Dalton Highway 9 Mile Hill research site. The phase change isotherm is represented as the dashed blue line and the temperature results are shown with a 2°F contour interval. Some of the measured temperatures along each thermistor string from May 29, 2010 are shown in black text superimposed on the contours.
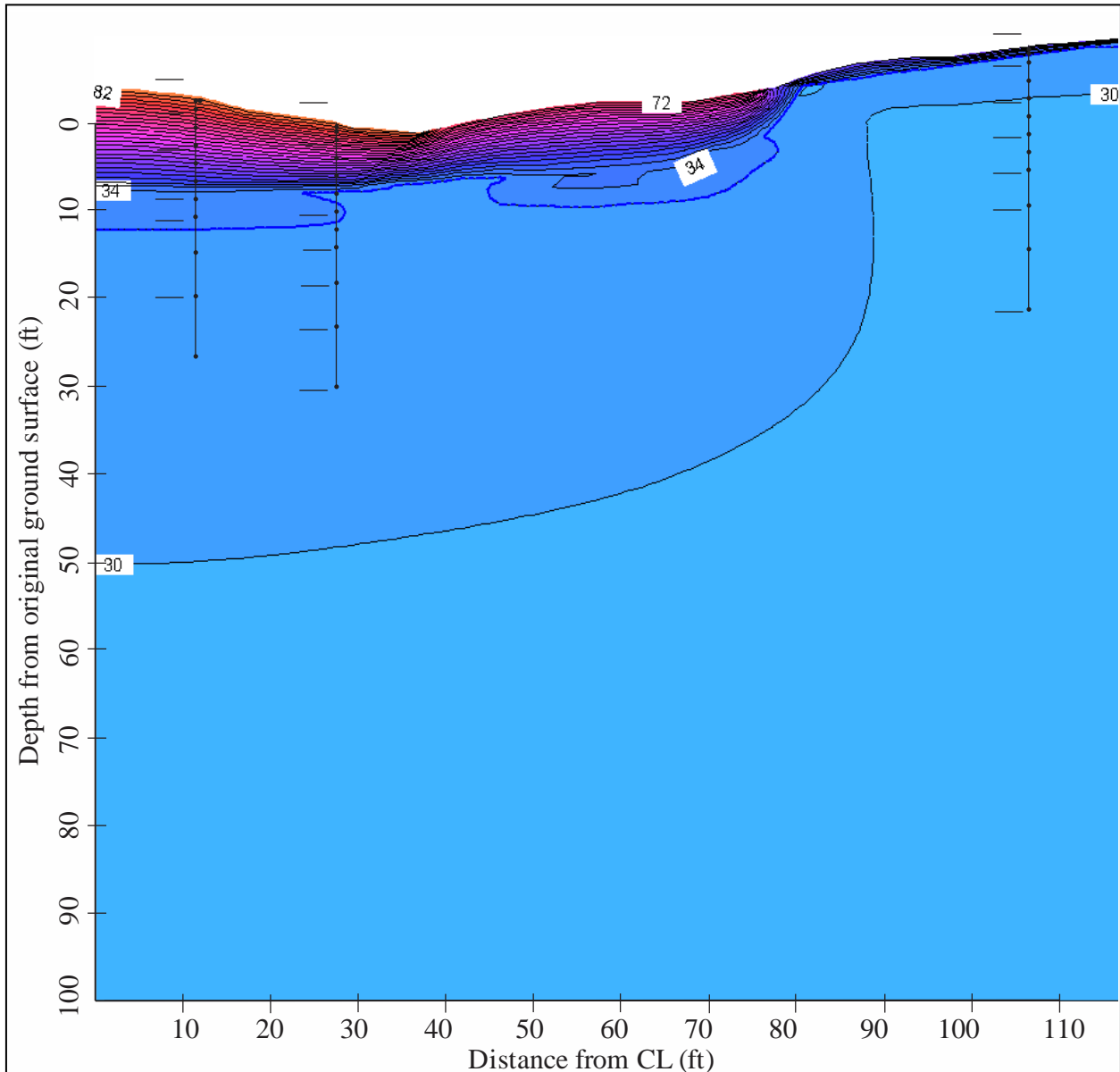
Figure 5.71. Thermal modeling results for July 1st, Run 3, Dalton Highway 9 Mile Hill research site. The phase change isotherm is represented as the dashed blue line and the temperature results are shown with a 2°F contour interval. Temperatures at the site were not yet measured for July 1st.
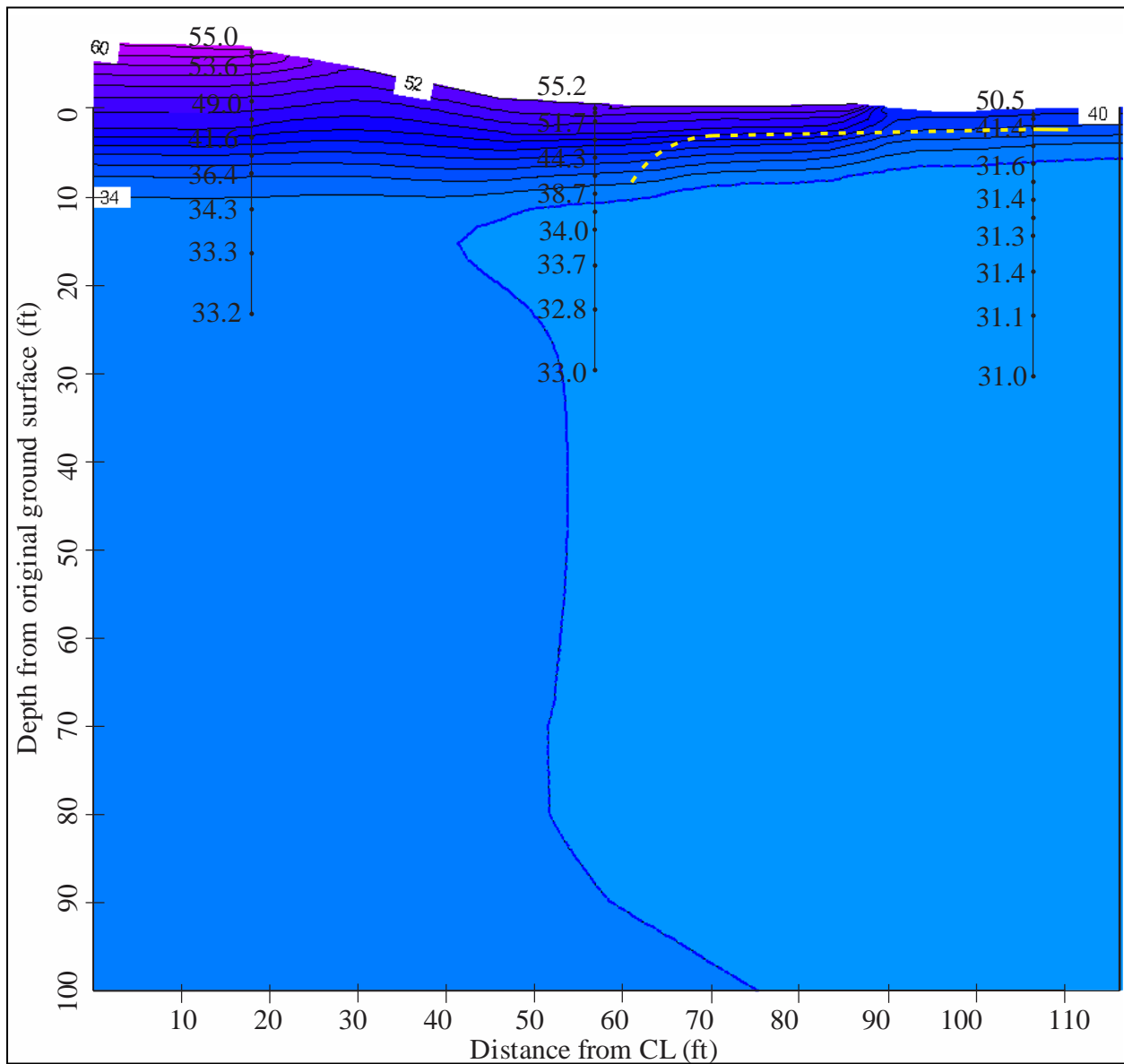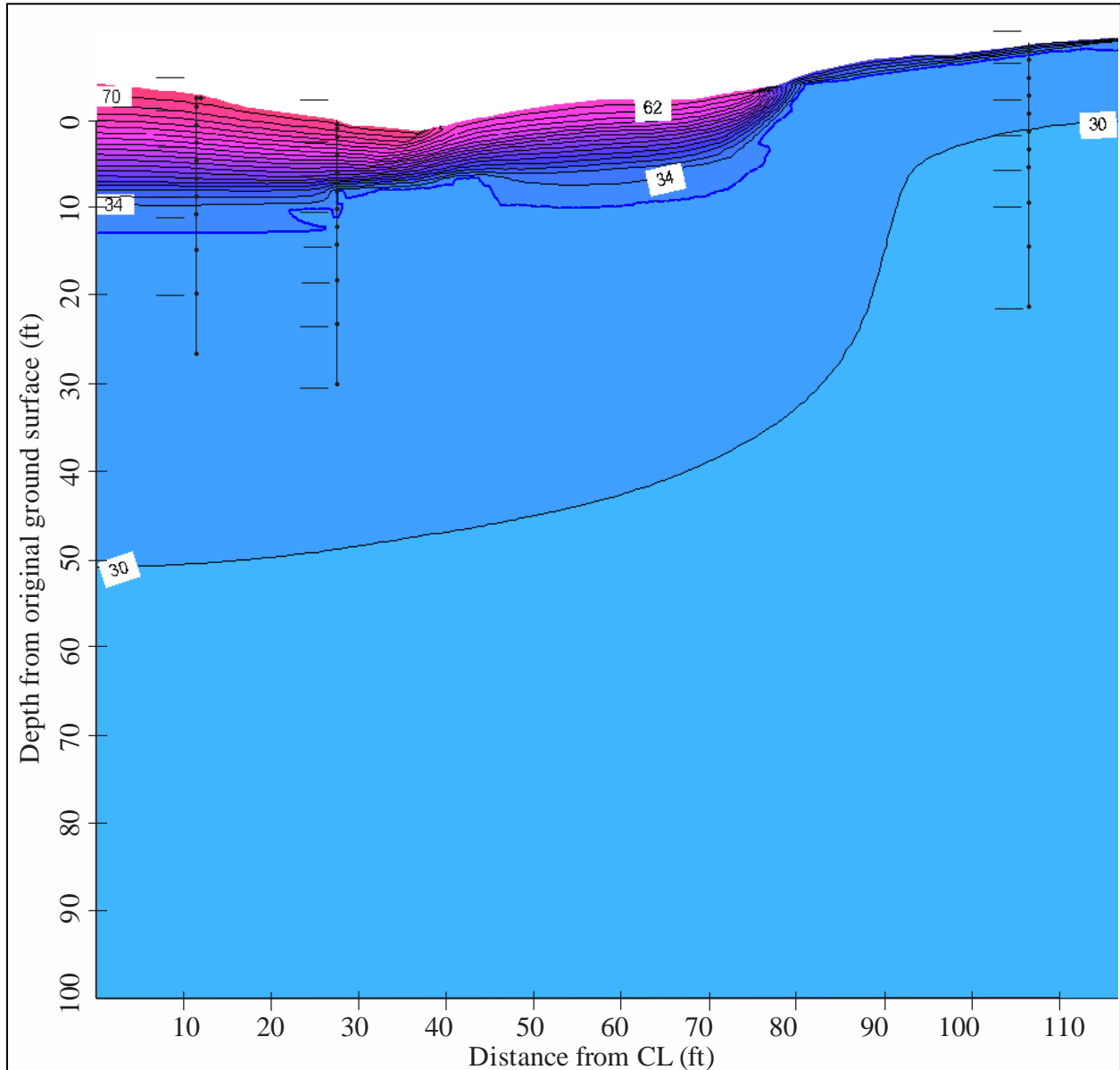
Figure 5.72. Thermal modeling results for August 1st, Run 3, Dalton Highway 9 Mile Hill research site. The phase change isotherm is represented as the dashed blue line and the temperature results are shown with a 2°F contour interval. Temperatures at the site were not yet measured for August 1st.
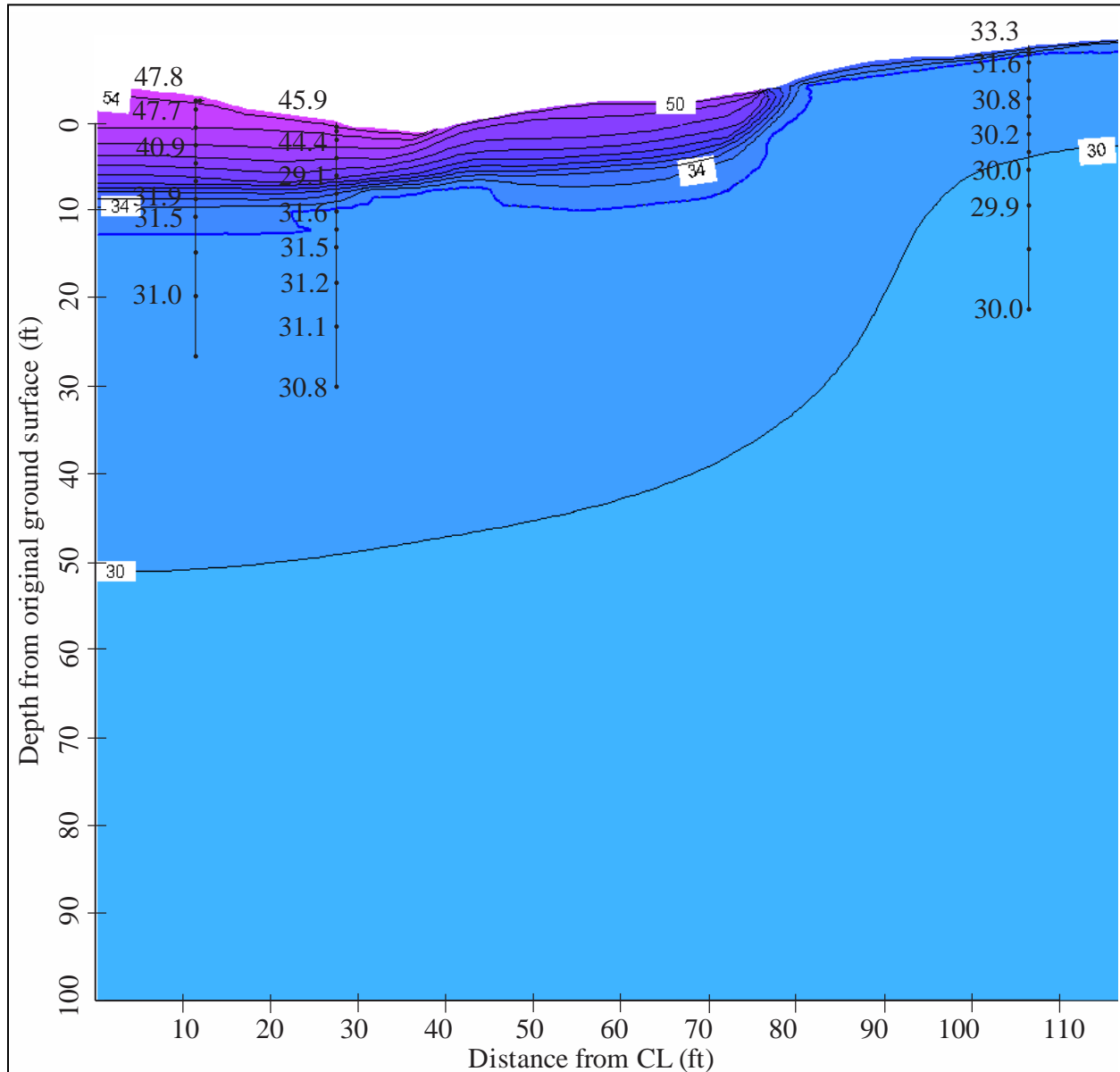
Figure 5.73. Thermal modeling results for September 1st, Run 3, Dalton Highway 9 Mile Hill research site. The phase change isotherm is represented as the dashed blue line and the temperature results are shown with a 2°F contour interval. Some of the measured temperatures along each thermistor string are shown in black text superimposed on the contours.
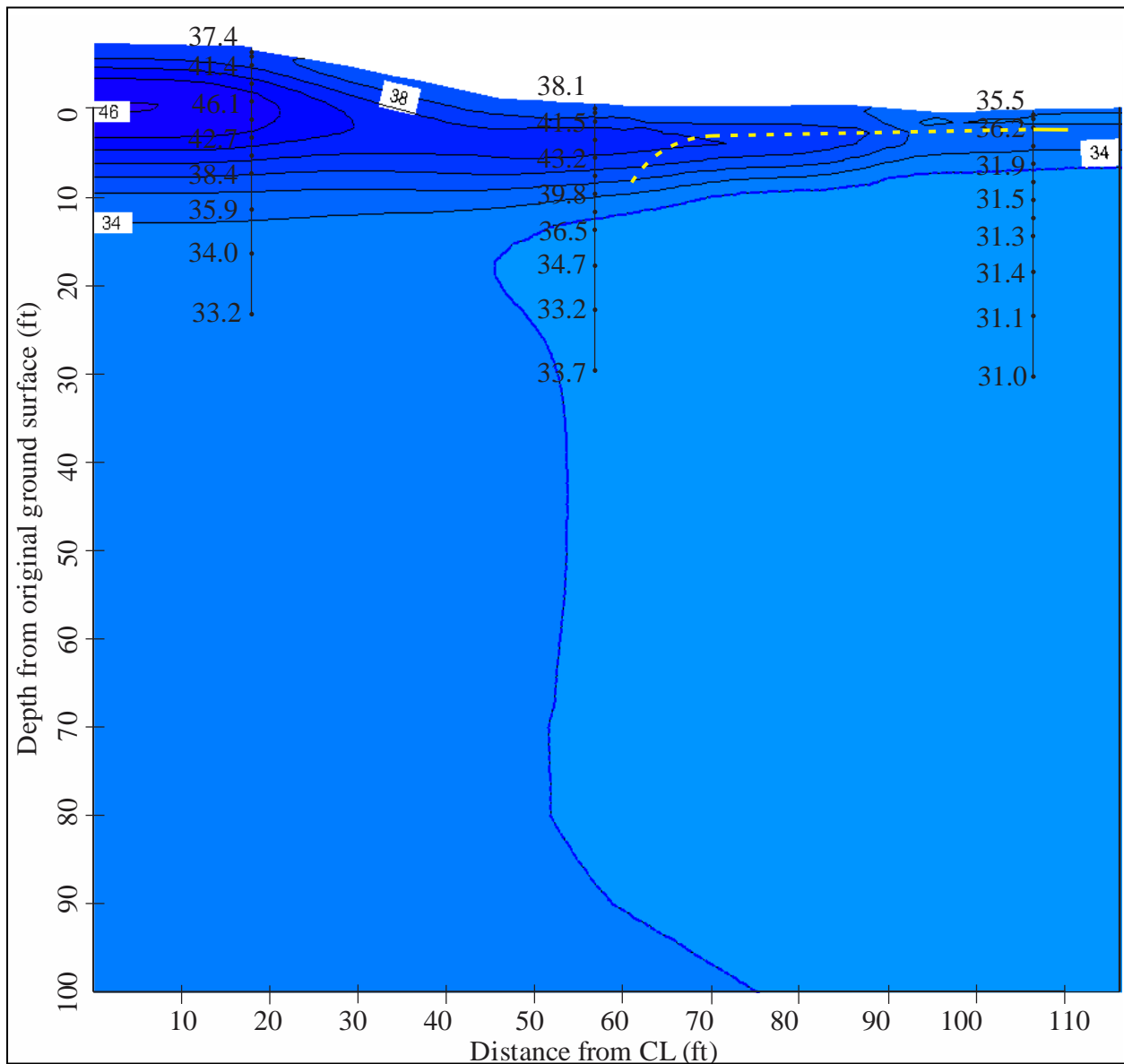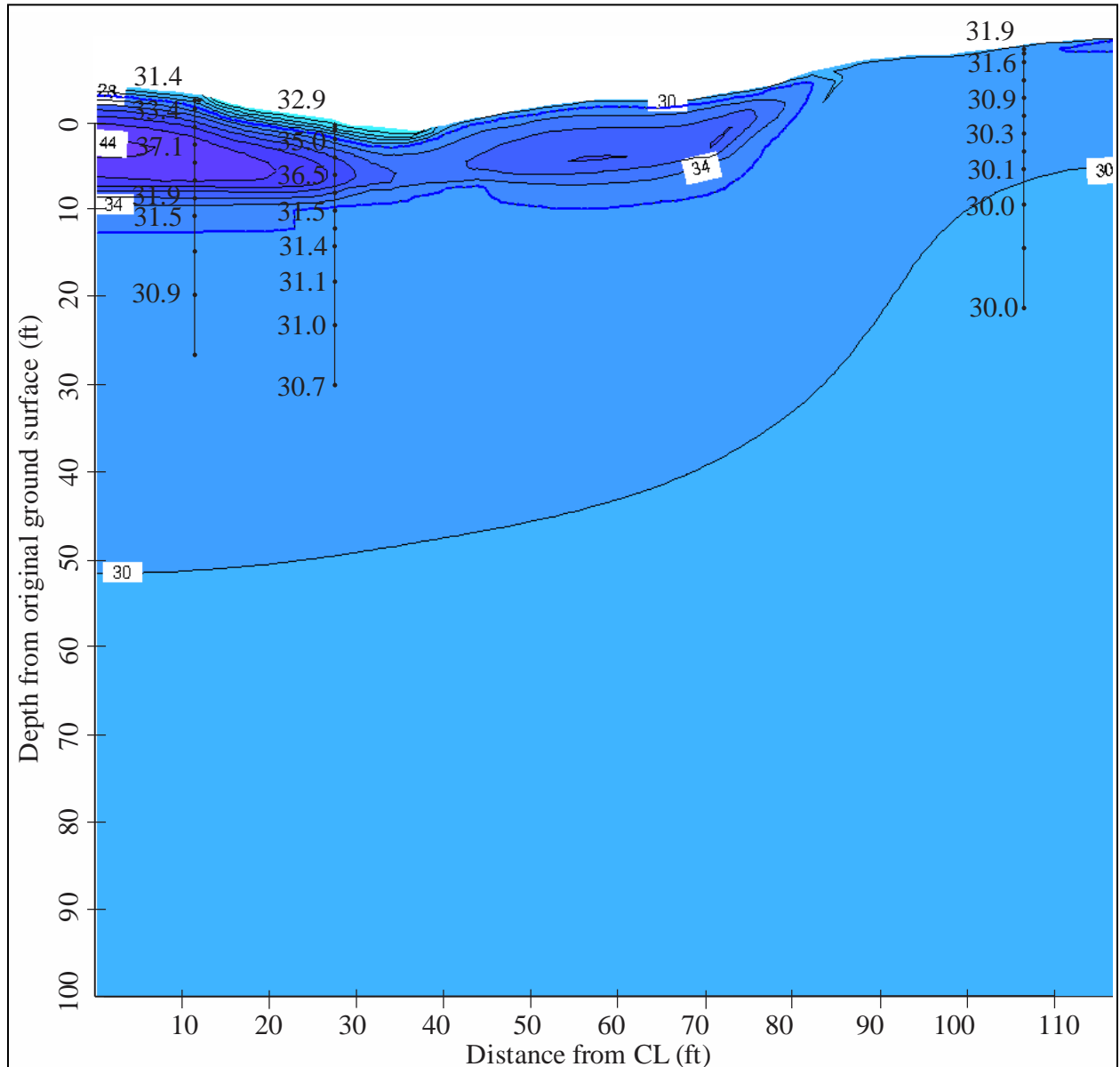
Figure 5.74. Thermal modeling results for October 1st, Run 3, Dalton Highway 9 Mile Hill research site. The phase change isotherm is represented as the dashed blue line and the temperature results are shown with a 2°F contour interval. Some of the measured temperatures along each thermistor string are shown in black text superimposed on the contours.
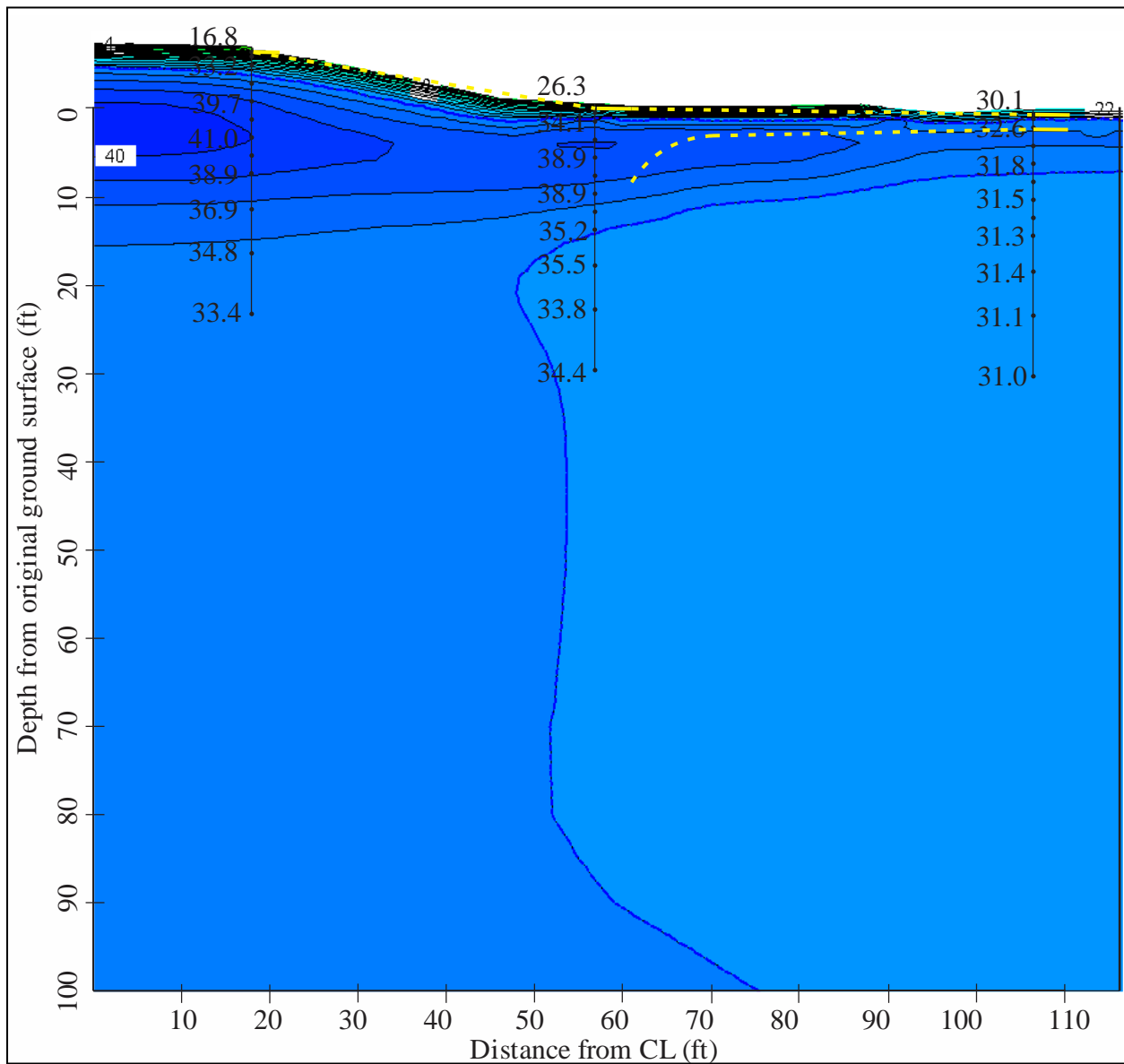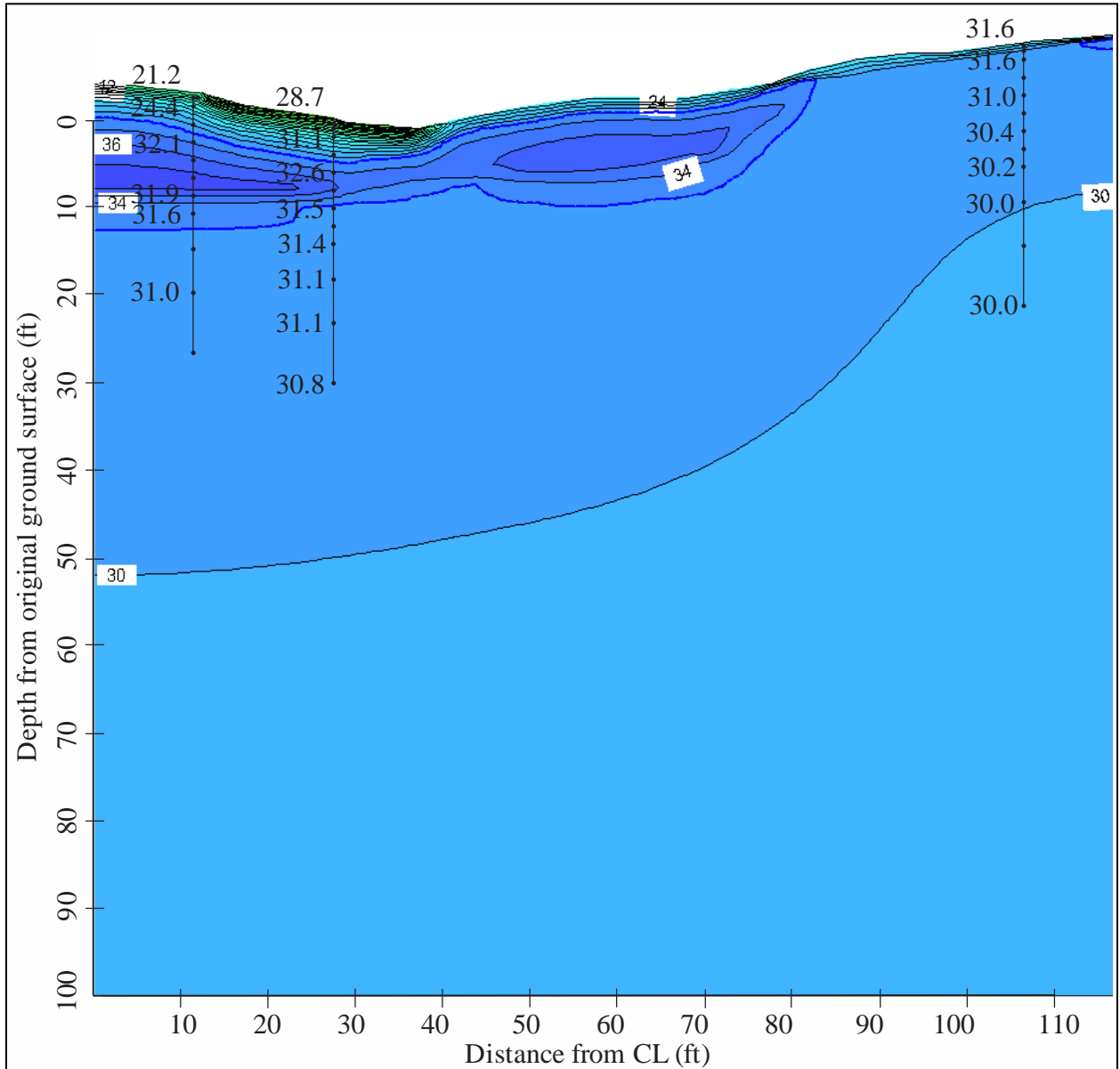
Figure 5.75. Thermal modeling results for November 1st, Run 3, Dalton Highway 9 Mile Hill research site. The phase change isotherm is represented as the dashed blue line and the temperature results are shown with a 2°F contour interval. Some of the measured temperatures along each thermistor string are shown in black text superimposed on the contours.
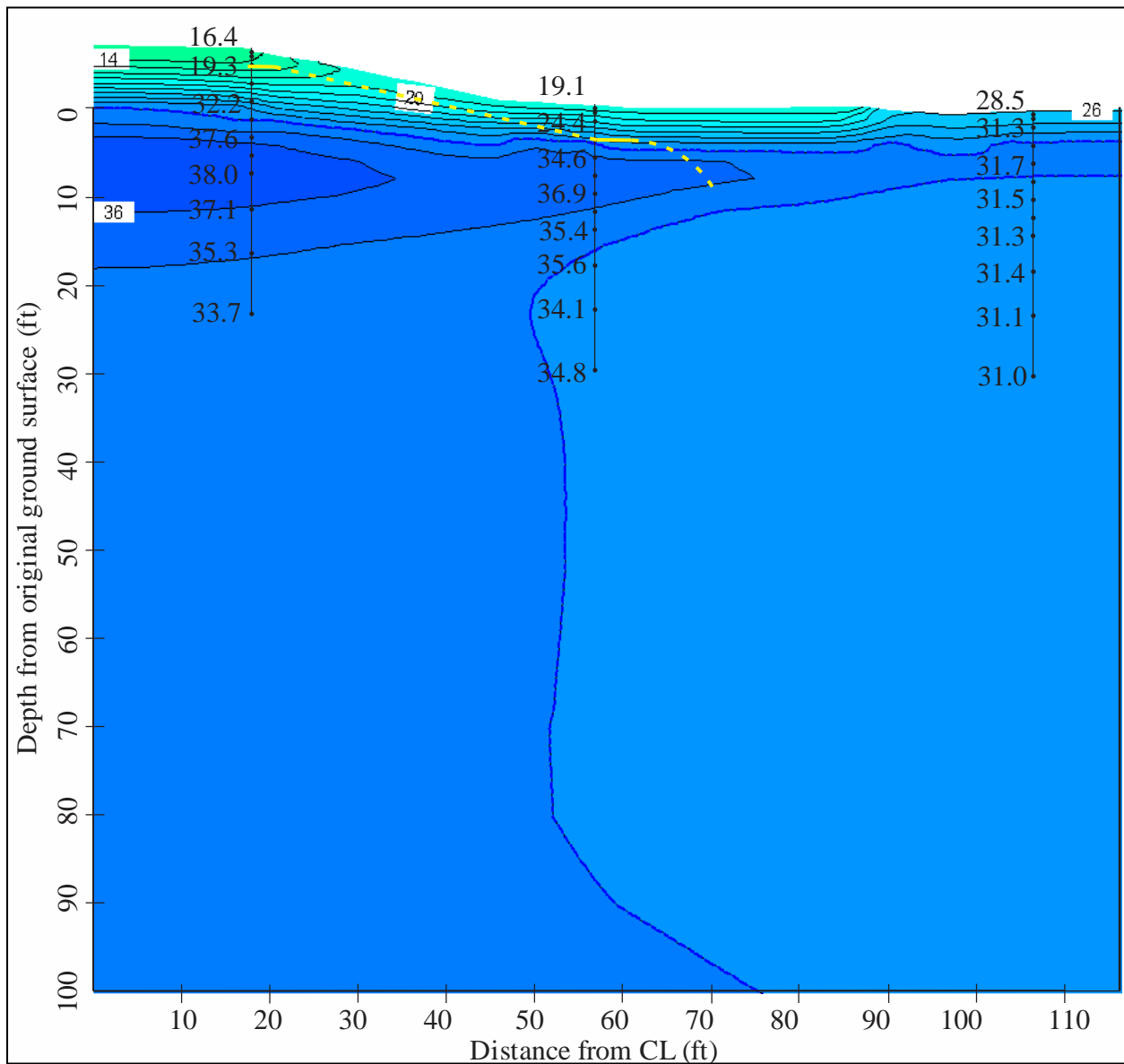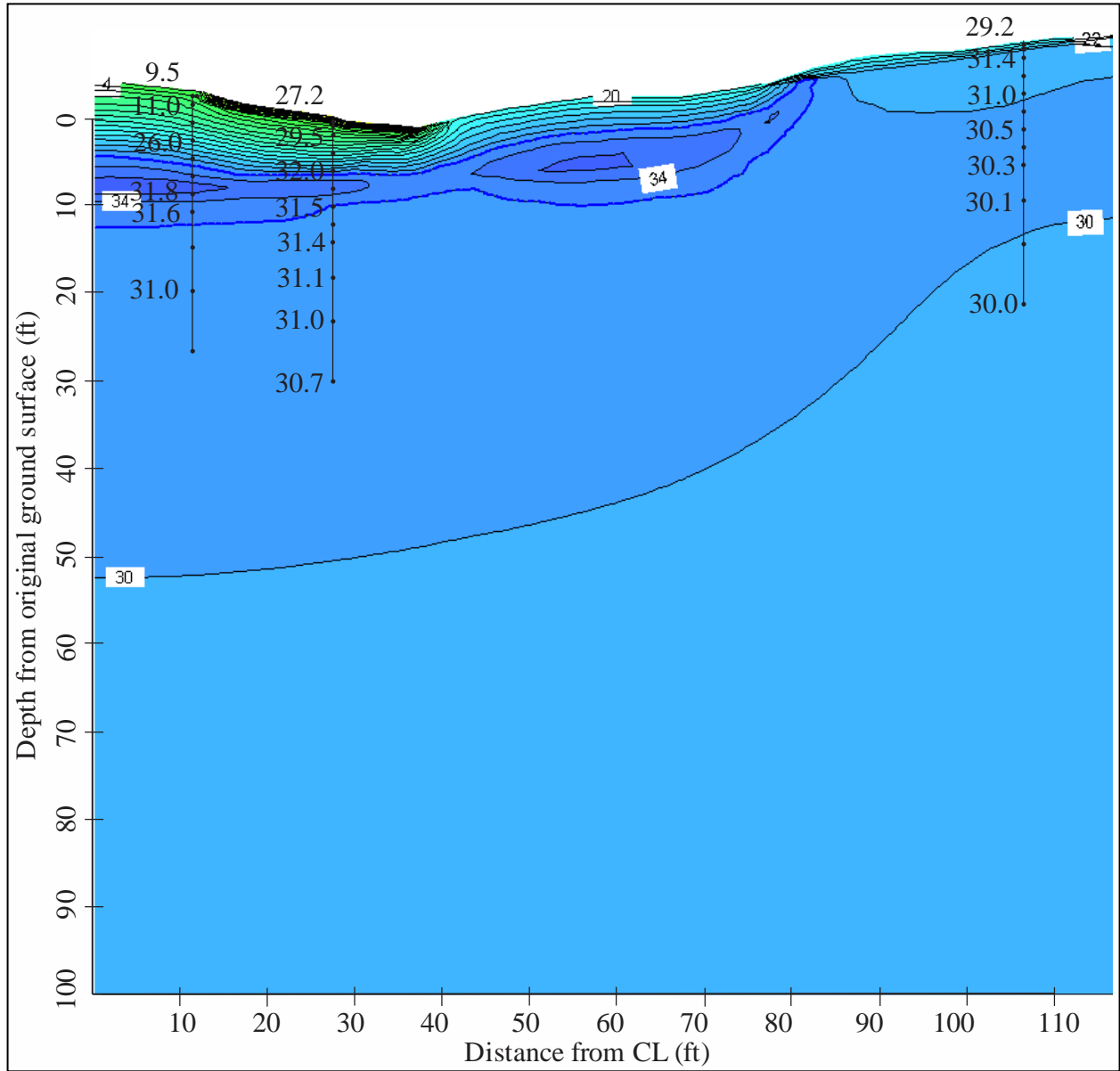
Figure 5.76. Thermal modeling results for December 1st, Run 3, Dalton Highway 9 Mile Hill research site. The phase change isotherm is represented as the dashed blue line and the temperature results are shown with a 2°F contour interval. Some of the measured temperatures along each thermistor string are shown in black text superimposed on the contours.

other for the rest of the year. Between the depths of 11.5 ft and 23.5 ft, the model is on average 1.6°F warmer than the measured temperatures. For the surface, the biggest discrepancy is in May and June, when the modeled temperatures are warmer by nearly 20°F; otherwise, the modeled surface temperatures are within 10°F of the measured temperatures.

The model results from Run 3 suggest that there is a thaw bulb under the highway embankment and the cleared area next to the highway that persists throughout the winter reaching a maximum depth of 16 feet under the shoulder and approximately 12 feet under the toe; however, the measured temperatures indicate that the active layer completely freezes by December. This model iteration overestimates the depth of thaw by as much as 4 ft below the embankment. For the undisturbed location, the modeled active layer depth reaches a maximum in September of 1.6 ft, which is within the range suggested by the measured temperatures. The development of the thaw bulb in Run 3 may be attributed to incorrect n-factors applied over the surfaces of the embankment and previously cleared area.

In an attempt to better match the modeled depth of thaw to that measured, the n-factors were adjusted in Run 4. While in all preceding model iterations an estimated input parameter was replaced with that either measured at the site or from soils obtained at the site, this model iteration is the first where an estimated parameter was replaced with another estimated parameter in an effort to fine-tune the model. The adjusted n-factors used in Run 4 are listed in Table 5.10. These values were chosen based on analysis of the surface temperatures in the previous model results. With the exception of the adjusted n-factors, Run 4 was similar to Run 3. The model results are presented in Figures 5.77 through 5.88. The measured and modeled temperatures for each of the selected depths were compared, and these comparisons are tabulated in Appendix E. Additionally, Table 5.9 contains a summary of the phase change isotherm depths for this model iteration.

Table 5.10. Adjusted n-factors used in Run 4, Dalton Highway 9 Mile Hill research site

Surface	Original n-factors		Adjusted n-factors	
	n_t	n_f	n_t	n_f
Gravel road	1.5	0.9	1.1	0.7
Gravel slope	1.5	0.6	1.1	0.4
Cleared area	1.2	0.4	0.8	0.3
Spruce forest	0.37	0.29	0.32	0.2

Adjusting the n-factors resulted in more accurately modeled surface temperatures at the expense of accurately modeled temperatures at depth. The modeled temperatures below 10 ft were too cold on average by 1°F to 2°F for each of the thermistor locations. The modeled surface temperatures at the shoulder location improved, now being 27°F too cold in the winter and 6°F too warm in the summer. Additionally, the modeled shoulder surface temperatures are within approximately 5°F of the measured temperatures.

The change in n-factors also resulted in a more accurate thaw bulb configuration. While the modeled thaw bulb persists longer than what the measured temperatures suggest, the soil beneath
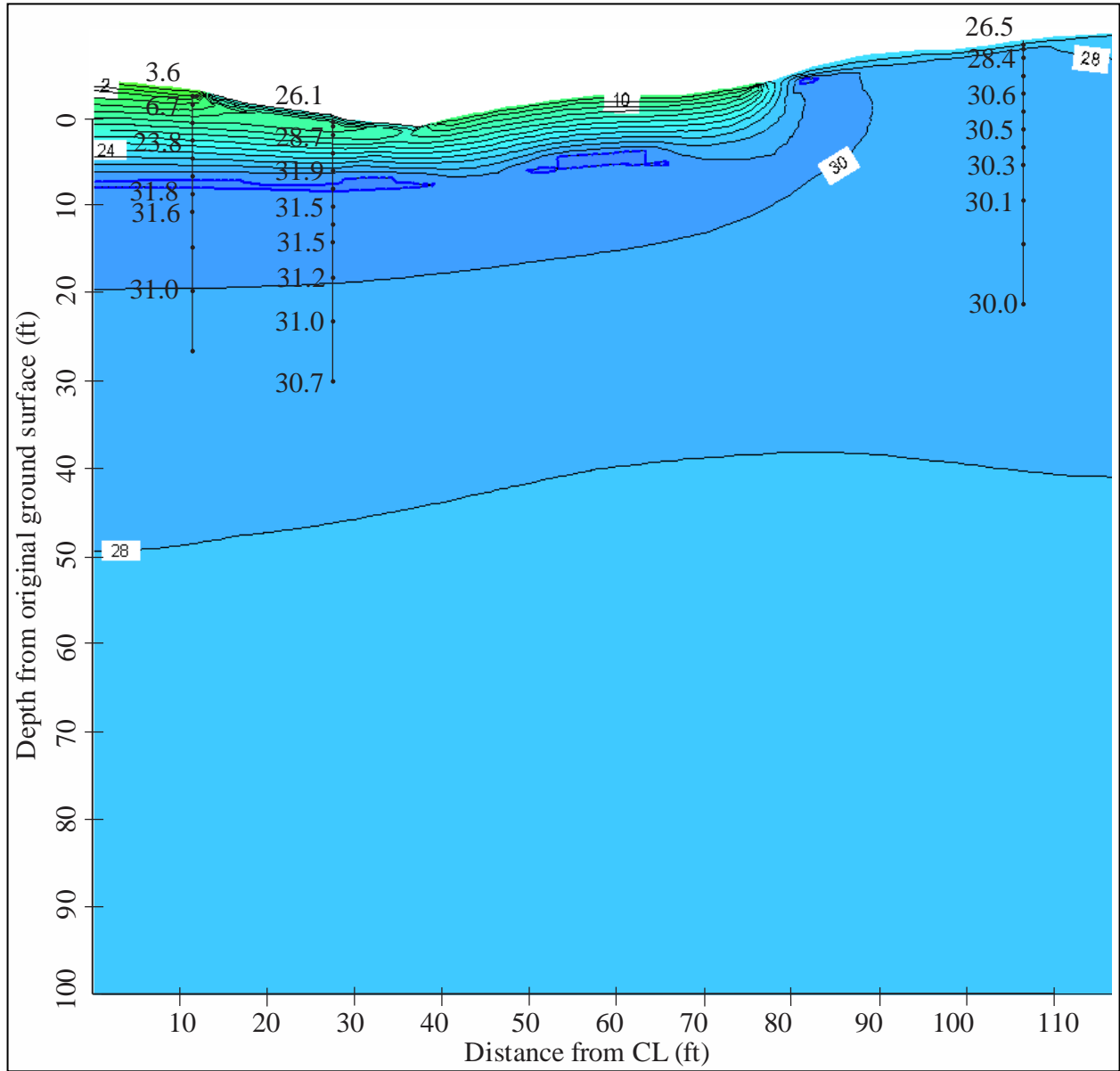
Figure 5.77. Thermal modeling results for January 1ˢᵗ, Run 4, Dalton Highway 9 Mile Hill research site. The phase change isotherm is represented as the dashed blue line and the temperature results are shown with a 2°F contour interval. Some of the measured temperatures along each thermistor string are shown in black text superimposed on the contours.
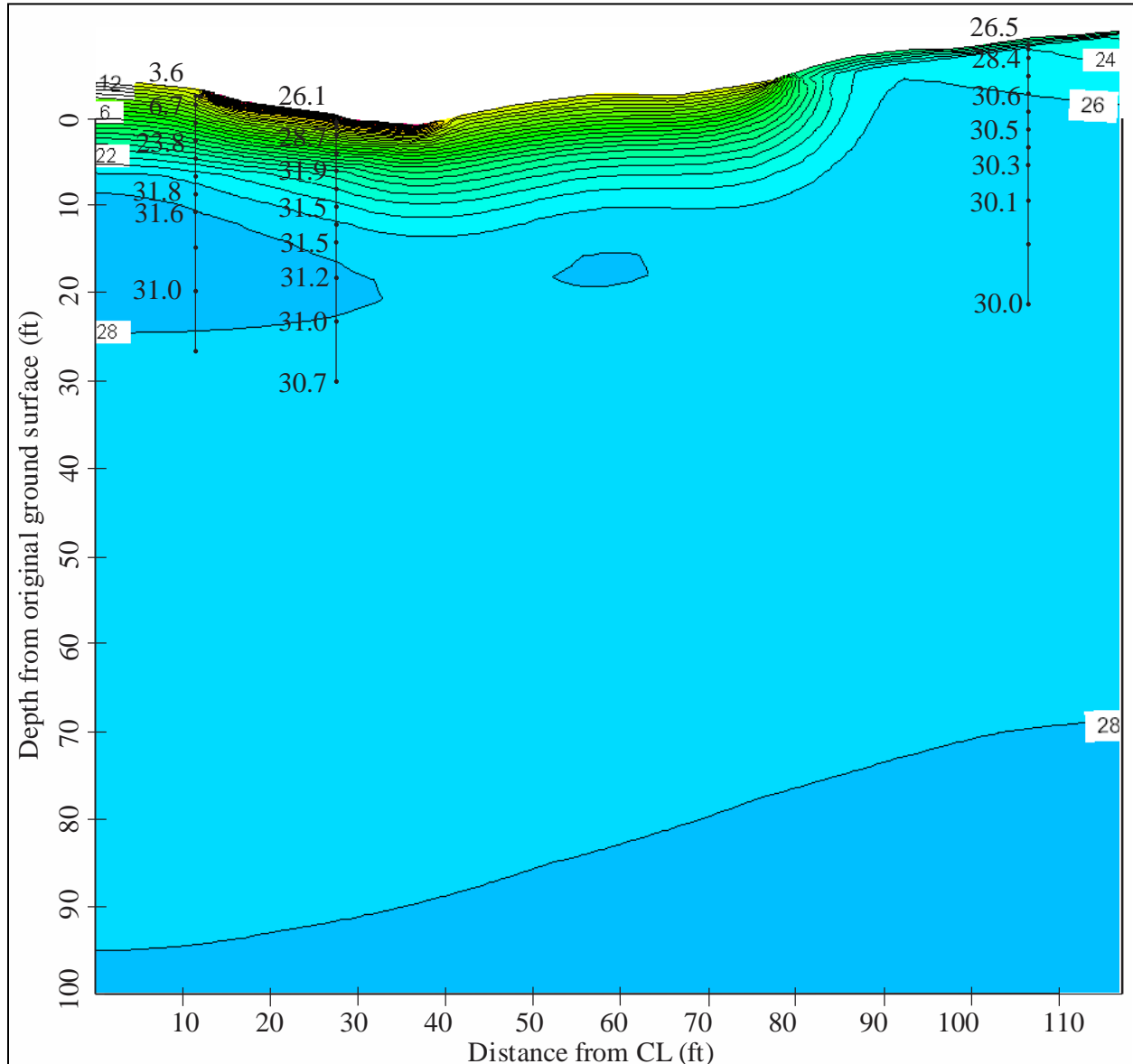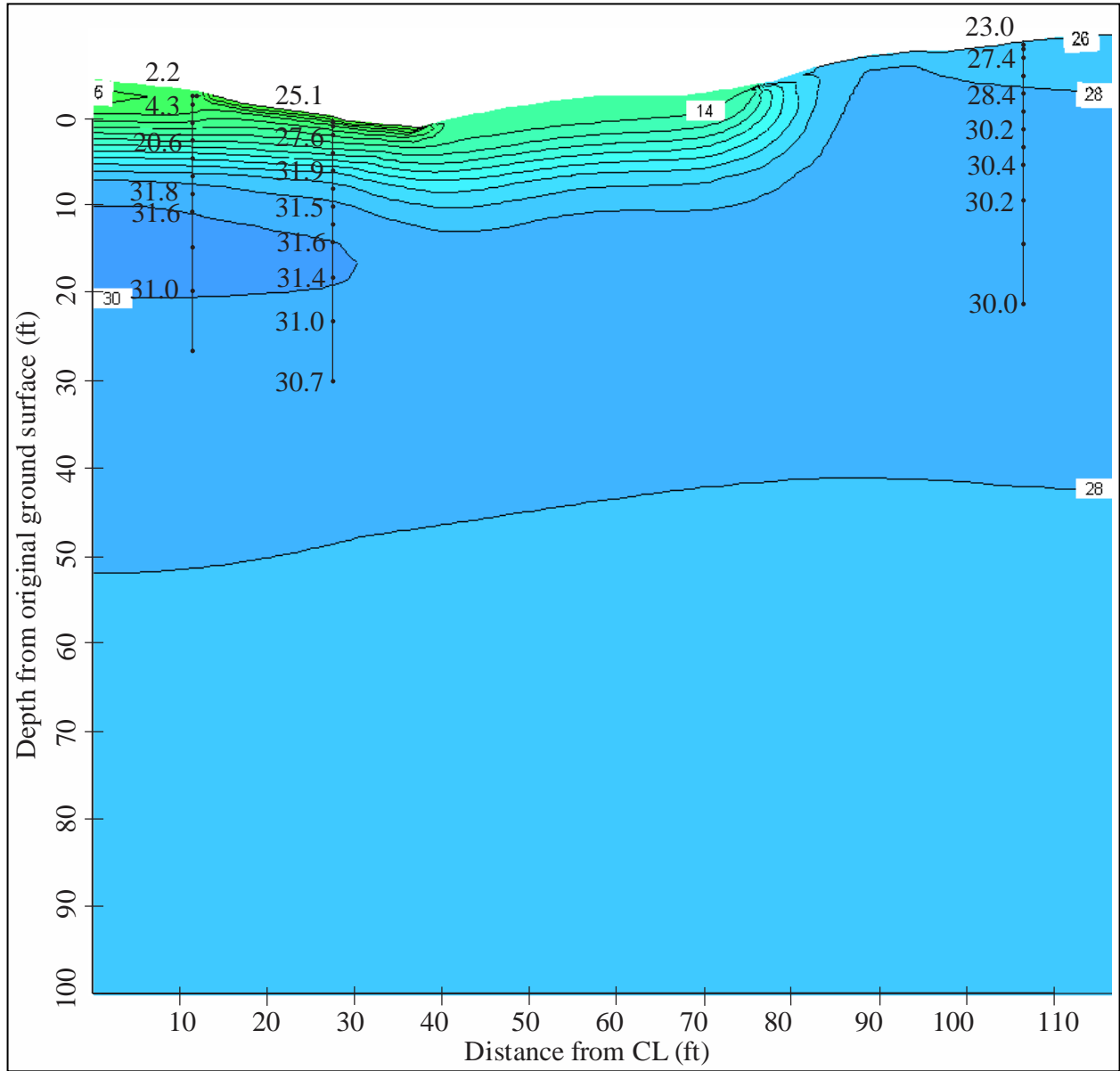
Figure 5.78. Thermal modeling results for February 1st, Run 4, Dalton Highway 9 Mile Hill research site. The phase change isotherm is represented as the dashed blue line and the temperature results are shown with a 2°F contour interval. Some of the measured temperatures along each thermistor string are shown in black text superimposed on the contours.
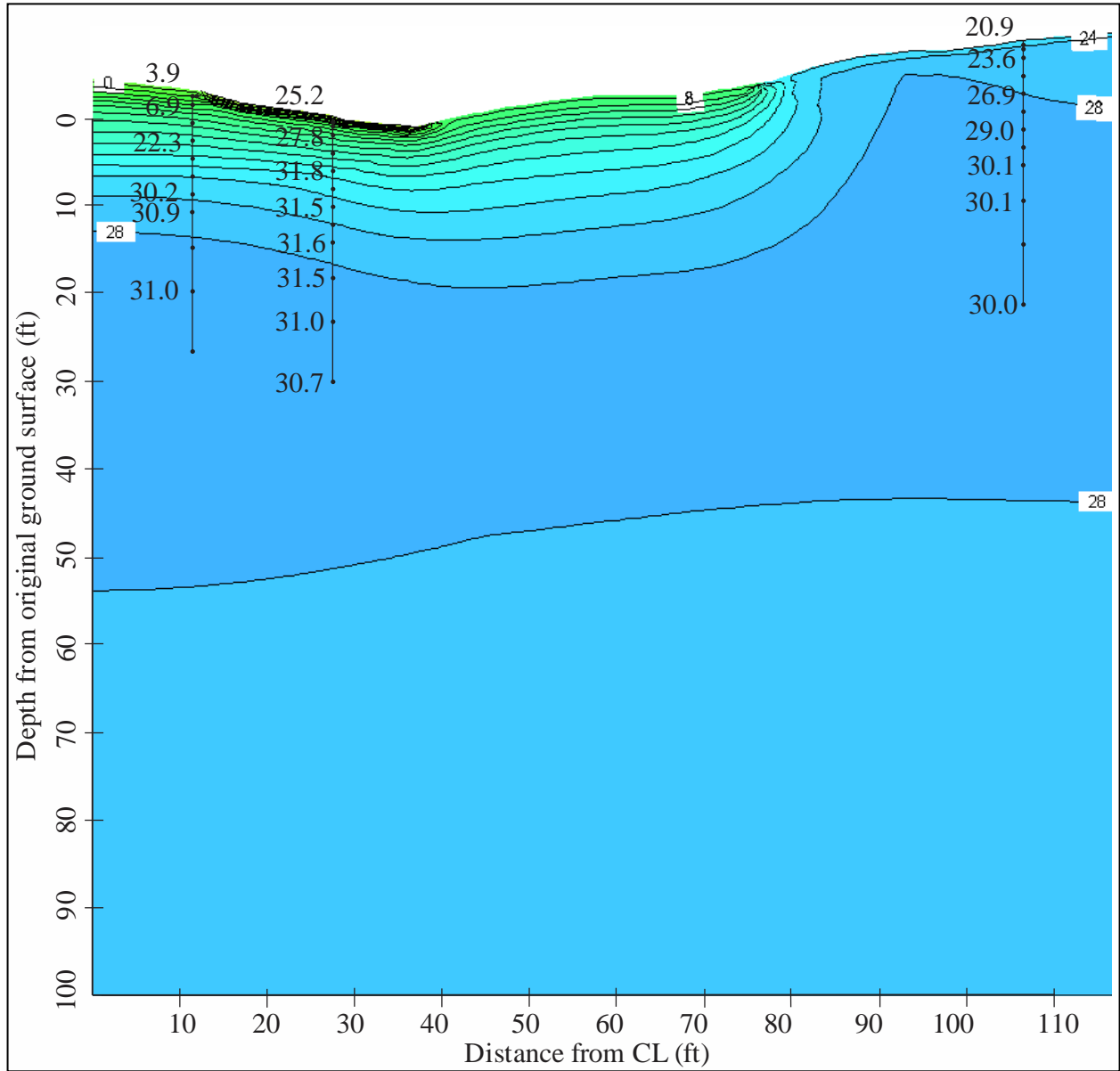
Figure 5.79. Thermal modeling results for March 1st, Run 4, Dalton Highway 9 Mile Hill research site. The phase change isotherm is represented as the dashed blue line and the temperature results are shown with a 2°F contour interval. Some of the measured temperatures along each thermistor string are shown in black text superimposed on the contours.
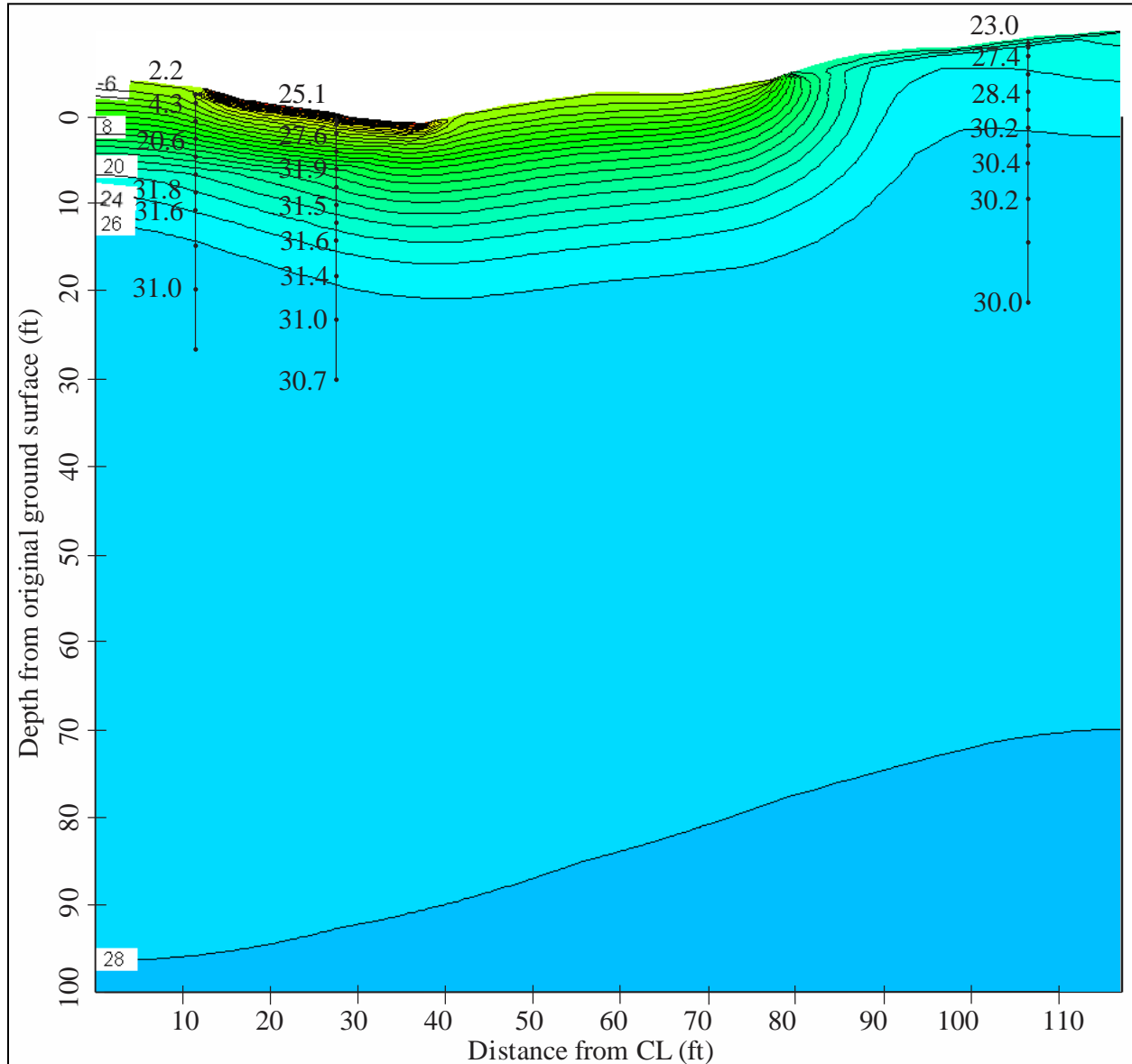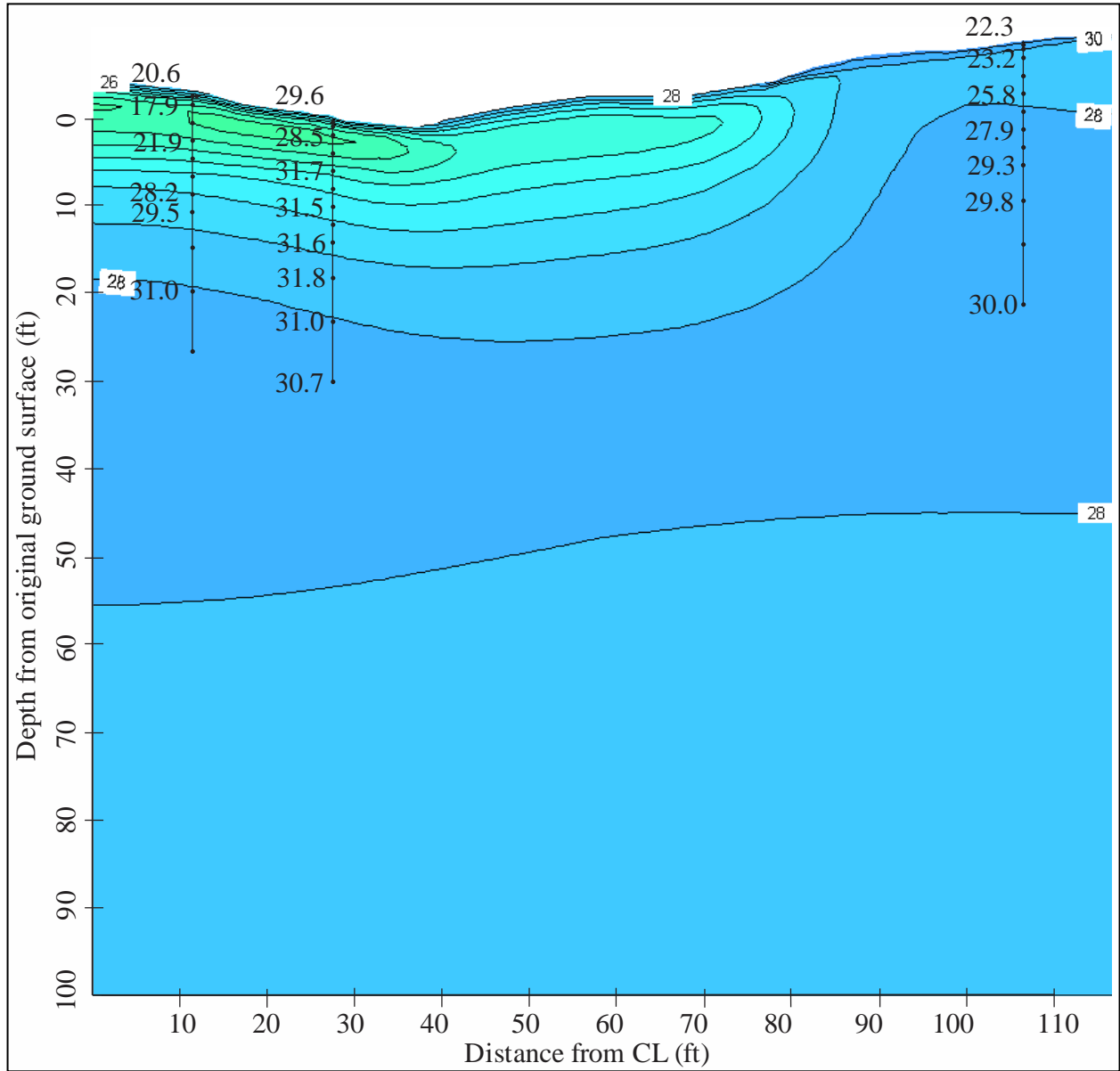
Figure 5.80. Thermal modeling results for April 1st, Run 4, Dalton Highway 9 Mile Hill research site. The phase change isotherm is represented as the dashed blue line and the temperature results are shown with a 2°F contour interval. Some of the measured temperatures along each thermistor string are shown in black text superimposed on the contours.
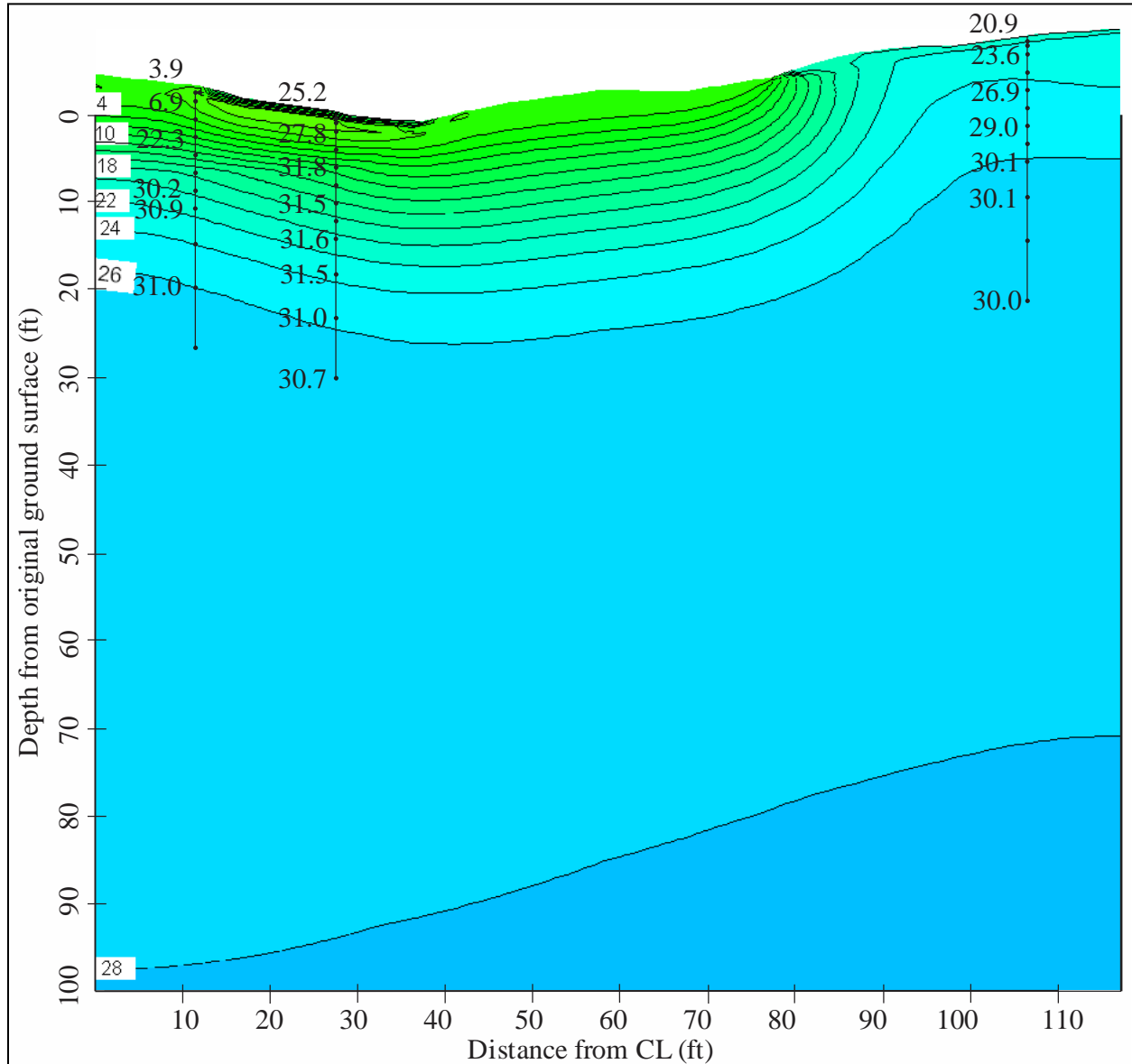
144
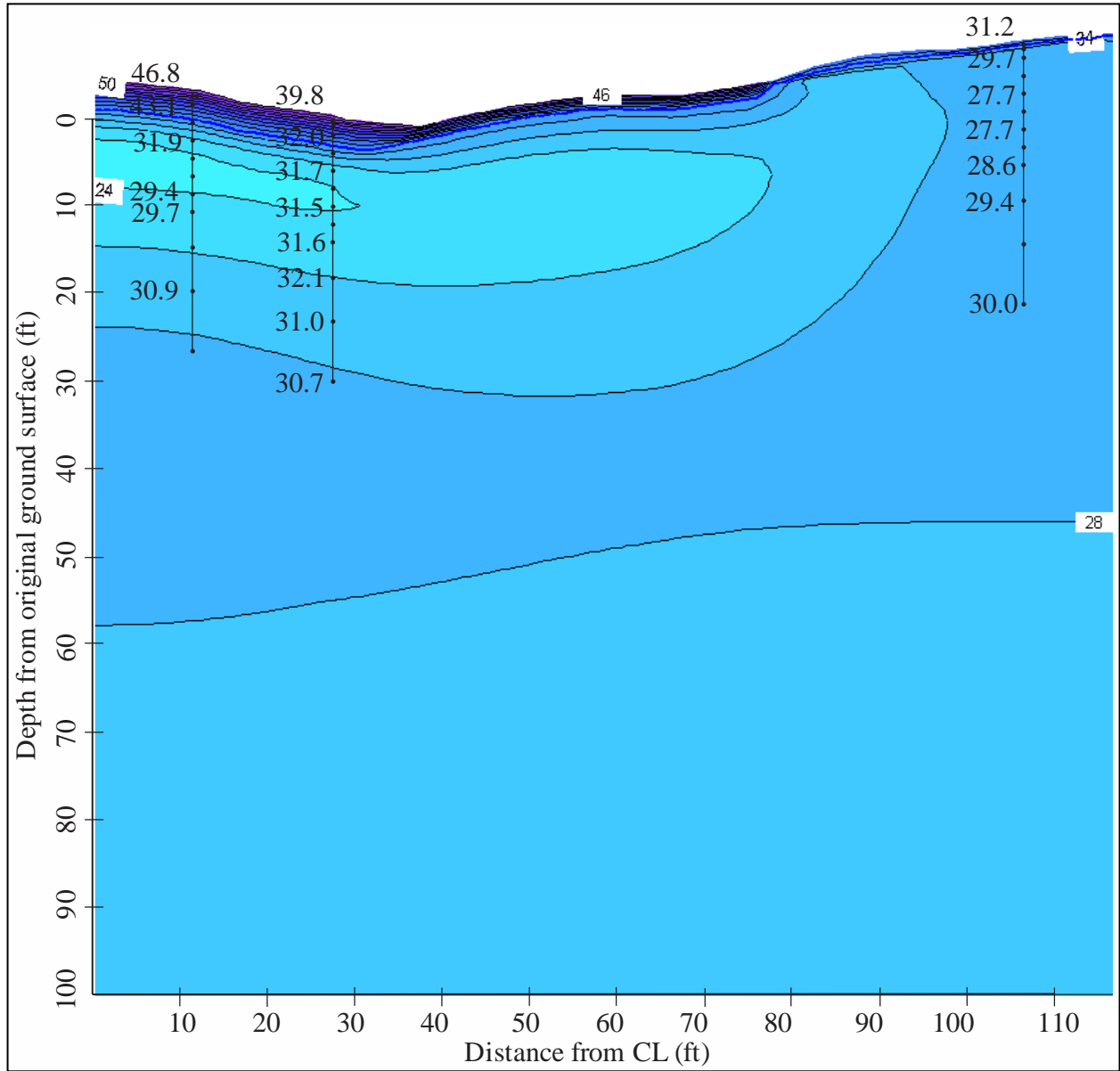
Figure 5.81. Thermal modeling results for May 1st, Run 4, Dalton Highway 9 Mile Hill research site. The phase change isotherm is represented as the dashed blue line and the temperature results are shown with a 2°F contour interval. Some of the measured temperatures along each thermistor string are shown in black text superimposed on the contours.
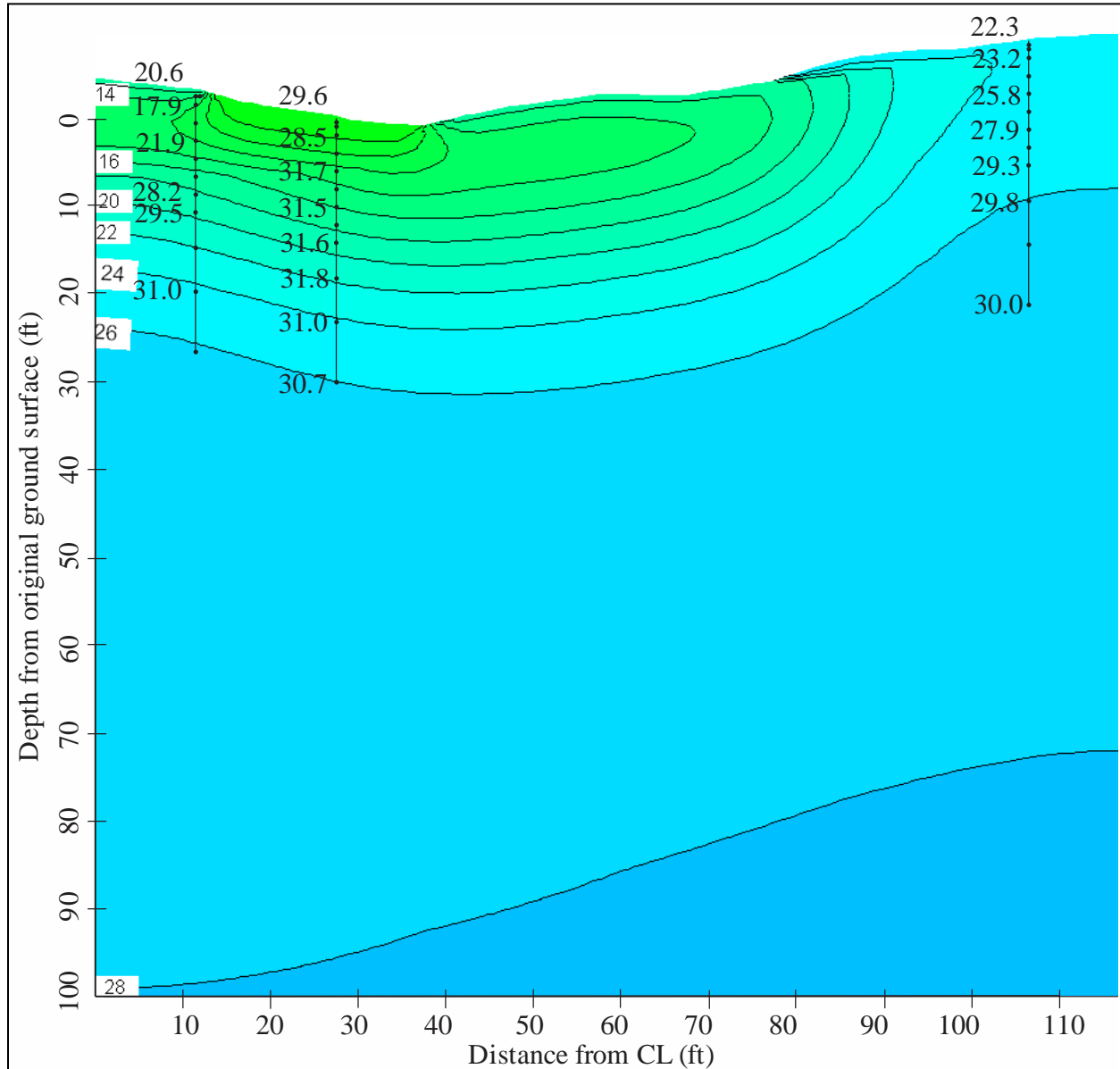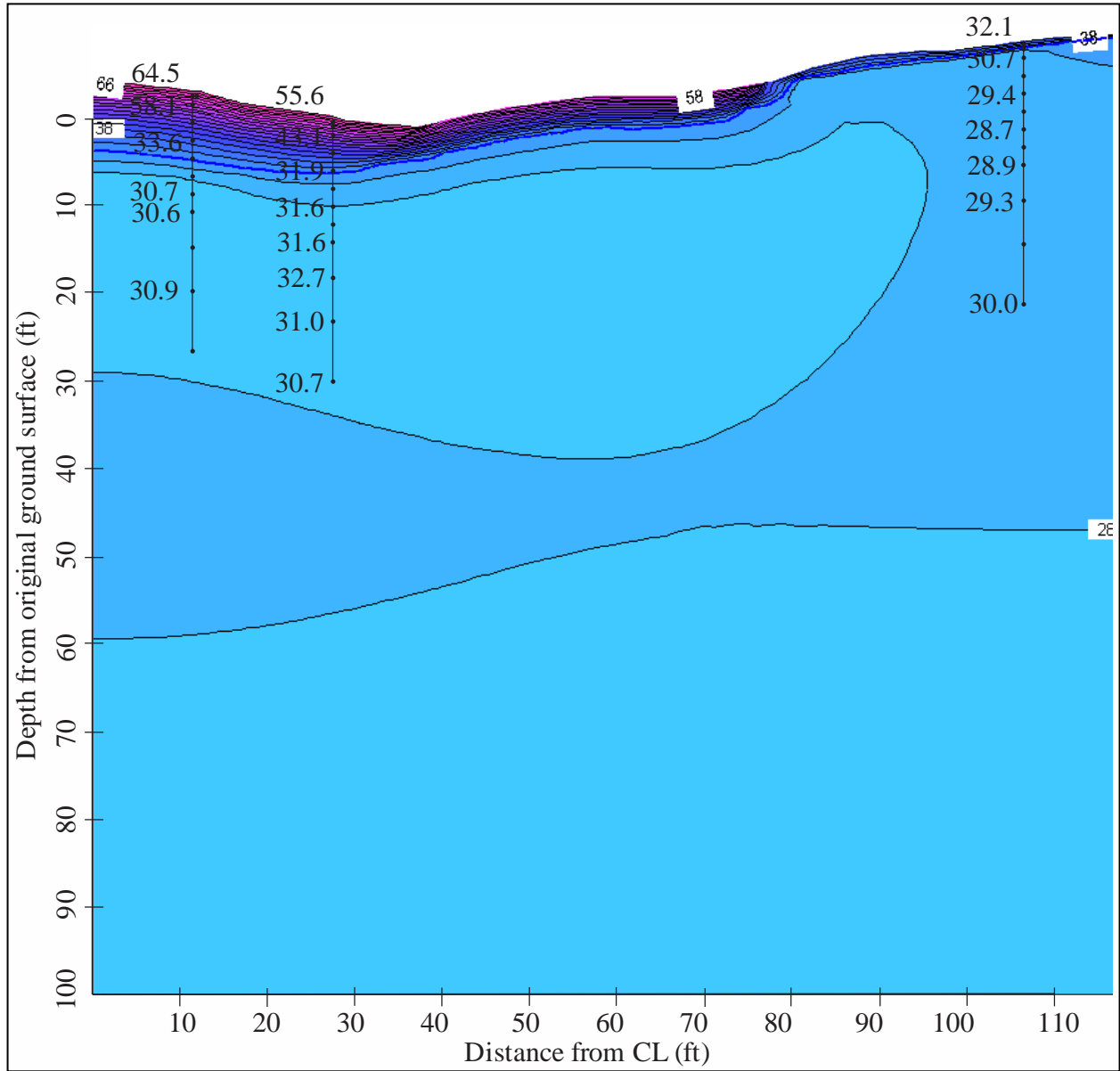
Figure 5.82. Thermal modeling results for June 1st, Run 4, Dalton Highway 9 Mile Hill research site. The phase change isotherm is represented as the dashed blue line and the temperature results are shown with a 2°F contour interval. Some of the measured temperatures along each thermistor string from May 29, 2010 are shown in black text superimposed on the contours.
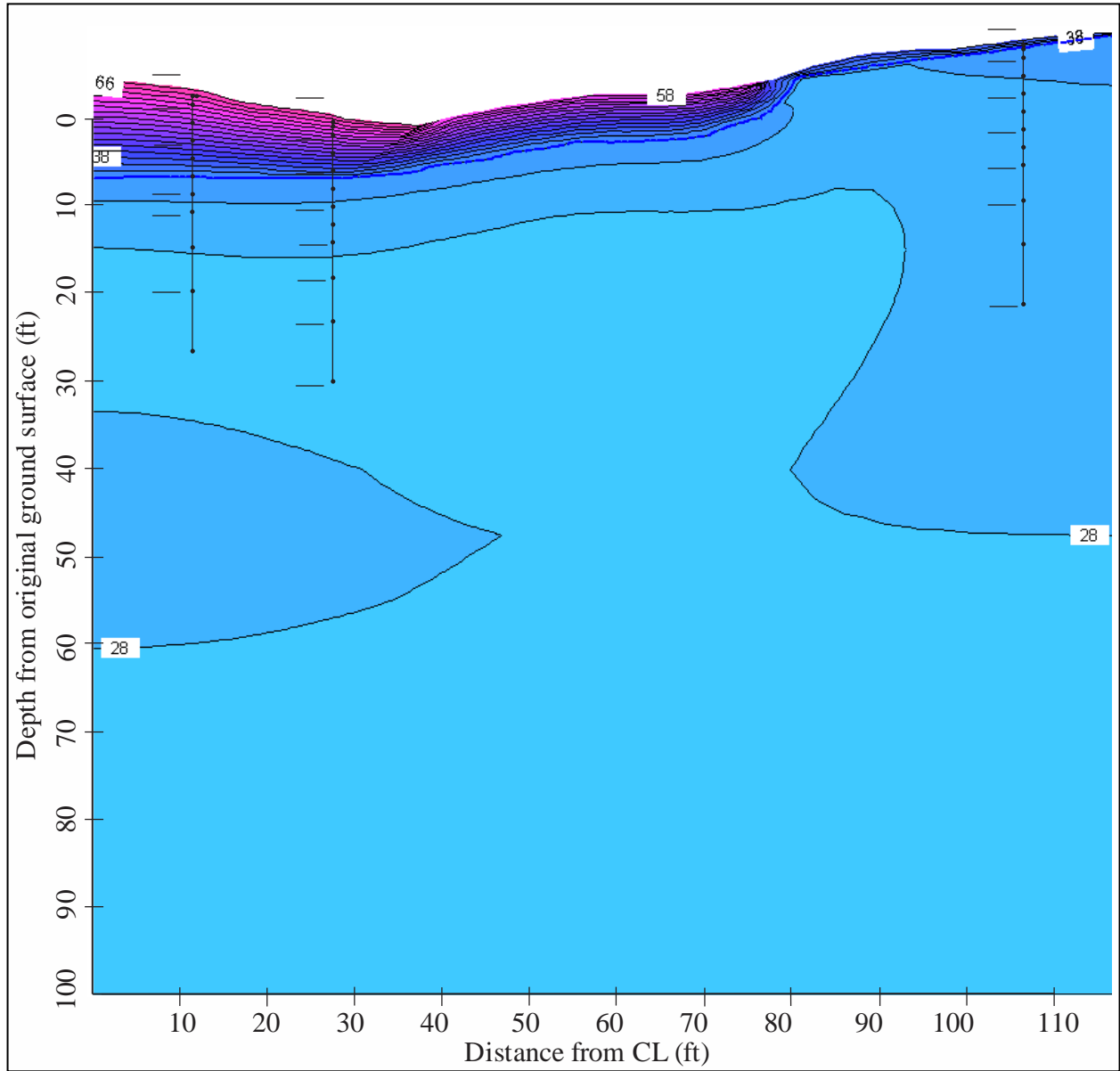
Figure 5.83. Thermal modeling results for July 1st, Run 4, Dalton Highway 9 Mile Hill research site. The phase change isotherm is represented as the dashed blue line and the temperature results are shown with a 2°F contour interval. Temperatures at the site were not yet measured for July 1st.
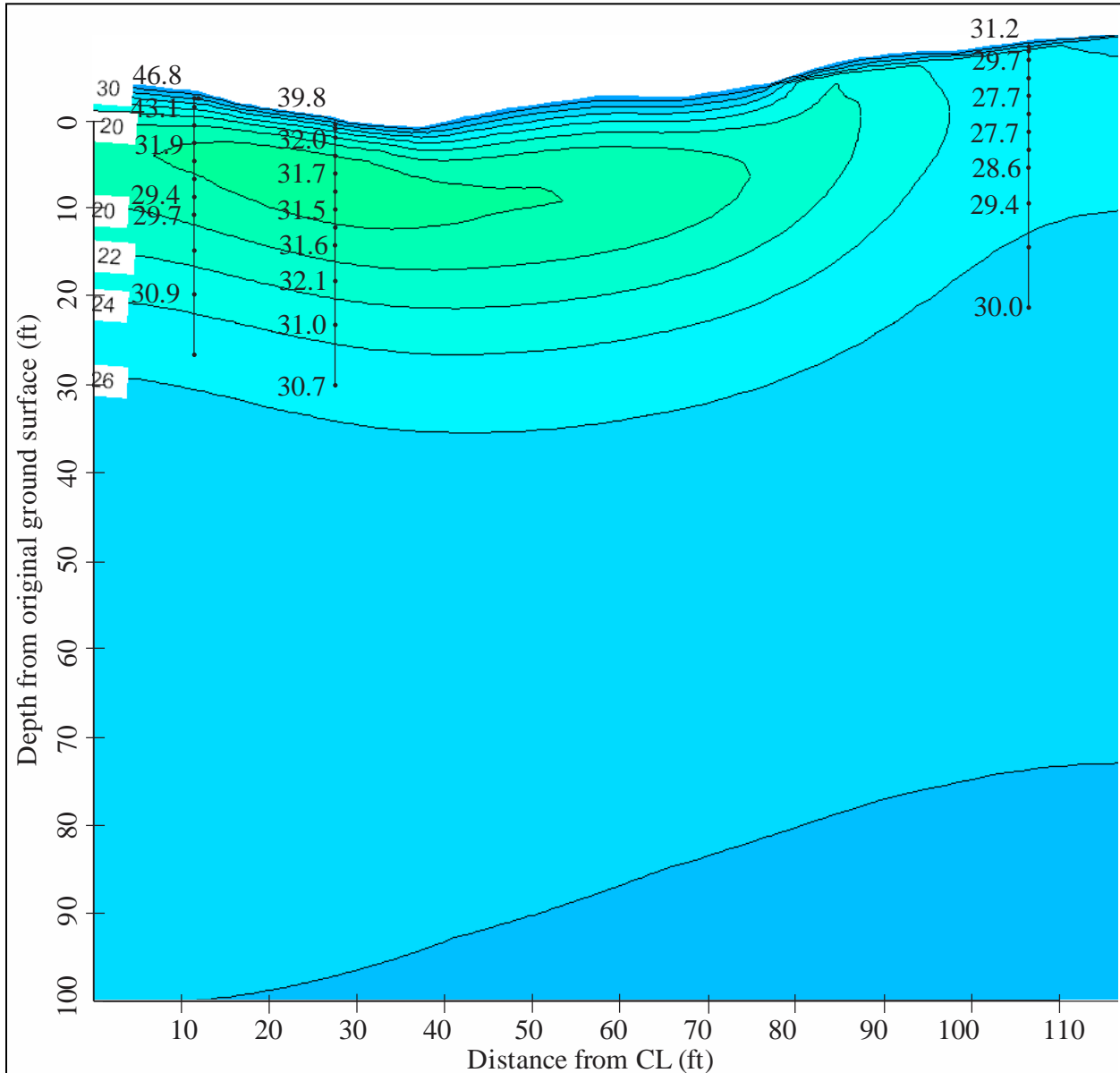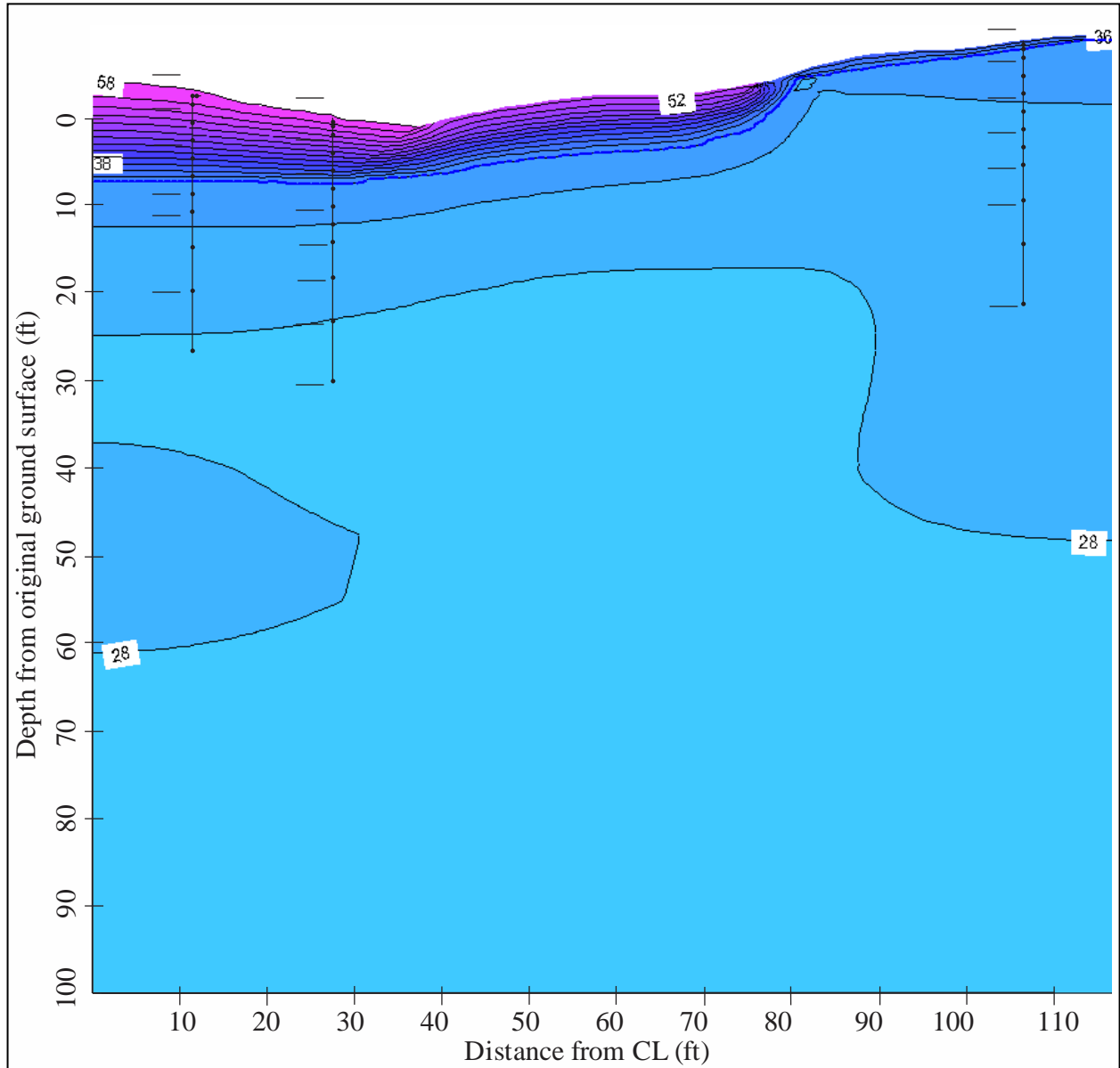
Figure 5.84. Thermal modeling results for August 1st, Run 4, Dalton Highway 9 Mile Hill research site. The phase change isotherm is represented as the dashed blue line and the temperature results are shown with a 2°F contour interval. Temperatures at the site were not yet measured for July 1st.
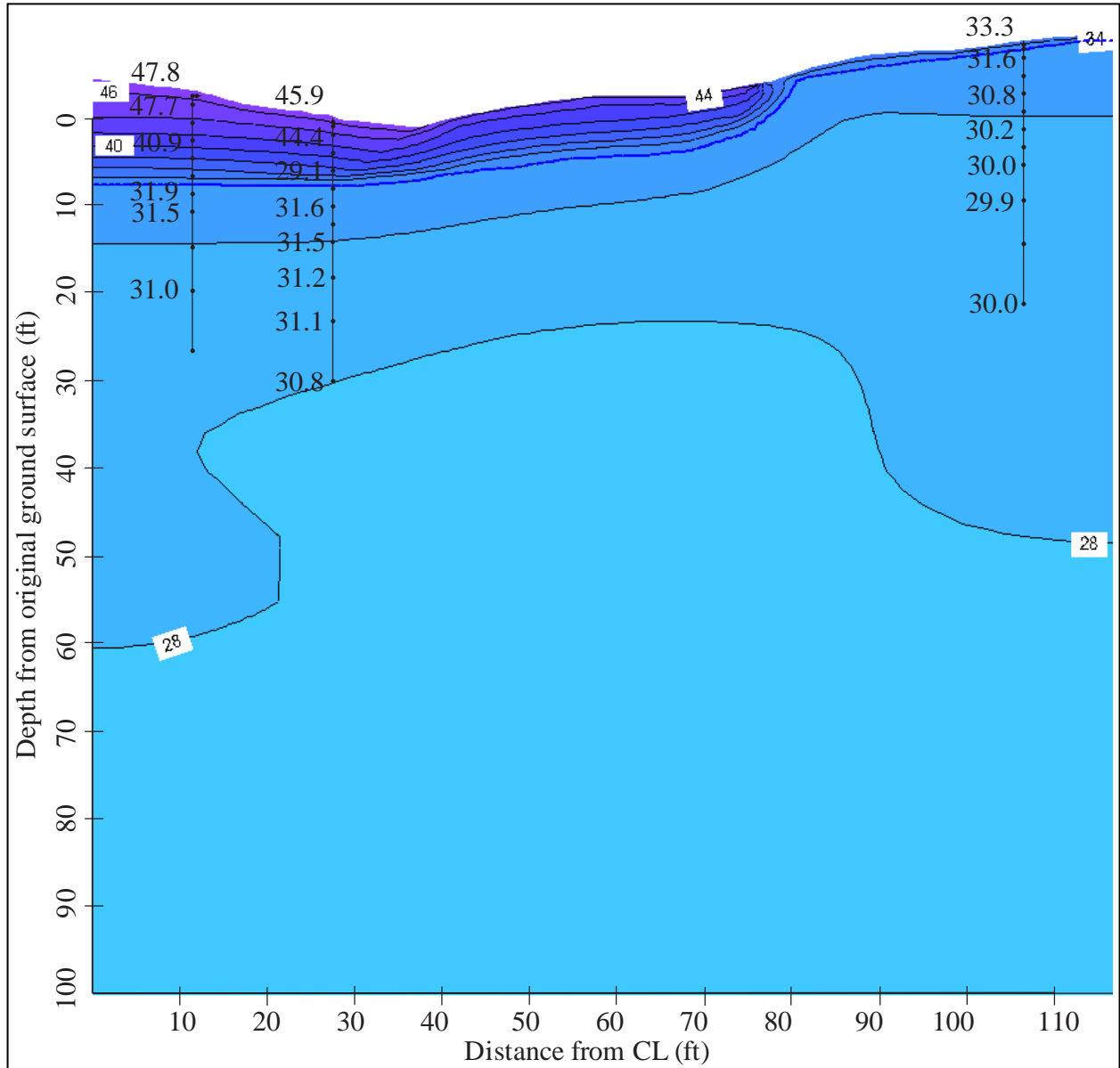
Figure 5.85. Thermal modeling results for September 1st, Run 4, Dalton Highway 9 Mile Hill research site. The phase change isotherm is represented as the dashed blue line and the temperature results are shown with a 2°F contour interval. Some of the measured temperatures along each thermistor string are shown in black text superimposed on the contours.
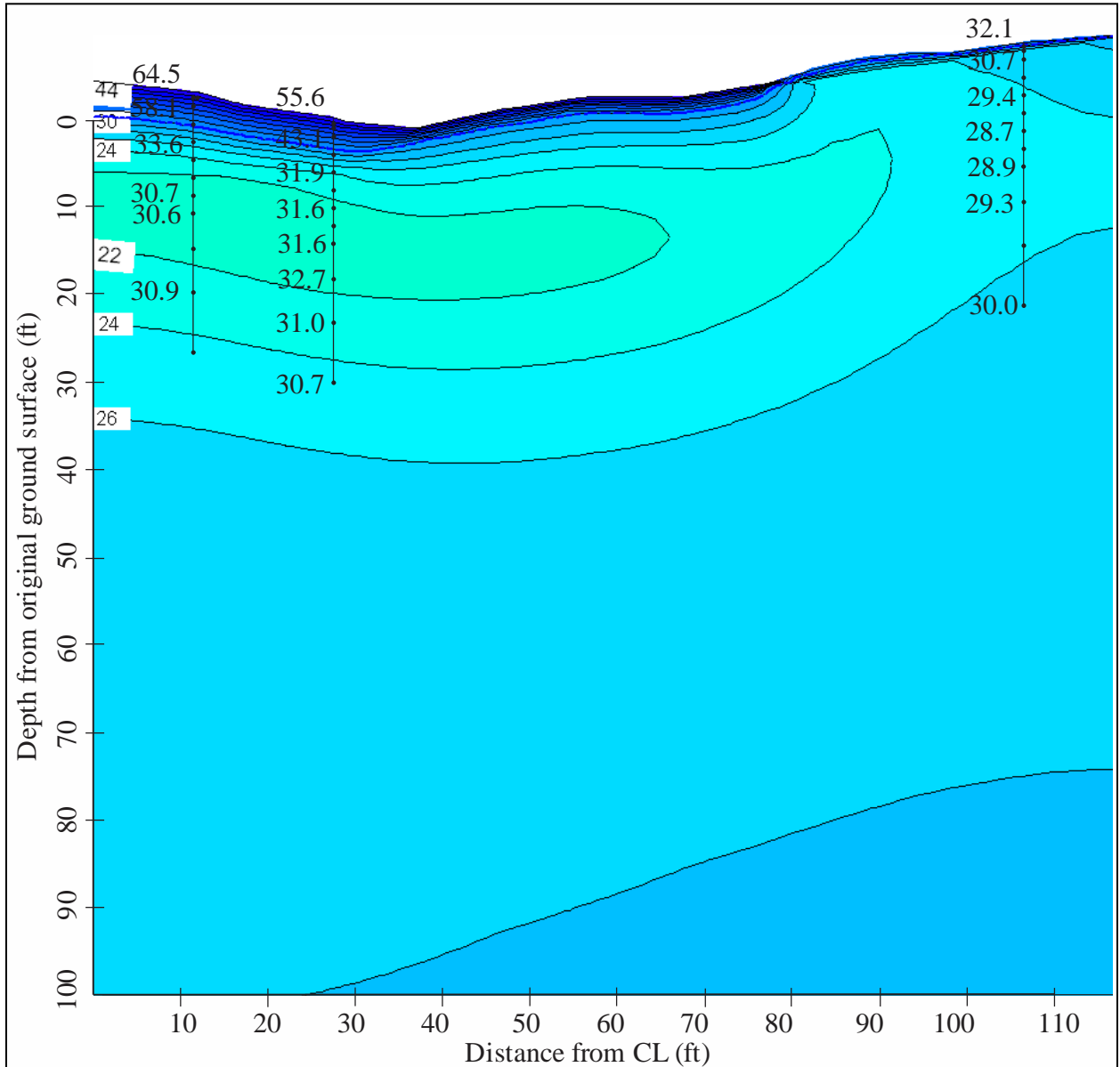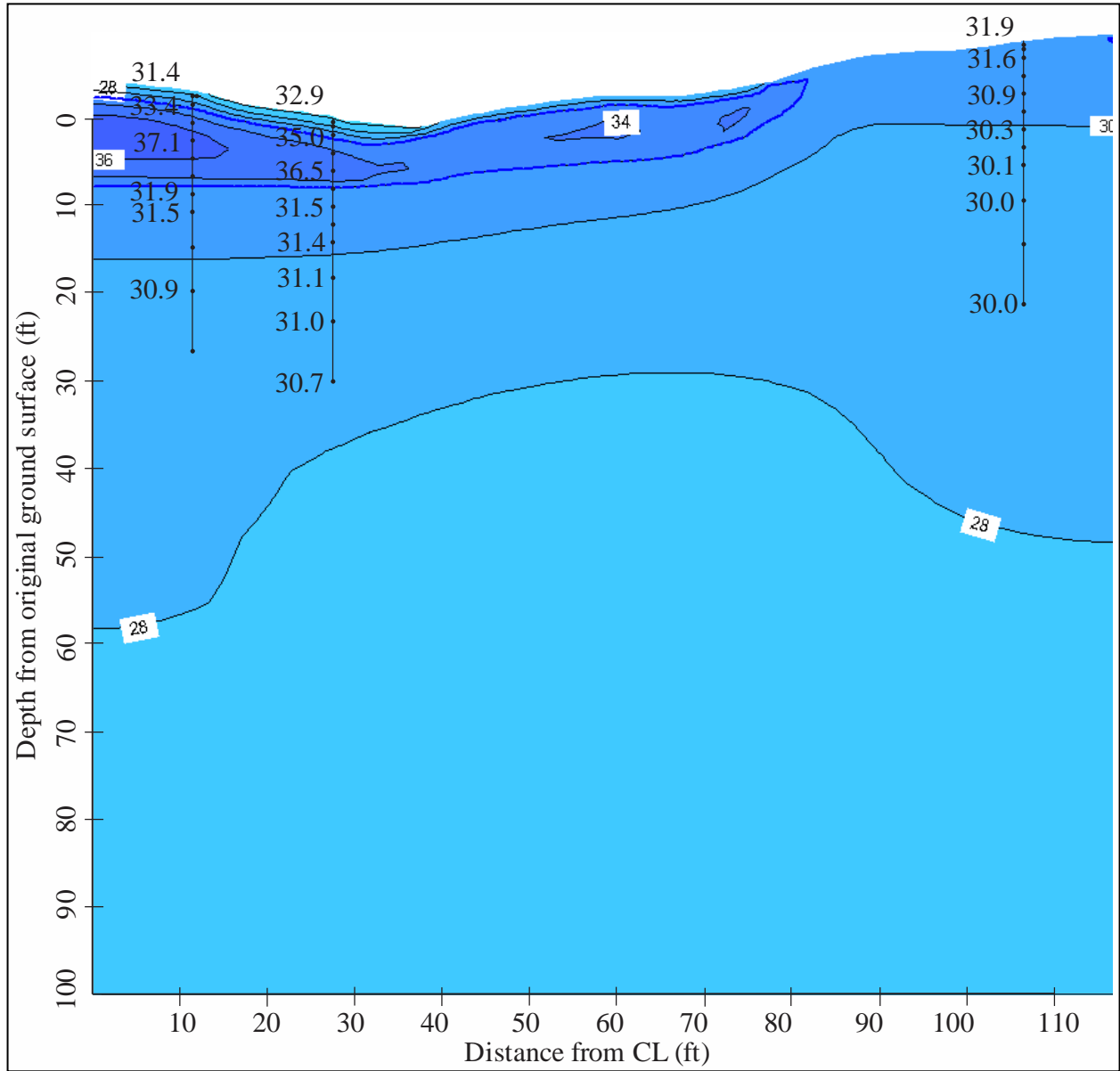
Figure 5.86. Thermal modeling results for October 1st, Run 4, Dalton Highway 9 Mile Hill research site. The phase change isotherm is represented as the dashed blue line and the temperature results are shown with a 2°F contour interval. Some of the measured temperatures along each thermistor string are shown in black text superimposed on the contours.
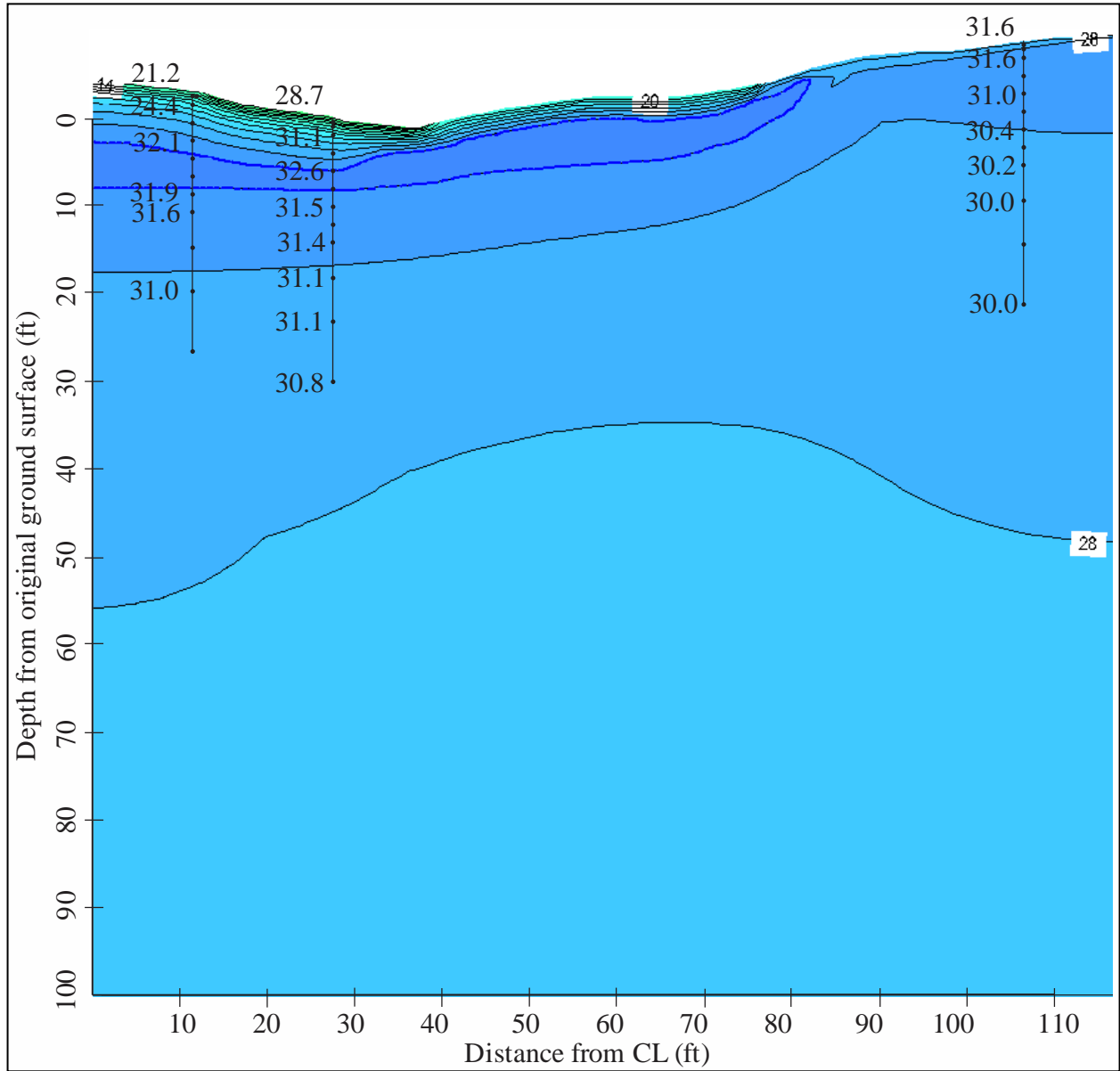
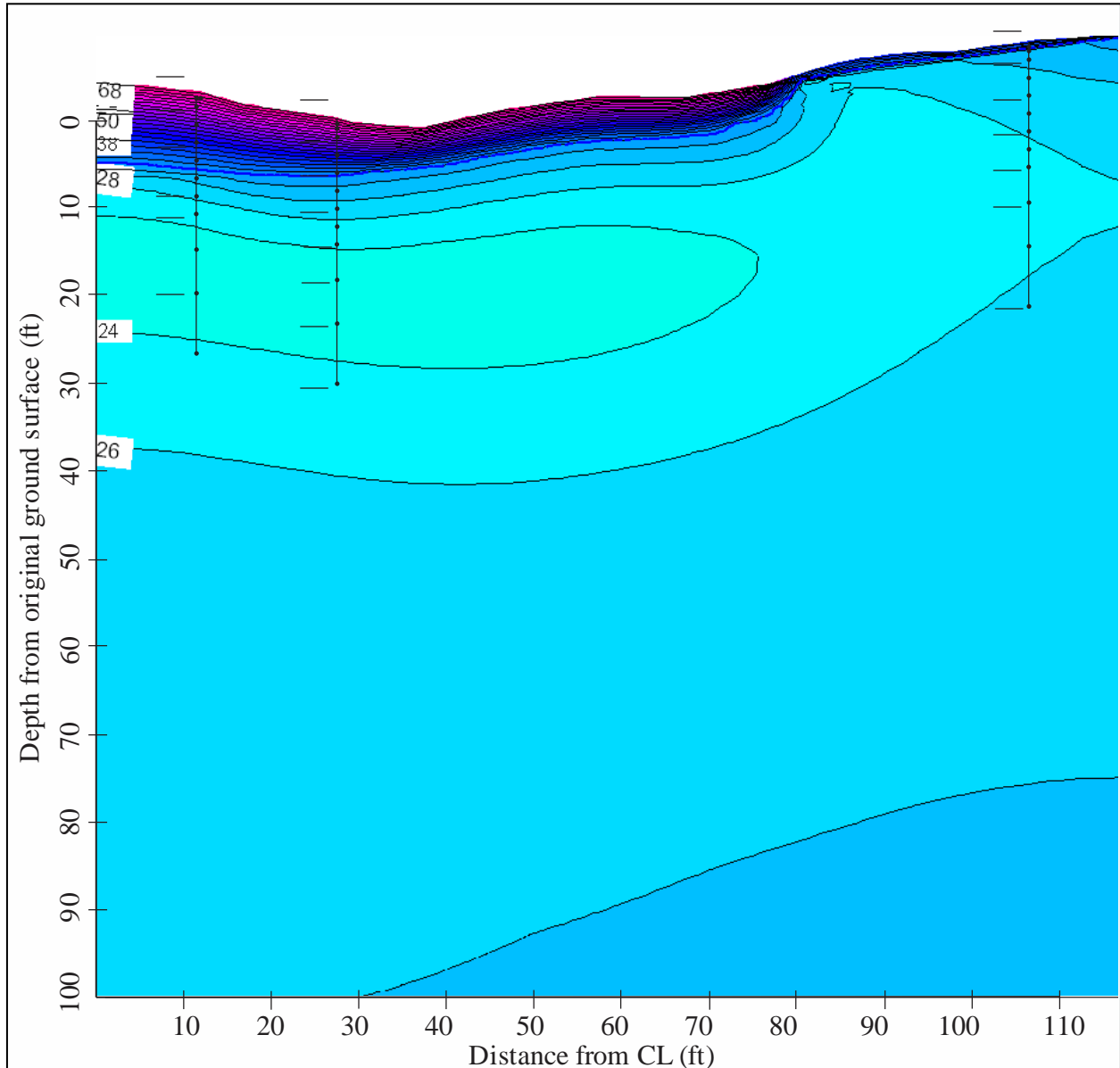Figure 5.87. Thermal modeling results for November 1st, Run 4, Dalton Highway 9 Mile Hill research site. The phase change isotherm is represented as the dashed blue line and the temperature results are shown with a 2°F contour interval. Some of the measured temperatures along each thermistor string are shown in black text superimposed on the contours.
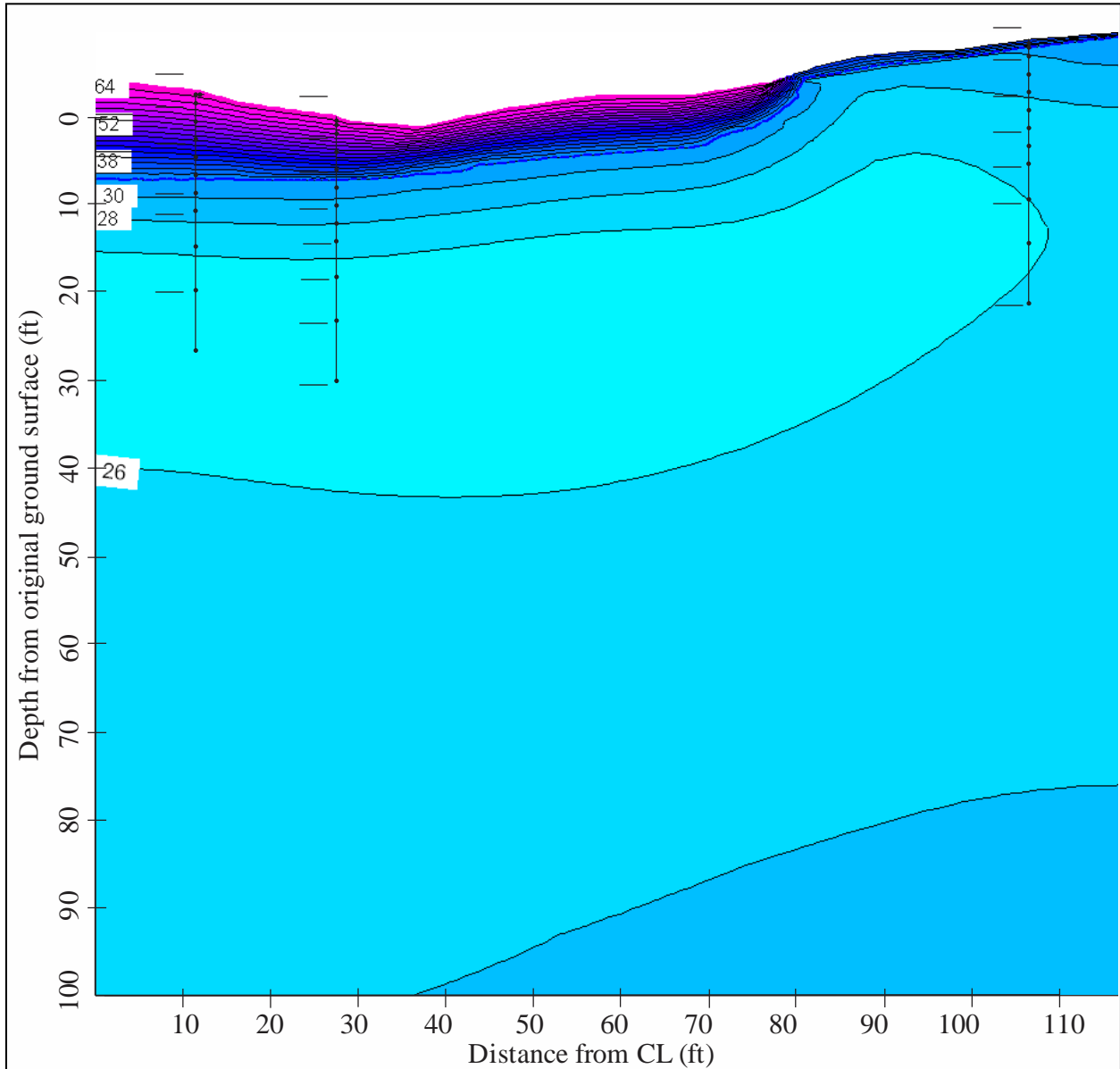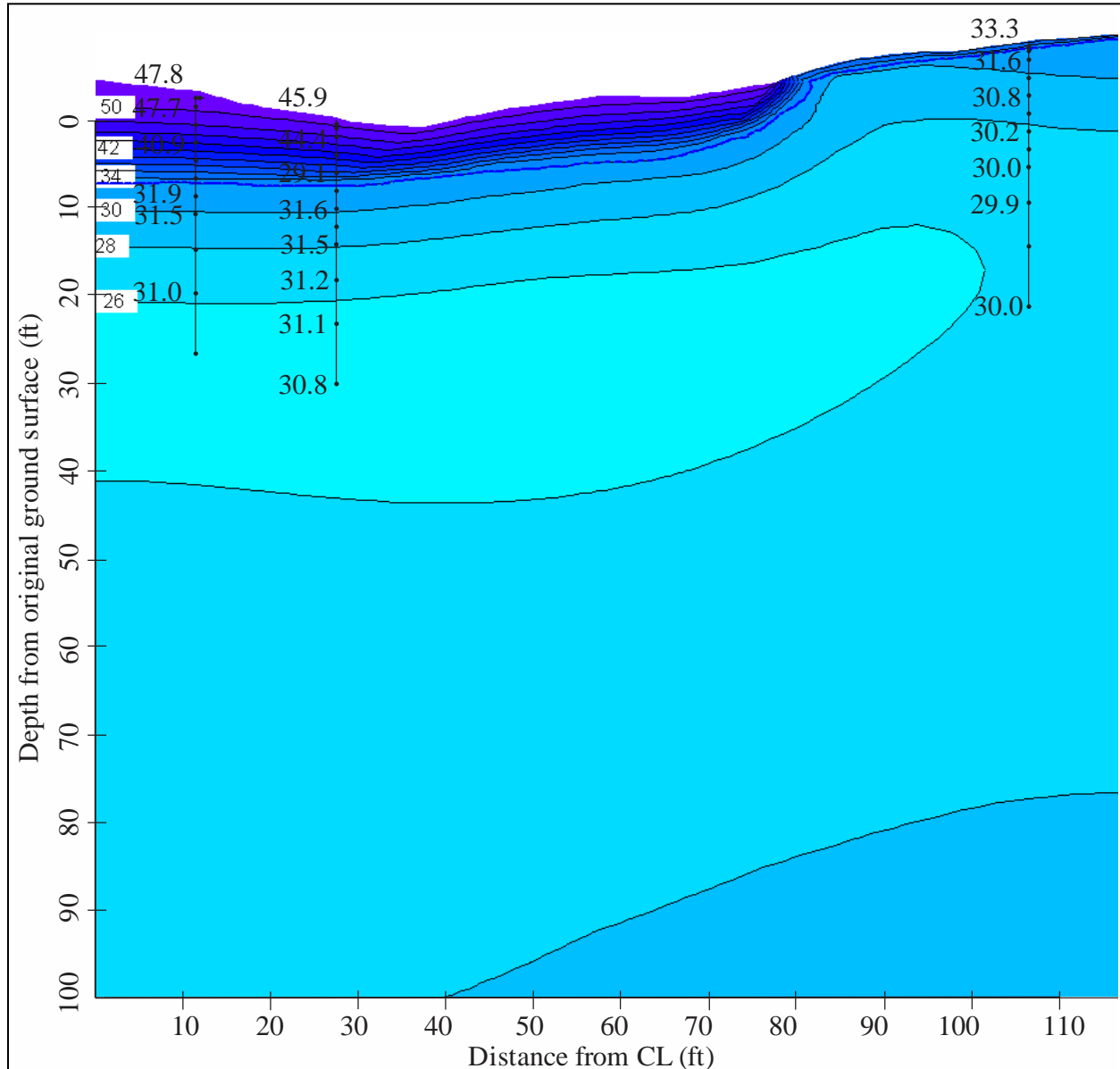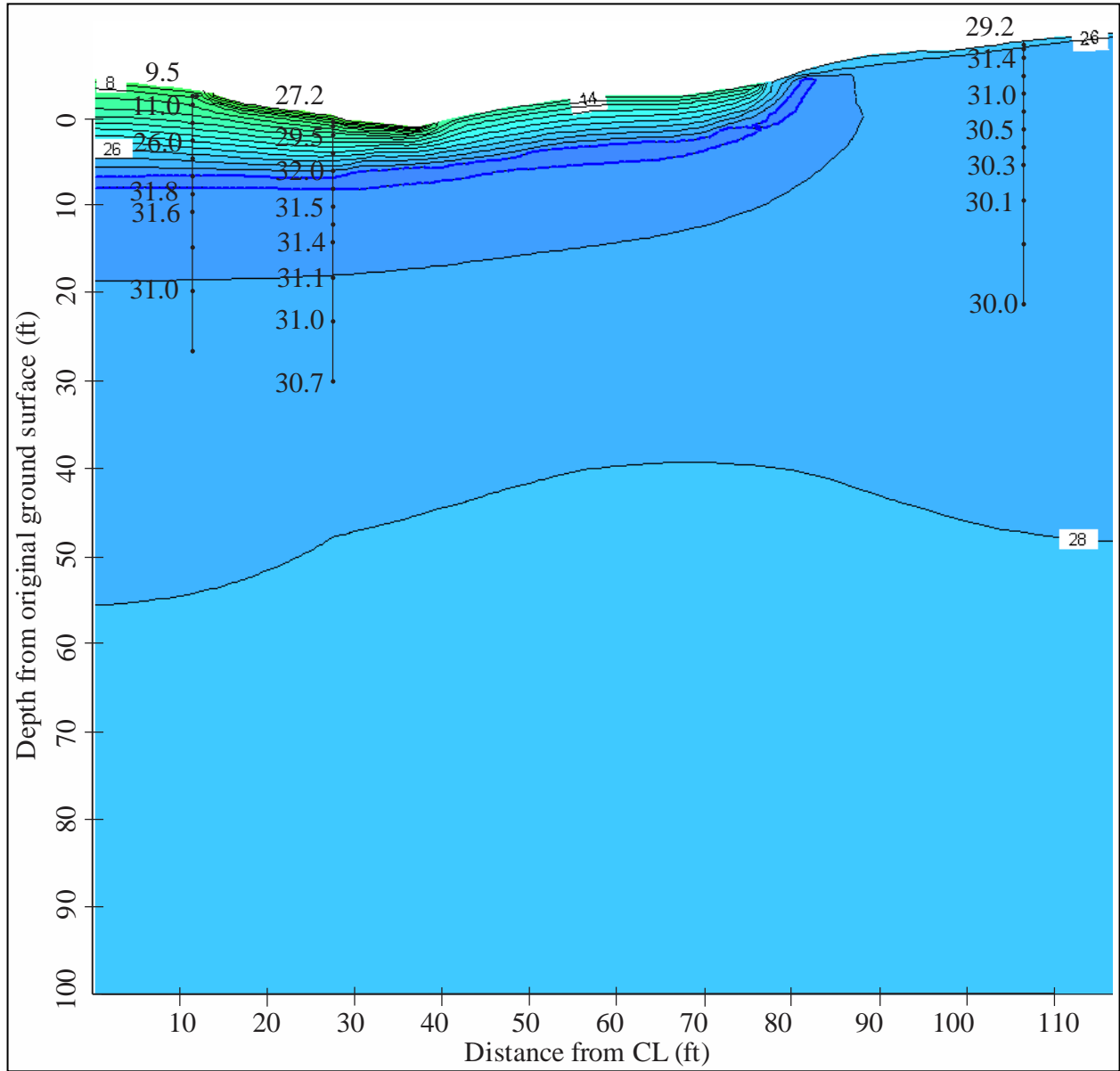
Figure 5.88. Thermal modeling results for December 1st, Run 4, Dalton Highway 9 Mile Hill research site. The phase change isotherm is represented as the dashed blue line and the temperature results are shown with a 2°F contour interval. Some of the measured temperatures along each thermistor string are shown in black text superimposed on the contours.

the embankment and cleared area does freeze back in the late winter months. The modeled active layer depth at both the shoulder and toe locations occurs in January at approximately 11 ft and 9 ft, respectively. The modeled active layer depth at the undisturbed location occurs in September at 1.4 ft. All of these depths are within the ranges indicated from analysis of the measured data.

5.4 Summary of Modeling Results and Recommendations

For each research location, the most critical parameter is the surface boundary condition, which can be separated into air temperature and modifying *n*-factors. The historic air temperature available from the internet provided an approximation of the regional climate for each research location; however, each historic air temperature function produced model results that were too cold by several degrees Fahrenheit. This is understandable, considering the age of the historical data, the distance of the each measuring station from its related research site, and in the case of the Livengood air temperature data, the spotty nature of the readings.

Using the air temperatures measured at each site resulted in much better agreement between the measured and modeled temperatures, especially in the undisturbed permafrost areas. Using the site specific data, the modeled temperatures typically were within 1°F to 2°F of the measured temperatures at depths below 10 ft. The modeled temperatures in the upper 10 ft of soil at each location demonstrated more deviation from the measured temperatures; however, the magnitude of these deviations may be reduced by acquiring a longer record of measured air temperatures at each research location, which would have the effect of smoothing the average daily air temperature.

The effects of adjusting the *n*-factors at each site are mixed. For both sites, using the adjusted *n*-factors improved the accuracy of the modeled surface temperatures of the embankment. For the Richardson Highway MP 113 research site, adjusting the *n*-factors resulted in a deeper active layer depth in the embankment (i.e., maximum depth of freeze), and in the undisturbed area (i.e., maximum depth of thaw). The model overestimated the actual active layer depths for these locations, as indicated by the measured temperatures. The change in surface temperatures resulted in cooler temperatures at the toe location and increased inaccuracy in the thaw bulb configuration. In contrast, for the Dalton Highway 9 Mile Hill research site, adjusting the *n*-factors eliminated the thaw bulb in the late winter months, and resulted in active layer depths that more closely correspond to those measured.

In contrast to the surface temperature, changing the thermal conductivity of the soil has very little effect on the overall model results. In other words, careful estimation of thermal conductivity from published data is sufficient in thermal modeling. Using an unfrozen water content function appropriate for the clayey soil at the Richardson Highway MP 113 research location slightly improved the model results through changes in the thaw bulb configuration. The use of a soil- and site-specific unfrozen water content function will have the greatest effect when soils demonstrating high unfrozen water content (i.e., clay) are present.

Overall, the final model for the Dalton Highway 9 Mile Hill location produced active layer depths that closely matched those indicated from measured temperature data. Of the two sites, the Dalton site is more critical in terms of thaw settlement, since the embankment directly overlies ice-rich permafrost. It is important to keep in mind that while fine-tuning the model was

possible for this research project, for most cases when modeling is needed, site-specific soil temperatures are not available.

To reiterate, the driving input parameter is the surface boundary condition. Determining the surface temperatures for a project location will produce the most benefit in the thermal modeling of future embankment designs in permafrost regions. This can be accomplished by installing a weather station to measure air temperature. Additionally, measuring soil surface temperature to calculate representative *n*-factors for a surface type may help to eliminate some of the guess work. However, due to the variation of natural surfaces and the spatial variation of snow cover, one surface temperature measurement will not be representative of the entire site, and thus should not be substituted for air temperature measurements.

Gravimetric moisture content is routinely determined for field samples. Although volumetric moisture content is not, this value can be calculated from the gravimetric moisture content and the dry unit weight of a soil sample. If thermal modeling is planned for a project area, the geotechnical field investigation and sampling program can be improved by collecting soil samples of known volume, or by determining a sample's volume once in the laboratory using the wax coating method. These results are easily combined with the soil's dry weight to yield dry unit weight. Performing this exercise on ice-rich samples will yield values for the percent of ice in a sample, which has some effect on the thermal conductivity of the soil (see Appendix H). Additionally, if the foundation soils in the project area have a high clay content, high organic content, or are saline, soil samples should be collected for unfrozen water content measurements. Appendix H contains general guidelines for selecting input parameters, should site-specific values not be available for a project area.

Although climate warming scenarios were not included in the present analysis, these research results suggest that such scenarios should be considered given the importance of the surface boundary condition. Finally, both of the sites modeled consisted of long-established embankments that may have finally reached a thermal equilibrium with the foundation soils. To further investigate modeled embankments, a newly constructed embankment over permafrost should be instrumented and modeled.

CHAPTER 6 – ARCHIVED TEMPERATURE DATA

One of the research objectives of this project was to conduct a review of previously measured temperature data from other locations within Northern Region. This data was in data base form, but not systematically named or organized, and some of the files were corrupted. As a first step, the readable data files were converted into Excel 2003 files. These files, each renamed to include "readable_modified" in the file name, were organized into folders named with the project title: Airport, Alder Creek, Bonanza Creek, Canyon Creek, Chitina, CRREL, Engineer Creek, Fairhill, and Farmers. The files for each project within each folder were combined into one Excel file, which was given a name that indicated this, such as "AIRPORT MASTER.xls."

Finally, all of the data were combined into one compilation Excel 2007 file: "HISTORICAL TEMP DATA_MASTER FILE.xlsx." Within this file are nine worksheets, one for each project location. At the top of each worksheet is a header that contains the general location of the temperature readings, the years during which the temperatures were collected, the names of the Excel 2003 files that are combined, and the names of the related reports via their pdf titles. If the locations of the temperature sensor could be determined, this information is included within each worksheet immediately below the header.

We searched the AK DOT&PF's Research, Development, and Technology Transfer resources webpage (http://www.dot.state.ak.us/stwddes/research/resources.shtml) for related reports. We also contacted David Esch, the lead engineer on many of these research projects, for any additional information that he could provide. The projects, their locations, and the related reports are summarized in Table 6.1.

A compact disc at the back of this report contains all of the electronic data. This includes the raw data as supplied in its original format, the reorganized and reformatted data files, and electronic copies of all of the related reports.

Table 6.1. Summary of historical temperature data collection.

Project name	Location	Related reports
Airport	Exact location unknown; somewhere along Airport Road, Fairbanks	---
Alder Creek	Parks Highway, near Ester	McHattie et al. (1983)
Bonanza Creek	~25 miles W of Fairbanks, Parks Highway, on Bonanza Creek	Esch (1978), McHattie et al. (1983)
Canyon Creek	~66 miles SE of Fairbanks, Richardson Hwy	Esch and Livingston (1978), McHattie et al. (1983), Reckard et al. (1988)
Chitina	Outside Chitina, AK	Esch (1972), Esch (1986), Esch (1994)
CRREL	Exact location unknown; USA-CRREL Alaska Field Station off Farmer's loop	Esch (1982), Esch (1984)
Engineer Creek	Exact location unknown, Steese Highway, ~9 mi from Fairbanks	Osterkamp et al. (1979)
Fairhill	Fairhill Frontage Road, between Farmer's Loop and Fox	Esch and Jurick (1980)
Farmers	Exact location unknown, along Farmer's Loop	---

CHAPTER 7 – REFERENCES

Andersland, O. B., and Ladanyi, B. (2004). *Frozen Ground Engineering*, 2nd ed.: John Wiley and Sons, Inc., Hoboken, NJ.

Braley, W. A. and Zarling, J. P. (1990). *MUT1D: Multilayer User-Friendly Thermal Model in 1 Dimension*: FHWA-AK-RD-90-02, Alaska Department of Transportation and Public Facilities, Fairbanks, Alaska.

Carslaw, H. S., and Jaeger, J. C. (1986). *Conduction of Heat in Solids*, 2nd Ed: Oxford University Press, New York, NY.

Coduto, D. P. (1999). *Geotechnical Engineering – Principles and Practices*: Prentice Hall, Upper Saddle River, NJ.

Darrow, M. (2006). *Glenn Highway MP 172-189 Rehabilitation*: IM-TEA-OA1-4(6), AKSAS 60922, Northern Region, Alaska Department of Transportation and Public Facilities, Fairbanks, Alaska.

Darrow, M. M., Huang, S. L., Akagawa, S. (2009). "Adsorbed cation effects on the frost susceptibility of natural soils." *Cold Regions Science and Technology*, 55, 263-277.

Das, B. M. (1998). *Principles of Geotechnical Engineering*, 4th ed: PWS Publishing Co., Boston, Ma.

Decagon Devices, Inc. (2006). *KD2 Pro Operator's Manual*: Decagon Devices, Inc., Pullman, Wa.

Esch, D. C. (1972). *Control of Permafrost Degradation beneath a Roadway by Subgrade Insulation*: State of Alaska, Department of Highways, Materials Division, Juneau, Alaska.

Esch, D. C. (1978). *Road Embankment Design Alternatives over Permafrost*: Alaska Department of Transportation and Public Facilities, Fairbanks, Alaska.

Esch, D. C. (1982). *Prethawing by Surface Modifications*: AK-RD-83-23, Alaska Department of Transportation and Public Facilities, Division of Planning and Programming Research Section, Fairbanks, Alaska.

Esch, D. C. (1984). *Surface Modifications for Thawing of Permafrost*: AK-RD-85-10, Alaska Department of Transportation and Public Facilities, Fairbanks, Alaska.

Esch, D. C. (1986). *Insulation Performance beneath Roads and Airfields in Alaska*: AK-RD-87-17, Alaska Department of Transportation and Public Facilities, Fairbanks, Alaska.

Esch, D. C. (1994). *Long Term Evaluation of Insulated Roads and Airfields in Alaska*: FHWA-AK-RD-94-18, Alaska Department of Transportation and Public Facilities, Juneau, Alaska.

Esch, D. C., and Jurick, R. (1980). *Construction History of Permafrost Insulation with Polystyrene Beadboard Roadway Test Section, Fairhill Frontage Road*: Alaska Department of Transportation and Public Facilities, Division of Planning and Programming Research Section, Fairbanks, Alaska.

Esch, D. C., and Livingston, H. (1978). *Performance of a Roadway with a Peat Underlay over Permafrost*: AK-RD-78-01, Alaska Department of Transportation and Public Facilities, Fairbanks, Alaska.

Ferrians, Jr., O. J., Nichols, D. R., Williams, J. R. (1983) "Copper River Basin." In Péwé, T. L., and Reger, R. D., eds., *Guidebook to Permafrost and Quaternary Geology along the Richardson and Glenn Highways, Alaska*: Alaska Division of Geological and Geophysical Surveys, Guidebook 1, 137-175.

Gosink, J. P., Osterkamp, T. E., Kawasaki, K. (1986). *A Comparison of Two Finite Element Models for the Prediction of Permafrost Temperatures*: AK-RD-87-06, Alaska Department of Transportation and Public Facilities, Fairbanks, Alaska.

Hillel, D. (1980). *Fundamentals of Soil Physics*: Academic Press, New York, NY.

Huang, S. L., Bray, M. T., Akagawa, S., Fukuda, M. (2004). "Field investigations of soil heave by a large diameter chilled gas pipeline experiment, Fairbanks, Alaska." *Journal of Cold Regions Engineering*, 18(1), 2-34.

Kersten, M. S. (1949). *Laboratory Research for the Determination of the Thermal Properties of Soils: Final Report*: University of Minnesota, Engineering Experiment Station, St. Paul, MN.

Krahn, J. (2004). *Thermal modeling with TEMP/W: an engineering methodology*. GEO-SLOPE International, Ltd., Calgary.

McHattie, R. L., Esch, D. C., Zarling, J. P., Connor, B., Goering, D. J. (1983). *Experimental Roadways on Permafrost: Three Interim Study Reports as Presented to the 4th International Permafrost Conference*: AK-RD-84-1, Alaska Department of Transportation and Public Facilities, Division of Planning and Programming Research Section, Fairbanks, Alaska.

Osterkamp, T. E., Jurick, R. W., Gislason, G. A., Akasofu, S. I. (1979). *Electrical Resistivity Measurements in Permafrost Terrain at the Engineer Creek Road Cut, Fairbanks, Alaska*: Alaska Department of Transportation and Public Facilities, Division of Planning and Research, Fairbanks, Alaska.

Platts, W. R. (1965). *Materials Investigation, Simpson Hill Slide*: F-071-2(5), Alaska Department of Highways, Materials Section, Fairbanks, Alaska.

Reckard, M., Esch, D., McHattie, R. (1988). *Peat used as Roadway Insulation over Permafrost: Results from the Canyon Creek Site*: AK-RD-88-11, Alaska Department of Transportation and Public Facilities, Fairbanks, Alaska.

Rowland, J. (2010). *Dalton Highway 9 Mile North Supplemental Geotechnical Report*: NH-F-065-2(3), AKSAS 64899, Northern Region Materials Section, Alaska Department of Transportation and Public Facilities, Fairbanks, Alaska.

Schlichting, S. J., and Darrow, M. M. (2006). *Dalton Highway 9 Mile Hill North*: NH-F-065-2(3), AKSAS 64899, Northern Region, Alaska Department of Transportation and Public Facilities, Fairbanks, Alaska.

Shur, Y., and Kanevskiy, M. (2010). *Geotechnical Investigations for the Dalton Highway Innovation Project as a Case Study of the Ice-rich Syngenetic Permafrost*: AUTC 207122, Institute of Northern Engineering, Fairbanks, Alaska.

Shur, Y., and Zhestkova, T. (2003). "Cryogenic structure of a glacio-lacustrine deposit." *Proc., Permafrost: Eighth International Conference*, University of Zurich, Zurich, Switzerland, 1051-1056.

STATE OF ALASKA DOT/PF
Northern Region Materials
Geology Section

FINAL TEST HOLE LOG

Project	TEMP/W Verification
Project Number	AUTC RR08.11, AKSAS 62223

Test Hole Number	TH08-1650
Total Depth	34.5 feet
Dates Drilled	11/7/2008 - 11/8/2008
Station, Offset	
Latitude, Longitude	N62.08238°, W145.4368°
Elevation	

Field Geologist	M. DARROW
Field Crew	T. JOHNSON, S. PARKER, J. CLINE, P. CALVIN
TH Finalized By	M. DARROW
Equipment Type	CME 45 Truck
Weather	overcast, ~+10 deg F
Vegetation	spruce to 10" dia, willow, cranberries

Ground Water Data

	While Drilling	After Drilling
Depth in (ft.)		
Time		
Date		
Symbol		

GENERAL COMMENTS:
Located in trees to east of hwy, west of Copper R.

SUBSURFACE MATERIAL

Bn ORG MAT
   w/ silt

Bn SILT
   dry to moist, sl Org, dry to moist; -0.5 degC @ 0.5, +0.4 degC @ 1.2

SAMPLE 08-4070 (2.5-4.5): NM 19.3%
   40% recov; 0.9 degC

Gy Fat CLAY
   w/ Cobbles
   moist, w/ scattered sand & gravel; w/ visible ice below 6.5; Vx, Vr, ice vein
   1/4" thick @ 13.5; massive ice @ 31.0, 32.5-33.5 (based on drill rxn)
SAMPLE 08-4071 (5.0-10.0):
   40% recov, sample from 7.5-10.0; -0.1 degC. CS liner (9.0-9.4): VOL MC
   48.2%, ku=0.633 Btu/ft*hr*F, kf=0.824 Btu/ft*hr*F

SAMPLE 08-4072 (10.0-12.5):
   100% recov, -0.1 degC. CS liner: A (11.2-11.6): VOL MC 48.5%, B
   (11.6-12.0): ku=0.70 Btu/ft*hr*F, kf=0.967 Btu/ft*hr*F

SAMPLE 08-4073 (12.5-15.0):
   100% recov; 4.0 degC at bottom - friction?! CS liner: A (12.5-13.0):
   VOL MC 37.3%, B (13.0-13.5): VOL MC 31.0%, ku=0.815 Btu/ft*hr*F,
   kf=1.16 Btu/ft*hr*F, C (13.5 - 14.0): VOL MC 24.4%

SAMPLE 08-4075 (15.0-17.0):
   100% recov, sleeve fractured, sample discarded
SAMPLE 08-4074 (15.5-16.0): NM 17.1%

SAMPLE 08-4076 (20.0-22.0):
   sampler destroyed. CS liner (21.0-21.5): ku=0.761 Btu/ft*hr*F, kf=0.948
   Btu/ft*hr*F

SAMPLE 08-4077 (28.5-29.5):
   20% recov. CS liner (29.0-29.5): ku=0.774 Btu/ft*hr*F, kf=0.986
   Btu/ft*hr*F

Drilling Method: Backhoe Excavator; H-S Auger

Sample Data:

Method	Number	Blow Count
SS	08-4070	4 / 7 / 8 / 8
CS	08-4071	
CS	08-4072	
CS	08-4073	
SS	08-4074 / 08-4075	12 / 24 / 32 / 38
CS	08-4076	
CS	08-4077 / 08-4078	

Depth column: 0 to 30 feet

Note: Unless otherwise noted, all samples are taken with 1-3/8-in. ID Standard Penetration Sampler driven with 140 lb. hammer with 30-in. drop. ☐ CME Auto Hammer ☒ Cathead Rope Method

Side text: NR AKDOT TEST HOLE LOG - USCS_NEW AUTC_DOTPF THERMAL RESEARCH_CHRISTINE.GPJ NR_AKDOT_PRECON_USCS_06_28_07.GDT 7/28/10

STATE OF ALASKA DOT/PF
Northern Region Materials
Geology Section

FINAL TEST HOLE LOG

Test Hole Number   TH08-1650

Drilling Method	Depth in (Feet)	Casing Blows / ft	Method	Number	Blow Count	Sample Interval	N-Value	Frozen	Graphic Log	SUBSURFACE MATERIAL
H-S Auger	30		AUGER	08-4079						SAMPLE 08-4078 (29.0-29.5): NM 24.5%
	31									
	32									
	33									
	34									SAMPLE 08-4079 (33.5-34.5): CH, 96.3% -200, LL 65, PI 38
										BOH

Drilling Notes: lost continuous sampler at 22.0; drilled to 25.0 to retrieve sampler; installed thermistor string to 30.0; backfilled with 17 50-lb bags of sand

FINAL TEST HOLE LOG

Project	TEMP/W Verification
Project Number	AUTC RR08.11, AKSAS 62223

Test Hole Number	TH08-1651
Total Depth	5 feet
Dates Drilled	11/8/2008 - 11/8/2008
Station, Offset	
Latitude, Longitude	N62.08241°, W145.43677°
Elevation	

Field Geologist	M. DARROW
Field Crew	T. JOHNSON, S. PARKER, J. CLINE, P. CALVIN
TH Finalized By	M. DARROW
Equipment Type	CME 45 Truck
Weather	overcast, ~+10 deg F
Vegetation	spruce to 10" dia, willow, cranberries

GENERAL COMMENTS:
Located ~10 ft to west of TH08-1650

SUBSURFACE MATERIAL

Depth	Material
0	ORG MAT w/ silt
1	Bn SILT dry to moist
5	BOH Gy Lean CLAY

Drilling Method: H-SPAuger Excavator / Backhoe

Drilling Notes: installed post for instrumentation

Note: Unless otherwise noted, all samples are taken with 1-3/8-in. ID Standard Penetration Sampler driven with 140 lb. hammer with 30-in. drop. ☐ CME Auto Hammer ☒ Cathead Rope Method

NR AKDOT TEST HOLE LOG - USCS_NEW AUTC_DOTPF THERMAL RESEARCH_CHRISTINE.GPJ NR_AKDOT_PRECON_USCS_06_28_07.GDT 7/28/10

FINAL TEST HOLE LOG

Project	TEMP/W Verification	Test Hole Number	TH08-1652
Project Number	AUTC RR08.11, AKSAS 62223	Total Depth	7 feet

Field Geologist	M. DARROW		Dates Drilled	11/8/2008 - 11/8/2008
Field Crew	T. JOHNSON, S. PARKER, J. CLINE, P. CALVIN		Station, Offset	
		Equipment Type	CME 45 Truck	
		Weather	overcast, ~+10 deg F	Latitude, Longitude	N62.08235°, W145.43727°
TH Finalized By	M. DARROW	Vegetation		Elevation	

Ground Water Data

	While Drilling	After Drilling
Depth in (ft.)		
Time		
Date		
Symbol		

GENERAL COMMENTS:
Located 40" east of pavement on shoulder, at break in slope

SUBSURFACE MATERIAL

Drilling Method	Depth in (Feet)	Casing Blows / ft	Method	Number	Blow Count	N-Value
H-S Auger / Backhoe Excavator	0–7		SS	08-4080	9 / 50	

Gy-Bn Well-graded GRAVEL
  w/ Silt & Sand (fill)
  dry to moist

SAMPLE 08-4080 (4.5-5.5): NM 3.2%
  SS bouncing on rock

BOH

Drilling Notes: drive line broke at 2 pm; hole abandoned 11/9/08 because truck was slipping down embankment

Note: Unless otherwise noted, all samples are taken with 1-3/8-in. ID Standard Penetration Sampler driven with 140 lb. hammer with 30-in. drop. ☐ CME Auto Hammer   ☒ Cathead Rope Method

NR AKDOT TEST HOLE LOG - USCS NEW AUTC_DOTPF THERMAL RESEARCH_CHRISTINE.GPJ NR_AKDOT_PRECON_USCS_06_28_07.GDT 7/28/10

163

FINAL TEST HOLE LOG

STATE OF ALASKA DOT/PF
Northern Region Materials
Geology Section

Project	TEMP/W Verification
Project Number	AUTC RR08.11, AKSAS 62223

Test Hole Number	TH08-1652b
Total Depth	40 feet
Dates Drilled	11/9/2008 - 11/9/2008
Station, Offset	
Latitude, Longitude	N62.0823°, W145.43723°
Elevation	

Field Geologist	M. DARROW
Field Crew	T. JOHNSON, S. PARKER, J. CLINE, P. CALVIN
TH Finalized By	M. DARROW

Equipment Type	CME 45 Truck
Weather	overcast, ~+10 deg F
Vegetation	

Ground Water Data

	While Drilling	After Drilling
Depth in (ft.)		
Time		
Date		
Symbol		

GENERAL COMMENTS:
Located at edge of pavement, right (east) shoulder

SUBSURFACE MATERIAL

Drilling Method: H-S Auger

Depth (ft)	Method	Number	Blow Count	N-Value	Description
0–0.3	AUGER	08-4082			ASPHALT 4" thick
	AUGER	08-4081			Gy Well-graded SAND w/ Silt & Gravel (fill) (base course?)
					SAMPLE 08-4082 (0.3-0.6): SW-SM, 8.9% -200, NV, NP
					Gy Well-graded GRAVEL w/ Silt & Sand (fill) w/ Cobbles
					SAMPLE 08-4081 (0.6-5.5): GW-GM, 6.2% -200, NV, NP combined with sample from TH08-1652
	AUGER	08-4083 08-4084 08-4085			SAMPLE 08-4083 (5.5-6.5): NM 1.6%
					Bn Silty SAND w/ Gravel
					SAMPLE 08-4084 (6.5-6.7): NM 10.0%, ORG 2.5%
	SS	08-4086	3 / 11 / 12	23	SAMPLE 08-4085 (6.5-7.0): SM, 16.2% -200, NV, NP SAMPLE 08-4086 (8.0-9.5): NM 19.4% 25% recov
	SS	08-4087	5 / 10 / 15 / 23	25	Gy Sandy Silty CLAY w/ occ. Gr SAMPLE 08-4087 (10.0-12.0): NM 15.7% 30% recov; 5.1 degC
	SS	08-4088 08-4089	5 / 15 / 27 / 36	42	SAMPLE 08-4088 (15.0-17.0): CL-ML, 56.8% -200, LL 19, PI 5 5.0 degC SAMPLE 08-4089 (15.5-16.0): NM 12.2%
	SS	08-4090	9 / 14 / 16 / 18	30	Gy Sandy Lean CLAY w/ Gravel w/ Cobbles 2" dia Gr 25.0-27.0 SAMPLE 08-4090 (20.0-22.0): NM 10.7% 90% recov.; 4.6 degC
	SS	08-4092 08-4091	7 / 13 / 13 / 13	26	SAMPLE 08-4092 (25.0-26.5): CL, 55.5% -200, LL 24, PI 10 2.4 degC SAMPLE 08-4091 (25.5-26.0): NM 15.5%

Note: Unless otherwise noted, all samples are taken with 1-3/8-in. ID Standard Penetration Sampler driven with 140 lb. hammer with 30-in. drop. ☐ CME Auto Hammer ☒ Cathead Rope Method

NR AKDOT TEST HOLE LOG - USCS NEW AUTC_DOTPF THERMAL RESEARCH_CHRISTINE.GPJ NR_AKDOT_PRECON_USCS_06_28_07.GDT 7/28/10

FINAL TEST HOLE LOG

STATE OF ALASKA DOT/PF
Northern Region Materials
Geology Section

Test Hole Number <u>TH08-1652b</u>

Drilling Method	Depth in (Feet)	Casing Blows / ft	Method	Number	Blow Count	Sample Interval	N-Value	Frozen	Graphic Log	SUBSURFACE MATERIAL
	30									
			SS	08-4093	15					SAMPLE 08-4093 (30.0-31.5):
	31				39		91			stopped hammer on 4th interval; 100% recov, 4.6 degC
					52					
	32				28					
	33									←
H-S Auger	34									
	35									
	36									
	37									
	38									
	39									
	40									BOH

Drilling Notes: heated asphalt w/ weed burner to get hole started; installed thermistor string to 30.0; backfilled w/ sand from M&O

STATE OF ALASKA DOT/PF
Northern Region Materials
Geology Section

FINAL TEST HOLE LOG

Project	TEMP/W Verification	Test Hole Number TH08-1653
Project Number	AUTC RR08.11, AKSAS 62223	Total Depth 39.5 feet
Field Geologist M. DARROW		Dates Drilled 11/9/2008 - 11/9/2008
Field Crew T. JOHNSON, S. PARKER, J. CLINE, P. CALVIN	Equipment Type CME 45 Truck	Station, Offset
	Weather overcast, ~+10 deg F	Latitude, Longitude N62.08237°, W145.43712°
TH Finalized By M. DARROW	Vegetation	Elevation

Ground Water Data

	While Drilling	After Drilling
Depth in (ft.)	24.0	
Time	17:30	
Date	11/9/08	
Symbol	▼	

GENERAL COMMENTS:
Located at toe

SUBSURFACE MATERIAL

Gy Well-graded GRAVEL
  w/ Silt & Sand (fill)
  w/ Cobbles

Bn-Gy Well-graded SAND
  w/ Gravel
  moist, w/ pea gravel; wet below 24.0 (French drain)

SAMPLE 08-4094 (7.0-9.0):
  50% recov; 3.0 degC

SAMPLE 08-4095 (9.5-10.0): NM 4.4%
  40% recov

0% recov

SAMPLE 08-4096 (15.5-16.0): NM 5.9%
  30% recov; 3.0 degC; SpG=2.724

0% recov

SAMPLE 08-4097 (19.5-20.0): NM 4.9%
  20% recov

SAMPLE 08-4098 (25.0-25.5): NM 11.3%
  80% recov; base of drain (sand sample)
Gy Sandy Lean CLAY
SAMPLE 08-4099 (25.5-26.0): NM 35.1%

SAMPLE 08-4100 (29.5-31.5): NM 27.7%

Sample Data columns — Drilling Method: Backhoe Excavator (0–5), H-S Auger (below); Method SS; Sample Numbers and Blow Counts:

Depth	Method	Number	Blow Count	N-Value
7–9	SS	08-4094	5 / 5 / 5 / 5	10
9.5–11	SS	08-4095	3 / 3 / 4 / 4	7
12–14	SS		5 / 5 / 6 / 6	11
15–16.5	SS	08-4096	4 / 4 / 3 / 3	7
17.5–19	SS		5 / 6 / 8 / 6	14
19.5–21	SS	08-4097	4 / 4 / 2 / 4	6
25–26	SS	08-4098 / 08-4099	6 / 5 / 11 / 17	
30			5	

Note: Unless otherwise noted, all samples are taken with 1-3/8-in. ID Standard Penetration Sampler driven with 140 lb. hammer with 30-in. drop. ☐ CME Auto Hammer ☒ Cathead Rope Method

NR AKDOT TEST HOLE LOG - USCS_NEW AUTC_DOTPF THERMAL RESEARCH_CHRISTINE.GPJ NR_AKDOT_PRECON_USCS_06_28_07.GDT 7/28/10

STATE OF ALASKA DOT/PF
Northern Region Materials
Geology Section

FINAL TEST HOLE LOG

Test Hole Number   TH08-1653

Drilling Method	Depth in (Feet)	Casing Blows / ft	Method	Number	Blow Count	Sample Interval	N-Value	Frozen	Graphic Log	SUBSURFACE MATERIAL
H-S Auger	30		SS	08-4100	12		28			30% recov; 2.4 degC
	31				16					
					22					
	32									
	33									
	34									
	35									
	36									
	37									
	38									
	39									BOH

Drilling Notes: broke cathead hammer on sample 08-4100; hole collapsed @ 24.0 & could not install thermistor string

FINAL TEST HOLE LOG

STATE OF ALASKA DOT/PF
Northern Region Materials
Geology Section

Project	TEMP/W Verification
Project Number	AUTC RR08.11, AKSAS 62223

Test Hole Number	TH08-1654
Total Depth	35.5 feet
Dates Drilled	11/10/2008 - 11/10/2008
Station, Offset	
Latitude, Longitude	N62.08236°, W145.43706°
Elevation	

Field Geologist — M. DARROW
Field Crew — T. JOHNSON, J. CLINE
TH Finalized By — M. DARROW

Equipment Type — CME 45 Truck
Weather — overcast, ~+10 deg F
Vegetation —

Ground Water Data

	While Drilling	After Drilling
Depth in (ft.)		
Time		
Date		
Symbol		

GENERAL COMMENTS:
Located 9' east of toe

SUBSURFACE MATERIAL

Drilling Method: Backhoe Excavator (0 to ~14), S-S Auger (below)

Gy Silty GRAVEL
w/ Sand (fill)
dry to moist

Bn Gravelly SILT

Bn-Gy Sandy Silty CLAY
w/ Cobbles
moist, w/ occ Gr; Gy 6.5-27.0, Gy-Bl below 27.0; may be massive ice
34.5-35.5 (based on drill rxn)

Sample Data:
Method: AUGER
Number: 08-4101, 08-4102

SAMPLE 08-4101 (14.0-16.0): CL-ML, 64.5% -200, LL 21, PI 7

SAMPLE 08-4102 (15.0-15.5): NM 14.2%

Note: Unless otherwise noted, all samples are taken with 1-3/8-in. ID Standard Penetration Sampler driven with 140 lb. hammer with 30-in. drop. ☐ CME Auto Hammer ☒ Cathead Rope Method

FINAL TEST HOLE LOG

STATE OF ALASKA DOT/PF
Northern Region Materials
Geology Section

Test Hole Number   TH08-1654

Drilling Method	Depth in (Feet)	Casing Blows / ft	Method	Number	Blow Count	Sample Interval	N-Value	Frozen	Graphic Log	SUBSURFACE MATERIAL
S-S Auger	30									
	31									
	32									
	33									
	34									
	35									BOH

Drilling Notes: up to 1000 psi down pressure at bottom (rest of TH at 400 psi);
clay plug @ 23.0 after drilling, broke through & installed thermistor string to 30.0;
backfilled w/ sand from M&O; some sand bridging, may be voids at depth

NR AKDOT TEST HOLE LOG - USCS NEW AUTC_DOTPF THERMAL RESEARCH_CHRISTINE.GPJ NR_AKDOT_PRECON_USCS_06_28_07.GDT 7/28/10

STATE OF ALASKA DOT/PF
Northern Region Materials
Geology Section

FINAL TEST HOLE LOG

Project	TEMP/W Verification	
Project Number	AUTC RR08.11, AKSAS 62223	

Field Geologist	M. DARROW
Field Crew	J. ROWLAND, J. CLINE, J. LOVE, C. MCCABE
TH Finalized By	M. DARROW

Equipment Type	CME 850
Weather	smokey, ~+65 deg F
Vegetation	moss, spruce < 4" dia

Test Hole Number	TH09-1400
Total Depth	6 feet
Dates Drilled	8/4/2009 - 8/4/2009
Station, Offset	
Latitude, Longitude	N65.54682°, W148.89235°
Elevation	

Ground Water Data

	While Drilling	After Drilling
Depth in (ft.)		
Time		
Date		
Symbol		

GENERAL COMMENTS:
Located ~94 ft to west of hwy (CL) in trees

SUBSURFACE MATERIAL

Bn ORG MAT
  moist, (Sphagnum moss and Labrador tea)
Bn-Gy SILT
  Gy below 1.0, wet when thawed

BOH

Drilling Notes: installed post for instrumentation

Drilling Method: H-S Auger

Note: Unless otherwise noted, all samples are taken with 1-3/8-in. ID Standard Penetration Sampler driven with 140 lb. hammer with 30-in. drop. ☒ CME Auto Hammer ☐ Cathead Rope Method

NR AKDOT TEST HOLE LOG - USCS_NEW AUTC_DOTPF THERMAL RESEARCH_CHRISTINE.GPJ NR_AKDOT_PRECON_USCS_06_28_07.GDT 7/28/10

FINAL TEST HOLE LOG

STATE OF ALASKA DOT/PF
Northern Region Materials
Geology Section

Project	TEMP/W Verification
Project Number	AUTC RR08.11, AKSAS 62223

Test Hole Number	TH09-1401
Total Depth	32.5 feet
Dates Drilled	8/4/2009 - 8/4/2009
Station, Offset	
Latitude, Longitude	N65.54682°, W148.89243°
Elevation	

Field Geologist	M. DARROW
Field Crew	J. ROWLAND, J. CLINE, J. LOVE, C. MCCABE
TH Finalized By	M. DARROW
Equipment Type	CME 850
Weather	smokey, ~+65 deg F
Vegetation	moss, spruce < 4" dia

Ground Water Data

	While Drilling	After Drilling
Depth in (ft.)		
Time		
Date		
Symbol		

GENERAL COMMENTS:
Undisturbed hole, located ~107 ft west of hwy (CL) in trees

SUBSURFACE MATERIAL

Drilling Method: H-S Auger

Bn ORG MAT
moist, (Sphagnum moss and Labrador tea)

Bn SILT
Org, Gy below 1.3 ft, friable w/ visible ice

SAMPLE 09-6600 (2.5-4.5):
100% recov, SS liner: A (2.5-3.0): ku=0.61 Btu/ft*hr*F, kf=0.892 Btu/ft*hr*F; B (3.0-3.5): ku=0.402 Btu/ft*hr*F, kf=1.036 Btu/fr*hr*F; C (3.5-4.0): VOL MC 86.1%; F (4.0-4.5): ku=0.38 Btu/ft*hr*F, kf=1.036 Btu/ft*hr*F

SAMPLE 09-6601 (6.5-7.5): ML, 90% -200, NM 65.8%, NV, NP
100% recov

100% recov

SAMPLE 09-6602 (12.0-12.5): NM 53.8%, ORG 6.0%
100% recov

100% recov

Wh ICE
w/ Silt
dry silt at 18.0 w/ large ice crystals; sampler dropped suddenly at 19.0

100% recov

80% recov

100% recov

100% recov

100% recov

Sample Data

Depth (ft)	Method	Number	Blow Count	Recov
2.5-4.5	SS	09-6600	6, 10, 12, 15	
6.5-7.5	SS	09-6601	7, 12, 13, 12	
8.5-10	SS		10, 15, 13, 13	
11.5-12.5	SS	09-6602	9, 13, 13, 15	
13-15	SS		11, 14, 14, 15	
15.5-17	SS		6, 11, 13, 10	
18-20	SS		2, 1, 1, 5	
23-24.5	SS		6, 8, 9	
25-26.5	SS		7, 9, 11, 9	
28-29.5	SS		5, 8, 8, 14	

Note: Unless otherwise noted, all samples are taken with 1-3/8-in. ID Standard Penetration Sampler driven with 140 lb. hammer with 30-in. drop. ☒ CME Auto Hammer ☐ Cathead Rope Method

NR AKDOT TEST HOLE LOG - USCS_NEW AUTC_DOTPF THERMAL RESEARCH_CHRISTINE.GPJ NR_AKDOT_PRECON_USCS_06_28_07.GDT 7/28/10

FINAL TEST HOLE LOG

STATE OF ALASKA DOT/PF
Northern Region Materials
Geology Section

Test Hole Number   TH09-1401

Drilling Method	Depth in (Feet)	Casing Blows / ft	Method	Number	Blow Count	Sample Interval	N-Value	Frozen	Graphic Log	SUBSURFACE MATERIAL
H-S Auger	30									30
	31		SS		8					100% recov 31
					10					
	32				14					32
					18					BOH

Drilling Notes: installed thermistor string to 30.0; backfilled w/ sand; installed 107 sensor 2" below surface; backfilled with thawing silt and covered w/ original organic mat

FINAL TEST HOLE LOG

Project	TEMP/W Verification	Test Hole Number TH09-1402
Project Number	AUTC RR08.11, AKSAS 62223	Total Depth 28 feet

Field Geologist	M. DARROW	Dates Drilled 8/5/2009 - 8/5/2009
Field Crew	J. ROWLAND, J. CLINE, J. LOVE, C. MCCABE	Station, Offset
	Equipment Type CME 850	
	Weather smokey, ~+50 deg F	Latitude, Longitude N65.54693°, W148.89194°
TH Finalized By	M. DARROW	Elevation
	Vegetation	

Ground Water Data

	While Drilling	After Drilling
Depth in (ft.)		
Time		
Date		
Symbol		

GENERAL COMMENTS:
Shoulder hole, located ~12 ft west of hwy (CL)

SUBSURFACE MATERIAL

Drilling Method: H-S Auger

Depth (Feet)	Method	Number	Blow Count	N-Value
0–3.5	AUGER	09-6603		
3.0–3.5	AUGER	09-6604		
7–9	SS		4 / 4 / 4 / 3	8
11.5–12.0	SS	09-6605	3 / 6 / 9 / 10	
13–15	SS		6 / 10 / 9 / 14	
16–18	SS		8 / 8 / 10 / 22	
18–20	SS		4 / 10 / 8 / 20	
20–22	SS		5 / 8 / 11 / 17	
22–24	SS		8 / 12 / 12 / 16	
24–26	SS		9 / 9 / 11 / 16	
26–28	SS		6 / 9 / 11 / 17	

Bn Well-graded SAND
   w/ Clay & Gravel (fill)
   moist, moist to wet below 8.0; fill composed of clayey chert
SAMPLE 09-6603 (0.0-3.5): SW-SC, 11.4% -200, LL 19, PI 4

SAMPLE 09-6604 (3.0-3.5): NM 2.6%

Gy SILT
   Org, wet when thawed
SAMPLE 09-6605 (11.5-12.0): NM 39.7%, ORG 7.1%
Wh ICE

BOH

Drilling Notes: pilot bit broke off at bottom of hole; hole abandoned

Note: Unless otherwise noted, all samples are taken with 1-3/8-in. ID Standard Penetration Sampler driven with 140 lb. hammer with 30-in. drop. ☒ CME Auto Hammer ☐ Cathead Rope Method

FINAL TEST HOLE LOG

STATE OF ALASKA DOT/PF
Northern Region Materials
Geology Section

Project	TEMP/W Verification	
Project Number	AUTC RR08.11, AKSAS 62223	

Test Hole Number	TH09-1403
Total Depth	35 feet
Dates Drilled	8/5/2009 - 8/5/2009
Station, Offset	
Latitude, Longitude	N65.54694°, W148.89198°
Elevation	

Field Geologist	M. DARROW
Field Crew	J. ROWLAND, J. CLINE, J. LOVE, C. MCCABE
TH Finalized By	M. DARROW
Equipment Type	CME 850
Weather	smokey, ~+50 deg F
Vegetation	

Ground Water Data

	While Drilling	After Drilling
Depth in (ft.)		
Time		
Date		
Symbol		

GENERAL COMMENTS:
Shoulder hole (appx 3' north of 1402), located ~12 ft west of hwy (CL)

SUBSURFACE MATERIAL

Columns: Drilling Method | Depth in (Feet) | Casing Blows / ft | Sample Data (Method | Number | Blow Count | Sample Interval | N-Value) | Frozen | Graphic Log

Drilling Method: S-S Auger

0–10 ft: Bn Well-graded SAND w/ Clay & Gravel (fill), moist

10 ft: Gy SILT, wet when thawed

11 ft: ICE

Note: Unless otherwise noted, all samples are taken with 1-3/8-in. ID Standard Penetration Sampler driven with 140 lb. hammer with 30-in. drop. ☒ CME Auto Hammer ☐ Cathead Rope Method

NR AKDOT TEST HOLE LOG - USCS_NEW AUTC_DOTPF THERMAL RESEARCH_CHRISTINE.GPJ NR_AKDOT_PRECON_USCS_06_28_07.GDT 7/28/10

STATE OF ALASKA DOT/PF
Northern Region Materials
Geology Section

FINAL TEST HOLE LOG

Test Hole Number   TH09-1403

Drilling Method	Depth in (Feet)	Casing Blows / ft	Method	Number	Blow Count	Sample Interval	N-Value	Frozen	Graphic Log	SUBSURFACE MATERIAL	
S-S Auger	30										30
	31										31
	32										32
	33										33
	34										34
	35									BOH	35

Drilling Notes: installed therm. string to 29.5 (entire string is 0.5 ft UP): 1.0 ft sensor @ 0.5 ft; 0.5 ft sensor is bent over in trench horizontally at 0.8 ft b/w surface; installed 107 sensor at 0.4 ft b/w surface above vert. string; backfilled surface w/ emb. mat'l

NR AKDOT TEST HOLE LOG - USCS NEW AUTC_DOTPF THERMAL RESEARCH_CHRISTINE.GPJ NR_AKDOT_PRECON_USCS_06_28_07.GDT 7/28/10

FINAL TEST HOLE LOG

STATE OF ALASKA DOT/PF
Northern Region Materials
Geology Section

Field Geologist	M. DARROW
Field Crew	J. ROWLAND, J. CLINE, J. LOVE, C. MCCABE
TH Finalized By	M. DARROW

Project	TEMP/W Verification
Project Number	AUTC RR08.11, AKSAS 62223
Equipment Type	CME 850
Weather	rainy, ~+50 deg F
Vegetation	willow/alder brush to 8', grass

Test Hole Number	TH09-1404
Total Depth	39 feet
Dates Drilled	8/6/2009 - 8/6/2009
Station, Offset	
Latitude, Longitude	N65.5469°, W148.892°
Elevation	

GENERAL COMMENTS:
Toe hole, located ~29 ft west of hwy (CL), in ditch at edge of gravel

Ground Water Data

	While Drilling	After Drilling
Depth in (ft.)		
Time		
Date		
Symbol		

SUBSURFACE MATERIAL

Drilling Method: AUGER / S-S Auger

Sample Data — Method: AUGER, Number: 09-6606

- Bn Well-graded SAND
  w/ Clay & Gravel
  dry to moist

- Gy SILT
  wet when thawed
  SAMPLE 09-6606 (6.0-6.5): NM 30.3%

- ICE

- Gy SILT
  w/ visible ice

- ICE
  w/ silt; white below 29.0

Note: Unless otherwise noted, all samples are taken with 1-3/8-in. ID Standard Penetration Sampler driven with 140 lb. hammer with 30-in. drop. ☒ CME Auto Hammer ☐ Cathead Rope Method

NR AKDOT TEST HOLE LOG - USCS NEW AUTC_DOTPF THERMAL RESEARCH_CHRISTINE.GPJ NR_AKDOT_PRECON_USCS_06_28_07.GDT 7/28/10

STATE OF ALASKA DOT/PF
Northern Region Materials
Geology Section

FINAL TEST HOLE LOG

Test Hole Number   TH09-1404

Drilling Method	Depth in (Feet)	Casing Blows / ft	Method	Number	Blow Count	Sample Interval	N-Value	Frozen	Graphic Log	SUBSURFACE MATERIAL
S-S Auger	30		AUGER	09-6607						
	31									
	32									
	33									
	34									
	35									
	36									Bn ICE
	37									w/ schist chips (icy colluvium) SAMPLE 09-6607 (36.0-36.5): NM 61.6%
	38									
	39									BOH

Drilling Notes: installed therm. string to 30.0; installed 107 sensor at 0.4 ft b/w surface; backfilled with SA, SI, & GR from surrounding surface

NR AKDOT TEST HOLE LOG - USCS NEW AUTC_DOTPF THERMAL RESEARCH_CHRISTINE.GPJ NR_AKDOT_PRECON_USCS_06_28_07.GDT 7/28/10

STATE OF ALASKA DEPARTMENT OF TRANSPORTATION
NORTHERN REGION
LABORATORY TESTING REPORT

PROJECT NAME: TEMP/W Verification
PROJECT NUMBER: AUTC RR08.11
AKSAS NUMBER: 62223
SAMPLED BY: M. DARROW
MATERIAL SOURCE: RICH 113

		TH08-1650 2.5-4.5 N62.08238° W145.4368° **08-4070** 7-Nov-08	TH08-1650 15.5-16.0 N62.08238° W145.4368° **08-4074** 7-Nov-08	TH08-1650 29.0-29.5 N62.08238° W145.4368° **08-4078** 7-Nov-08	TH08-1650 33.5-34.5 N62.08238° W145.4368° **08-4079** 7-Nov-08	TH08-1652 4.5-5.5 N62.08235° W145.43727° **08-4080** 8-Nov-08	TH08-1652b 0.6-5.5 N62.0823° W145.43723° **08-4081** 9-Nov-08	TH08-1652b 0.3-0.6 N62.0823° W145.43723° **08-4082** 9-Nov-08
% Passing	**3"**						100	
	2"						97	100
	1.5"						96	97
Gravel	**1.0"**						87	96
	0.75"						81	94
	0.5"						67	86
	0.375"						59	80
	#4						42	63
	#8						32	50
	#10						30	48
	#16				100		26	39
	#30				99		20	28
Sand	**#40**				99		17	23
	#50				99		14	19
	#60				98		12	17
	#80				98		10	14
	#100				98		9	12
Silt/Clay	**#200**				96.3		6.2	8.9
	0.02				103.6			
Hydro	**0.005**				95.4			
	0.002				80.8			
	0.001				60.2			
LIQUID LIMIT					65		NV	NV
PLASTIC INDEX					38		NP	NP
USCS CLASSIFICATION					CH		GW-GM	SW-SM
USCS SOIL DESCRIPTION								
NATURAL MOISTURE		19.3	17.1	24.5		3.2		
ORGANICS								
SP. GR. (FINE)					2.49			2.66
SP. GR. (COARSE)								
MAX. DRY DENSITY								
OPTIMUM MOISTURE								
L.A. ABRASION								
DEGRAD. FACTOR								
SODIUM SULF. (CRSE)								
SODIUM SULF. (FINE)								
NORDIC ABRASION								
REMARKS								

GENERAL COMMENTS

Gradation is based on material passing the 3" sieve, according to Alaska Test Method T-7.

[1]Organic content determination is based on the results of the ATM T-6 test method.

(Soil descriptions shown in parentheses are based on field determinations.)

USCS Soil Description Abbreviations: WG = Well-graded; PG = Poorly-graded; E = Elastic; L = Lean; F = Fat

PROJECT NAME: TEMP/W Verification
PROJECT NUMBER: AUTC RR08.11
AKSAS NUMBER: 62223
SAMPLED BY: M. DARROW
MATERIAL SOURCE: RICH 113

TEST HOLE NUMBER DEPTH (feet) LATITUDE LONGITUDE LAB NUMBER DATE SAMPLED	TH08-1652b 5.5-6.5 N62.0823° W145.43723° 08-4083 9-Nov-08	TH08-1652b 6.5-6.7 N62.0823° W145.43723° 08-4084 9-Nov-08	TH08-1652b 6.5-7.0 N62.0823° W145.43723° 08-4085 9-Nov-08	TH08-1652b 8.0-9.5 N62.0823° W145.43723° 08-4086 9-Nov-08	TH08-1652b 10.0-12.0 N62.0823° W145.43723° 08-4087 9-Nov-08	TH08-1652b 15.0-17.0 N62.0823° W145.43723° 08-4088 9-Nov-08	TH08-1652b 15.5-16.0 N62.0823° W145.43723° 08-4089 9-Nov-08
% Passing 3"							
2"							
1.5"			100				
1.0"			98			100	
Gravel 0.75"			95			98	
0.5"			84			96	
0.375"			78			95	
#4			65			93	
#8			55			90	
#10			53			90	
#16			47			88	
#30			38			84	
Sand #40			32			81	
#50			26			77	
#60			24			75	
#80			21			70	
#100			20			67	
Silt/Clay #200			16.2			56.8	
0.02						38.8	
Hydro 0.005						23.7	
0.002						15.9	
0.001						11.3	
LIQUID LIMIT			NV			19	
PLASTIC INDEX			NP			5	
USCS CLASSIFICATION			SM			CL-ML	
USCS SOIL DESCRIPTION							
NATURAL MOISTURE	1.6	10.0		19.4	15.7		12.2
ORGANICS		2.5					
SP. GR. (FINE)		2.75				2.74	
SP. GR. (COARSE)							
MAX. DRY DENSITY							
OPTIMUM MOISTURE							
L.A. ABRASION							
DEGRAD. FACTOR							
SODIUM SULF. (CRSE)							
SODIUM SULF. (FINE)							
NORDIC ABRASION							
REMARKS		sl Org [1]					

GENERAL COMMENTS
Gradation is based on material passing the 3" sieve, according to Alaska Test Method T-7.
[1]Organic content determination is based on the results of the ATM T-6 test method.
(Soil descriptions shown in parentheses are based on field determinations.)
USCS Soil Description Abbreviations: WG = Well-graded; PG = Poorly-graded; E = Elastic; L = Lean; F = Fat

PROJECT NAME: TEMP/W Verification
PROJECT NUMBER: AUTC RR08.11
AKSAS NUMBER: 62223
SAMPLED BY: M. DARROW
MATERIAL SOURCE: RICH 113

		TH08-1652b	TH08-1652b	TH08-1652b	TH08-1653	TH08-1653	TH08-1653	TH08-1653
TEST HOLE NUMBER								
DEPTH (feet)		20.0-22.0	25.5-26.0	25.0-26.5	9.5-10.0	15.5-16.0	19.5-20.0	25.0-25.5
LATITUDE		N62.0823°	N62.0823°	N62.0823°	N62.08237°	N62.08237°	N62.08237°	N62.08237°
LONGITUDE		W145.43723°	W145.43723°	W145.43723°	W145.43712°	W145.43712°	W145.43712°	W145.43712°
LAB NUMBER		**08-4090**	**08-4091**	**08-4092**	**08-4095**	**08-4096**	**08-4097**	**08-4098**
DATE SAMPLED		9-Nov-08	9-Nov-08	9-Nov-08	9-Nov-08	9-Nov-08	9-Nov-08	9-Nov-08
% Passing	**3"**							
	2"							
	1.5"			100				
Gravel	**1.0"**			88				
	0.75"			87				
	0.5"			85				
	0.375"			83				
	#4			81				
	#8			78				
	#10			77				
	#16			75				
	#30			73				
Sand	**#40**			71				
	#50			69				
	#60			68				
	#80			64				
	#100			62				
Silt/Clay	**#200**			55.5				
	0.02							
Hydro	**0.005**							
	0.002							
	0.001							
LIQUID LIMIT				24				
PLASTIC INDEX				10				
USCS CLASSIFICATION				CL				
USCS SOIL DESCRIPTION								
NATURAL MOISTURE		10.7	15.5		4.4	5.9	4.9	11.3
ORGANICS								
SP. GR. (FINE)						2.72		
SP. GR. (COARSE)								
MAX. DRY DENSITY								
OPTIMUM MOISTURE								
L.A. ABRASION								
DEGRAD. FACTOR								
SODIUM SULF. (CRSE)								
SODIUM SULF. (FINE)								
NORDIC ABRASION								
REMARKS								

GENERAL COMMENTS

Gradation is based on material passing the 3" sieve, according to Alaska Test Method T-7.

[1]Organic content determination is based on the results of the ATM T-6 test method.

(Soil descriptions shown in parentheses are based on field determinations.)

USCS Soil Description Abbreviations: WG = Well-graded; PG = Poorly-graded; E = Elastic; L = Lean; F = Fat

STATE OF ALASKA DEPARTMENT OF TRANSPORTATION
NORTHERN REGION
LABORATORY TESTING REPORT

PROJECT NAME: TEMP/W Verification
PROJECT NUMBER: AUTC RR08.11
AKSAS NUMBER: 62223
SAMPLED BY: M. DARROW
MATERIAL SOURCE: RICH 113

TEST HOLE NUMBER DEPTH (feet) LATITUDE LONGITUDE LAB NUMBER DATE SAMPLED	TH08-1653 25.5-26.0 N62.08237° W145.43712° **08-4099** 9-Nov-08	TH08-1653 29.5-31.5 N62.08237° W145.43712° **08-4100** 9-Nov-08	TH08-1654 14.0-16.0 N62.08236° W145.43706° **08-4101** 10-Nov-08	TH08-1654 15.0-15.5 N62.08236° W145.43706° **08-4102** 10-Nov-08			
% Passing **3"** **2"** **1.5"** **1.0"** *Gravel* **0.75"** **0.5"** **0.375"** **#4**			100 98 98 96				
#8 **#10** **#16** **#30** *Sand* **#40** **#50** **#60** **#80** **#100**			93 93 90 86 83 80 78 75 73				
Silt/Clay **#200**			64.5				
0.02 *Hydro* **0.005** **0.002** **0.001**							
LIQUID LIMIT PLASTIC INDEX USCS CLASSIFICATION			21 7 CL-ML				
USCS SOIL DESCRIPTION							
NATURAL MOISTURE ORGANICS SP. GR. (FINE) SP. GR. (COARSE) MAX. DRY DENSITY OPTIMUM MOISTURE L.A. ABRASION DEGRAD. FACTOR SODIUM SULF. (CRSE) SODIUM SULF. (FINE) NORDIC ABRASION	35.1	27.7		14.2			
REMARKS							

GENERAL COMMENTS Gradation is based on material passing the 3" sieve, according to Alaska Test Method T-7.

[1]Organic content determination is based on the results of the ATM T-6 test method.

(Soil descriptions shown in parentheses are based on field determinations.)

USCS Soil Description Abbreviations: WG = Well-graded; PG = Poorly-graded; E = Elastic; L = Lean; F = Fat

PROJECT NAME: TEMP/W Verification
PROJECT NUMBER: AUTC RR08.11
AKSAS NUMBER: 62223
SAMPLED BY: M. DARROW
MATERIAL SOURCE: DALTON 9 MILE

TEST HOLE NUMBER	TH09-1401	TH09-1401	TH09-1402	TH09-1402	TH09-1402	TH09-1404	TH09-1404
DEPTH (feet)	6.5-7.5	12.0-12.5	0.0-3.5	3.0-3.5	11.5-12.0	6.0-6.5	36.0-36.5
LATITUDE	N65.54682°	N65.54682°	N65.54693°	N65.54693°	N65.54693°	N65.5469°	N65.5469°
LONGITUDE	W148.89243°	W148.89243°	W148.89194°	W148.89194°	W148.89194°	W148.892°	W148.892°
LAB NUMBER	**09-6601**	**09-6602**	**09-6603**	**09-6604**	**09-6605**	**09-6606**	**09-6607**
DATE SAMPLED	4-Aug-09	4-Aug-09	5-Aug-09	5-Aug-09	5-Aug-09	6-Aug-09	6-Aug-09
% Passing **3"**							
2"							
1.5"			100				
1.0"			99				
Gravel **0.75"**			96				
0.5"			88				
0.375"			81				
#4			64				
#8			48				
#10			46				
#16			37				
#30			28				
Sand **#40**	100		25				
#50	99		22				
#60	98		21				
#80	97		18				
#100	95		16				
Silt/Clay **#200**	90.0		11.4				
0.02							
Hydro **0.005**							
0.002							
0.001							
LIQUID LIMIT	NV		19				
PLASTIC INDEX	NP		4				
USCS CLASSIFICATION	ML		SW-SC				
USCS SOIL DESCRIPTION							
NATURAL MOISTURE	65.8	53.8		2.6	39.7	30.3	61.6
ORGANICS		6.0			7.1		
SP. GR. (FINE)							
SP. GR. (COARSE)							
MAX. DRY DENSITY							
OPTIMUM MOISTURE							
L.A. ABRASION							
DEGRAD. FACTOR							
SODIUM SULF. (CRSE)							
SODIUM SULF. (FINE)							
NORDIC ABRASION							
REMARKS		Org [1]			Org [1]		

GENERAL COMMENTS

Gradation is based on material passing the 3" sieve, according to Alaska Test Method T-7.

[1]Organic content determination is based on the results of the ATM T-6 test method.

(Soil descriptions shown in parentheses are based on field determinations.)

USCS Soil Description Abbreviations: WG = Well-graded; PG = Poorly-graded; E = Elastic; L = Lean; F = Fat

APPENDIX C – AUTOMATED DATA ACQUISITION SYSTEM PARTS LIST

Table C.1. Parts list for the Automated Data Acquisition Systems (ADAS) used for this project.

Device	Quantity at each research location	
	Richardson Hwy MP113 site	Dalton Hwy 9 Mile Hill site
Data Acquisition		
CR1000 Measurement & Control Datalogger, with extended temperature testing	1	1
AM16/32B 16 or 32 Channel Relay Multiplexer with extended temperature testing	1	1
MUXPOWER-L-2 Multiplexer Power/Reset Cable	1	1
MUXSIGNAL-L-2 Multiplexer Signal Cable	1	1
ENC14/16-NC-NM weather-resistant 14"x16" enclosure	1	1
Telemetry		
RF450 900MHz 1W Spread Spectrum Radio	2	1
Field power Cable 12Vdc Plug to Pigtail, 2 ft	1	1
Wall Charger 12Vdc 800mA Output, 100-240 Vac 50-60Hz w/ barrel plug, 6ft cable	1	---
900MHz 3dBd omni antenna w/ Type N female & mounting hardware	2	1
Data cable null modem DB9 male to male, 1ft	2	---
Moxa portserver	1	---
RF450 Diagnostics & Programming cable w/ software	1	---
Power		
SP20 20 Watt solar panel	1	1
100 Amp-Hr Concorde deep cycle batteries	3	3
PS100 12 Vdc power supply w/ charging regulator and 7 Amp-Hr sealed battery	1	---
Sun Saver charge controller	1	1
Battery enclosure	1	1
Software and connecting cables		
LOGGERNET datalogger support software	1	
SC32B optically isolated RS-232 interface	1	
USB to serial interface connector	1	
CR1000KD Keyboard/Display for CR1000	1	

The following tables contain the raw data obtained from the KD2 Pro thermal conductivity soil probe; these raw data values are given in SI units. Samples 4071A, 4072B, 4073B, 4076, and 4077 were taken from TH08-1650 at the Richardson Highway MP 113 location; samples 6600 A, B, and F were taken from TH09-1401 at the Dalton 9 Mile Hill location.

Table D.1. Thermal conductivity data for Sample 4071A.

Bath Temperature (Cº)	KD2 Pro Reading		Sample Temperature	
	W/m·K	r^2	Before test (Cº)	After test (Cº)
-20	1.412	1.0000	-20.20	-20.19
	1.415	1.0000		
	1.425	1.0000		
-15	1.421	1.0000	-15.05	-15.05
	1.426	1.0000		
	1.432	1.0000		
-10	1.464	1.0000	-10.14	-10.12
	1.461	1.0000		
	1.453	1.0000		
-7.5	1.492	1.0000	-7.57	-7.56
	1.482	1.0000		
	1.475	1.0000		
-5	1.783	1.0000	-5.06	-5.04
	1.773	1.0000		
	1.775	1.0000		
-4	1.931	1.0000	-4.05	-4.03
	1.950	1.0000		
	1.944	1.0000		
-3	2.283	0.9999	-2.96	-2.96
	2.377	0.9999		
	2.317	0.9999		
-2	1.057	1.0000	-2.04	-2.03
	1.056	1.0000		
	1.065	1.0000		
-1	1.071	1.0000	-1.07	-1.05
	1.083	1.0000		
	1.083	1.0000		
-0.5	1.074	1.0000	-0.51	-0.51
	1.074	1.0000		
	1.083	1.0000		
-0.2	1.085	1.0000	-0.25	-0.25
	1.091	1.0000		
	1.090	1.0000		
5	1.092	1.0000	4.97	4.97
	1.102	1.0000		
	1.094	1.0000		
10	1.093	1.0000	9.98	9.98
	1.099	1.0000		
	1.102	1.0000		

Table D.2. Thermal conductivity data for Sample 4072B.

Bath Temperature (Cº)	KD2 Pro Reading		Sample Temperature	
	W/m·K	r^2	Before test (Cº)	After test (Cº)
-20	1.668	1.0000	-19.86	-19.85
	1.663	1.0000		
	1.692	1.0000		
-15	1.814	1.0000	-15.04	-15.03
	1.831	1.0000		
	1.833	1.0000		
-10	1.695	0.9999	-9.91	-9.91
	1.693	0.9999		
	1.699	0.9999		
-7.5	1.201	0.9999	-7.51	-7.50
	1.203	1.0000		
	1.206	1.0000		
-5	1.189	1.0000	-5.05	-5.05
	1.189	1.0000		
	1.193	1.0000		
-4	1.208	1.0000	-4.01	-4.01
	1.211	0.9999		
	1.204	1.0000		
-3	1.215	1.0000	-3.05	-3.05
	1.206	0.9999		
	1.212	1.0000		
-2	1.204	1.0000	-2.02	-2.01
	1.199	1.0000		
	1.205	1.0000		
-1	1.033	0.9999	-1.03	-1.03
	1.067	0.9999		
	1.069	1.0000		
-0.5	1.211	1.0000	-0.54	-0.53
	1.217	1.0000		
	1.214	1.0000		
-0.2	1.207	1.0000	-0.24	-0.23
	1.214	1.0000		
	1.218	1.0000		
5	1.207	1.0000	4.94	4.95
	1.209	1.0000		
	1.219	1.0000		
10	1.209	1.0000	9.97	9.99
	1.206	1.0000		
	1.217	1.0000		

Table D.3. Thermal conductivity data for Sample 4073B.

Bath Temperature (C°)	KD2 Pro Reading		Sample Temperature	
	W/m·K	r^2	Before test (C°)	After test (C°)
-20	1.830	0.9999	-19.97	-19.85
	1.762	0.9999		
	1.910	1.0000		
-15	2.009	0.9999	-15.01	-14.96
	1.944	1.0000		
	1.960	0.9999		
-10	2.027	1.0000	-9.98	-9.96
	2.005	1.0000		
	1.991	1.0000		
-7.5	2.078	1.0000	-7.46	-7.42
	2.086	0.9999		
	2.068	1.0000		
-5	2.258	1.0000	-5.03	-5.01
	2.263	1.0000		
	2.245	1.0000		
-4	2.286	1.0000	-4.00	-3.99
	2.141	0.9997		
	2.169	0.9999		
-3	2.187	0.9999	-2.98	-2.98
	2.141	0.9997		
	2.169	0.9999		
-2	2.478	1.0000	-2.03	-2.00
	2.502	1.0000		
	2.533	1.0000		
-1	1.404	1.0000	-0.95	-0.90
	1.343	1.0000		
	1.381	1.0000		
-0.5	1.420	1.0000	-0.51	-0.51
	1.352	1.0000		
	1.385	1.0000		
-0.2	1.405	1.0000	-0.19	-0.19
	1.409	1.0000		
	1.402	1.0000		
5	1.405	1.0000	4.99	4.99
	1.414	1.0000		
	1.413	1.0000		
10	1.395	1.0000	10.00	10.00
	1.405	1.0000		
	1.412	1.0000		

Table D.4. Thermal conductivity data for Sample 4076.

Bath Temperature (Cº)	KD2 Pro Reading		Sample Temperature	
	W/m·K	r^2	Before test (Cº)	After test (Cº)
-20	1.648	0.9999	-20.01	-20.00
	1.630	1.0000		
	1.615	0.9999		
-15	1.626	1.0000	-15.02	-15.01
	1.631	0.9999		
	1.658	0.9999		
-10	1.620	1.0000	-10.02	-10.02
	1.647	1.0000		
	1.655	0.9999		
-7.5	1.659	1.0000	-7.55	-7.55
	1.668	1.0000		
	1.660	1.0000		
-5	1.740	1.0000	-5.06	-5.06
	1.699	1.0000		
	1.711	1.0000		
-4	1.758	1.0000	-4.07	-4.06
	1.729	1.0000		
	1.716	1.0000		
-3	1.787	0.9999	-3.07	-3.07
	1.743	1.0000		
	1.757	1.0000		
-2	2.005	1.0000	-2.09	-2.09
	1.926	1.0000		
	1.929	1.0000		
-1	2.700	0.9999	-1.14	-1.13
	2.644	0.9999		
	2.571	1.0000		
-0.5	1.218	0.9996	-0.51	-0.51
	1.219	0.9996		
	1.213	0.9996		
-0.2	1.282	1.0000	-0.23	-0.23
	1.288	1.0000		
	1.284	1.0000		
5	1.309	1.0000	4.97	4.96
	1.317	1.0000		
	1.324	1.0000		
10	1.320	1.0000	9.98	9.98
	1.313	1.0000		
	1.320	1.0000		

Table D.5. Thermal conductivity data for Sample 4077.

Bath Temperature (Cº)	KD2 Pro Reading		Sample Temperature	
	W/m·K	r^2	Before test (Cº)	After test (Cº)
-20	1.613	0.9999	-19.95	-19.84
	1.606	0.9999		
	1.657	0.9999		
-15	1.691	0.9999	-14.99	-14.96
	1.679	0.9999		
	1.717	0.9999		
-10	1.688	0.9999	-10.02	-9.99
	1.704	0.9999		
	1.729	0.9999		
-7.5	1.776	0.9999	-7.51	-7.39
	1.786	0.9999		
	1.788	0.9999		
-5	1.264	1.0000	-4.97	-4.96
	1.235	1.0000		
	1.256	1.0000		
-4	1.286	1.0000	-4.02	-4.01
	1.26	1.0000		
	1.281	1.0000		
-3	1.295	0.9999	-2.97	-2.91
	1.276	0.9999		
	1.286	0.9999		
-2	1.313	1.0000	-1.99	-1.93
	1.28	1.0000		
	1.293	1.0000		
-1	1.281	1.0000	-1.00	-0.99
	1.28	1.0000		
	1.308	1.0000		
-0.5	1.343	1.0000	-0.50	-0.53
	1.291	1.0000		
	1.324	1.0000		
-0.2	1.337	1.0000	-0.20	-0.19
	1.309	1.0000		
	1.334	1.0000		
5	1.359	1.0000	5.04	5.05
	1.319	1.0000		
	1.338	1.0000		
10	1.346	1.0000	9.99	9.99
	1.33	1.0000		
	1.343	1.0000		

Table D.6. Thermal conductivity data for Sample 6600A.

Bath Temperature (C°)	KD2 Pro Reading		Sample Temperature	
	W/m·K	r^2	Before test (C°)	After test (C°)
-20	1.728	0.9999	-20.01	-20.00
	1.735	0.9999		
	1.748	0.9999		
-15	1.654	0.9999	-14.98	-14.98
	1.647	0.9999		
	1.646	0.9999		
-10	1.536	1.0000	-9.99	-9.99
	1.546	1.0000		
	1.547	1.0000		
-7.5	1.536	0.9999	-7.53	-7.53
	1.546	1.0000		
	1.547	0.9999		
-5	1.767	0.9999	-5.05	-5.05
	1.771	0.9999		
	1.774	0.9999		
-4	2.052	0.9999	-4.06	-4.05
	2.084	0.9999		
	2.072	0.9999		
-3	2.391	0.9999	-3.09	-3.09
	2.375	0.9999		
	2.403	0.9999		
-2	3.239	0.9999	-2.03	-2.02
	3.245	1.0000		
	3.282	0.9999		
-1	3.104	0.9981	-1.04	-1.02
	3.076	0.9981		
	3.301	0.9981		
-0.5	2.052	0.9996	-0.55	-0.54
	2.032	0.9997		
	2.029	0.9997		
-0.2	1.047	1.0000	-0.23	-0.23
	1.057	1.0000		
	1.064	1.0000		
5	1.051	1.0000	4.98	4.99
	1.058	1.0000		
	1.056	1.0000		
10	1.061	1.0000	10.00	10.01
	1.068	0.9999		
	1.069	0.9999		

Table D.7. Thermal conductivity data for Sample 6600B.

Bath Temperature (Cº)	KD2 Pro Reading		Sample Temperature	
	W/m·K	r^2	Before test (Cº)	After test (Cº)
-20	1.812	0.9999	-19.98	-19.98
	1.834	0.9999		
	1.806	0.9999		
-15	1.802	1.0000	-14.98	-14.98
	1.785	0.9999		
	1.803	1.0000		
-10	1.795	1.0000	-9.99	-9.98
	1.794	0.9999		
	1.793	1.0000		
-7.5	1.743	0.9999	-7.50	-7.50
	1.761	1.0000		
	1.756	0.9999		
-5	1.775	0.9999	-5.03	-5.03
	1.766	0.9999		
	1.772	0.9999		
-4	1.795	1.0000	-4.04	-4.03
	1.805	0.9999		
	1.801	0.9999		
-3	1.904	0.9999	-3.02	-3.01
	1.887	0.9999		
	1.880	0.9999		
-2	2.593	0.9999	-2.01	-2.00
	2.597	1.0000		
	2.580	0.9999		
-1	3.626	1.0000	-1.01	-1.01
	3.716	0.9999		
	3.699	0.9999		
-0.5	0.888	0.9945	-0.51	-0.51
	1.061	0.9999		
	1.044	0.9999		
-0.2	0.935	1.0000	-0.24	-0.24
	1.006	1.0000		
	1.009	1.0000		
5	0.702	1.0000	5.04	5.04
	0.691	1.0000		
	0.692	1.0000		
10	0.940	1.0000	9.97	10.00
	0.701	1.0000		
	0.704	1.0000		

Table D.8. Thermal conductivity data for Sample 6600F.

Bath Temperature (Cº)	KD2 Pro Reading		Sample Temperature	
	W/m·K	r^2	Before test (Cº)	After test (Cº)
-20	1.757	0.9999	-20.08	-20.08
	1.763	0.9999		
	1.771	0.9999		
-15	1.721	0.9999	-15.02	-15.01
	1.731	0.9999		
	1.740	0.9999		
-10	1.793	0.9999	-10.02	-10.02
	1.801	0.9999		
	1.787	0.9999		
-7.5	1.792	0.9999	-7.49	-7.47
	1.811	0.9999		
	1.795	0.9999		
-5	1.818	0.9999	-5.06	-5.05
	1.831	0.9999		
	1.807	0.9999		
-4	1.850	0.9999	-4.03	-4.01
	1.851	0.9999		
	1.847	0.9999		
-3	1.972	0.9999	-2.99	-2.99
	1.949	1.0000		
	1.942	0.9999		
-2	2.239	0.9999	-2.05	-2.04
	2.227	0.9999		
	2.237	0.9999		
-1	4.094	1.0000	-0.99	-0.99
	4.098	1.0000		
	4.133	0.9999		
-0.5	1.202	0.9996	-0.52	-0.52
	1.271	0.9998		
	1.271	0.9998		
-0.2	0.785	1.0000	-0.87	-0.84
	0.767	1.0000		
	0.759	1.0000		
5	0.654	1.0000	4.98	4.98
	0.657	1.0000		
	0.661	1.0000		
10	0.656	1.0000	9.99	10.00
	0.657	1.0000		
	0.661	1.0000		

Table E.1. Measured versus modeled temperatures for the undisturbed thermistor string, Run 1b, Richardson Highway MP 113 research site. For each month and at each selected depth, the upper left temperature is that measured by the thermistor bead. The lower left temperature in parentheses and italics is the modeled temperature estimated to the nearest 0.5°F. The number to the right is the difference between the two temperatures to the left. Temperatures were compared for the first day of each month in 2009.

Depth (ft)	Temperatures (°F)											
	January		February		March		April		May		June	
0.5	14.4 *(19.0)*	-4.6	26.2 *(21.0)*	5.2	25.1 *(23.0)*	2.1	27.0 *(28.0)*	-1.0	33.9 *(33.0)*	0.9	43.5 *(36.0)*	7.5
2	27.3 *(21.5)*	5.8	30.5 *(22.0)*	8.5	30.0 *(23.5)*	6.5	28.2 *(27.0)*	1.2	30.5 *(30.0)*	0.5	31.7 *(31.5)*	0.2
6	31.7 *(26.5)*	5.2	31.6 *(25.0)*	6.6	31.5 *(25.0)*	6.5	31.2 *(27.0)*	4.2	31.0 *(29.0)*	2.0	31.0 *(30.0)*	1.0
10	31.6 *(29.0)*	2.6	31.6 *(27.0)*	4.6	31.6 *(26.5)*	5.1	31.5 *(27.0)*	4.5	31.5 *(29.0)*	2.5	31.5 *(29.0)*	2.5
14	31.3 *(29.0)*	2.3	31.4 *(28.5)*	2.9	31.3 *(27.5)*	3.8	31.3 *(27.5)*	3.8	31.3 *(29.0)*	2.3	31.3 *(29.0)*	2.3
18	31.4 *(29.0)*	2.4	31.4 *(29.0)*	2.4	31.4 *(28.5)*	2.9	31.4 *(28.0)*	3.4	31.4 *(29.0)*	2.4	31.4 *(29.0)*	2.4
23	31.2 *(29.0)*	2.2	31.2 *(29.0)*	2.2	31.1 *(29.0)*	2.1	31.1 *(28.5)*	2.6	31.1 *(29.0)*	2.1	31.1 *(29.0)*	2.1
30	31.1 *(29.0)*	2.1	31.0 *(29.0)*	2.0	31.0 *(29.0)*	2.0	31.0 *(29.0)*	2.0	31.0 *(29.0)*	2.0	31.0 *(29.0)*	2.0

Table E.1 (continued).

Depth	Temperatures (°F)											
(ft)	July		August		September		October		November		December	
0.5	49.8 (40.0)	9.8	57.9 (41.0)	16.9	50.5 (37.0)	13.5	35.5 (35.0)	0.5	30.1 (27.0)	3.1	28.5 (21.0)	7.5
2	35.9 (34.0)	1.9	41.9 (35.0)	6.9	41.4 (35.0)	6.4	36.2 (35.0)	1.2	32.6 (32.0)	0.6	31.3 (26.0)	5.3
6	31.1 (30.5)	0.6	31.3 (31.0)	0.3	31.6 (31.5)	0.1	31.9 (31.5)	0.4	31.8 (31.5)	0.3	31.7 (32.0)	0.3
10	31.4 (29.5)	1.9	31.4 (30.0)	1.4	31.4 (30.5)	0.9	31.5 (31.0)	0.5	31.5 (31.0)	0.5	31.5 (31.0)	0.5
14	31.3 (29.0)	2.3	31.3 (29.0)	2.3	31.3 (30.0)	1.3	31.3 (31.0)	0.3	31.3 (31.0)	0.3	31.3 (31.0)	0.3
18	31.4 (29.0)	2.4	31.4 (29.0)	2.4	31.4 (29.5)	1.9	31.4 (31.0)	0.4	31.4 (31.0)	0.4	31.4 (31.0)	0.4
23	31.1 (29.0)	2.1	31.1 (28.5)	2.6	31.1 (29.0)	2.1	31.1 (31.0)	0.1	31.1 (31.0)	0.1	31.1 (31.0)	0.1
30	31.0 (29.0)	2.0	31.0 (29.0)	2.0	31.0 (29.0)	2.0	31.0 (31.0)	0.0	31.0 (31.0)	0.0	31.0 (31.0)	0.0

Table E.2. Measured versus modeled temperatures for the toe thermistor string, Run 1b, Richardson Highway MP 113 research site. For each month and at each selected depth, the upper left temperature is that measured by the thermistor bead. The lower left temperature in parentheses and italics is the modeled temperature estimated to the nearest 0.5°F. The number to the right is the difference between the two temperatures to the left. Temperatures were compared for the first day of each month in 2009.

Depth (ft)	Temperatures (°F)											
	January		February		March		April		May		June	
0.5	15.2 *(9.0)*	6.2	19.0 *(-1.0)*	20.0	16.9 *(0.0)*	16.9	23.8 *(17.0)*	6.8	39.8 *(39.0)*	0.8	54.3 *(59.0)*	-4.7
2	23.6 *(8.0)*	15.6	22.4 *(5.0)*	17.4	19.9 *(8.0)*	11.9	23.4 *(17.0)*	6.4	29.9 *(31.0)*	-1.1	45.2 *(46.0)*	-0.8
6	32.7 *(23.0)*	9.7	31.8 *(17.0)*	14.8	31.0 *(16.0)*	15.0	30.0 *(17.5)*	12.5	30.4 *(25.0)*	5.4	30.9 *(30.0)*	0.9
10	35.2 *(32.0)*	3.2	34.0 *(26.5)*	7.5	33.3 *(23.0)*	10.0	32.7 *(21.0)*	11.7	32.4 *(23.5)*	8.9	32.2 *(27.5)*	4.7
14	35.7 *(31.5)*	4.2	34.7 *(30.0)*	4.7	34.0 *(27.5)*	6.5	33.4 *(25.0)*	8.4	32.9 *(25.0)*	7.9	32.6 *(27.0)*	5.6
18	33.7 *(31.0)*	2.7	35.1 *(31.0)*	4.1	34.5 *(29.5)*	5.0	34.0 *(27.5)*	6.5	33.6 *(26.5)*	7.1	33.2 *(27.0)*	6.2
23	34.6 *(30.5)*	4.1	34.4 *(30.5)*	3.9	34.1 *(30.0)*	4.1	33.8 *(29.0)*	4.8	33.4 *(28.5)*	4.9	33.1 *(28.0)*	5.1
30	35.1 *(30.5)*	4.6	34.7 *(30.0)*	4.7	34.3 *(30.0)*	4.3	33.8 *(30.0)*	3.8	33.5 *(29.0)*	4.5	33.1 *(29.0)*	4.1

Table E.2 (continued).

Depth (ft)	Temperatures (°F)											
	July		August		September		October		November		December	
0.5	63.8 (65.0)	1.2	67.5 (65.0)	2.5	55.2 (57.0)	-1.8	38.1 (43.0)	-4.9	26.3 (9.0)	17.3	19.1 (9.0)	10.1
2	51.2 (55.0)	-3.8	57.9 (55.0)	2.9	51.7 (53.0)	-1.3	41.5 (41.0)	0.5	34.1 (25.0)	9.1	24.4 (13.0)	11.4
6	33.1 (33.0)	0.1	42.1 (35.0)	7.5	44.3 (37.0)	7.3	43.2 (37.0)	6.2	38.9 (35.0)	3.9	34.6 (32.0)	2.6
10	32.2 (30.0)	2.2	35.2 (30.5)	4.7	38.7 (31.5)	7.2	39.8 (32.0)	7.8	38.9 (32.0)	6.9	36.9 (32.0)	4.9
14	32.5 (29.0)	3.5	33.0 30.0)	3.0	34.0 (31.0)	3.0	36.5 (31.0)	5.5	35.2 (31.0)	4.2	35.4 (31.5)	3.9
18	33.0 (29.0)	4.0	32.9 (29.0)	3.9	33.7 (30.0)	3.7	34.7 (31.0)	3.7	35.5 (31.0)	4.5	35.6 (31.0)	4.6
23	32.9 (29.0)	3.9	32.7 (29.0)	3.7	32.8 (30.0)	2.8	33.2 (31.0)	2.2	33.8 (31.0)	2.8	34.1 (31.0)	3.1
30	32.9 (29.5)	3.4	32.7 (29.5)	3.2	33.0 (30.0)	3.0	33.7 (31.0)	2.7	34.4 (31.0)	3.4	34.8 (31.0)	3.8

Table E.3. Measured versus modeled temperatures for the embankment thermistor string, Run 1b, Richardson Highway MP 113 research site. For each month and at each selected depth, the upper left temperature is that measured by the thermistor bead. The lower left temperature in parentheses and italics is the modeled temperature estimated to the nearest 0.5°F. The number to the right is the difference between the two temperatures to the left. Temperatures were compared for the first day of each month in 2009.

Depth (ft)	Temperatures (°F)											
	January		February		March		April		May		June	
0.5	-16.7 *(0.5)*	-17.2	7.5 *(-21.0)*	28.5	12.8 *(3.0)*	9.8	28.1 *(17.0)*	11.1	50.9 *(41.0)*	9.9	57.5 *(65.0)*	-7.5
2	0.7 *(3.0)*	-2.3	12.7 *(-5.0)*	17.7	15.3 *(5.0)*	10.3	25.7 *(17.0)*	8.7	40.6 *(31.5)*	9.1	52.9 *(55.0)*	-2.1
6	29.0 *(19.0)*	10.0	27.5 *(25.0)*	2.5	26.0 *(19.0)*	7.0	26.7 *(22.0)*	4.7	30.5 *(31.0)*	-0.5	34.5 *(40.0)*	-5.5
10	34.7 *(31.5)*	3.2	33.3 *(29.5)*	3.8	32.4 *(29.0)*	3.4	31.8 *(29.0)*	2.8	31.6 *(31.0)*	0.6	31.7 *(32.0)*	-0.3
14	36.1 *(35.0)*	1.1	34.9 *(34.0)*	0.9	34.0 *(33.0)*	1.0	33.3 *(33.0)*	0.3	32.9 *(33.0)*	-0.1	32.6 *(33.0)*	-0.4
18	36.5 *(34.0)*	2.5	35.6 *(34.0)*	1.6	35.0 *(33.0)*	2.0	34.3 *(33.0)*	1.3	33.8 *(33.0)*	0.8	33.4 *(33.0)*	0.4
23	35.6 *(33.5)*	2.1	35.2 *(33.5)*	1.7	34.9 *(33.0)*	1.9	34.5 *(33.0)*	1.5	34.1 *(33.0)*	1.1	33.7 *(33.0)*	0.7
30	34.2 *(32.5)*	1.7	34.2 *(32.5)*	1.7	34.2 *(32.5)*	1.7	34.1 *(32.5)*	1.6	33.9 *(32.5)*	1.4	33.7 *(32.5)*	1.2

Table E.3 (continued).

Depth (ft)	Temperatures (°F)											
	July		August		September		October		November		December	
0.5	67.1 (75.0)	-7.9	70.4 (75.0)	-4.6	55.0 (61.0)	-6.0	37.4 (41.0)	-3.6	16.8 (5.0)	11.8	16.4 (-23.0)	39.4
2	56.7 (68.0)	-11.3	63.3 (69.0)	-5.7	53.6 (59.5)	-5.9	41.4 (43.0)	-1.6	33.2 (15.0)	18.2	19.3 (-1)	20.3
6	39.6 (49.0)	-9.4	47.6 (53.0)	-5.4	49.0 (50.5)	-1.5	46.1 (45.0)	1.1	39.7 (35.0)	4.7	32.2 (24.0)	8.2
10	31.8 (38.0)	-6.2	35.8 (40.5)	-4.7	41.6 (41.0)	0.6	42.7 (41.0)	1.7	41.0 (37.0)	4.0	37.6 (33.5)	4.1
14	32.5 (34.5)	-2.0	33.0 (34.5)	-1.5	36.4 (35.0)	1.4	38.4 (35.0)	3.4	38.9 (35.0)	3.9	38.0 (35.0)	3.0
18	33.2 (34.0)	-0.8	33.1 (34.0)	-0.9	34.3 (34.0)	0.3	35.9 (34.0)	1.9	36.9 (34.0)	2.9	37.1 (34.0)	3.1
23	33.4 (33.5)	-0.1	33.2 (33.5)	-0.3	33.3 (33.5)	-0.2	34.0 (33.5)	0.5	34.8 (33.5)	1.3	35.3 (33.5)	1.8
30	33.5 (32.5)	1.0	33.3 (32.5)	0.8	33.2 (32.5)	0.7	33.2 (32.5)	0.7	33.4 (32.5)	0.9	33.7 (33.0)	0.7

Table E.4. Measured versus modeled temperatures for the undisturbed thermistor string, Run 4, Richardson Highway MP 113 research site. For each month and at each selected depth, the upper left temperature is that measured by the thermistor bead. The lower left temperature in parentheses and italics is the modeled temperature estimated to the nearest 0.5°F. The number to the right is the difference between the two temperatures to the left. Temperatures were compared for the first day of each month in 2009.

Depth (ft)	Temperatures (°F)											
	January		February		March		April		May		June	
0.5	14.4 *(15.0)*	-0.6	26.2 *(20.0)*	6.2	25.1 *(24.5)*	0.6	27.0 *(31.5)*	-4.5	33.9 *(36.0)*	-2.1	43.5 *(40.0)*	3.5
2	27.3 *(20.0)*	7.3	30.5 *(22.0)*	8.5	30.0 *(25.0)*	5.0	28.2 *(29.5)*	-1.3	30.5 *(31.5)*	-1.0	31.7 *(34.0)*	-2.3
6	31.7 *(32.5)*	-0.8	31.6 *(27.0)*	4.6	31.5 *(27.0)*	4.5	31.2 *(29.0)*	2.2	31.0 *(29.5)*	1.5	31.0 *(31.0)*	0.0
10	31.6 *(31.5)*	0.1	31.6 *(30.0)*	1.6	31.6 *(28.5)*	3.1	31.5 *(28.5)*	3.0	31.5 *(29.0)*	1.5	31.5 *(29.5)*	2.0
14	31.3 *(31.5)*	-0.2	31.4 *(30.5)*	0.9	31.3 *(30.0)*	1.3	31.3 *(29.0)*	2.3	31.3 *(29.5)*	1.8	31.3 *(29.0)*	2.3
18	31.4 *(31.5)*	-0.1	31.4 *(30.5)*	0.9	31.4 *(30.5)*	0.9	31.4 *(30.0)*	1.4	31.4 *(29.5)*	1.9	31.4 *(29.5)*	1.9
23	31.2 *(31.5)*	-0.3	31.2 *(31.0)*	0.2	31.1 *(31.0)*	0.1	31.1 *(30.5)*	0.6	31.1 *(30.5)*	0.6	31.1 *(30.5)*	0.6
30	31.1 *(31.5)*	-0.4	31.0 *(31.0)*	0.0	31.0 *(31.0)*	0.0	31.0 *(31.0)*	0.0	31.0 *(31.0)*	0.0	31.0 *(31.0)*	0.0

Table E.4 (continued).

Depth (ft)	Temperatures (°F)											
	July		August		September		October		November		December	
0.5	49.8 (42.0)	7.8	57.9 (40.0)	7.9	50.5 (38.0)	12.5	35.5 (33.0)	2.5	30.1 (25.0)	5.1	28.5 (27.5)	1.0
2	35.9 (35.0)	0.9	41.9 (38.0)	3.9	41.4 (36.5)	4.9	36.2 (33.0)	3.2	32.6 (32.0)	0.6	31.3 (29.0)	2.3
6	31.1 (31.0)	0.1	31.3 (31.5)	-0.2	31.6 (31.5)	0.1	31.9 (31.5)	0.4	31.8 (32.0)	-0.2	31.7 (32.0)	-0.3
10	31.4 (31.0)	0.4	31.4 (31.0)	0.4	31.4 (31.0)	0.4	31.5 (31.0)	0.5	31.5 (31.0)	0.5	31.5 (31.0)	0.5
14	31.3 (30.5)	0.8	31.3 (31.0)	0.3	31.3 (31.0)	0.3	31.3 (31.0)	0.3	31.3 (31.0)	0.3	31.3 (31.0)	0.3
18	31.4 (30.0)	1.4	31.4 (31.0)	0.4	31.4 (31.0)	0.4	31.4 (31.0)	0.4	31.4 (31.0)	0.4	31.4 (31.0)	0.4
23	31.1 (30.5)	0.6	31.1 (31.0)	0.1	31.1 (31.0)	0.1	31.1 (31.0)	0.1	31.1 (31.0)	0.1	31.1 (31.0)	0.1
30	31.0 (31.0)	0.0	31.0 (31.0)	0.0	31.0 (31.0)	0.0	31.0 (31.0)	0.0	31.0 (31.0)	0.0	31.0 (31.0)	0.0

Table E.5. Measured versus modeled temperatures for the toe thermistor string, Run 4, Richardson Highway MP 113 research site. For each month and at each selected depth, the upper left temperature is that measured by the thermistor bead. The lower left temperature in parentheses and italics is the modeled temperature estimated to the nearest 0.5°F. The number to the right is the difference between the two temperatures to the left. Temperatures were compared for the first day of each month in 2009.

Depth (ft)	Temperatures (°F)											
	January		February		March		April		May		June	
0.5	15.2 (-8.0)	23.2	19.0 (-6.0)	25.0	16.9 (14.0)	2.9	23.8 (31.5)	-7.7	39.8 (48.0)	-8.2	54.3 (66.0)	-11.7
2	23.6 (16.0)	7.6	22.4 (4.0)	18.4	19.9 (13.5)	6.4	23.4 (23.5)	-0.1	29.9 (34.0)	-4.1	45.2 (52.0)	-6.8
6	32.7 (25.0)	7.7	31.8 (21.0)	10.8	31.0 (22.0)	9.0	30.0 (21.5)	8.5	30.4 (29.0)	1.4	30.9 (31.5)	-0.6
10	35.2 (32.5)	2.7	34.0 (32.0)	2.0	33.3 (29.0)	4.3	32.7 (26.5)	6.2	32.4 (28.5)	2.9	32.2 (31.0)	1.2
14	35.7 (31.5)	4.2	34.7 (31.5)	3.2	34.0 (31.5)	2.5	33.4 (30.0)	3.4	32.9 (29.5)	3.4	32.6 (31.0)	1.6
18	33.7 (31.5)	2.2	35.1 (31.5)	3.6	34.5 (31.5)	3.0	34.0 (31.0)	3.0	33.6 (30.5)	3.1	33.2 (31.0)	2.2
23	34.6 (31.5)	3.1	34.4 (31.5)	2.9	34.1 (31.5)	2.6	33.8 (31.5)	2.3	33.4 (31.0)	2.4	33.1 (31.5)	1.6
30	35.1 (31.5)	3.6	34.7 (31.5)	3.2	34.3 (31.5)	2.8	33.8 (31.5)	2.3	33.5 (31.5)	2.0	33.1 (31.5)	1.6

Table E.5 (continued).

Depth (ft)	Temperatures (°F)											
	July		August		September		October		November		December	
0.5	63.8 (78.0)	-14.2	67.5 (67.5)	0.0	55.2 (61.0)	-5.8	38.1 (38.5)	-0.4	26.3 (12.0)	14.3	19.1 (12.0)	7.1
2	51.2 (60.0)	-8.8	57.9 (67.0)	-9.1	51.7 (56.5)	-4.8	41.5 (41.0)	0.5	34.1 (28.0)	6.1	24.4 (18.0)	6.4
6	33.1 (36.5)	-3.4	42.1 (43.0)	-0.9	44.3 (41.0)	3.3	43.2 (41.0)	2.2	38.9 (38.5)	0.4	34.6 (33.0)	1.6
10	32.2 (31.5)	0.7	35.2 (31.5)	3.7	38.7 (32.0)	6.7	39.8 (32.0)	7.8	38.9 (33.0)	5.9	36.9 (35.0)	1.9
14	32.5 (31.5)	1.0	33.0 (31.5)	1.5	34.0 (31.5)	2.5	36.5 (31.5)	5.5	35.2 (31.5)	3.7	35.4 (31.5)	3.9
18	33.0 (31.5)	1.5	32.9 (31.5)	1.4	33.7 (31.5)	2.2	34.7 (31.5)	3.2	35.5 (31.5)	4.0	35.6 (31.5)	4.1
23	32.9 (31.5)	1.4	32.7 (31.5)	1.2	32.8 (31.5)	1.3	33.2 (31.5)	1.7	33.8 (31.5)	2.3	34.1 (31.5)	2.6
30	32.9 (31.5)	1.4	32.7 (31.5)	1.2	33.0 (31.5)	1.5	33.7 (31.5)	2.2	34.4 (31.5)	2.9	34.8 (31.5)	3.3

Table E.6. Measured versus modeled temperatures for the embankment thermistor string, Run 4, Richardson Highway MP 113 research site. For each month and at each selected depth, the upper left temperature is that measured by the thermistor bead. The lower left temperature in parentheses and italics is the modeled temperature estimated to the nearest 0.5°F. The number to the right is the difference between the two temperatures to the left. Temperatures were compared for the first day of each month in 2009.

Depth (ft)	Temperatures (°F)											
	January		February		March		April		May		June	
0.5	-16.7 *(-12.0)*	-4.7	7.5 *(-8.0)*	15.5	12.8 *(12.0)*	0.8	28.1 *(32.0)*	-3.9	50.9 *(56.0)*	-5.1	57.5 *(86.0)*	-28.5
2	0.7 *(9.0)*	-8.3	12.7 *(-1.0)*	13.7	15.3 *(9.0)*	6.3	25.7 *(24.5)*	1.2	40.6 *(46.0)*	-5.4	52.9 *(66.0)*	-13.1
6	29.0 *(22.0)*	7.0	27.5 *(20.0)*	7.5	26.0 *(23.0)*	3.0	26.7 *(24.5)*	2.2	30.5 *(34.0)*	-3.5	34.5 *(46.0)*	-11.5
10	34.7 *(38.0)*	-3.3	33.3 *(32.0)*	1.3	32.4 *(32.0)*	0.4	31.8 *(32.0)*	-0.2	31.6 *(32.0)*	-0.4	31.7 *(37.5)*	-5.8
14	36.1 *(38.5)*	-2.4	34.9 *(38.0)*	-3.1	34.0 *(38.0)*	-4.0	33.3 *(36.5)*	-3.2	32.9 *(36.5)*	-3.6	32.6 *(37.0)*	-4.4
18	36.5 *(37.0)*	-0.5	35.6 *(37.0)*	-1.4	35.0 *(37.0)*	-2.0	34.3 *(37.0)*	-2.7	33.8 *(37.0)*	-3.2	33.4 *(37.0)*	-3.6
23	35.6 *(36.0)*	-0.4	35.2 *(36.0)*	-0.8	34.9 *(36.0)*	-1.1	34.5 *(36.0)*	-1.5	34.1 *(36.0)*	-1.9	33.7 *(36.0)*	-2.3
30	34.2 *(35.0)*	-0.8	34.2 *(35.0)*	-0.8	34.2 *(35.0)*	-0.8	34.1 *(35.0)*	-0.9	33.9 *(35.0)*	-1.1	33.7 *(35.0)*	-1.3

Table E.6 (continued).

Depth	Temperatures (°F)										
(ft)	July		August		September		October		November		December	
0.5	67.1 (86.0)	-18.9	70.4 (76.5)	-6.1	55.0 (68.0)	-13.0	37.4 (41.0)	-3.6	16.8 (10.0)	6.8	16.4 (8.0)	8.4
2	56.7 (61.0)	-4.3	63.3 (69.5)	-6.2	53.6 (64.0)	-10.4	41.4 (42.0)	-0.6	33.2 (22.0)	11.2	19.3 (28.0)	-8.7
6	39.6 (51.0)	-11.4	47.6 (61.0)	-13.4	49.0 (54.5)	-5.5	46.1 (48.0)	-1.9	39.7 (40.0)	-0.3	32.2 (33.5)	-1.3
10	31.8 (41.0)	-9.2	35.8 (46.5)	-10.7	41.6 (45.0)	-3.4	42.7 (45.0)	-2.3	41.0 (43.0)	-2.0	37.6 (37.5)	0.1
14	32.5 (37.5)	-5.0	33.0 (37.5)	-4.5	36.4 (37.5)	-1.1	38.4 (37.5)	0.9	38.9 (38.0)	0.9	38.0 (38.0)	0.0
18	33.2 (37.0)	-3.8	33.1 (37.0)	-3.9	34.3 (37.0)	-2.7	35.9 (37.0)	-1.1	36.9 (37.0)	-0.1	37.1 (37.0)	0.1
23	33.4 (36.0)	-2.6	33.2 (36.5)	-3.3	33.3 (36.0)	-2.7	34.0 (36.0)	-2.0	34.8 (36.5)	-1.7	35.3 (36.0)	-0.7
30	33.5 (35.0)	-1.5	33.3 (35.0)	-1.7	33.2 (35.0)	-1.8	33.2 (35.0)	-1.8	33.4 (35.0)	-0.6	33.7 (35.0)	-1.3

Table E.7. Measured versus modeled temperatures for the undisturbed thermistor string, Run 5, Richardson Highway MP 113 research site. For each month and at each selected depth, the upper left temperature is that measured by the thermistor bead. The lower left temperature in parentheses and italics is the modeled temperature estimated to the nearest 0.5°F. The number to the right is the difference between the two temperatures to the left. Temperatures were compared for the first day of each month in 2009.

Depth (ft)	Temperatures (°F)											
	January		February		March		April		May		June	
0.5	14.4 *(14.0)*	0.4	26.2 *(20.0)*	6.2	25.1 *(25.0)*	0.1	27.0 *(32.0)*	-5.0	33.9 *(36.0)*	-2.1	43.5 *(42.0)*	1.5
2	27.3 *(19.0)*	8.3	30.5 *(23.0)*	7.5	30.0 *(26.0)*	4.0	28.2 *(30.5)*	-2.3	30.5 *(31.5)*	-1.0	31.7 *(34.0)*	-2.3
6	31.7 *(30.0)*	1.7	31.6 *(29.0)*	2.6	31.5 *(28.0)*	3.5	31.2 *(29.0)*	2.2	31.0 *(29.5)*	1.5	31.0 *(31.0)*	0.0
10	31.6 *(30.5)*	0.1	31.6 *(30.0)*	1.6	31.6 *(30.0)*	1.6	31.5 *(30.0)*	1.5	31.5 *(29.5)*	1.5	31.5 *(30.5)*	1.5
14	31.3 *(31.0)*	0.3	31.4 *(30.5)*	0.9	31.3 *(30.5)*	0.8	31.3 *(30.5)*	0.8	31.3 *(30.0)*	1.3	31.3 *(30.5)*	0.8
18	31.4 *(31.0)*	0.4	31.4 *(30.5)*	0.9	31.4 *(30.5)*	0.9	31.4 *(30.5)*	0.9	31.4 *(30.5)*	0.9	31.4 *(31.0)*	0.4
23	31.2 *(31.0)*	0.2	31.2 *(31.0)*	0.2	31.1 *(31.0)*	0.1	31.1 *(31.0)*	0.1	31.1 *(30.5)*	0.6	31.1 *(31.0)*	0.1
30	31.1 *(31.0)*	0.1	31.0 *(31.0)*	0.0	31.0 *(31.0)*	0.0	31.0 *(31.0)*	0.0	31.0 *(31.0)*	0.0	31.0 *(31.0)*	0.0

Table E.7 (continued).

Depth (ft)	Temperatures (°F)											
	July		August		September		October		November		December	
0.5	49.8 (42.0)	7.8	57.9 (40.0)	7.9	50.5 (39.0)	11.5	35.5 (33.0)	2.5	30.1 (24.0)	6.1	28.5 (28.0)	0.5
2	35.9 (36.0)	-0.1	41.9 (38.0)	3.9	41.4 (37.0)	4.4	36.2 (34.0)	2.2	32.6 (32.5)	0.1	31.3 (30.0)	1.3
6	31.1 (31.5)	-0.4	31.3 (31.5)	-0.2	31.6 (32.0)	-0.4	31.9 (32.0)	-0.1	31.8 (32.0)	-0.2	31.7 (32.0)	-0.3
10	31.4 (31.0)	0.4	31.4 (31.5)	-0.1	31.4 (31.5)	-0.1	31.5 (31.5)	0.0	31.5 (31.5)	0.0	31.5 (31.5)	0.5
14	31.3 (31.0)	0.3	31.3 (31.0)	0.3	31.3 (31.0)	0.3	31.3 (31.0)	0.3	31.3 (31.5)	-0.2	31.3 (31.5)	-0.2
18	31.4 (31.0)	0.4	31.4 (31.0)	0.4	31.4 (31.0)	0.4	31.4 (31.0)	0.4	31.4 (31.0)	0.4	31.4 (31.0)	0.4
23	31.1 (31.0)	0.1	31.1 (31.0)	0.1	31.1 (31.0)	0.1	31.1 (31.0)	0.1	31.1 (31.0)	0.1	31.1 (31.0)	0.1
30	31.0 (31.0)	0.0	31.0 (31.0)	0.0	31.0 (31.0)	0.0	31.0 (31.0)	0.0	31.0 (31.0)	0.0	31.0 (31.0)	0.0

Table E.8. Measured versus modeled temperatures for the toe thermistor string, Run 5, Richardson Highway MP 113 research site. For each month and at each selected depth, the upper left temperature is that measured by the thermistor bead. The lower left temperature in parentheses and italics is the modeled temperature estimated to the nearest 0.5°F. The number to the right is the difference between the two temperatures to the left. Temperatures were compared for the first day of each month in 2009.

Depth (ft)	Temperatures (°F)											
	January		February		March		April		May		June	
0.5	15.2 (-12.0)	27.2	19.0 (-6.0)	25.0	16.9 (8.0)	8.9	23.8 (32.0)	-8.2	39.8 (54.0)	-14.2	54.3 (86.0)	-31.7
2	23.6 (-2.0)	25.6	22.4 (4.0)	18.4	19.9 (12.0)	7.9	23.4 (24.0)	-0.6	29.9 (34.0)	-4.1	45.2 (54.0)	-8.8
6	32.7 (23.0)	9.7	31.8 (19.0)	12.8	31.0 (20.0)	11.0	30.0 (21.0)	9.0	30.4 (27.5)	2.9	30.9 (31.5)	-0.6
10	35.2 (33.0)	2.2	34.0 (29.0)	5.0	33.3 (27.0)	6.3	32.7 (26.0)	6.7	32.4 (27.5)	4.9	32.2 (29.0)	3.2
14	35.7 (34.0)	1.7	34.7 (32.5)	2.2	34.0 (32.0)	2.0	33.4 (30.5)	2.9	32.9 (30.0)	2.9	32.6 (30.5)	2.1
18	33.7 (33.5)	0.2	35.1 (33.0)	2.1	34.5 (32.5)	2.0	34.0 (32.0)	2.0	33.6 (31.5)	2.1	33.2 (31.0)	2.2
23	34.6 (32.0)	2.6	34.4 (32.0)	2.2	34.1 (32.0)	2.1	33.8 (32.0)	1.8	33.4 (32.5)	0.9	33.1 (32.0)	1.1
30	35.1 (31.5)	3.6	34.7 (32.0)	2.7	34.3 (31.5)	2.8	33.8 (32.0)	1.8	33.5 (32.0)	1.5	33.1 (32.0)	1.1

Table E.8 (continued).

Depth	Temperatures (°F)										
(ft)	July		August		September		October		November		December	
0.5	63.8 (86.0)	-22.2	67.5 (69.0)	-1.5	55.2 (62.0)	-6.8	38.1 (39.0)	-0.9	26.3 (8.0)	18.3	19.1 (13.0)	6.1
2	51.2 (62.0)	-10.8	57.9 (67.0)	-9.1	51.7 (59.0)	-7.3	41.5 (42.0)	-0.5	34.1 (32.0)	2.1	24.4 (19.0)	5.4
6	33.1 (38.0)	-4.9	42.1 (45.0)	-2.9	44.3 (48.0)	-3.7	43.2 (45.5)	-2.3	38.9 (41.0)	-2.1	34.6 (33.0)	1.6
10	32.2 (31.5)	0.7	35.2 (34.0)	1.2	38.7 (37.0)	1.7	39.8 (39.0)	0.8	38.9 (38.0)	0.9	36.9 (36.5)	0.4
14	32.5 (31.0)	0.5	33.0 (31.5)	1.5	34.0 (31.5)	2.5	36.5 (33.0)	3.5	35.2 (34.0)	1.2	35.4 (34.5)	0.9
18	33.0 (31.5)	1.5	32.9 (31.5)	1.4	33.7 (31.5)	2.2	34.7 (31.5)	3.2	35.5 (31.5)	4.0	35.6 (32.5)	3.1
23	32.9 (31.5)	1.4	32.7 (31.5)	1.2	32.8 (31.5)	1.3	33.2 (31.5)	1.7	33.8 (31.5)	2.3	34.1 (31.5)	2.6
30	32.9 (32.0)	0.9	32.7 (32.0)	0.7	33.0 (31.5)	1.5	33.7 (31.5)	2.2	34.4 (31.5)	2.9	34.8 (31.5)	3.3

Table E.9. Measured versus modeled temperatures for the embankment thermistor string, Run 4, Richardson Highway MP 113 research site. For each month and at each selected depth, the upper left temperature is that measured by the thermistor bead. The lower left temperature in parentheses and italics is the modeled temperature estimated to the nearest 0.5°F. The number to the right is the difference between the two temperatures to the left. Temperatures were compared for the first day of each month in 2009.

Depth (ft)	Temperatures (°F)											
	January		February		March		April		May		June	
0.5	-16.7 (-12.0)	-4.7	7.5 (2.0)	5.5	12.8 (12.0)	0.8	28.1 (32.0)	-3.9	50.9 (56.0)	-5.1	57.5 (86.0)	-28.5
2	0.7 (-6.0)	5.3	12.7 (-2.0)	14.7	15.3 (8.0)	7.3	25.7 (24.0)	1.7	40.6 (46.0)	-5.4	52.9 (66.0)	-13.1
6	29.0 (18.0)	11.0	27.5 (18.0)	9.5	26.0 (18.0)	8.0	26.7 (20.5)	6.2	30.5 (31.0)	-0.5	34.5 (43.0)	-8.5
10	34.7 (31.0)	3.7	33.3 (28.0)	5.3	32.4 (26.0)	6.4	31.8 (25.5)	6.3	31.6 (29.0)	2.6	31.7 (33.0)	-1.3
14	36.1 (36.5)	-0.4	34.9 (34.0)	0.9	34.0 (32.0)	2.0	33.3 (31.0)	2.3	32.9 (31.0)	1.9	32.6 (31.0)	-1.6
18	36.5 (37.0)	-0.5	35.6 (36.5)	-0.9	35.0 (34.5)	0.5	34.3 (34.0)	0.3	33.8 (33.0)	0.8	33.4 (33.0)	-0.4
23	35.6 (36.0)	-0.4	35.2 (35.5)	-0.3	34.9 (35.0)	-0.1	34.5 (35.0)	-0.5	34.1 (35.0)	-0.9	33.7 (34.5)	-0.8
30	34.2 (34.5)	-0.3	34.2 (35.0)	-0.8	34.2 (34.5)	-0.3	34.1 (34.5)	-0.4	33.9 (35.0)	-1.1	33.7 (35.0)	-1.3

Table E.9 (continued).

Depth (ft)	Temperatures (°F)																
	July			August			September			October			November			December	
0.5	67.1 (86.0)	-18.9		70.4 (76.0)	-5.6		55.0 (68.0)	-13.0		37.4 (40.0)	-2.6		16.8 (10.0)	6.8		16.4 (8.0)	8.4
2	56.7 (72.0)	-15.3		63.3 (76.0)	-12.7		53.6 (65.0)	-11.4		41.4 (42.0)	-0.6		33.2 (22.0)	11.2		19.3 (11.0)	8.3
6	39.6 (51.0)	-11.4		47.6 (60.0)	-12.4		49.0 (57.0)	-8.0		46.1 (49.0)	-2.9		39.7 (40.0)	-0.3		32.2 (29.0)	3.2
10	31.8 (40.0)	-8.2		35.8 (48.0)	-12.2		41.6 (50.0)	-8.4		42.7 (48.0)	-5.3		41.0 (43.0)	-2.0		37.6 (36.5)	1.1
14	32.5 (33.5)	-1.0		33.0 (36.0)	-3.0		36.4 (40.0)	-3.6		38.4 (42.0)	-3.6		38.9 (41.5)	-2.6		38.0 (39.0)	-1.0
18	33.2 (33.0)	0.2		33.1 (33.0)	0.1		34.3 (35.0)	-0.7		35.9 (36.5)	-0.6		36.9 (38.0)	-1.1		37.1 (38.0)	-0.9
23	33.4 (34.0)	-0.6		33.2 (33.5)	-0.3		33.3 (33.0)	0.3		34.0 (34.0)	0.0		34.8 (35.0)	-0.2		35.3 (35.5)	-0.2
30	33.5 (35.0)	-1.5		33.3 (35.0)	-1.7		33.2 (34.5)	-1.3		33.2 (34.0)	-0.8		33.4 (34.0)	-0.6		33.7 (34.5)	-0.8

Table E.10. Measured versus modeled temperatures for the undisturbed thermistor string, Run 6, Richardson Highway MP 113 research site. For each month and at each selected depth, the upper left temperature is that measured by the thermistor bead. The lower left temperature in parentheses and italics is the modeled temperature estimated to the nearest 0.5°F. The number to the right is the difference between the two temperatures to the left. Temperatures were compared for the first day of each month in 2009.

Depth (ft)	Temperatures (°F)											
	January		February		March		April		May		June	
0.5	14.4 *(12.0)*	2.4	26.2 *(19.0)*	7.2	25.1 *(23.0)*	2.1	27.0 *(31.0)*	-4.0	33.9 *(36.0)*	-2.1	43.5 *(44.0)*	-0.5
2	27.3 *(19.0)*	8.3	30.5 *(21.0)*	9.5	30.0 *(24.0)*	6.0	28.2 *(29.0)*	-0.8	30.5 *(31.5)*	-1.0	31.7 *(34.0)*	-2.3
6	31.7 *(30.0)*	1.7	31.6 *(29.5)*	2.1	31.5 *(27.0)*	4.5	31.2 *(27.0)*	4.2	31.0 *(29.5)*	1.5	31.0 *(30.0)*	1.0
10	31.6 *(30.5)*	0.1	31.6 *(30.5)*	1.1	31.6 *(30.0)*	1.6	31.5 *(29.0)*	2.5	31.5 *(29.5)*	1.5	31.5 *(29.0)*	2.5
14	31.3 *(31.0)*	0.3	31.4 *(30.5)*	0.9	31.3 *(30.5)*	0.8	31.3 *(30.5)*	0.8	31.3 *(30.0)*	1.3	31.3 *(30.5)*	0.8
18	31.4 *(31.0)*	0.4	31.4 *(31.0)*	0.4	31.4 *(31.0)*	0.4	31.4 *(30.5)*	0.9	31.4 *(30.5)*	0.9	31.4 *(31.0)*	0.4
23	31.2 *(31.0)*	0.2	31.2 *(31.0)*	0.2	31.1 *(31.0)*	0.1	31.1 *(31.0)*	0.1	31.1 *(31.0)*	0.1	31.1 *(31.0)*	0.1
30	31.1 *(31.0)*	0.1	31.0 *(31.0)*	0.0	31.0 *(31.0)*	0.0	31.0 *(31.0)*	0.0	31.0 *(31.0)*	0.0	31.0 *(31.0)*	0.0

Table E.10 (continued).

Depth (ft)	Temperatures (°F)																
	July			August			September			October			November			December	
0.5	49.8 (42.0)	7.8		57.9 (43.0)	4.9		50.5 (40.0)	10.5		35.5 (34.0)	1.5		30.1 (28.0)	2.1		28.5 (27.0)	1.5
2	35.9 (36.0)	-0.1		41.9 (40.0)	1.9		41.4 (38.0)	3.4		36.2 (34.5)	1.7		32.6 (33.0)	-0.4		31.3 (29.0)	2.3
6	31.1 (31.5)	-0.4		31.3 (31.5)	-0.2		31.6 (32.0)	-0.4		31.9 (32.5)	-0.6		31.8 (33.0)	-1.2		31.7 (33.0)	-1.3
10	31.4 (31.0)	0.4		31.4 (31.5)	-0.1		31.4 (31.5)	-0.1		31.5 (31.5)	0.0		31.5 (31.5)	0.0		31.5 (31.5)	0.5
14	31.3 (31.0)	0.3		31.3 (31.0)	0.3		31.3 (31.0)	0.3		31.3 (31.0)	0.3		31.3 (31.5)	-0.2		31.3 (31.0)	0.3
18	31.4 (31.0)	0.4		31.4 (31.0)	0.4		31.4 (31.0)	0.4		31.4 (31.0)	0.4		31.4 (31.0)	0.4		31.4 (31.0)	0.4
23	31.1 (31.0)	0.1		31.1 (31.0)	0.1		31.1 (31.0)	0.1		31.1 (31.0)	0.1		31.1 (31.0)	0.1		31.1 (31.0)	0.1
30	31.0 (31.0)	0.0		31.0 (31.0)	0.0		31.0 (31.0)	0.0		31.0 (31.0)	0.0		31.0 (31.0)	0.0		31.0 (31.0)	0.0

Table E.11. Measured versus modeled temperatures for the toe thermistor string, Run 6, Richardson Highway MP 113 research site. For each month and at each selected depth, the upper left temperature is that measured by the thermistor bead. The lower left temperature in parentheses and italics is the modeled temperature estimated to the nearest 0.5°F. The number to the right is the difference between the two temperatures to the left. Temperatures were compared for the first day of each month in 2009.

Depth (ft)	Temperatures (°F)											
	January		February		March		April		May		June	
0.5	15.2 *(16.0)*	-0.8	19.0 *(0.0)*	19.0	16.9 *(12.0)*	4.9	23.8 *(31.5)*	-7.7	39.8 *(44.0)*	-4.2	54.3 *(60.0)*	-5.7
2	23.6 *(11.0)*	12.6	22.4 *(12.0)*	10.4	19.9 *(16.0)*	3.9	23.4 *(25.5)*	-2.1	29.9 *(32.0)*	-2.1	45.2 *(42.0)*	3.2
6	32.7 *(28.0)*	4.7	31.8 *(24.0)*	7.8	31.0 *(24.0)*	7.0	30.0 *(24.0)*	6.0	30.4 *(29.0)*	1.4	30.9 *(31.0)*	-0.1
10	35.2 *(33.0)*	2.2	34.0 *(32.0)*	2.0	33.3 *(29.0)*	4.3	32.7 *(28.0)*	4.7	32.4 *(29.5)*	2.9	32.2 *(30.0)*	2.2
14	35.7 *(33.0)*	2.7	34.7 *(32.5)*	2.2	34.0 *(32.0)*	2.0	33.4 *(31.0)*	2.4	32.9 *(30.5)*	2.4	32.6 *(31.0)*	1.6
18	33.7 *(32.0)*	1.7	35.1 *(32.0)*	3.1	34.5 *(32.0)*	2.5	34.0 *(32.0)*	2.0	33.6 *(31.0)*	2.6	33.2 *(31.0)*	2.2
23	34.6 *(31.5)*	3.1	34.4 *(31.5)*	2.9	34.1 *(31.5)*	2.6	33.8 *(32.0)*	1.8	33.4 *(31.5)*	1.9	33.1 *(31.5)*	1.6
30	35.1 *(31.5)*	3.6	34.7 *(31.5)*	3.2	34.3 *(31.5)*	2.8	33.8 *(31.5)*	2.3	33.5 *(31.5)*	2.0	33.1 *(31.5)*	1.6

Table E.11 (continued).

Depth (ft)	Temperatures (°F)										
	July		August		September		October		November		December	
0.5	63.8 (58.0)	5.8	67.5 (57.0)	10.5	55.2 (51.0)	4.2	38.1 (37.5)	0.6	26.3 (2.0)	24.3	19.1 (19.0)	0.1
2	51.2 (48.0)	3.2	57.9 (54.0)	3.9	51.7 (48.0)	3.7	41.5 (39.0)	2.5	34.1 (34.0)	0.1	24.4 (24.0)	0.4
6	33.1 (33.0)	0.1	42.1 (38.0)	4.1	44.3 (39.0)	5.3	43.2 (40.0)	3.2	38.9 (37.0)	1.9	34.6 (34.0)	0.6
10	32.2 (31.5)	0.7	35.2 (32.0)	3.2	38.7 (33.0)	5.7	39.8 (34.0)	5.8	38.9 (35.0)	3.9	36.9 (35.0)	1.9
14	32.5 (31.0)	0.5	33.0 (31.5)	1.5	34.0 (31.5)	2.5	36.5 (31.5)	5.0	35.2 (32.0)	3.2	35.4 (33.0)	2.4
18	33.0 (31.5)	1.5	32.9 (31.5)	1.4	33.7 (31.5)	2.2	34.7 (31.5)	3.2	35.5 (31.5)	4.0	35.6 (31.5)	4.1
23	32.9 (31.5)	1.4	32.7 (31.5)	1.2	32.8 (31.5)	1.3	33.2 (31.5)	1.7	33.8 (31.5)	2.3	34.1 (31.5)	2.6
30	32.9 (31.5)	1.4	32.7 (31.5)	1.2	33.0 (31.5)	1.5	33.7 (31.5)	2.2	34.4 (31.5)	2.9	34.8 (31.5)	3.3

Table E.12. Measured versus modeled temperatures for the embankment thermistor string, Run 6, Richardson Highway MP 113 research site. For each month and at each selected depth, the upper left temperature is that measured by the thermistor bead. The lower left temperature in parentheses and italics is the modeled temperature estimated to the nearest 0.5°F. The number to the right is the difference between the two temperatures to the left. Temperatures were compared for the first day of each month in 2009.

Depth (ft)	Temperatures (°F)											
	January		February		March		April		May		June	
0.5	-16.7 *(-8.0)*	8.7	7.5 *(-12.0)*	19.5	12.8 *(14.0)*	-2.8	28.1 *(32.0)*	-3.9	50.9 *(48.0)*	2.9	57.5 *(74.0)*	-16.5
2	0.7 *(1.0)*	-0.3	12.7 *(4.0)*	8.7	15.3 *(12.0)*	3.3	25.7 *(24.0)*	1.7	40.6 *(40.0)*	0.6	52.9 *(56.0)*	-3.1
6	29.0 *(23.0)*	6.0	27.5 *(21.0)*	6.5	26.0 *(22.0)*	4.0	26.7 *(22.0)*	4.7	30.5 *(30.0)*	0.5	34.5 *(40.0)*	-5.5
10	34.7 *(32.0)*	2.7	33.3 *(28.5)*	4.8	32.4 *(29.0)*	3.4	31.8 *(27.0)*	4.8	31.6 *(29.0)*	2.6	31.7 *(32.0)*	-0.3
14	36.1 *(35.0)*	1.1	34.9 *(33.5)*	1.4	34.0 *(32.0)*	2.0	33.3 *(31.0)*	2.3	32.9 *(31.0)*	1.9	32.6 *(31.0)*	-1.6
18	36.5 *(35.0)*	1.5	35.6 *(35.0)*	0.6	35.0 *(34.5)*	0.5	34.3 *(33.5)*	0.8	33.8 *(33.0)*	0.8	33.4 *(32.5)*	0.9
23	35.6 *(35.0)*	0.6	35.2 *(35.0)*	0.2	34.9 *(35.0)*	-0.1	34.5 *(35.0)*	-0.5	34.1 *(34.0)*	0.1	33.7 *(33.0)*	0.7
30	34.2 *(33.5)*	0.7	34.2 *(33.5)*	0.7	34.2 *(33.5)*	0.7	34.1 *(33.5)*	0.6	33.9 *(33.5)*	0.4	33.7 *(33.0)*	0.7

Table E.12 (continued).

Depth (ft)	Temperatures (°F)											
	July		August		September		October		November		December	
0.5	67.1 (74.0)	-6.9	70.4 (66.0)	4.4	55.0 (59.0)	-4.0	37.4 (39.0)	-1.6	16.8 (-4.0)	20.8	16.4 (13.0)	3.4
2	56.7 (60.0)	-3.3	63.3 (65.0)	-1.7	53.6 (56.0)	-2.4	41.4 (40.0)	1.4	33.2 (24.0)	9.2	19.3 (15.0)	4.3
6	39.6 (44.0)	-4.4	47.6 (52.0)	-4.4	49.0 (49.0)	0.0	46.1 (44.5)	1.6	39.7 (38.0)	1.7	32.2 (28.0)	4.2
10	31.8 (36.0)	-4.2	35.8 (42.0)	-6.2	41.6 (43.5)	-1.9	42.7 (43.0)	-0.3	41.0 (40.0)	1.0	37.6 (35.0)	2.6
14	32.5 (31.5)	1.0	33.0 (34.0)	-1.0	36.4 (36.0)	0.4	38.4 (38.0)	0.4	38.9 (38.0)	0.9	38.0 (37.0)	1.0
18	33.2 (32.5)	0.7	33.1 (33.0)	0.1	34.3 (33.5)	0.8	35.9 (35.0)	0.9	36.9 (35.5)	1.4	37.1 (36.0)	1.1
23	33.4 (33.0)	0.4	33.2 (33.0)	0.2	33.3 (33.0)	0.3	34.0 (33.5)	0.5	34.8 (33.5)	1.3	35.3 (34.0)	1.3
30	33.5 (33.0)	0.5	33.3 (33.0)	0.3	33.2 (33.0)	0.2	33.2 (33.0)	0.2	33.4 (33.0)	0.4	33.7 (33.0)	0.7

Table E.13. Measured versus modeled temperatures for the undisturbed thermistor string, Run 1, Dalton Highway 9 Mile Hill research site. For each month and at each selected depth, the upper left temperature is that measured by the thermistor bead. The lower left temperature in parentheses and italics is the modeled temperature estimated to the nearest 0.5°F. The number to the right is the difference between the two temperatures to the left. Temperatures were compared for the first day of each month from September through December 2009, and from January through May 2010. For June, the modeled temperatures were compared to the measured temperatures from May 29, 2010. Since measured temperatures for July and August have not been collected at the time of this writing, no comparison is made for these months. The thermistor at 23.0 failed after installation.

Depth (ft)	Temperatures (°F)											
	January		February		March		April		May		June	
0.5	26.5 *(22.0)*	4.5	23.0 *(20.0)*	3.0	20.9 *(22.0)*	-1.1	22.3 *(24.5)*	-2.2	31.2 *(28.0)*	3.2	32.1 *(30.0)*	2.1
2	28.4 *(24.5)*	3.9	27.4 *(23.0)*	4.4	23.6 *(22.5)*	1.1	23.2 *(24.5)*	-1.3	29.7 *(25.5)*	4.2	30.7 *(27.0)*	3.7
6	30.6 *(26.0)*	4.6	28.4 *(25.0)*	3.4	26.9 *(24.5)*	2.4	25.8 *(24.5)*	1.3	27.7 *(25.0)*	2.7	29.4 *(25.5)*	3.9
10	30.5 *(26.0)*	4.5	30.2 *(26.0)*	4.2	29.0 *(25.0)*	4.0	27.9 *(25.0)*	2.9	27.7 *(25.0)*	2.7	28.7 *(25.0)*	3.7
14	30.3 *(26.5)*	3.8	30.4 *(26.5)*	3.9	30.1 *(26.0)*	4.1	29.3 *(25.5)*	3.8	28.6 *(25.0)*	3.6	28.9 *(25.0)*	3.9
18	30.1 *(26.5)*	3.6	30.2 *(26.5)*	3.7	30.1 *(26.0)*	4.1	29.8 *(26.0)*	3.8	29.4 *(25.0)*	4.4	29.3 *(25.0)*	4.3
30	30.0 *(26.5)*	3.5	30.0 *(27.0)*	3.0	30.0 *(26.5)*	3.5	30.0 *(26.5)*	3.5	30.0 *(26.5)*	3.5	30.0 *(26.5)*	3.5

Table E.13 (continued).

Depth (ft)	Temperatures (°F)											
	July		August		September		October		November		December	
0.5	--- (32.0)	---	--- (32.0)	---	33.3 (32.5)	0.8	31.9 (30.5)	1.4	31.6 (26.0)	5.6	29.2 (24.0)	5.2
2	--- (29.0)	---	--- (30.0)	---	31.6 (31.0)	0.6	31.6 (30.0)	1.6	31.6 (28.5)	3.1	31.4 (27.5)	3.9
6	--- (27.0)	---	--- (28.5)	---	30.8 (29.5)	1.3	30.9 (29.0)	1.9	31.0 (29.0)	2.0	31.0 (27.0)	4.0
10	--- (26.0)	---	--- (27.0)	---	30.2 (27.5)	2.7	30.3 (28.5)	1.8	30.4 (28.5)	1.9	30.6 (27.0)	3.6
14	--- (25.0)	---	--- (27.0)	---	30.0 (27.0)	3.0	30.1 (27.5)	2.6	30.2 (27.5)	2.7	30.3 (27.0)	3.3
18	--- (25.0)	---	--- (26.0)	---	29.9 (27.0)	2.9	30.0 (27.0)	3.0	30.0 (27.5)	2.5	30.1 (27.0)	3.1
30	--- (26.0)	---	--- (26.5)	---	30.0 (26.5)	3.5	30.0 (27.0)	3.0	30.0 (27.0)	3.0	30.0 (27.0)	3.0

Table E.14. Measured versus modeled temperatures for the toe thermistor string, Run 1, Dalton Highway 9 Mile Hill research site.
For each month and at each selected depth, the upper left temperature is that measured by the thermistor bead. The lower left
temperature in parentheses and italics is the modeled temperature estimated to the nearest 0.5°F. The number to the right is the
difference between the two temperatures to the left. Temperatures were compared for the first day of each month from September
through December 2009, and from January through May 2010. For June, the modeled temperatures were compared to the measured
temperatures from May 29, 2010. Since measured temperatures for July and August have not been collected at the time of this writing,
no comparison is made for these months.

Depth (ft)	Temperatures (°F)											
	January		February		March		April		May		June	
0.5	26.1 (-20.0)	46.1	25.1 (-18.0)	43.1	25.2 (0.5)	24.7	29.6 (7.0)	22.6	39.8 (27.0)	12.8	55.6 (40.0)	15.6
2	28.7 (-4.0)	32.7	27.6 (-5.0)	32.6	27.8 (5.5)	22.3	28.5 (8.0)	20.5	32.0 (22.0)	10.0	43.1 (34.0)	9.1
6	31.9 (18.0)	13.9	31.9 (12.0)	19.9	31.8 (11.0)	20.8	31.7 (13.0)	18.7	31.7 (17.5)	14.2	31.9 (24.0)	7.9
10	31.5 (24.5)	7.0	31.5 (18.5)	13.0	31.5 (16.0)	15.5	31.5 (16.0)	15.5	31.5 (17.5)	14.0	31.6 (21.5)	10.1
14	31.5 (27.0)	4.5	31.6 (23.0)	8.6	31.6 (20.5)	11.1	31.6 (19.0)	12.6	31.6 (19.0)	12.6	31.6 (21.0)	10.6
18	31.2 (28.0)	3.2	31.4 (25.5)	5.9	31.5 (23.5)	8.0	31.8 (21.5)	10.3	32.1 (21.0)	11.1	32.7 (21.5)	11.2
23	31.0 (27.5)	3.5	31.0 (26.0)	5.0	31.0 (25.5)	5.5	31.0 (24.5)	6.5	31.0 (23.0)	8.0	31.0 (23.0)	8.0
30	30.7 (27.5)	3.2	30.7 (26.5)	4.2	30.7 (26.5)	4.2	30.7 (26.0)	4.7	30.7 (25.0)	5.7	30.7 (25.0)	5.7

Table E.14 (continued).

Depth (ft)	Temperatures (°F)										
	July		August		September		October		November		December	
0.5	--- (68.0)	---	--- (64.0)	---	45.9 (50.0)	-4.1	32.9 (27.0)	5.9	28.7 (12.0)	16.7	27.2 (-1.0)	28.2
2	--- (59.0)	---	--- (58.0)	---	44.4 (47.5)	-3.1	35.0 (32.0)	3.0	31.1 (16.0)	15.1	29.5 (7.0)	22.5
6	--- (32.0)	---	--- (39.0)	---	29.1 (37.0)	-7.9	36.5 (34.5)	2.0	32.6 (32.0)	0.6	32.0 (28.0)	4.0
10	--- (26.5)	---	--- (29.5)	---	31.6 (30.0)	1.6	31.5 (31.0)	0.5	31.5 (31.0)	0.5	31.5 (31.0)	0.5
14	--- (24.0)	---	--- (27.0)	---	31.5 (28.0)	3.5	31.4 (29.0)	2.4	31.4 (28.5)	2.9	31.4 (29.5)	1.9
18	--- (23.0)	---	--- (25.5)	---	31.2 (27.0)	4.2	31.1 (27.5)	3.6	31.1 (28.0)	3.1	31.1 (29.0)	2.1
23	--- (23.0)	---	--- (25.5)	---	31.1 (25.5)	5.6	31.0 (26.5)	4.5	31.1 (27.0)	4.1	31.0 (27.5)	3.5
30	--- (24.5)	---	--- (25.0)	---	30.8 (25.0)	5.8	30.7 (25.5)	5.2	30.8 (26.5)	4.3	30.7 (27.0)	3.7

Table E.15. Measured versus modeled temperatures for the embankment thermistor string, Run 1, Dalton Highway 9 Mile Hill research site. For each month and at each selected depth, the upper left temperature is that measured by the thermistor bead. The lower left temperature in parentheses and italics is the modeled temperature estimated to the nearest 0.5°F. The number to the right is the difference between the two temperatures to the left. Temperatures were compared for the first day of each month from September through December 2009, and from January through May 2010. For June, the modeled temperatures were compared to the measured temperatures from May 29, 2010. Since measured temperatures for July and August have not been collected at the time of this writing, no comparison is made for these months. Depths shown reflect the actual location of the thermistor beads in the boring. The thermistors at 9.5 ft, 17.5 ft, and 29.5 ft failed after installation.

Depth (ft)	Temperatures (°F)											
	January		February		March		April		May		June	
0.5	3.6 (-9.0)	12.6	2.2 (-6.0)	8.2	3.9 (1.0)	2.9	20.6 (14.0)	6.6	46.8 (28.0)	18.8	64.5 (43.0)	21.5
1.5	6.7 (-5.0)	11.7	4.3 (-4.0)	8.3	6.9 (1.0)	5.9	17.9 (12.0)	5.9	43.1 (25.0)	18.1	58.1 (39.0)	19.1
5.5	23.8 (13.0)	10.8	20.6 (8.0)	12.6	22.3 (8.0)	14.3	21.9 (12.0)	9.9	31.9 (17.5)	14.4	33.6 (27.0)	6.6
11.5	31.8 (27.0)	4.8	31.8 (22.0)	9.8	30.2 (19.5)	10.7	28.2 (18.5)	9.7	29.4 (19.0)	10.4	30.7 (21.5)	9.2
13.5	31.6 (28.0)	3.6	31.6 (24.0)	7.6	30.9 (21.0)	9.9	29.5 (19.5)	10.0	29.7 (19.5)	10.2	30.6 (21.0)	9.6
23.5	31.0 (28.0)	3.0	31.0 (26.5)	4.5	31.0 (26.0)	5.0	31.0 (24.5)	6.5	30.9 (23.0)	7.9	30.9 (23.0)	7.9

Table E.15 (continued).

Depth (ft)	Temperatures (°F)											
	July		August		September		October		November		December	
0.5	--- (68.0)	---	--- (64.0)	---	47.8 (50.5)	-2.7	31.4 (27.0)	4.4	21.2 (10.0)	11.2	9.5 (1.0)	8.5
1.5	--- (60.0)	---	--- (62.0)	---	47.7 (50.0)	-2.3	33.4 (32.0)	1.4	24.4 (12.0)	12.4	11.0 (5.0)	6.0
5.5	--- (42.0)	---	--- (48.0)	---	40.9 (44.0)	-3.1	37.1 (36.0)	1.1	32.1 (27.0)	5.1	26.0 (19.0)	7.0
11.5	--- (26.0)	---	--- (31.0)	---	31.9 (31.0)	0.9	31.9 (31.5)	0.4	31.9 (31.5)	0.4	31.8 (31.5)	0.3
13.5	--- (25.0)	---	--- (28.5)	---	31.5 (29.5)	2.0	31.5 (31.0)	0.5	31.6 (31.0)	0.6	31.6 (31.0)	0.6
23.5	--- (23.0)	---	--- (26.5)	---	31.0 (26.5)	4.5	30.9 (27.0)	3.9	31.0 (28.0)	3.0	31.0 (28.5)	2.5

Table E.16. Measured versus modeled temperatures for the undisturbed thermistor string, Run 3, Dalton Highway 9 Mile Hill research site. For each month and at each selected depth, the upper left temperature is that measured by the thermistor bead. The lower left temperature in parentheses and italics is the modeled temperature estimated to the nearest 0.5°F. The number to the right is the difference between the two temperatures to the left. Temperatures were compared for the first day of each month from September through December 2009, and from January through May 2010. For June, the modeled temperatures were compared to the measured temperatures from May 29, 2010. Since measured temperatures for July and August have not been collected at the time of this writing, no comparison is made for these months. The thermistor at 23.0 failed after installation.

Depth (ft)	Temperatures (°F)											
	January		February		March		April		May		June	
0.5	26.5 *(22.0)*	4.5	23.0 *(22.0)*	1.0	20.9 *(20.0)*	0.9	22.3 *(27.0)*	-4.7	31.2 *(34.0)*	-2.8	32.1 *(36.0)*	-3.9
2	28.4 *(26.0)*	2.4	27.4 *(25.0)*	2.4	23.6 *(25.0)*	-1.4	23.2 *(25.0)*	-1.8	29.7 *(30.0)*	-0.3	30.7 *(30.0)*	0.7
6	30.6 *(28.5)*	2.1	28.4 *(27.0)*	1.4	26.9 *(27.0)*	-0.1	25.8 *(27.0)*	-1.2	27.7 *(27.0)*	0.7	29.4 *(29.5)*	-0.1
10	30.5 *(28.0)*	2.5	30.2 *(28.5)*	1.7	29.0 *(28.0)*	1.0	27.9 *(28.0)*	-0.1	27.7 *(27.5)*	0.2	28.7 *(29.5)*	-0.8
14	30.3 *(29.0)*	1.3	30.4 *(29.0)*	1.4	30.1 *(28.5)*	1.6	29.3 *(28.5)*	0.8	28.6 *(28.0)*	0.6	28.9 *(29.5)*	-0.6
18	30.1 *(29.0)*	1.1	30.2 *(29.0)*	1.2	30.1 *(29.0)*	1.1	29.8 *(29.0)*	0.8	29.4 *(28.5)*	0.9	29.3 *(29.5)*	-0.2
30	30.0 *(29.0)*	1.0	30.0 *(29.5)*	0.5	30.0 *(29.5)*	0.5	30.0 *(29.0)*	1.0	30.0 *(29.0)*	1.0	30.0 *(29.5)*	0.5

Table E.16 (continued).

Depth (ft)	Temperatures (°F)											
	July		August		September		October		November		December	
0.5	--- *(40.0)*	---	--- *(38.0)*	---	33.3 *(36.0)*	-2.7	31.9 *(30.0)*	1.9	31.6 *(28.0)*	3.6	29.2 *(22.0)*	7.2
2	--- *(31.5)*	---	--- *(31.5)*	---	31.6 *(31.5)*	0.1	31.6 *(30.5)*	1.1	31.6 *(30.5)*	1.1	31.4 *(28.5)*	2.9
6	--- *(30.0)*	---	--- *(31.0)*	---	30.8 *(31.0)*	-0.2	30.9 *(31.0)*	-0.1	31.0 *(31.0)*	0.0	31.0 *(30.0)*	1.0
10	--- *(29.5)*	---	--- *(30.0)*	---	30.2 *(30.0)*	0.2	30.3 *(31.0)*	-0.7	30.4 *(31.0)*	-0.6	30.6 *(30.5)*	0.1
14	--- *(29.5)*	---	--- *(29.5)*	---	30.0 *(29.5)*	0.5	30.1 *(30.0)*	0.1	30.2 *(30.5)*	-0.3	30.3 *(31.0)*	-0.7
18	--- *(29.5)*	---	--- *(29.5)*	---	29.9 *(29.5)*	0.4	30.0 *(29.5)*	0.5	30.0 *(30.0)*	0.0	30.1 *(30.5)*	-0.4
30	--- *(29.5)*	---	--- *(29.5)*	---	30.0 *(29.5)*	0.5	30.0 *(29.5)*	0.5	30.0 *(29.5)*	0.5	30.0 *(29.5)*	0.5

Table E.17. Measured versus modeled temperatures for the toe thermistor string, Run 3, Dalton Highway 9 Mile Hill research site. For each month and at each selected depth, the upper left temperature is that measured by the thermistor bead. The lower left temperature in parentheses and italics is the modeled temperature estimated to the nearest 0.5°F. The number to the right is the difference between the two temperatures to the left. Temperatures were compared for the first day of each month from September through December 2009, and from January through May 2010. For June, the modeled temperatures were compared to the measured temperatures from May 29, 2010. Since measured temperatures for July and August have not been collected at the time of this writing, no comparison is made for these months.

Depth (ft)	Temperatures (°F)											
	January		February		March		April		May		June	
0.5	26.1 (-4.0)	30.1	25.1 (-8.0)	33.1	25.2 (-12.0)	37.2	29.6 (18.0)	11.6	39.8 (52.0)	-12.2	55.6 (82.0)	-26.4
2	28.7 (4.0)	24.7	27.6 (5.0)	22.6	27.8 (4.0)	23.8	28.5 (15.0)	13.5	32.0 (42.0)	-10.0	43.1 (62.0)	-18.9
6	31.9 (28.0)	3.9	31.9 (26.0)	5.9	31.8 (26.0)	5.8	31.7 (27.0)	4.7	31.7 (32.0)	-0.3	31.9 (37.0)	-5.1
10	31.5 (32.0)	-0.5	31.5 (32.0)	-0.5	31.5 (32.0)	-0.5	31.5 (32.0)	-0.5	31.5 (32.0)	-0.5	31.6 (32.0)	-0.4
14	31.5 (31.5)	0.0	31.6 (31.5)	0.1	31.6 (31.5)	0.1	31.6 (31.5)	0.1	31.6 (31.5)	0.1	31.6 (31.5)	0.1
18	31.2 (31.5)	-0.3	31.4 (31.5)	-0.1	31.5 (31.5)	0.0	31.8 (31.5)	0.3	32.1 (31.5)	0.6	32.7 (31.5)	1.2
23	31.0 (31.0)	0.0	31.0 (31.0)	0.0	31.0 (31.0)	0.0	31.0 (31.0)	0.0	31.0 (31.0)	0.0	31.0 (31.0)	0.0
30	30.7 (31.0)	-0.3	30.7 (31.0)	-0.3	30.7 (31.0)	-0.3	30.7 (31.0)	-0.3	30.7 (31.0)	-0.3	30.7 (31.0)	-0.3

Table E.17 (continued).

Depth (ft)	Temperatures (°F)											
	July		August		September		October		November		December	
0.5	--- *(80.0)*	---	--- *(70.0)*	---	45.9 *(54.0)*	-8.1	32.9 *(25.0)*	7.9	28.7 *(8.0)*	20.7	27.2 *(-8.0)*	35.2
2	--- *(71.0)*	---	--- *(64.0)*	---	44.4 *(51.0)*	-6.6	35.0 *(32.5)*	2.5	31.1 *(20.0)*	11.1	29.5 *(9.0)*	20.5
6	--- *(45.0)*	---	--- *(46.0)*	---	29.1 *(44.0)*	-14.9	36.5 *(39.0)*	-2.5	32.6 *(34.5)*	-1.9	32.0 *(30.0)*	2.0
10	--- *(32.0)*	---	--- *(32.0)*	---	31.6 *(32.0)*	-0.4	31.5 *(31.5)*	0.0	31.5 *(31.5)*	0.0	31.5 *(32.0)*	-0.5
14	--- *(31.5)*	---	--- *(31.5)*	---	31.5 *(31.5)*	0.0	31.4 *(31.5)*	-0.1	31.4 *(31.5)*	-0.1	31.4 *(31.5)*	-0.1
18	--- *(31.5)*	---	--- *(31.5)*	---	31.2 *(31.5)*	-0.3	31.1 *(31.0)*	0.1	31.1 *(31.5)*	-0.4	31.1 *(31.5)*	-0.4
23	--- *(31.0)*	---	--- *(31.0)*	---	31.1 *(31.0)*	0.1	31.0 *(31.0)*	0.0	31.1 *(31.0)*	0.1	31.0 *(31.0)*	0.0
30	--- *(31.0)*	---	--- *(31.0)*	---	30.8 *(31.0)*	-0.2	30.7 *(31.0)*	-0.3	30.8 *(31.0)*	-0.2	30.7 *(31.0)*	-0.3

Table E.18. Measured versus modeled temperatures for the embankment thermistor string, Run 3, Dalton Highway 9 Mile Hill research site. For each month and at each selected depth, the upper left temperature is that measured by the thermistor bead. The lower left temperature in parentheses and italics is the modeled temperature estimated to the nearest 0.5°F. The number to the right is the difference between the two temperatures to the left. Temperatures were compared for the first day of each month from September through December 2009, and from January through May 2010. For June, the modeled temperatures were compared to the measured temperatures from May 29, 2010. Since measured temperatures for July and August have not been collected at the time of this writing, no comparison is made for these months. Depths shown reflect the actual location of the thermistor beads in the boring. The thermistors at 9.5 ft, 17.5 ft, and 29.5 ft failed after installation.

Depth (ft)	Temperatures (°F)											
	January		February		March		April		May		June	
0.5	3.6 (-2.0)	5.6	2.2 (4.0)	-1.8	3.9 (-4.0)	7.9	20.6 (20.0)	0.6	46.8 (60.0)	-13.2	64.5 (82.0)	-17.5
1.5	6.7 (3.0)	3.7	4.3 (5.0)	-0.7	6.9 (0.0)	6.9	17.9 (15.0)	2.9	43.1 (46.0)	-2.9	58.1 (70.0)	-11.9
5.5	23.8 (18.0)	5.8	20.6 (14.0)	6.6	22.3 (18.0)	5.3	21.9 (19.0)	2.9	31.9 (31.5)	0.4	33.6 (44.0)	-10.4
11.5	31.8 (34.0)	-2.2	31.8 (34.0)	-2.2	30.2 (33.0)	-2.8	28.2 (32.0)	-3.8	29.4 (32.5)	-3.1	30.7 (33.0)	-2.3
13.5	31.6 (33.0)	-1.4	31.6 (32.5)	-0.9	30.9 (32.0)	-1.1	29.5 (32.0)	-2.5	29.7 (32.0)	-2.3	30.6 (32.0)	-1.4
23.5	31.0 (31.0)	0.0	31.0 (31.0)	0.0	31.0 (31.0)	0.0	31.0 (31.5)	-0.5	30.9 (31.0)	-0.1	30.9 (31.5)	-0.6

Table E.18 (continued).

Depth (ft)	Temperatures (°F)											
	July		August		September		October		November		December	
0.5	--- (81.5)	---	--- (70.5)	---	47.8 (54.0)	-6.2	31.4 (29.0)	2.4	21.2 (16.0)	5.2	9.5 (6.0)	3.5
1.5	--- (76.0)	---	--- (69.5)	---	47.7 (53.0)	-5.3	33.4 (33.0)	0.4	24.4 (22.0)	2.4	11.0 (11.0)	0.0
5.5	--- (56.0)	---	--- (58.0)	---	40.9 (50.0)	-9.1	37.1 (42.5)	-5.4	32.1 (33.5)	-1.4	26.0 (22.0)	4.0
11.5	--- (33.0)	---	--- (36.0)	---	31.9 (36.0)	-4.1	31.9 (36.0)	-4.1	31.9 (36.0)	-4.1	31.8 (35.5)	-3.7
13.5	--- (32.0)	---	--- (33.0)	---	31.5 (33.0)	-1.5	31.5 (33.0)	-1.5	31.6 (33.0)	-1.4	31.6 (33.0)	-1.4
23.5	--- (31.5)	---	--- (31.5)	---	31.0 (31.0)	0.0	30.9 (31.5)	-0.6	31.0 (31.5)	-0.5	31.0 (31.5)	-0.5

Table E.19. Measured versus modeled temperatures for the undisturbed thermistor string, Run 4, Dalton Highway 9 Mile Hill research site. For each month and at each selected depth, the upper left temperature is that measured by the thermistor bead. The lower left temperature in parentheses and italics is the modeled temperature estimated to the nearest 0.5°F. The number to the right is the difference between the two temperatures to the left. Temperatures were compared for the first day of each month from September through December 2009, and from January through May 2010. For June, the modeled temperatures were compared to the measured temperatures from May 29, 2010. Since measured temperatures for July and August have not been collected at the time of this writing, no comparison is made for these months. The thermistor at 23.0 failed after installation.

Depth (ft)	Temperatures (°F)											
	January		February		March		April		May		June	
0.5	26.5 (26.0)	0.5	23.0 (26.5)	-3.5	20.9 (24.0)	-3.1	22.3 (28.0)	-5.7	31.2 (32.0)	-0.8	32.1 (36.0)	-3.9
2	28.4 (28.5)	-0.1	27.4 (27.0)	0.4	23.6 (26.5)	-2.9	23.2 (29.5)	-6.3	29.7 (28.0)	1.7	30.7 (28.0)	2.7
6	30.6 (28.5)	2.1	28.4 (28.0)	0.4	26.9 (28.0)	-1.1	25.8 (29.0)	-3.2	27.7 (28.5)	-0.8	29.4 (28.5)	0.9
10	30.5 (29.0)	1.5	30.2 (28.5)	1.7	29.0 (28.5)	0.5	27.9 (28.0)	-0.1	27.7 (29.0)	-1.3	28.7 (29.0)	-0.3
14	30.3 (29.0)	1.3	30.4 (29.0)	1.4	30.1 (29.0)	1.1	29.3 (28.5)	0.8	28.6 (29.0)	-0.4	28.9 (29.0)	-0.1
18	30.1 (29.0)	1.1	30.2 (29.0)	1.2	30.1 (29.0)	1.1	29.8 (29.0)	0.8	29.4 (29.0)	0.4	29.3 (29.0)	0.3
30	30.0 (29.0)	1.0	30.0 (29.0)	1.0	30.0 (29.0)	1.0	30.0 (29.0)	1.0	30.0 (29.0)	1.0	30.0 (29.0)	1.0

Table E.19 (continued).

Depth (ft)	Temperatures (°F)										
	July		August		September		October		November		December
0.5	--- *(34.0)*	---	--- *(34.0)*	---	33.3 *(34.0)*	-0.7	31.9 *(31.0)*	0.9	31.6 *(28.0)*	3.6	29.2 *(26.5)*	2.7
2	--- *(31.0)*	---	--- *(31.5)*	---	31.6 *(31.5)*	0.1	31.6 *(31.0)*	0.6	31.6 *(30.5)*	1.1	31.4 *(28.0)*	3.4
6	--- *(29.5)*	---	--- *(30.0)*	---	30.8 *(31.0)*	-0.2	30.9 *(31.0)*	-0.1	31.0 *(31.0)*	0.0	31.0 *(28.5)*	2.5
10	--- *(29.0)*	---	--- *(29.5)*	---	30.2 *(29.5)*	0.7	30.3 *(30.0)*	0.3	30.4 *(30.0)*	0.4	30.5 *(29.0)*	1.5
14	--- *(29.0)*	---	--- *(29.0)*	---	30.0 *(29.5)*	0.5	30.1 *(29.5)*	0.6	30.2 *(29.5)*	0.7	30.3 *(29.0)*	1.3
18	--- *(29.0)*	---	--- *(29.0)*	---	29.9 *(29.0)*	0.9	30.0 *(29.0)*	1.0	30.0 *(29.0)*	1.0	30.1 *(29.0)*	1.1
30	--- *(29.0)*	---	--- *(29.0)*	---	30.0 *(29.0)*	1.0	30.0 *(29.0)*	1.0	30.0 *(29.0)*	1.0	30.0 *(29.0)*	1.0

Table E.20. Measured versus modeled temperatures for the toe thermistor string, Run 4, Dalton Highway 9 Mile Hill research site. For each month and at each selected depth, the upper left temperature is that measured by the thermistor bead. The lower left temperature in parentheses and italics is the modeled temperature estimated to the nearest 0.5°F. The number to the right is the difference between the two temperatures to the left. Temperatures were compared for the first day of each month from September through December 2009, and from January through May 2010. For June, the modeled temperatures were compared to the measured temperatures from May 29, 2010. Since measured temperatures for July and August have not been collected at the time of this writing, no comparison is made for these months.

Depth (ft)	Temperatures (°F)											
	January		February		March		April		May		June	
0.5	26.1 (12.0)	14.1	25.1 (6.0)	19.1	25.2 (-2.0)	27.2	29.6 (26.0)	3.6	39.8 (46.0)	-6.2	55.6 (60.0)	-4.4
2	28.7 (16.0)	12.7	27.6 (12.0)	15.6	27.8 (10.0)	17.8	28.5 (14.0)	14.5	32.0 (36.0)	-4.0	43.1 (50.0)	-6.9
6	31.9 (30.0)	1.9	31.9 (24.0)	7.9	31.8 (21.0)	10.8	31.7 (19.0)	12.7	31.7 (25.5)	6.2	31.9 (32.0)	-0.1
10	31.5 (31.5)	0.0	31.5 (28.5)	3.0	31.5 (25.0)	6.5	31.5 (23.0)	8.5	31.5 (24.0)	-7.5	31.6 (28.0)	3.6
14	31.5 (31.0)	0.5	31.6 (30.0)	1.6	31.6 (27.0)	4.6	31.6 (25.0)	6.6	31.6 (25.0)	6.6	31.6 (29.5)	2.1
18	31.2 (30.0)	1.2	31.4 (30.0)	1.4	31.5 (28.5)	3.0	31.8 (27.0)	4.8	32.1 (26.0)	6.1	32.7 (29.0)	3.7
23	31.0 (29.5)	1.5	31.0 (29.5)	1.5	31.0 (29.0)	2.0	31.0 (28.0)	3.0	31.0 (27.0)	4.0	31.0 (29.0)	2.0
30	30.7 (29.0)	1.7	30.7 (29.0)	1.7	30.7 (29.0)	1.7	30.7 (29.0)	1.7	30.7 (28.0)	2.7	30.7 (28.5)	2.2

Table E.20 (continued).

Depth (ft)	Temperatures (°F)											
	July		August		September		October		November		December	
0.5	--- (62.0)	---	--- (56.0)	---	45.9 (46.0)	-0.1	32.9 (27.0)	5.9	28.7 (16.0)	12.7	27.2 (8.0)	19.2
2	--- (54.0)	---	--- (52.0)	---	44.4 (44.0)	0.4	35.0 (31.0)	4.0	31.1 (24.0)	7.1	29.5 (16.0)	13.5
6	--- (37.0)	---	--- (38.0)	---	29.1 (37.0)	-7.9	36.5 (35.0)	1.5	32.6 (32.0)	0.6	32.0 (30.0)	2.0
10	--- (29.5)	---	--- (31.0)	---	31.6 (31.0)	0.6	31.5 (31.0)	0.5	31.5 (31.5)	0.0	31.5 (31.5)	0.0
14	--- (28.5)	---	--- (29.5)	---	31.5 (30.0)	1.5	31.4 (30.5)	0.9	31.4 (31.0)	0.4	31.4 (31.0)	0.4
18	--- (27.5)	---	--- (29.0)	---	31.2 (29.0)	2.2	31.1 (29.5)	1.6	31.1 (29.5)	0.6	31.1 (30.0)	1.1
23	--- (27.0)	---	--- (28.0)	---	31.1 (29.0)	2.1	31.0 (29.0)	1.0	31.1 (29.0)	2.1	31.0 (29.5)	1.5
30	--- (27.0)	---	--- (27.0)	---	30.8 (28.0)	2.8	30.7 (29.0)	1.7	30.8 (29.0)	1.8	30.7 (29.0)	1.7

Table E.21. Measured versus modeled temperatures for the embankment thermistor string, Run 4, Dalton Highway 9 Mile Hill research site. For each month and at each selected depth, the upper left temperature is that measured by the thermistor bead. The lower left temperature in parentheses and italics is the modeled temperature estimated to the nearest 0.5°F. The number to the right is the difference between the two temperatures to the left. Temperatures were compared for the first day of each month from September through December 2009, and from January through May 2010. For June, the modeled temperatures were compared to the measured temperatures from May 29, 2010. Since measured temperatures for July and August have not been collected at the time of this writing, no comparison is made for these months. Depths shown reflect the actual location of the thermistor beads in the boring. The thermistors at 9.5 ft, 17.5 ft, and 29.5 ft failed after installation.

Depth (ft)	Temperatures (°F)											
	January		February		March		April		May		June	
0.5	3.6 (4.0)	-0.4	2.2 (7.0)	-4.8	3.9 (2.0)	1.9	20.6 (26.0)	-5.4	46.8 (46.0)	0.8	64.5 (62.0)	2.5
1.5	6.7 (9.0)	-3.7	4.3 (7.0)	-2.7	6.9 (6.0)	0.9	17.9 (16.0)	1.9	43.1 (38.0)	5.1	58.1 (54.0)	4.1
5.5	23.8 (20.0)	3.8	20.6 (16.0)	4.6	22.3 (17.0)	5.3	21.9 (16.0)	5.9	31.9 (26.0)	5.9	33.6 (37.0)	-3.4
11.5	31.8 (31.5)	0.3	31.8 (29.0)	2.8	30.2 (25.5)	4.7	28.2 (24.0)	4.2	29.4 (24.0)	5.4	30.7 (27.5)	3.2
13.5	31.6 (31.5)	0.1	31.6 (30.0)	1.6	30.9 (27.0)	3.9	29.5 (25.0)	4.5	29.7 (25.0)	4.7	30.6 (27.5)	3.1
23.5	31.0 (30.0)	1.0	31.0 (30.0)	1.0	31.0 (29.0)	2.0	31.0 (28.0)	3.0	30.9 (27.0)	3.9	30.9 (27.0)	3.9

Table E.21 (continued).

Depth	Temperatures (°F)											
(ft)	July		August		September		October		November		December	
0.5	--- (64.0)	---	--- (57.0)	---	47.8 (46.5)	1.3	31.4 (28.0)	3.4	21.2 (16.0)	5.2	9.5 (10.0)	-0.5
1.5	--- (60.0)	---	--- (56.0)	---	47.7 (45.0)	2.7	33.4 (31.0)	2.4	24.4 (22.0)	2.4	11.0 (12.0)	-1.0
5.5	--- (46.0)	---	--- (46.0)	---	40.9 (41.0)	-0.1	37.1 (36.5)	0.6	32.1 (30.0)	2.1	26.0 (22.0)	4.0
11.5	--- (31.0)	---	--- (31.5)	---	31.9 (31.5)	0.4	31.9 (31.5)	0.4	31.9 (31.5)	0.4	31.8 (31.5)	0.3
13.5	--- (29.5)	---	--- (30.5)	---	31.5 (31.0)	0.5	31.5 (31.0)	0.5	31.6 (31.0)	0.6	31.6 (31.5)	0.1
23.5	--- (27.5)	---	--- (29.0)	---	31.0 (29.0)	2.0	30.9 (29.5)	1.4	31.0 (29.5)	2.5	31.0 (29.5)	1.5
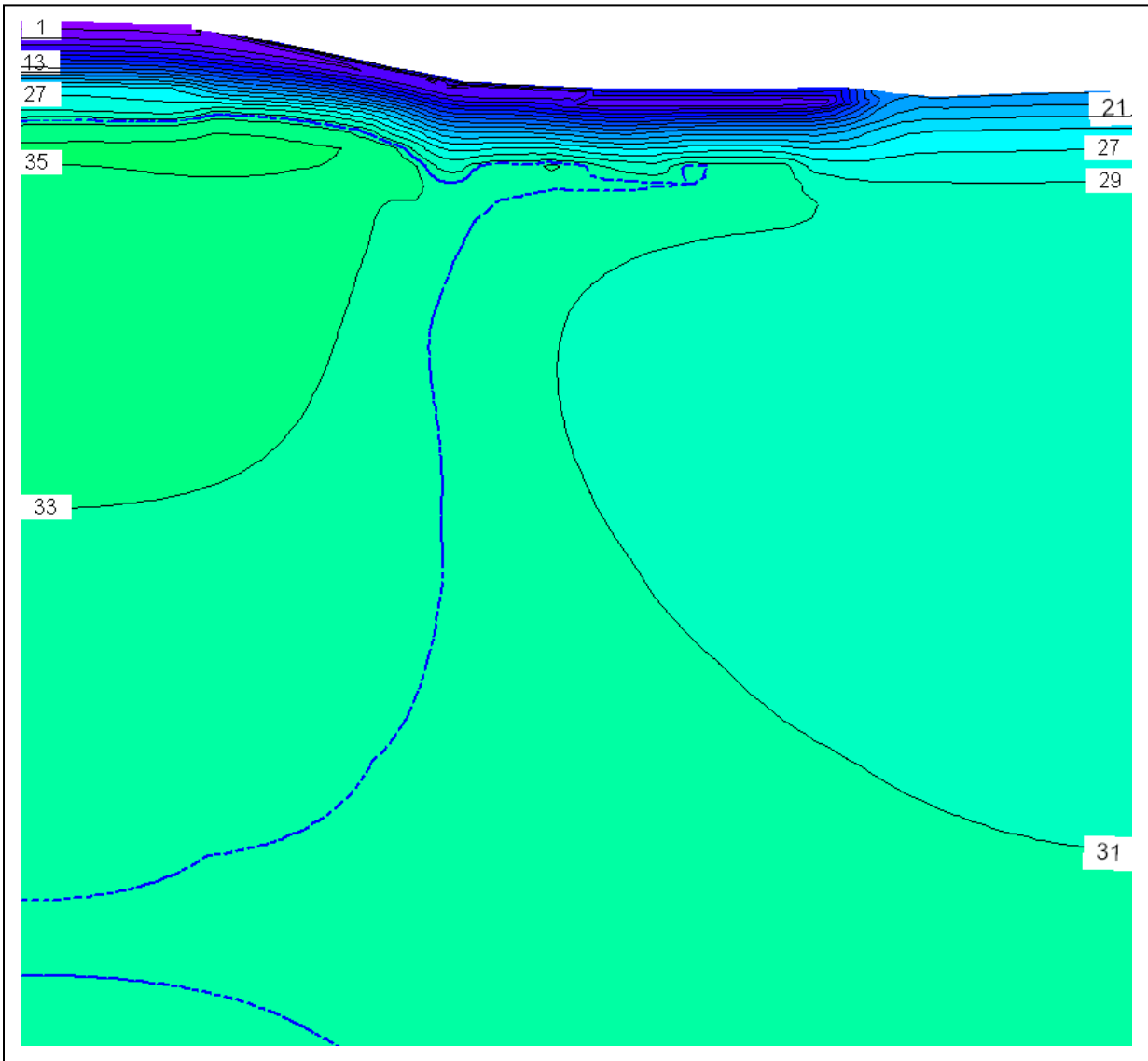
Figure F.1. Thermal modeling results for January 1st, Run 2, Richardson Highway MP 113 research site. The phase change isotherm is represented as the dashed blue line and the temperature results are shown with a 2°F contour interval.
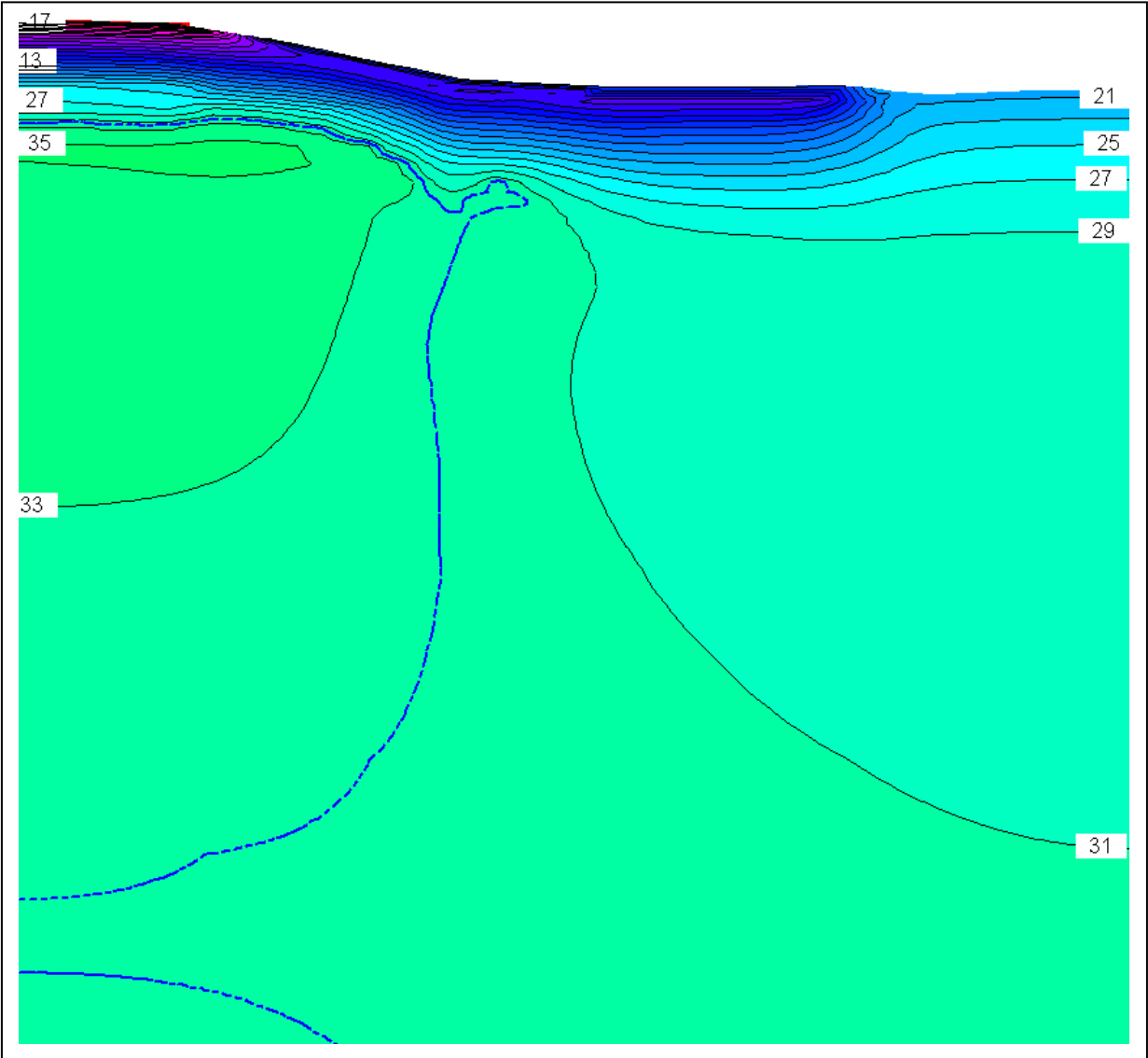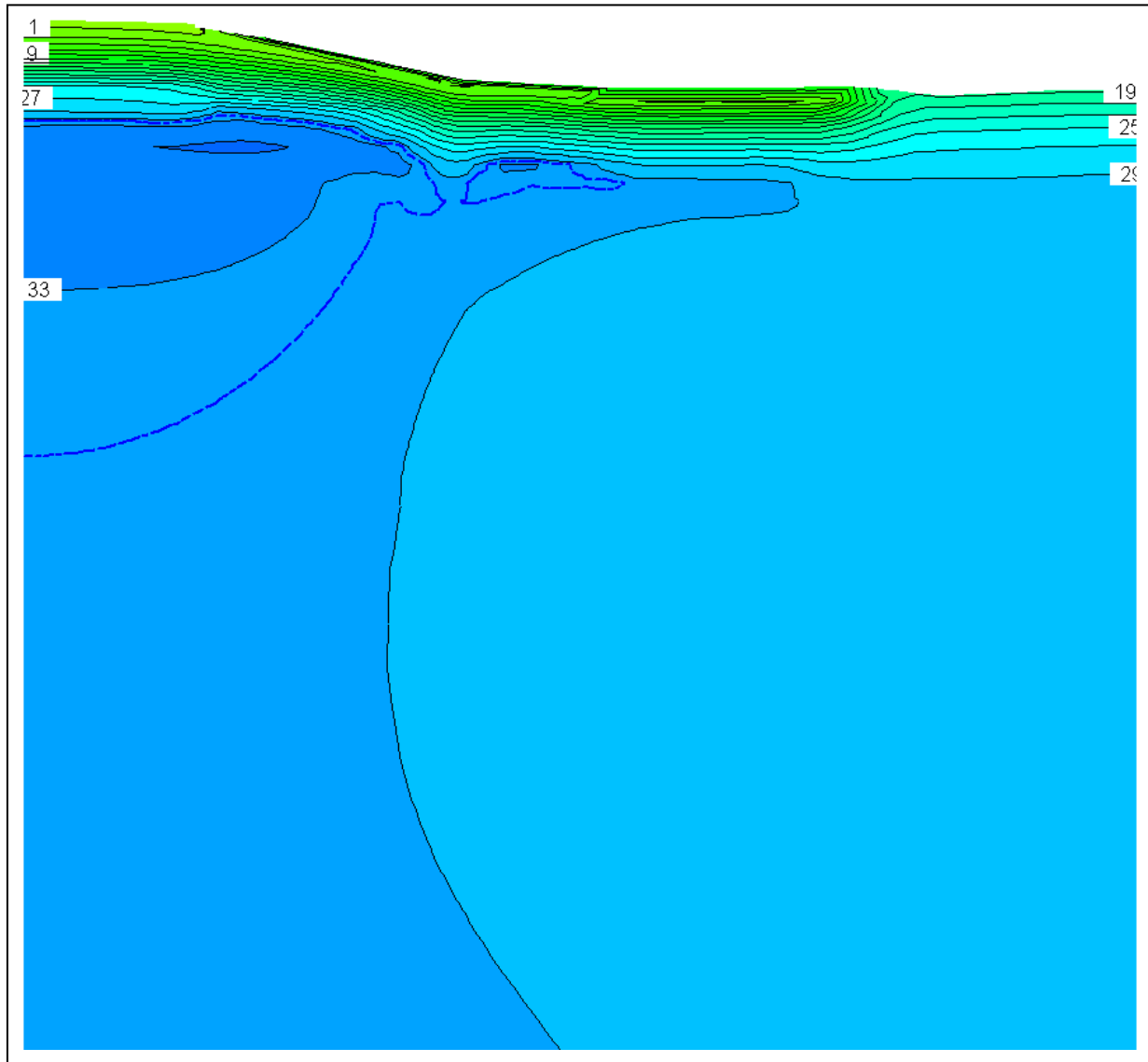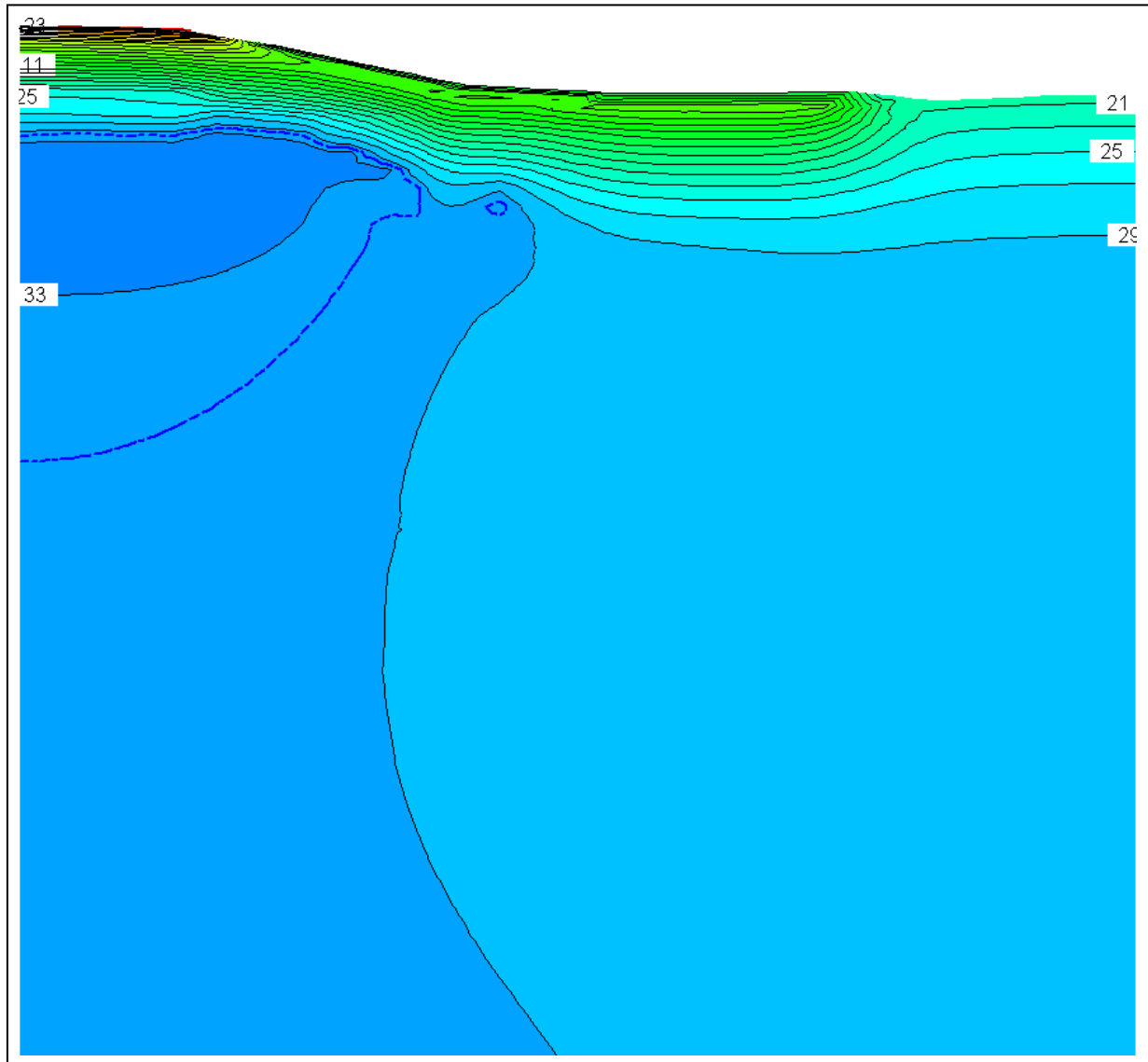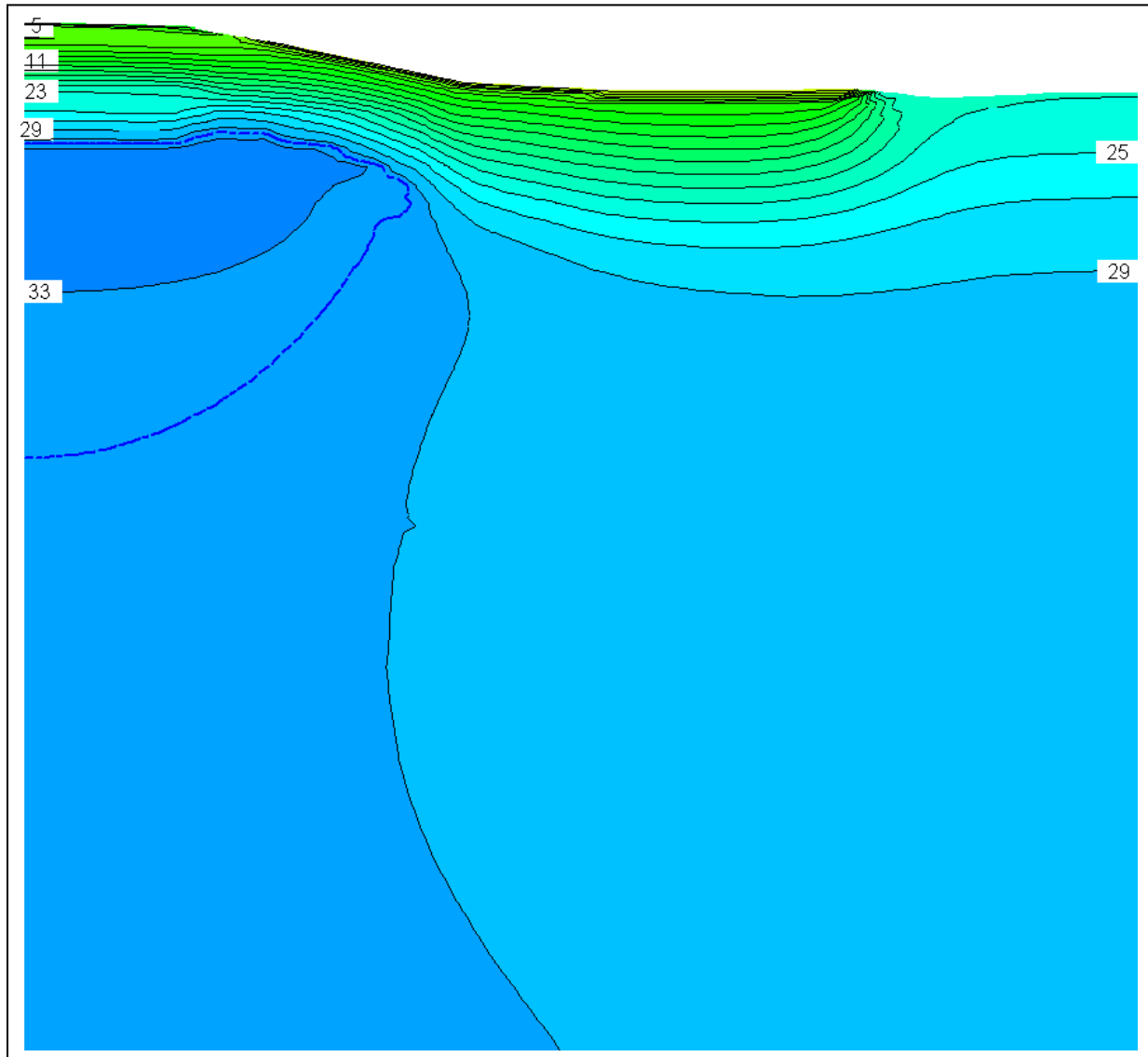
Figure F.2. Thermal modeling results for February 1st, Run 2, Richardson Highway MP 113 research site. The phase change isotherm is represented as the dashed blue line and the temperature results are shown with a 2°F contour interval.
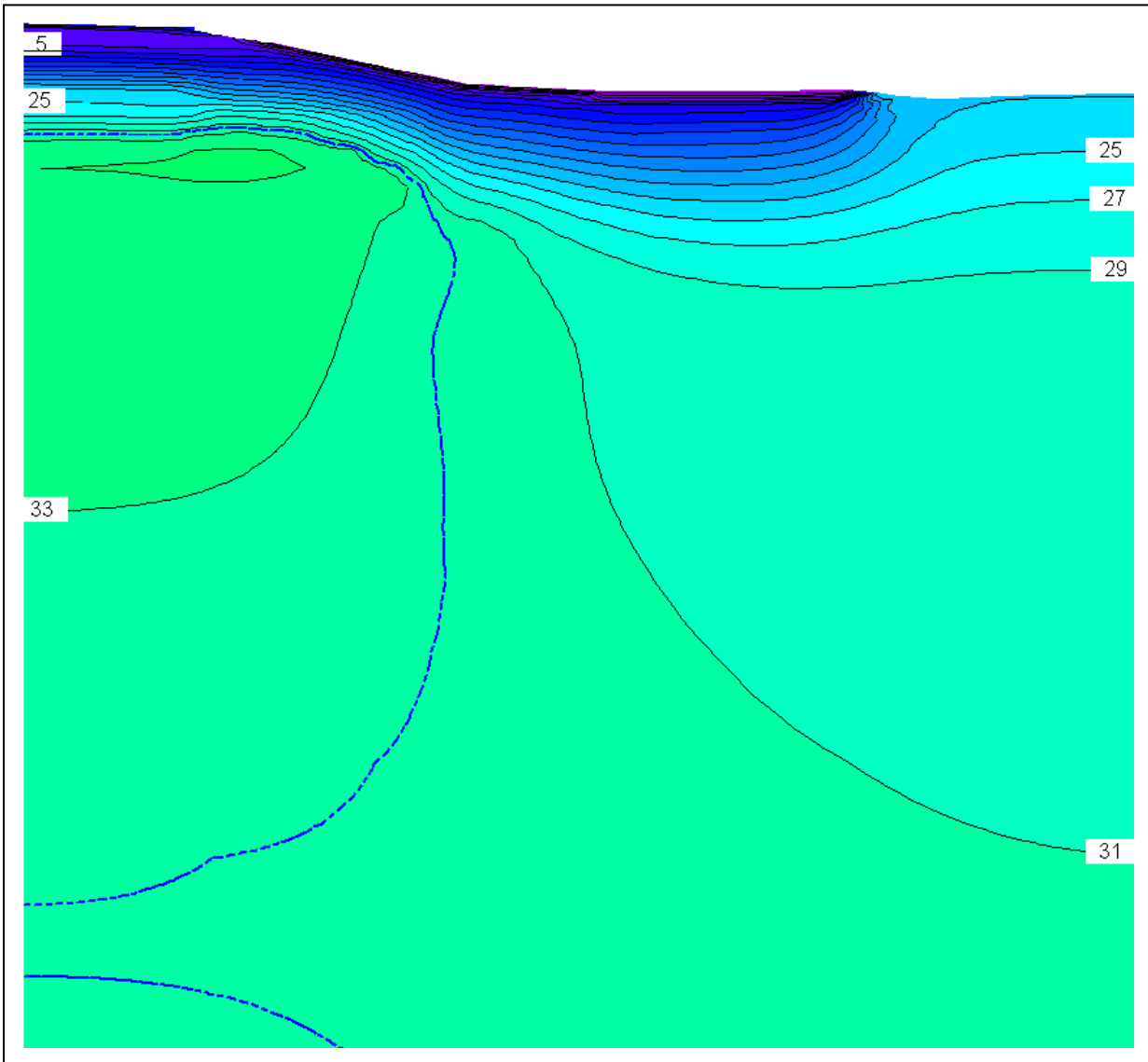
Figure F.3. Thermal modeling results for March 1st, Run 2, Richardson Highway MP 113 research site. The phase change isotherm is represented as the dashed blue line and the temperature results are shown with a 2°F contour interval.
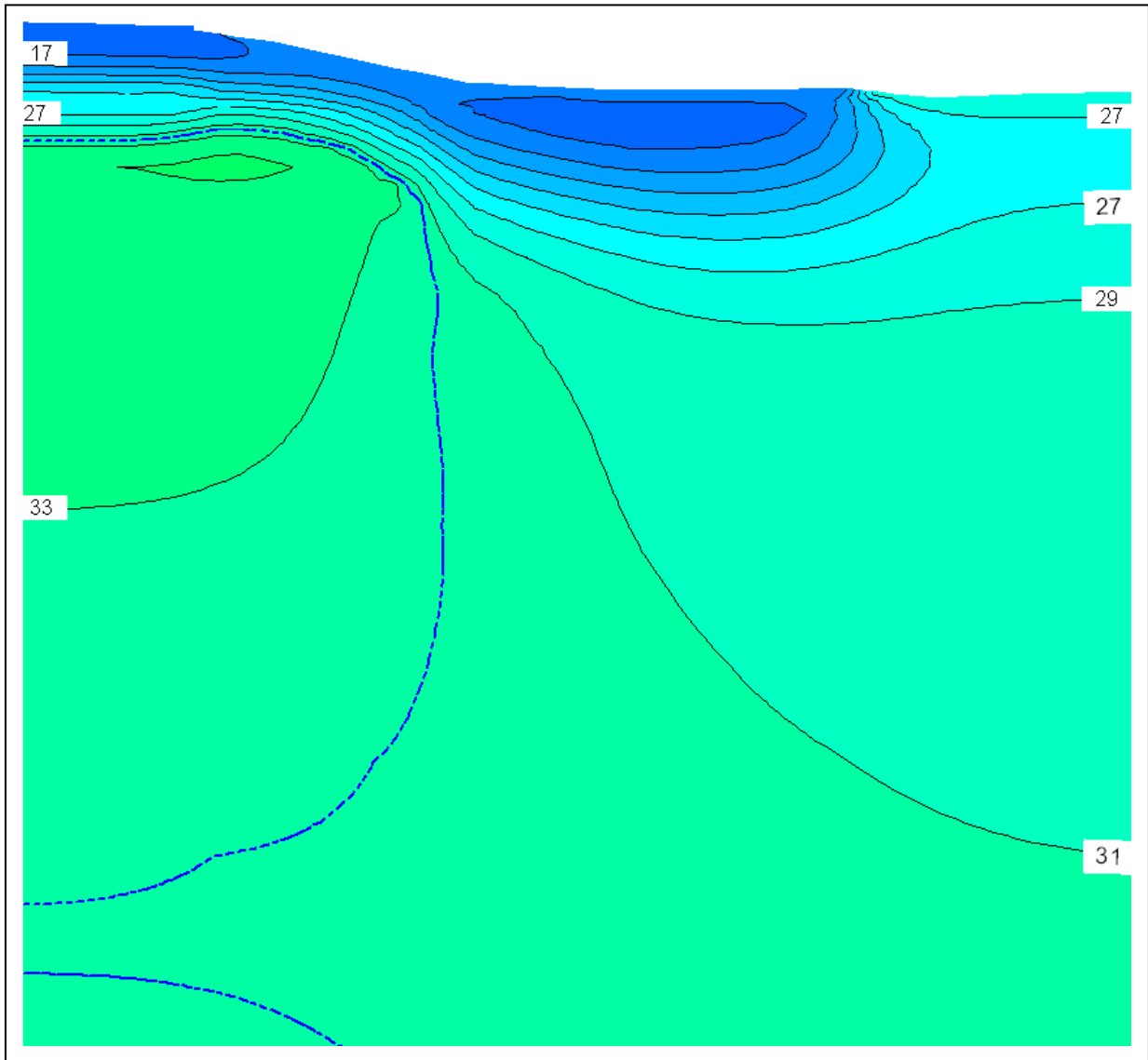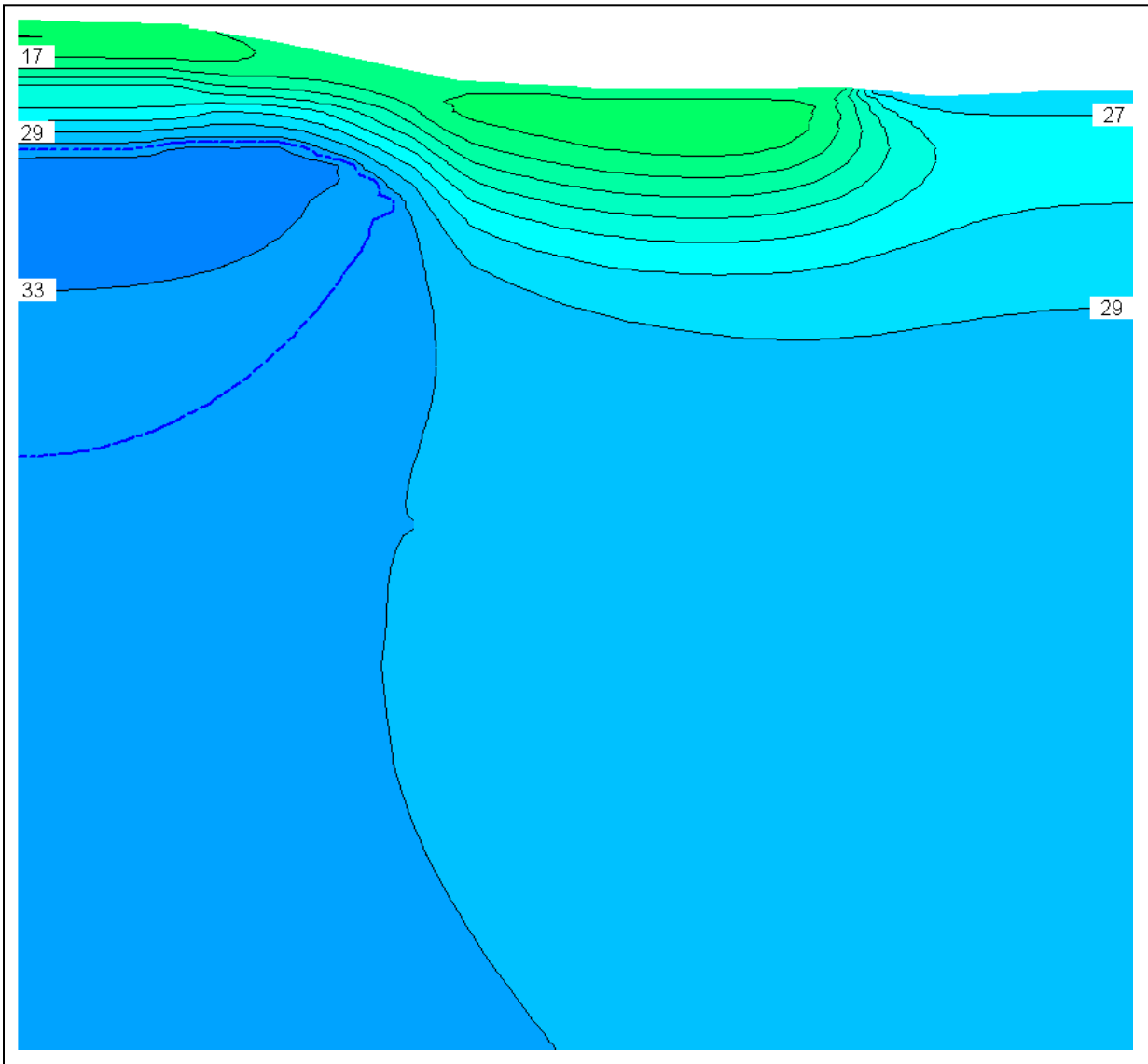
Figure F.4. Thermal modeling results for April 1st, Run 2, Richardson Highway MP 113 research site. The phase change isotherm is represented as the dashed blue line and the temperature results are shown with a 2°F contour interval.
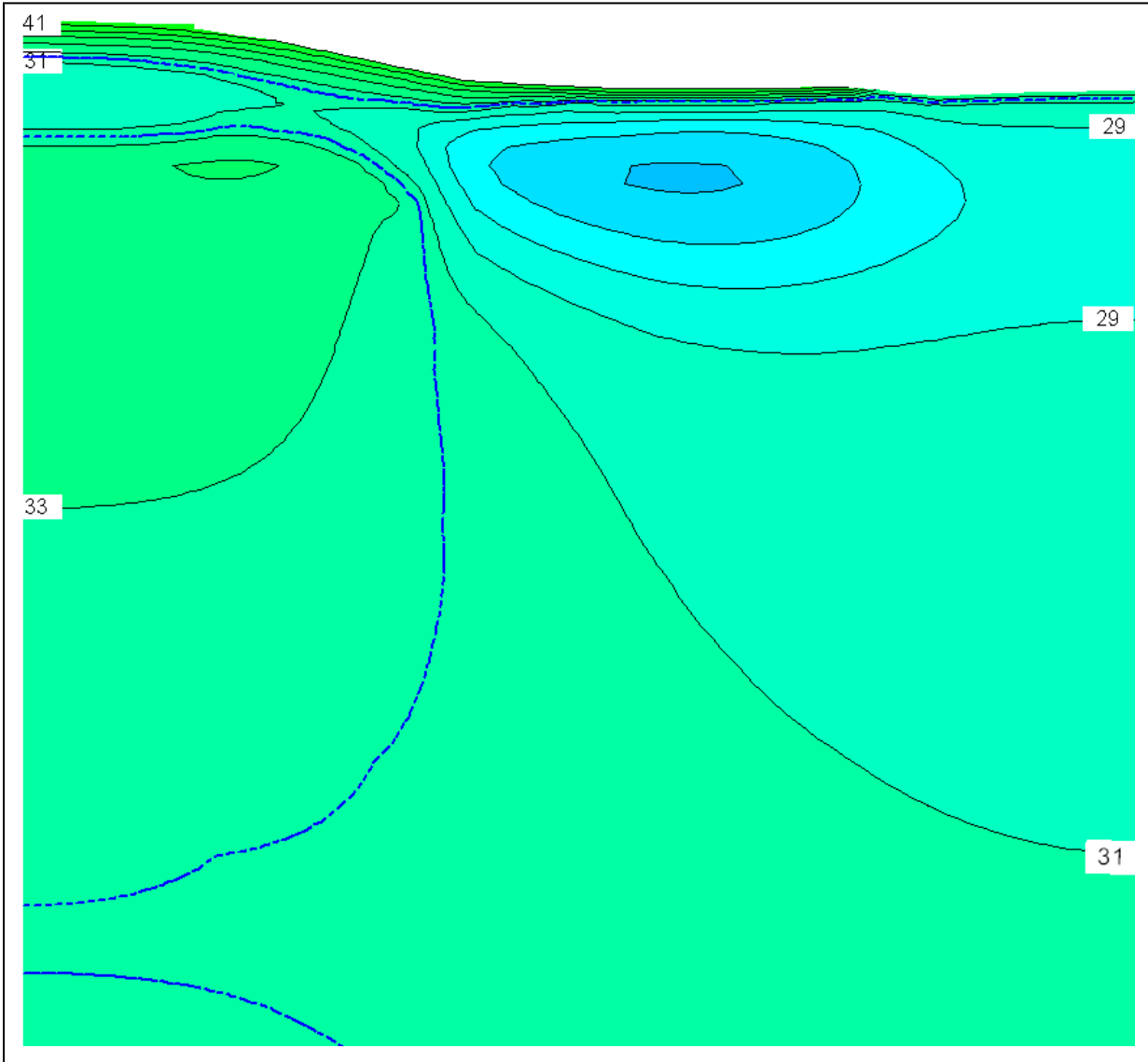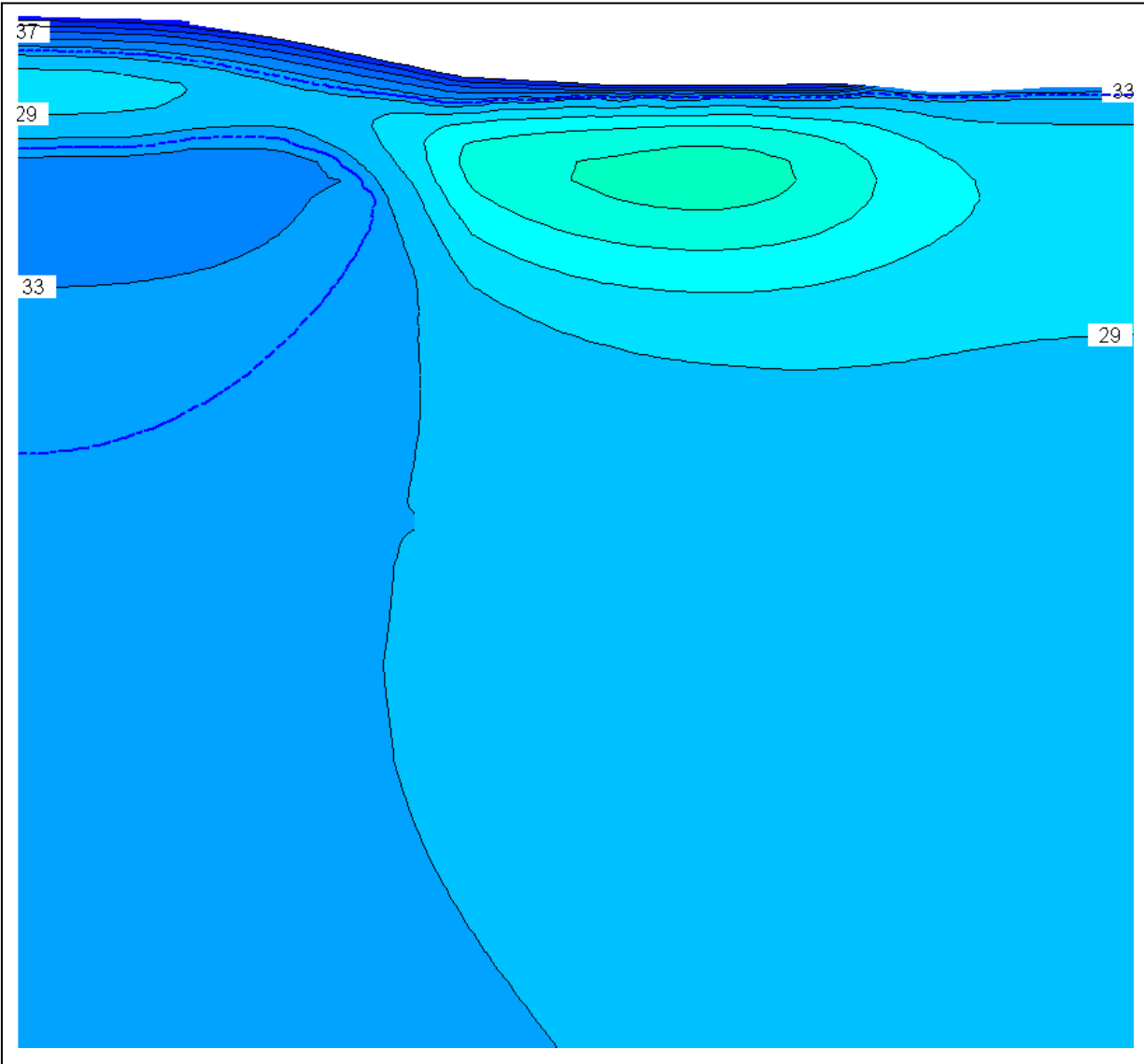
Figure F.5. Thermal modeling results for May 1st, Run 2, Richardson Highway MP 113 research site. The phase change isotherm is represented as the dashed blue line and the temperature results are shown with a 2°F contour interval.
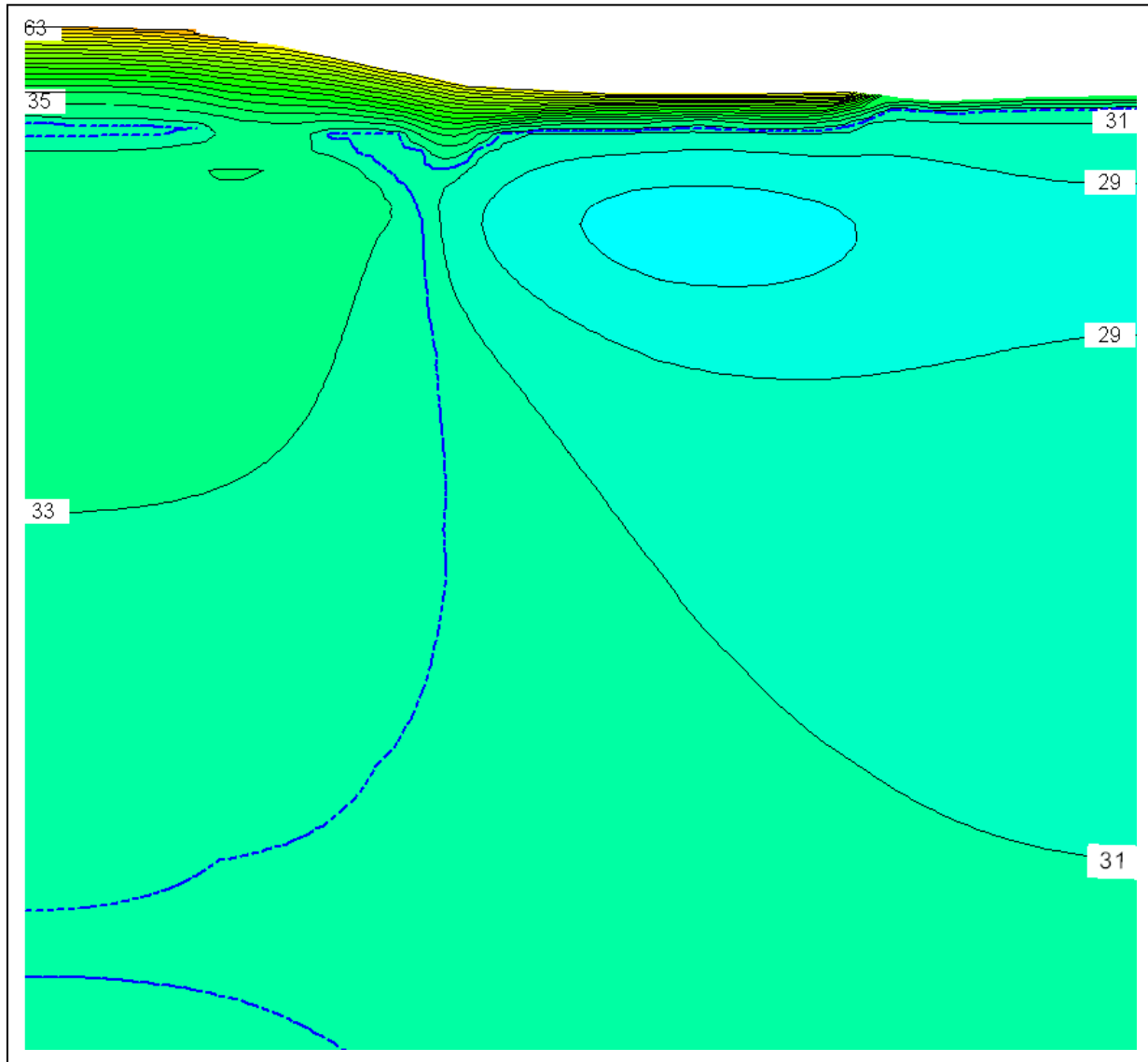
Figure F.6. Thermal modeling results for June 1st, Run 2, Richardson Highway MP 113 research site. The phase change isotherm is represented as the dashed blue line and the temperature results are shown with a 2°F contour interval.
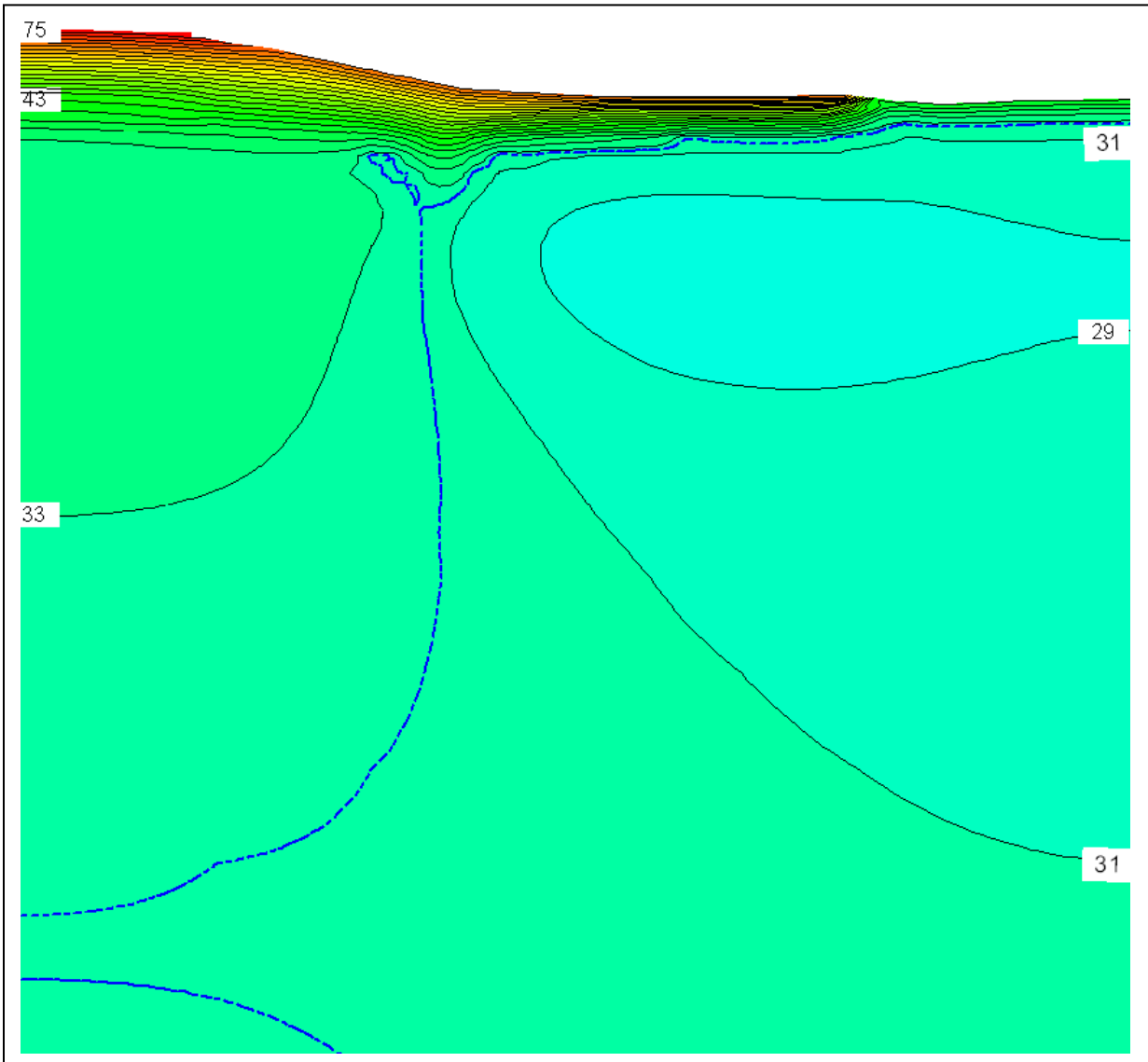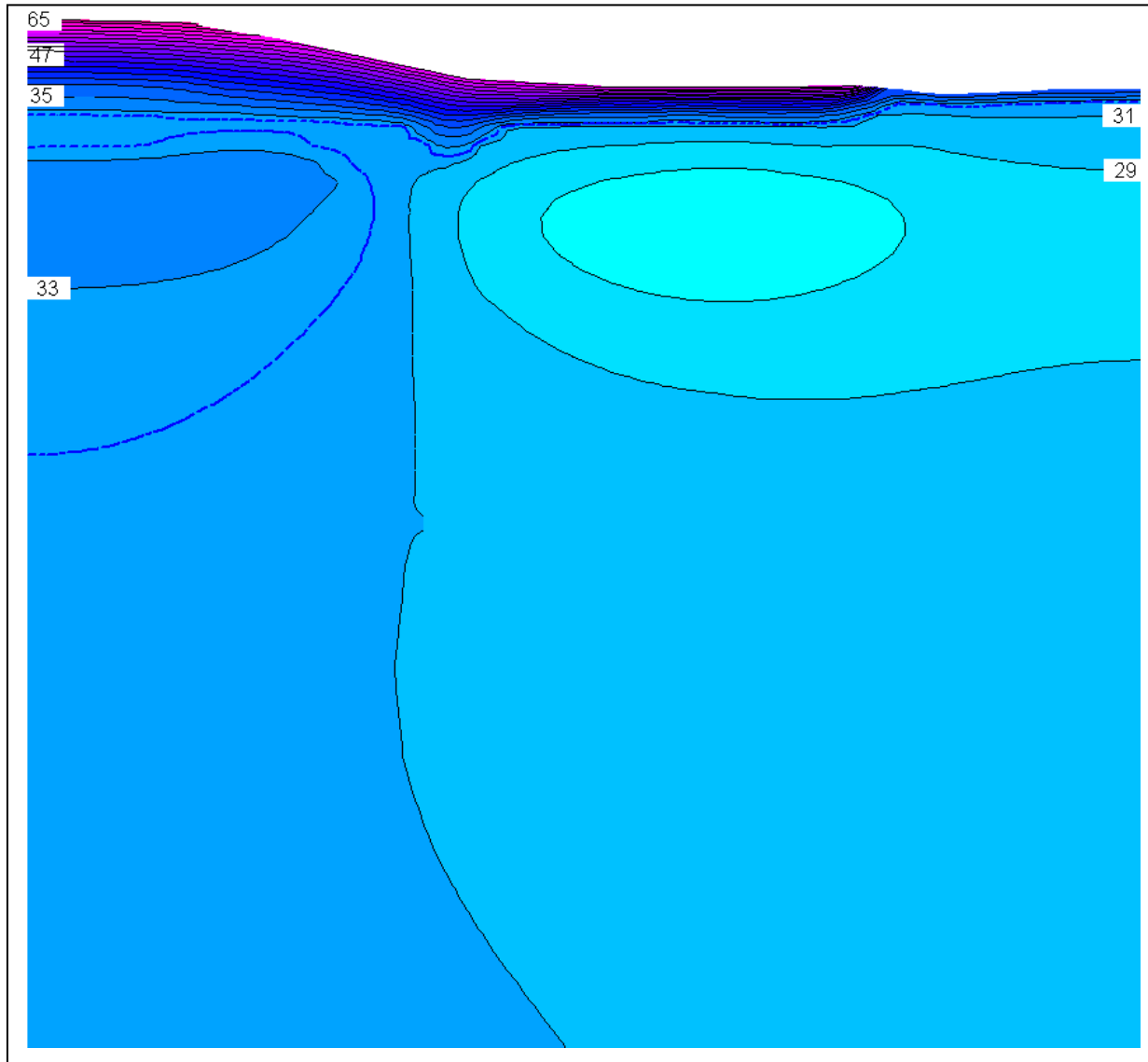
Figure F.7. Thermal modeling results for July 1st, Run 2, Richardson Highway MP 113 research site. The phase change isotherm is represented as the dashed blue line and the temperature results are shown with a 2°F contour interval.
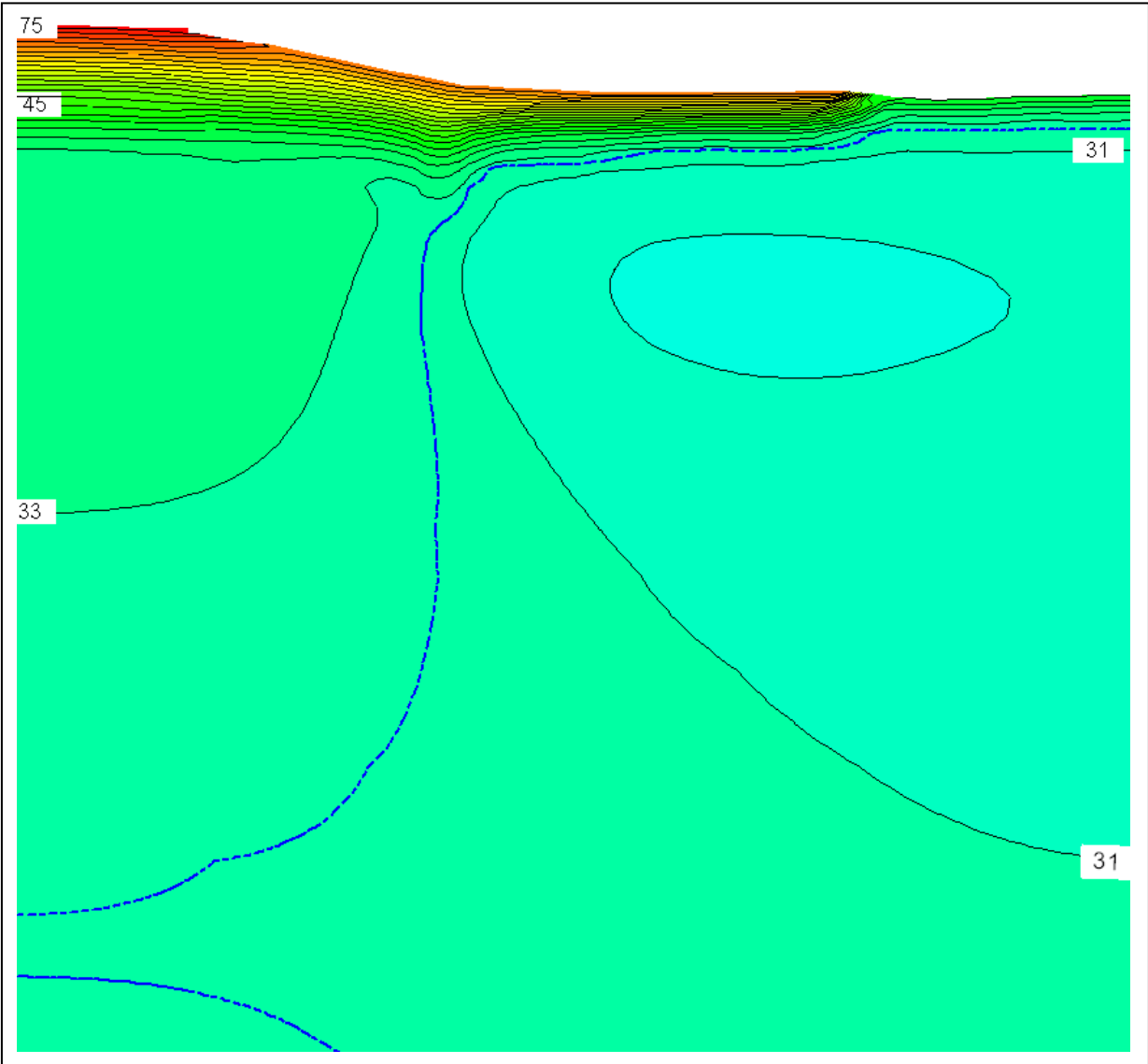
Figure F.8. Thermal modeling results for August 1st, Run 2, Richardson Highway MP 113 research site. The phase change isotherm is represented as the dashed blue line and the temperature results are shown with a 2°F contour interval.
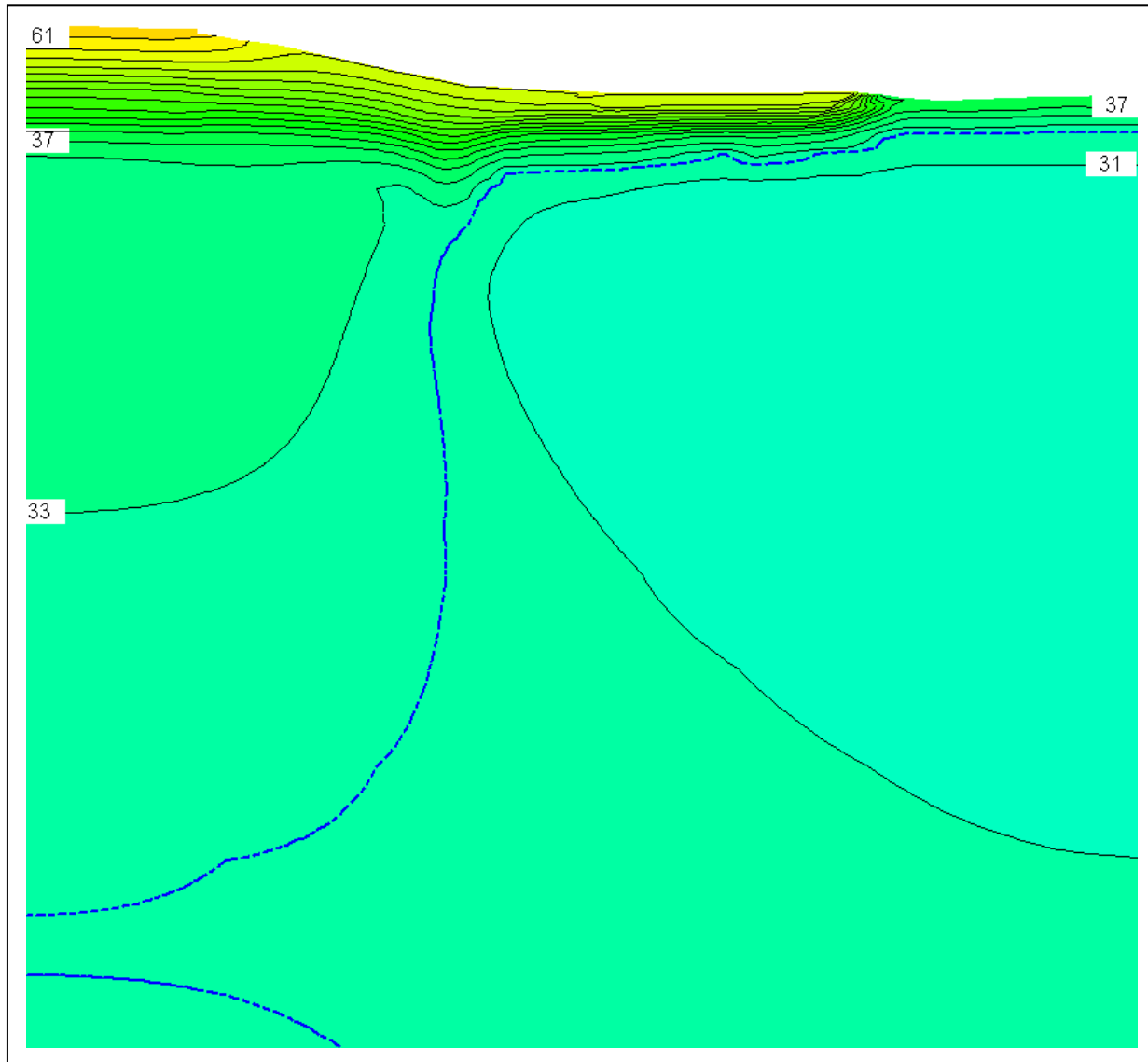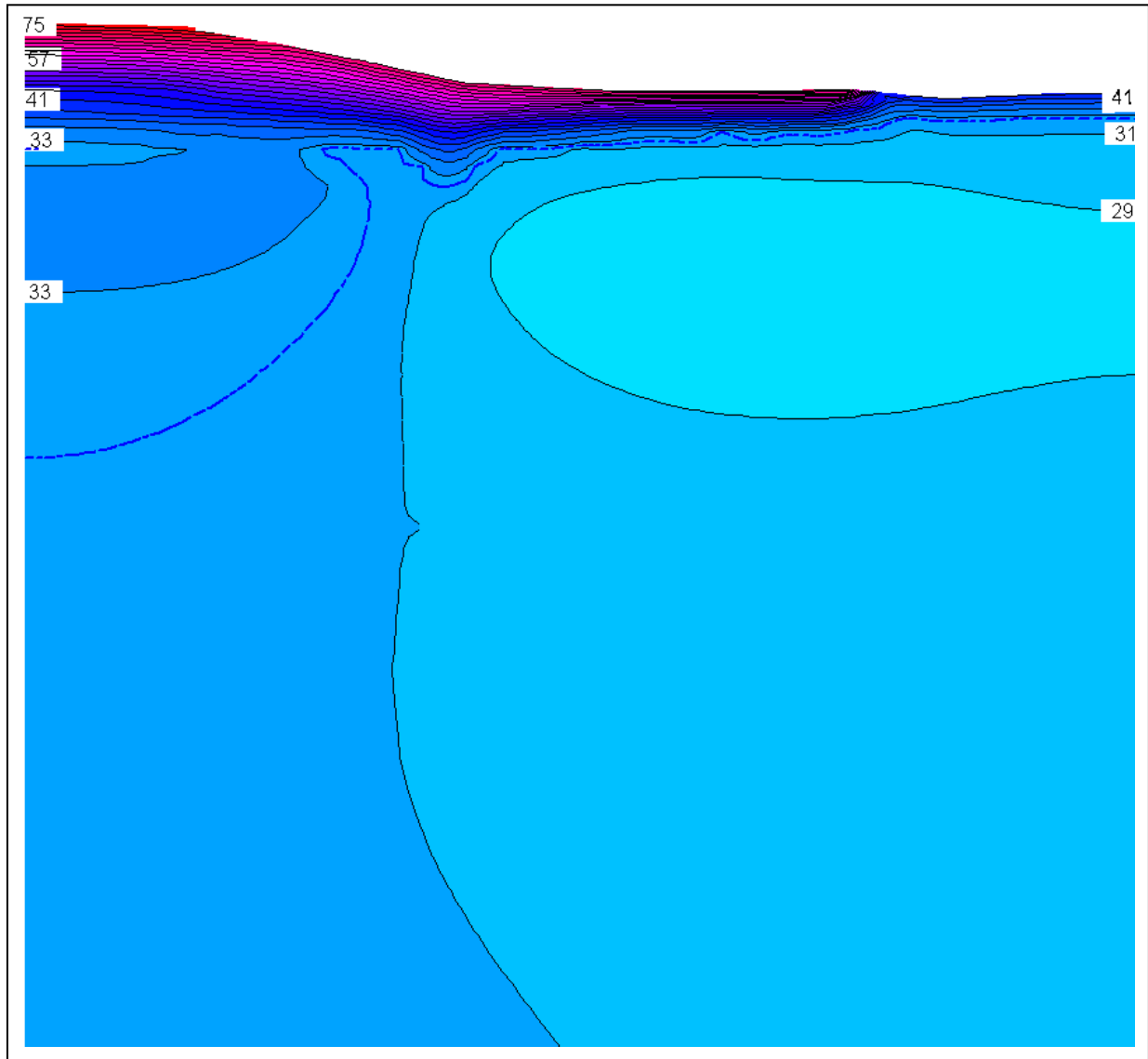
Figure F.9. Thermal modeling results for September 1st, Run 2, Richardson Highway MP 113 research site. The phase change isotherm is represented as the dashed blue line and the temperature results are shown with a 2°F contour interval.
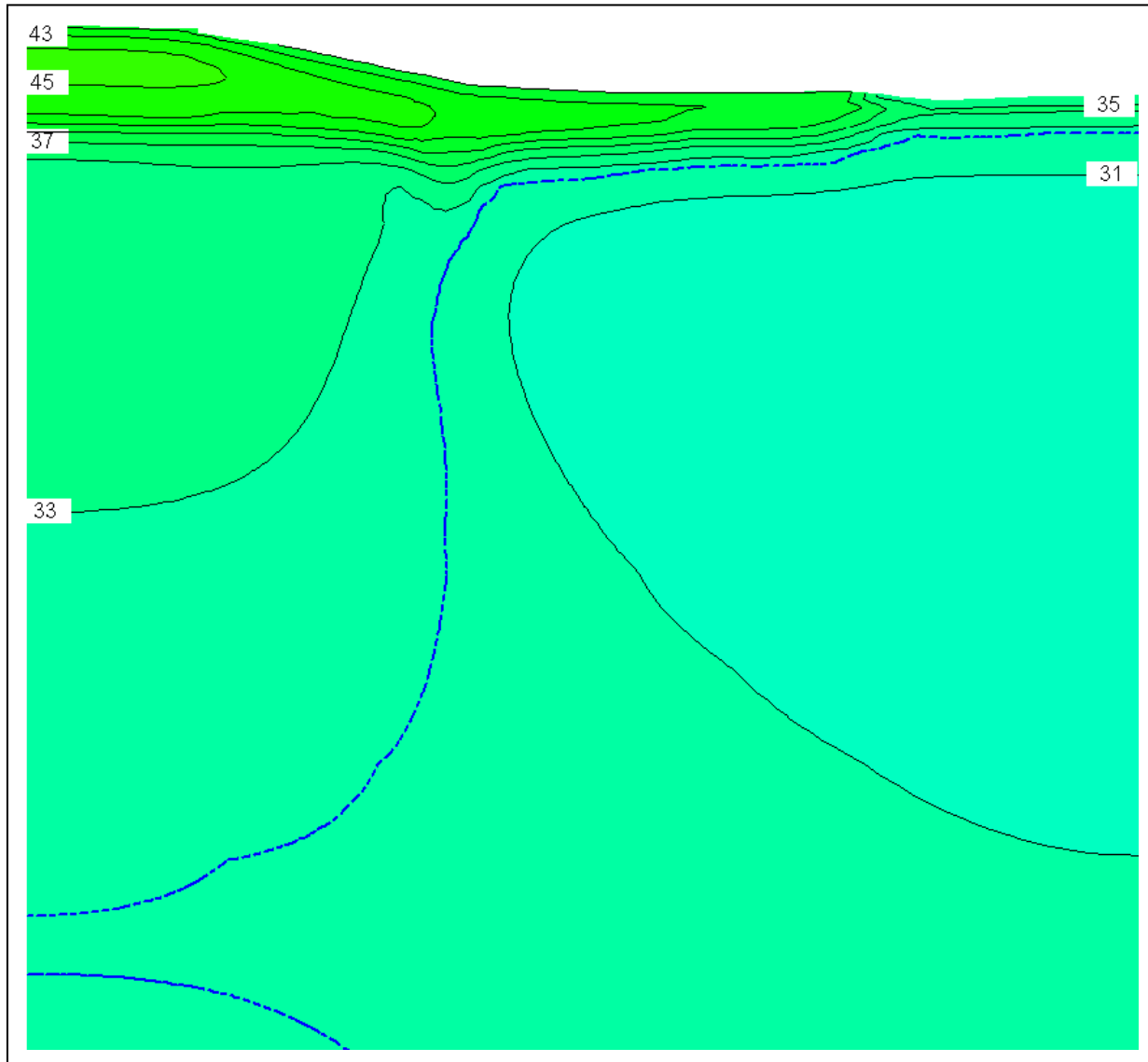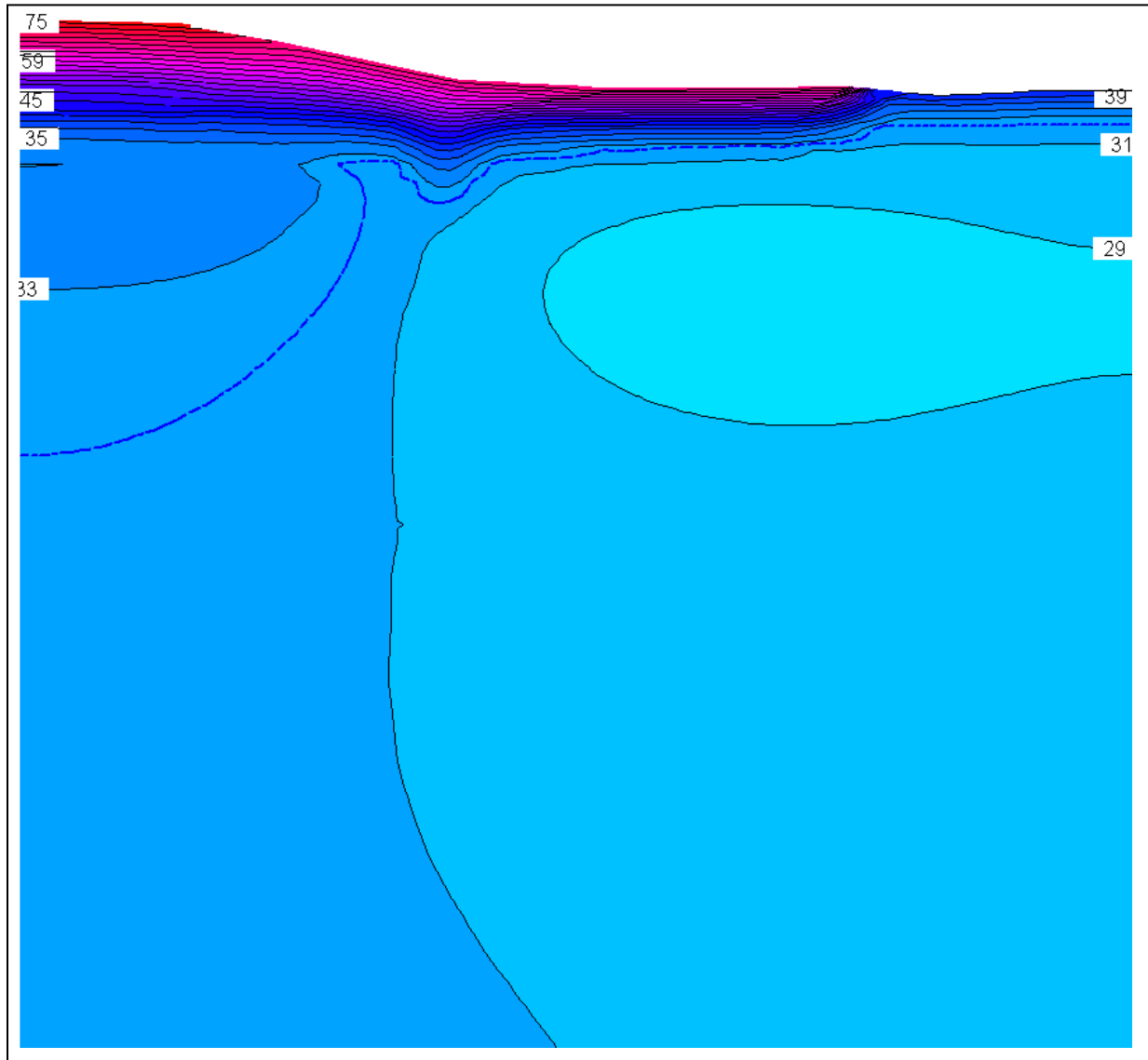
Figure F.10. Thermal modeling results for October 1st, Run 2, Richardson Highway MP 113 research site. The phase change isotherm is represented as the dashed blue line and the temperature results are shown with a 2°F contour interval.
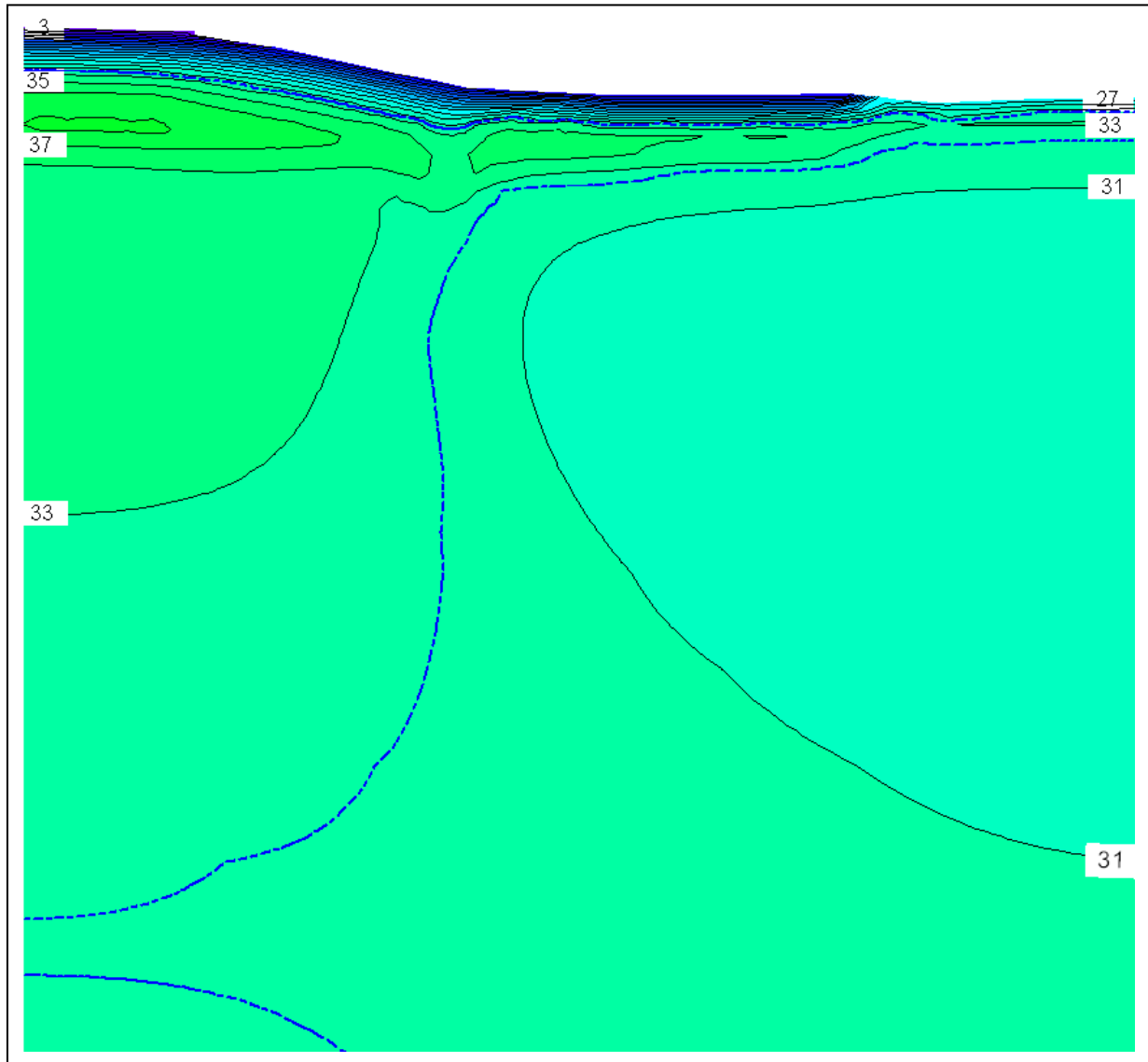
Figure F.11. Thermal modeling results for November 1st, Run 2, Richardson Highway MP 113
research site. The phase change isotherm is represented as the dashed blue line and the
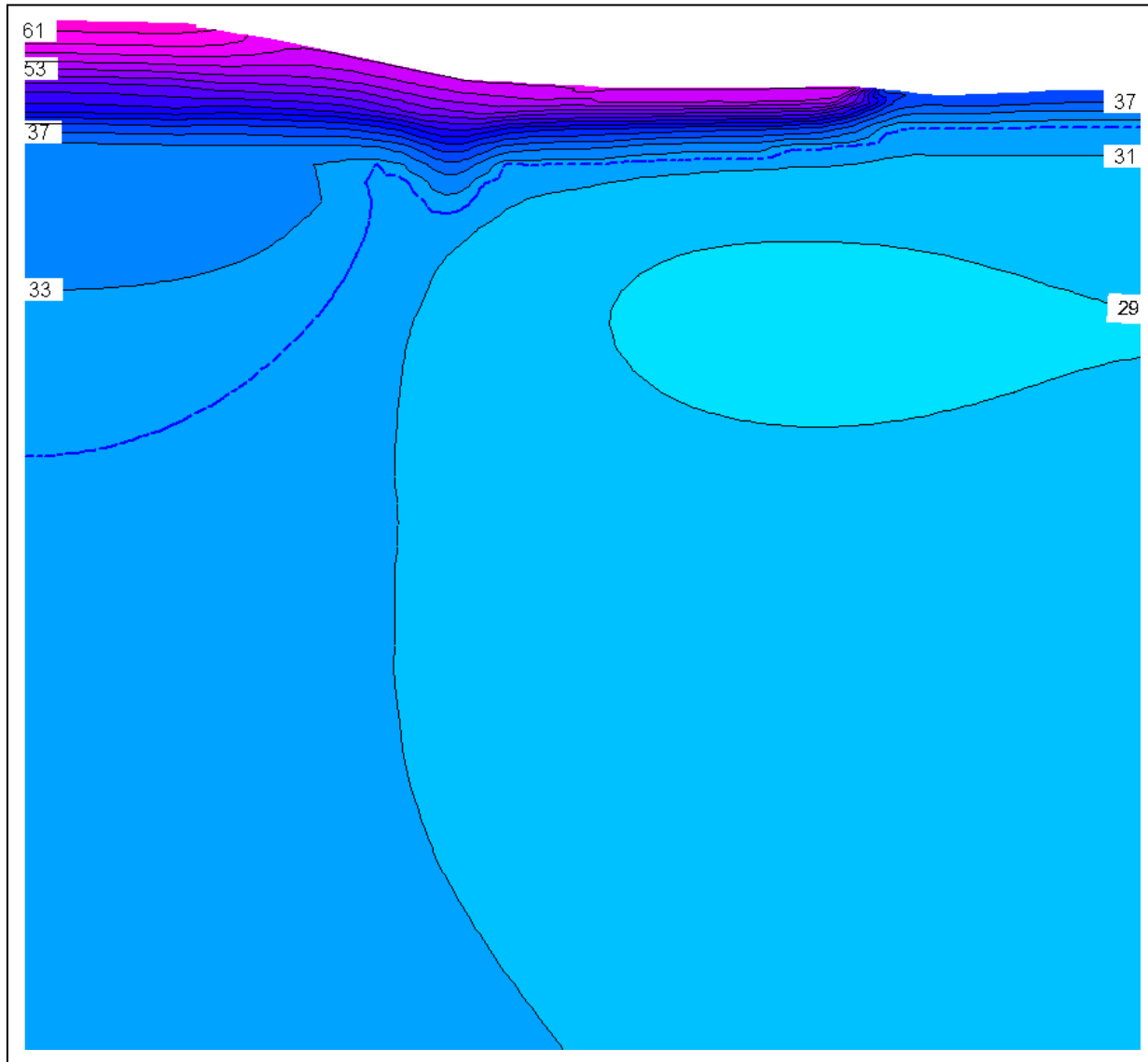temperature results are shown with a 2°F contour interval.
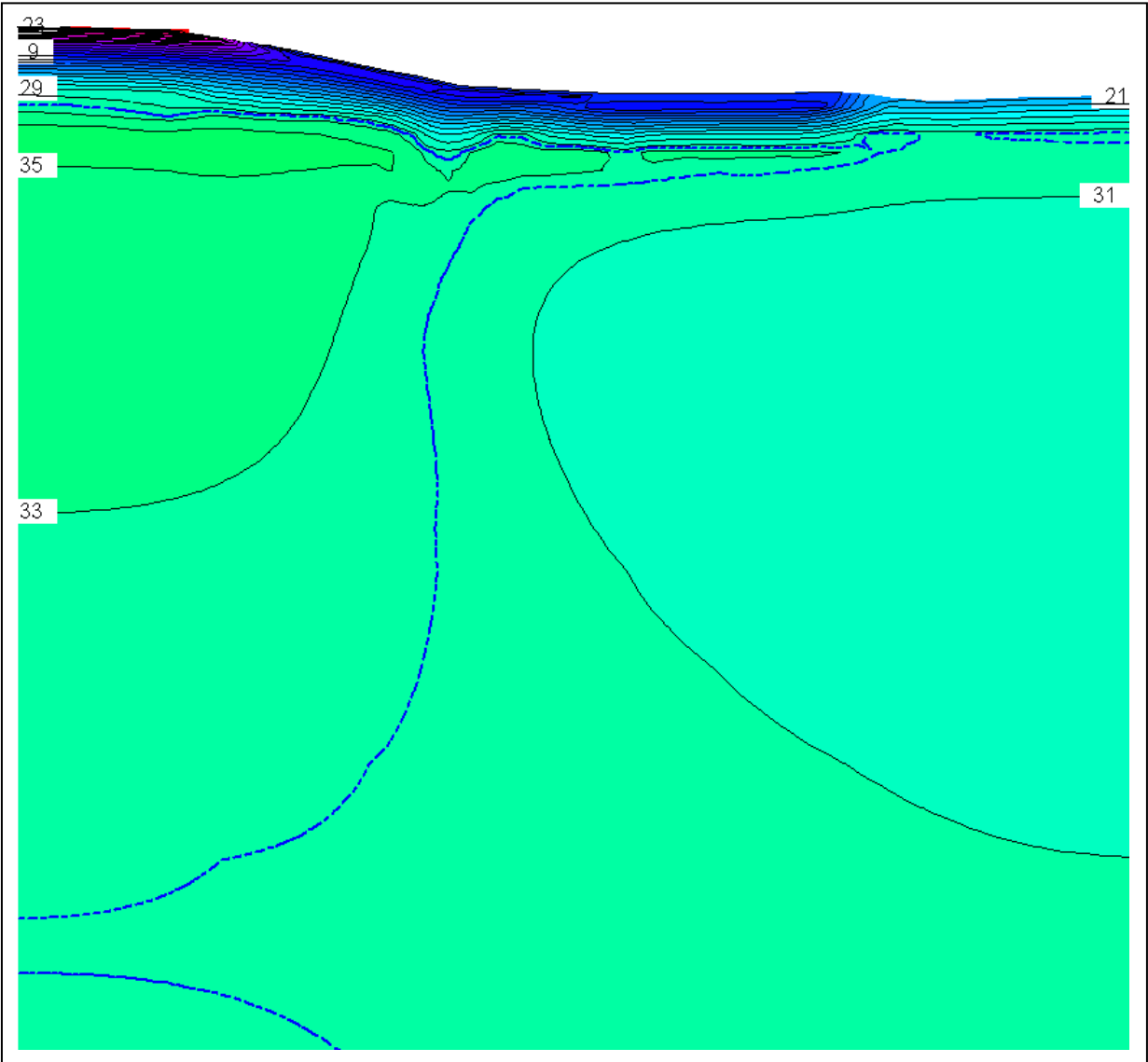
Figure F.12. Thermal modeling results for December 1st, Run 2, Richardson Highway MP 113 research site. The phase change isotherm is represented as the dashed blue line and the temperature results are shown with a 2°F contour interval.
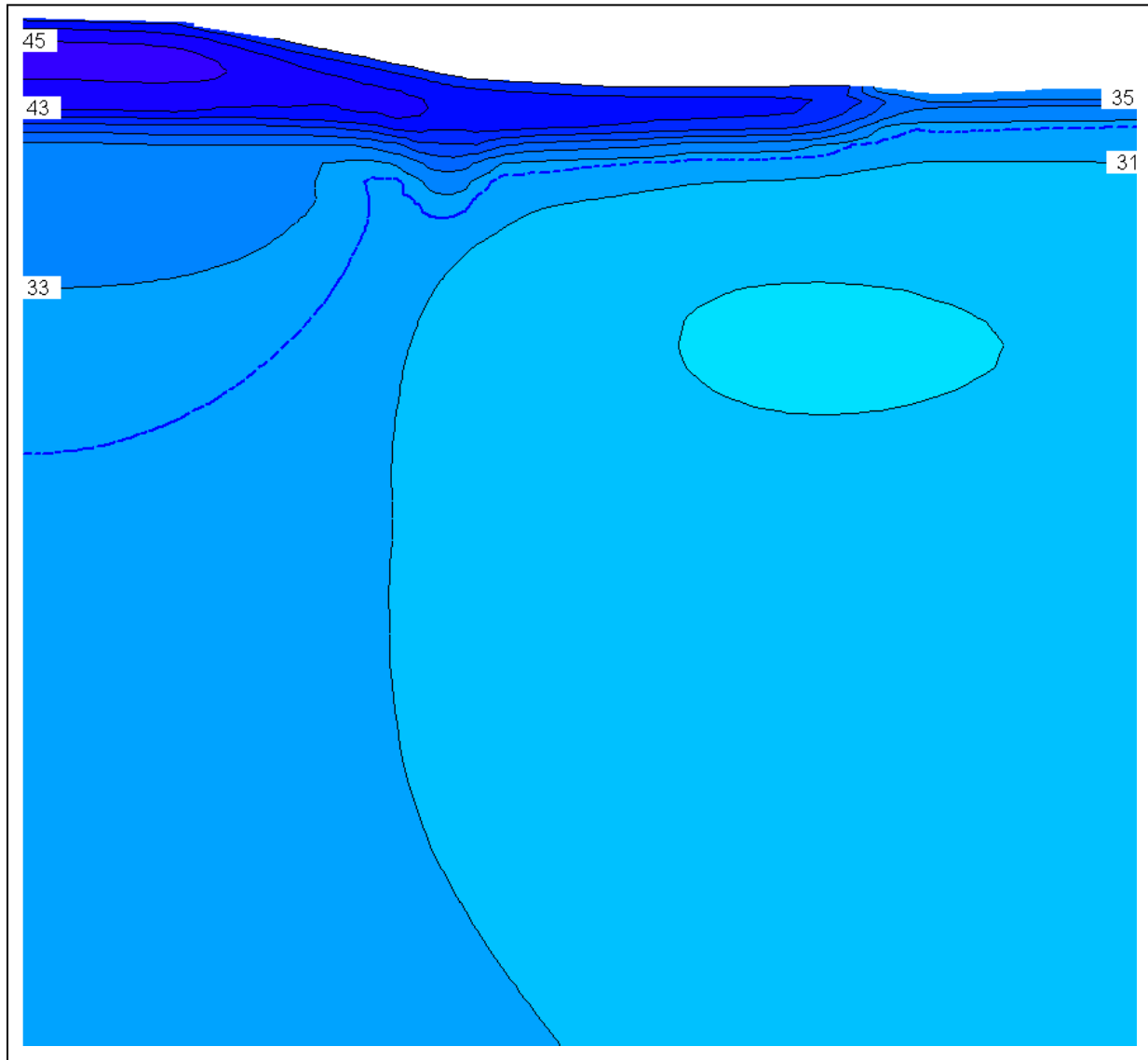
Figure F.13. Thermal modeling results for January 1st, Run 3, Richardson Highway MP 113 research site. The phase change isotherm is represented as the dashed blue line and the temperature results are shown with a 2°F contour interval.

Figure F.14. Thermal modeling results for February 1st, Run 3, Richardson Highway MP 113 research site. The phase change isotherm is represented as the dashed blue line and the temperature results are shown with a 2°F contour interval.
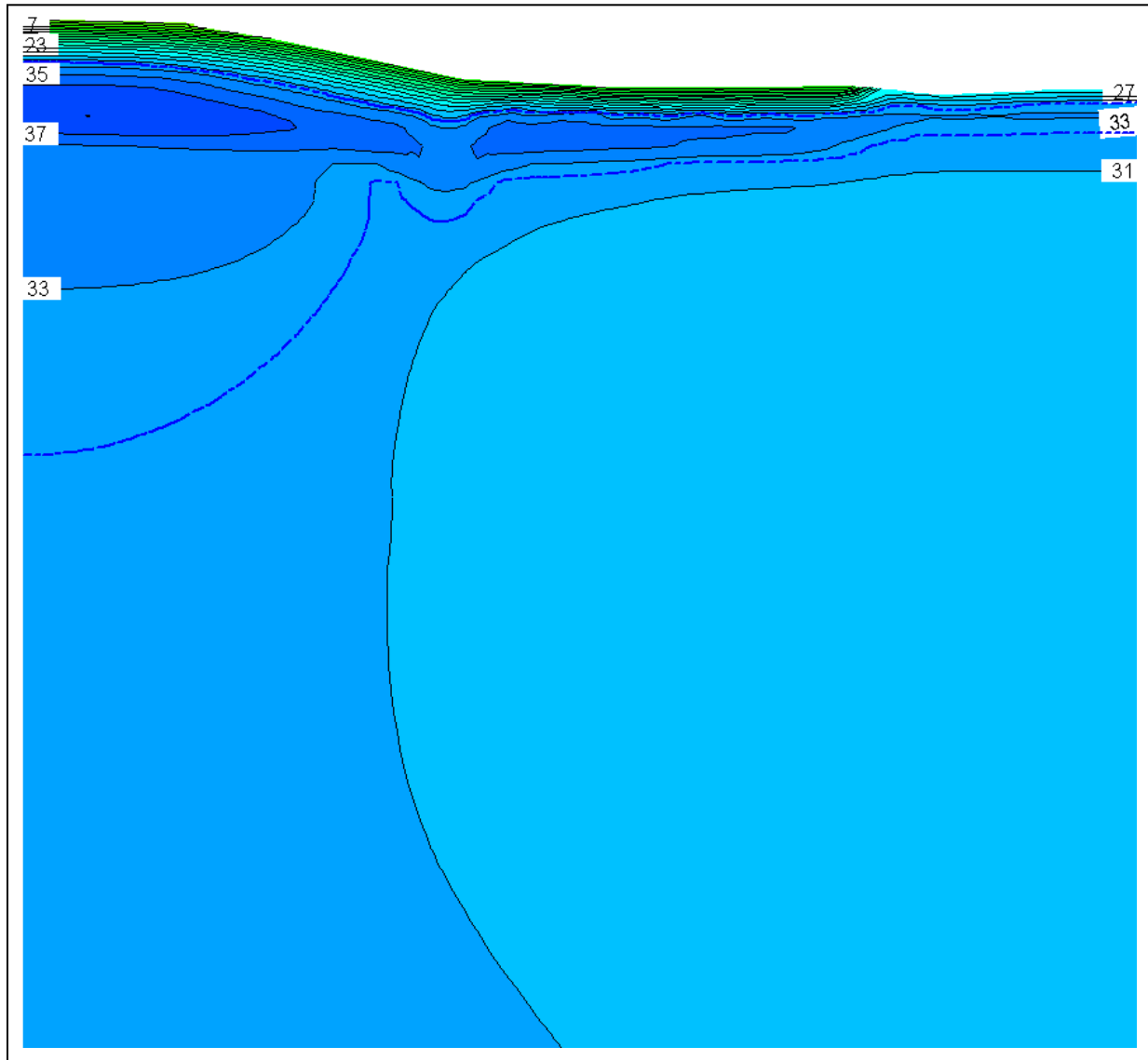
Figure F.15. Thermal modeling results for March 1st, Run 3, Richardson Highway MP 113 research site. The phase change isotherm is represented as the dashed blue line and the temperature results are shown with a 2°F contour interval.

Figure F.16. Thermal modeling results for April 1st, Run 3, Richardson Highway MP 113 research site. The phase change isotherm is represented as the dashed blue line and the temperature results are shown with a 2°F contour interval.
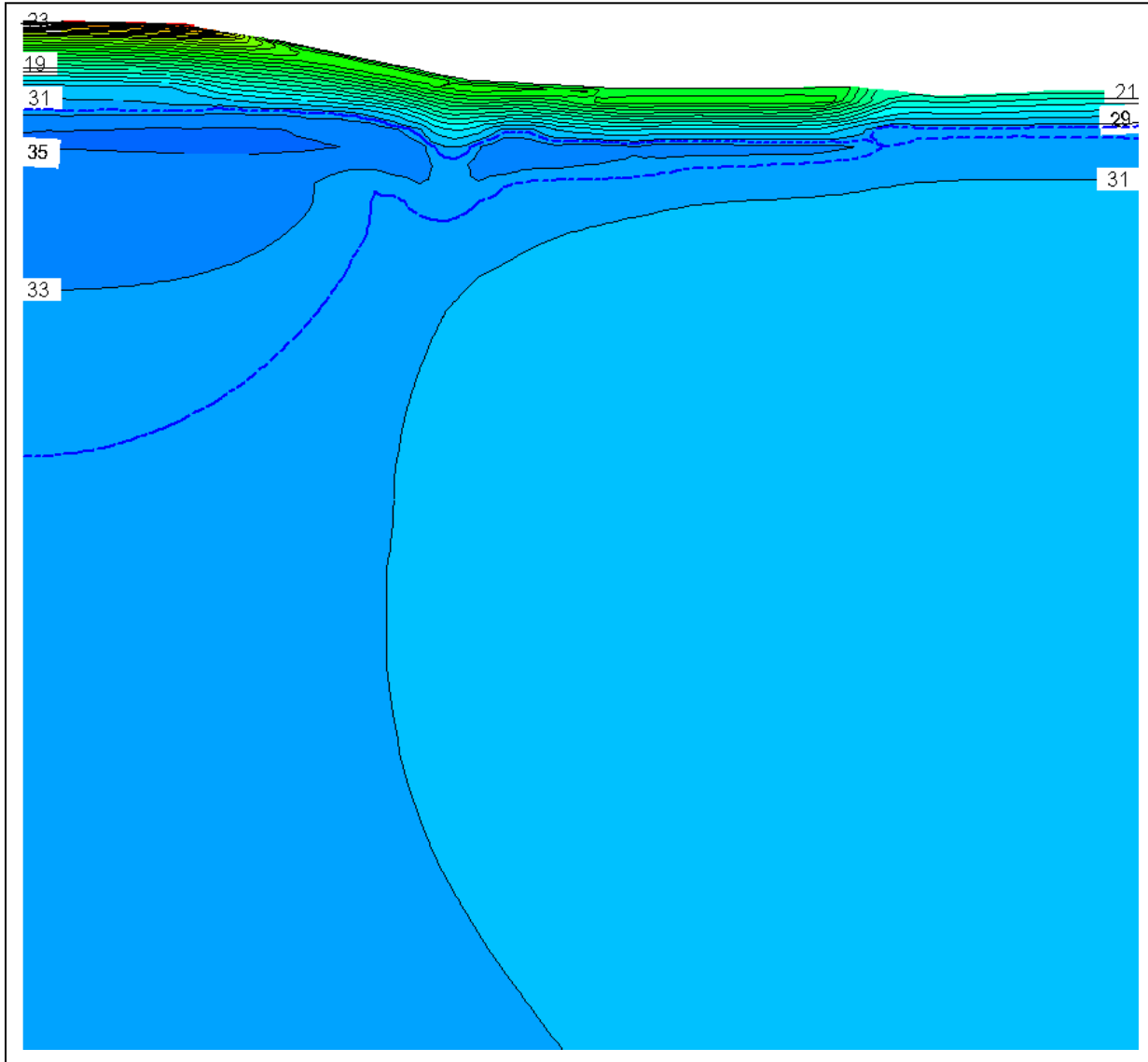
Figure F.17. Thermal modeling results for May 1st, Run 3, Richardson Highway MP 113 research site. The phase change isotherm is represented as the dashed blue line and the temperature results are shown with a 2°F contour interval.
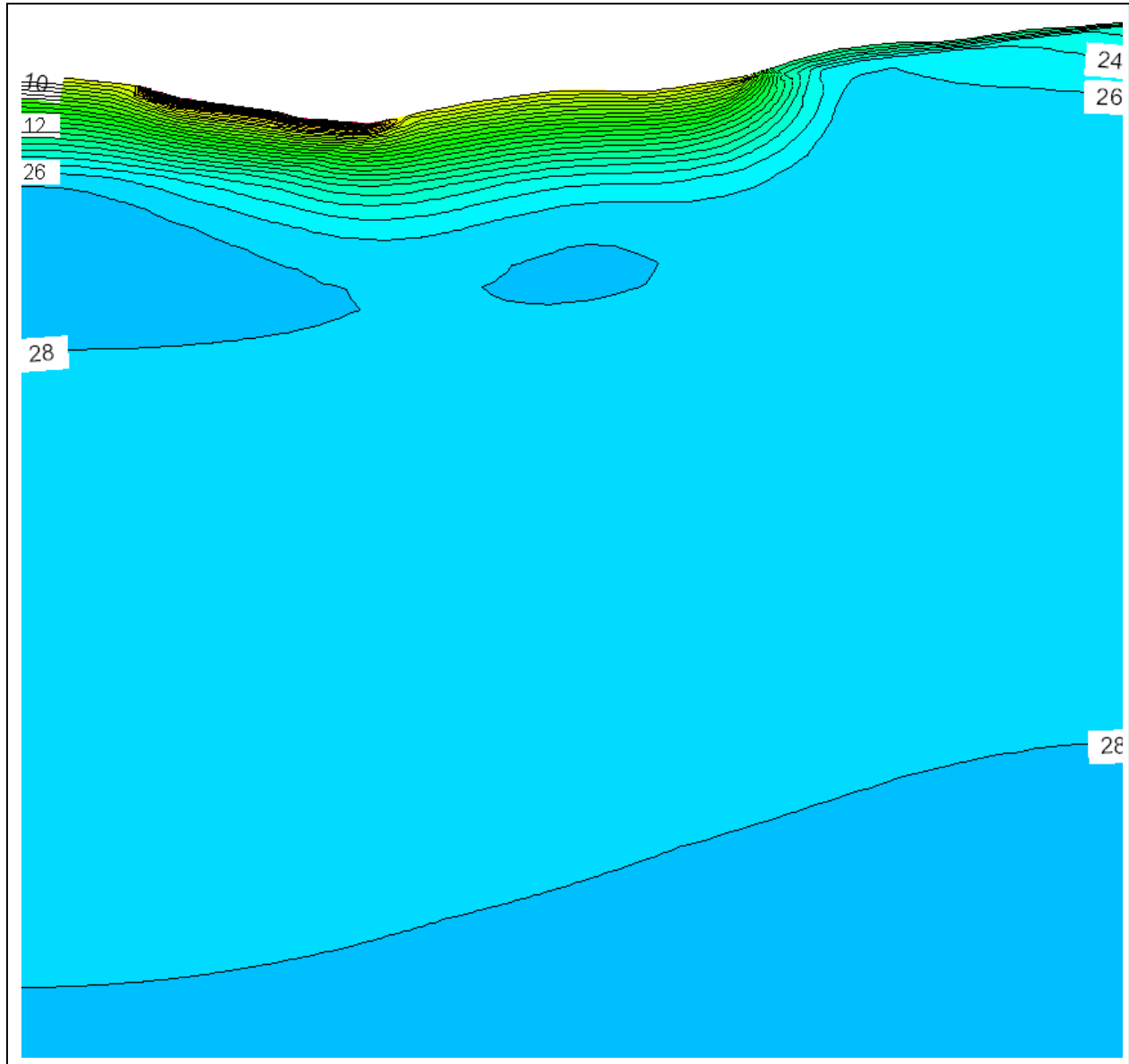
Figure F.18. Thermal modeling results for June 1st, Run 3, Richardson Highway MP 113 research site. The phase change isotherm is represented as the dashed blue line and the temperature results are shown with a 2°F contour interval.

Figure F.19. Thermal modeling results for July 1st, Run 3, Richardson Highway MP 113 research site. The phase change isotherm is represented as the dashed blue line and the temperature results are shown with a 2°F contour interval.
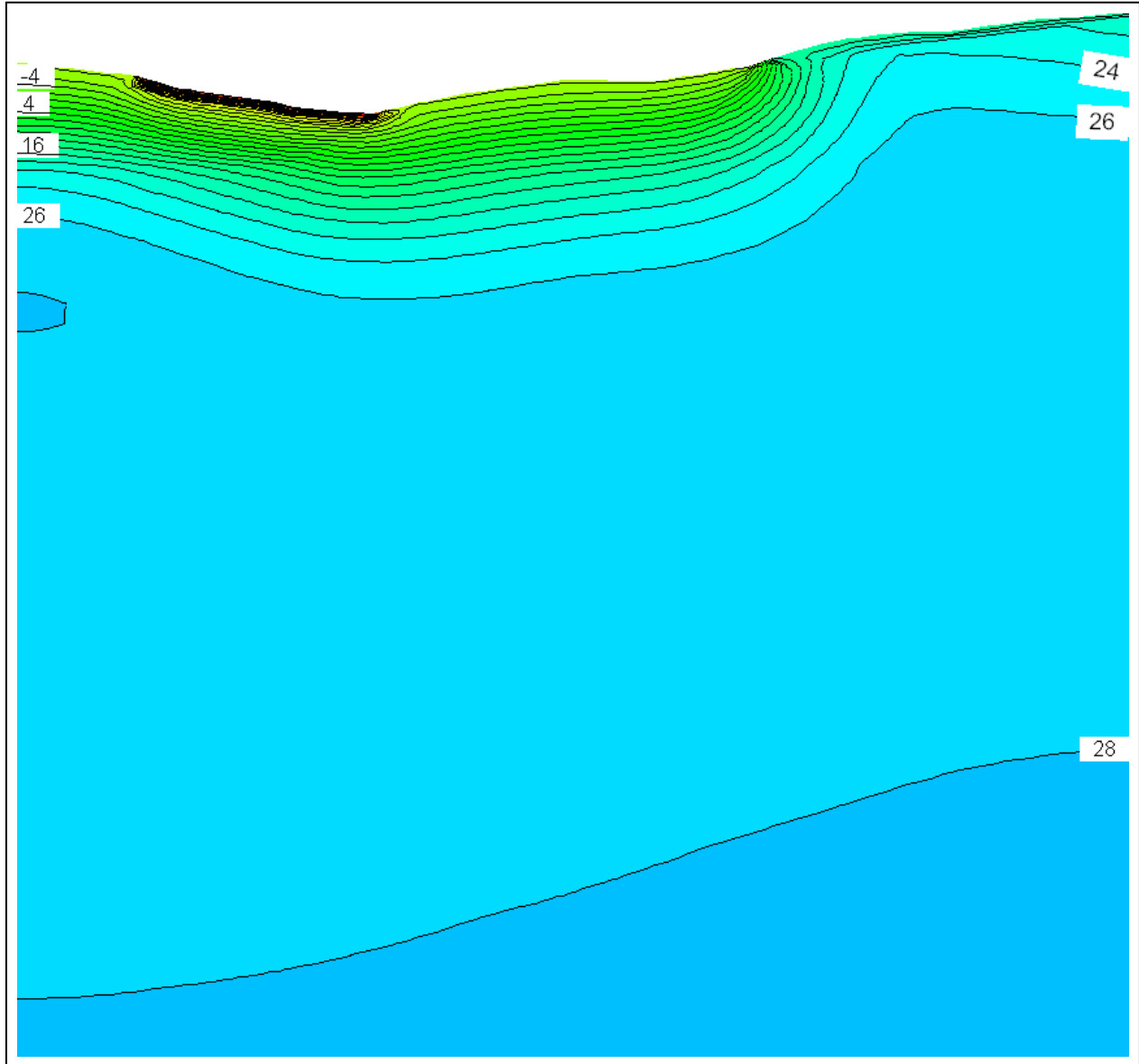
Figure F.20. Thermal modeling results for August 1st, Run 3, Richardson Highway MP 113 research site. The phase change isotherm is represented as the dashed blue line and the temperature results are shown with a 2°F contour interval.
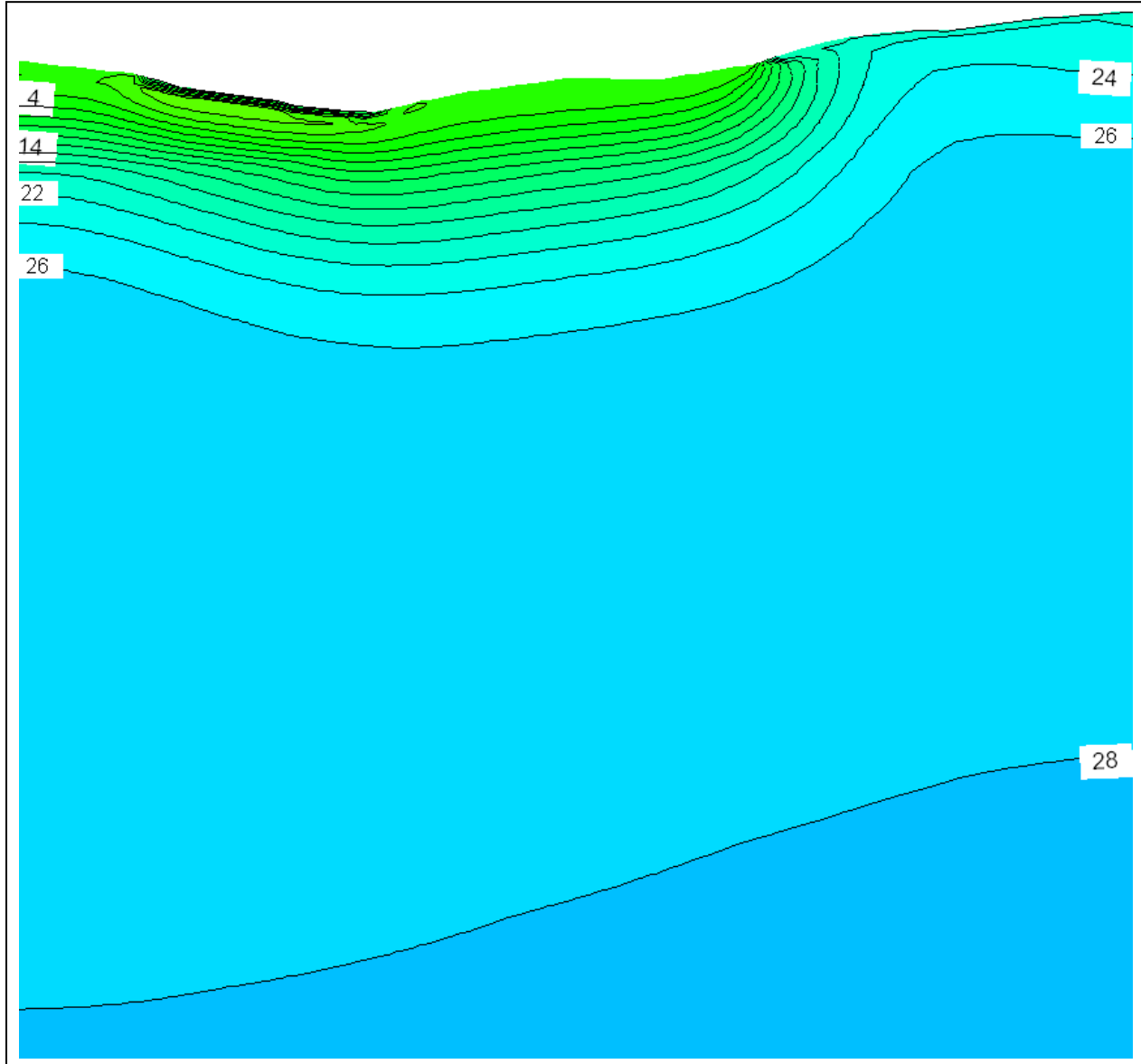
Figure F.21. Thermal modeling results for September 1st, Run 3, Richardson Highway MP 113 research site. The phase change isotherm is represented as the dashed blue line and the temperature results are shown with a 2°F contour interval.

Figure F.22. Thermal modeling results for October 1st, Run 3, Richardson Highway MP 113 research site. The phase change isotherm is represented as the dashed blue line and the temperature results are shown with a 2°F contour interval.
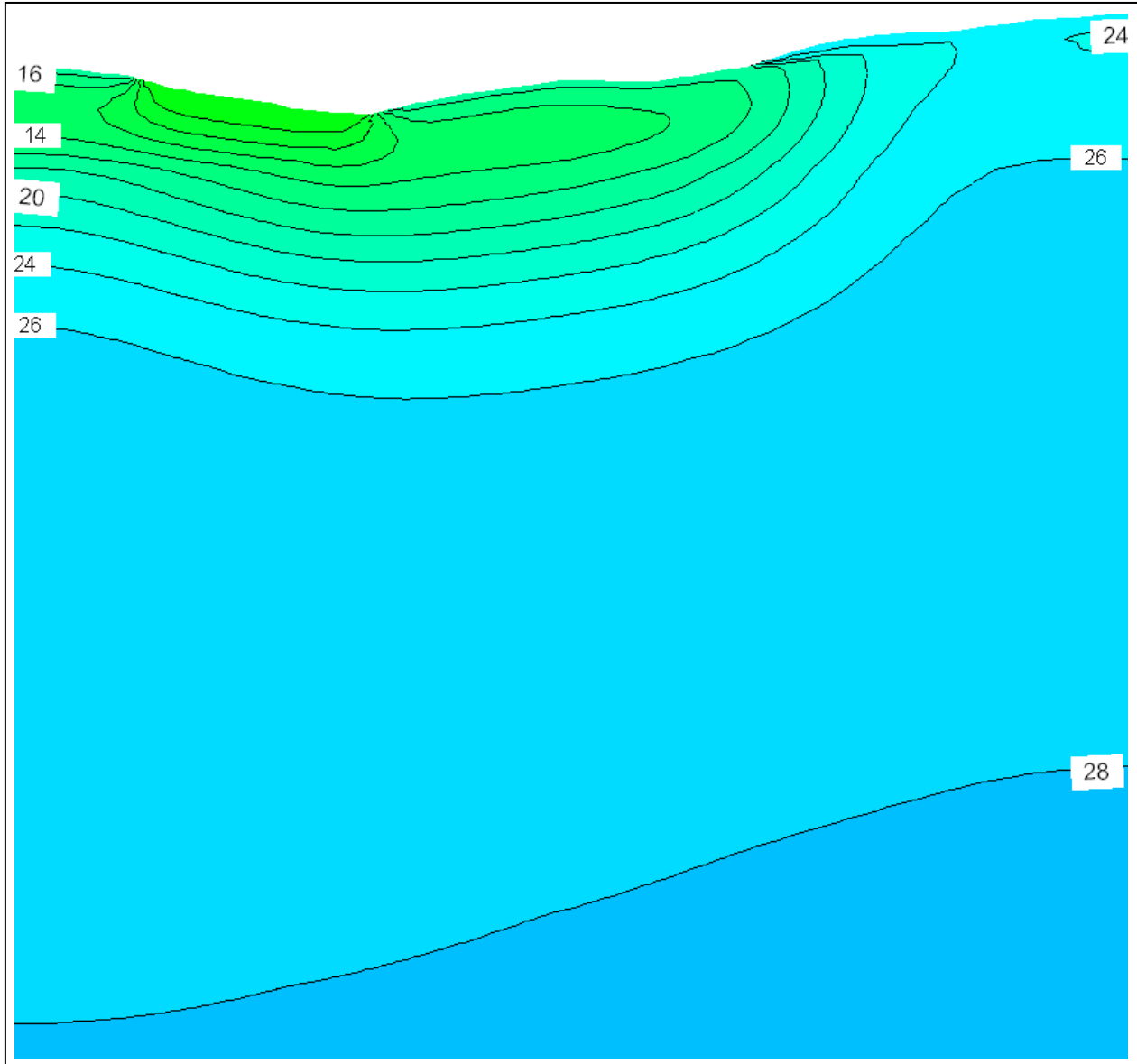
Figure F.23. Thermal modeling results for November 1st, Run 3, Richardson Highway MP 113 research site. The phase change isotherm is represented as the dashed blue line and the temperature results are shown with a 2°F contour interval.

Figure F.24. Thermal modeling results for December 1st, Run 3, Richardson Highway MP 113 research site. The phase change isotherm is represented as the dashed blue line and the temperature results are shown with a 2°F contour interval.
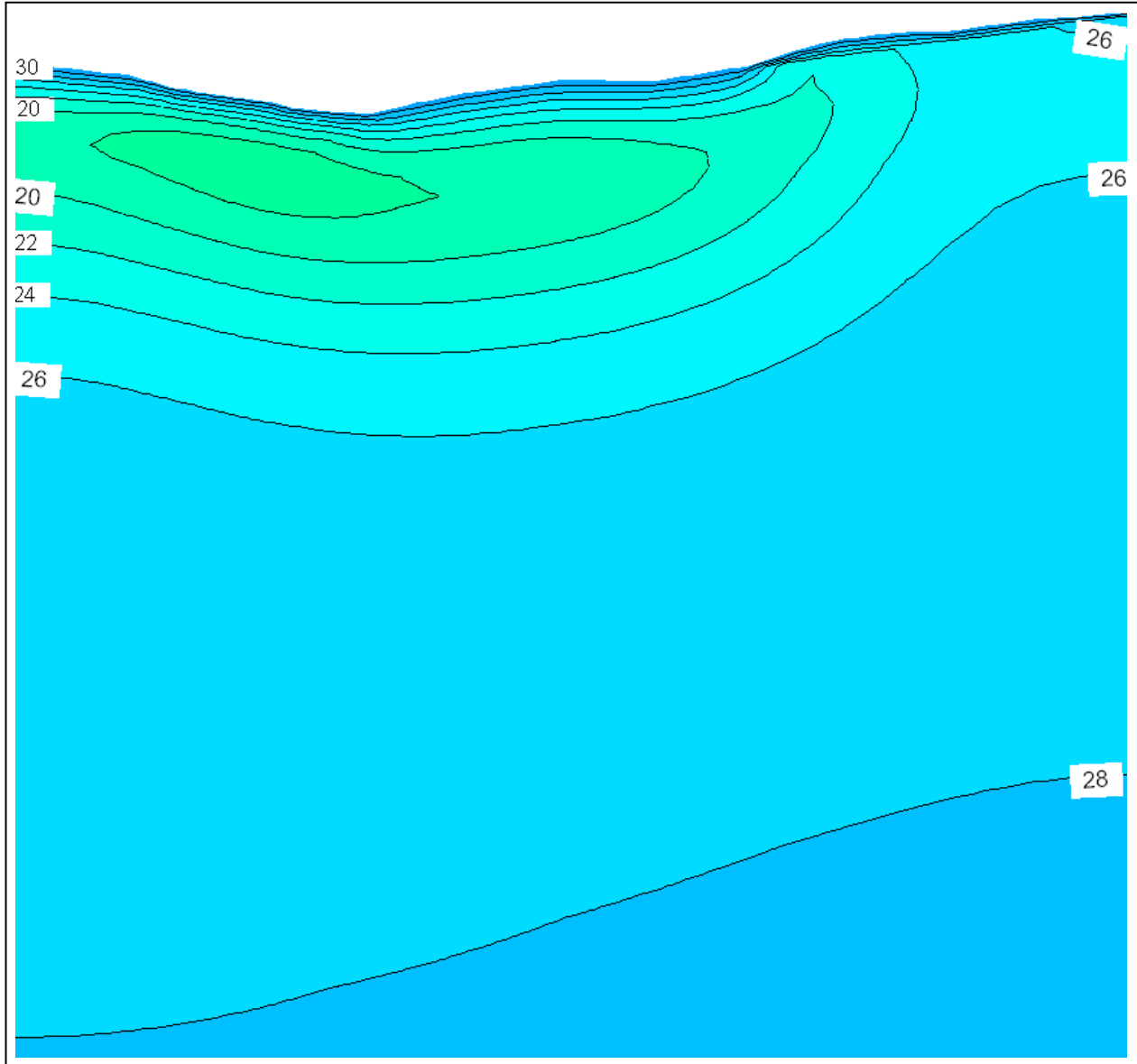
Figure G.1. Thermal modeling results for January 1st, Run 2, Dalton Highway 9 Mile Hill research site. The phase change isotherm is represented as the dashed blue line and the temperature results are shown with a 2°F contour interval.
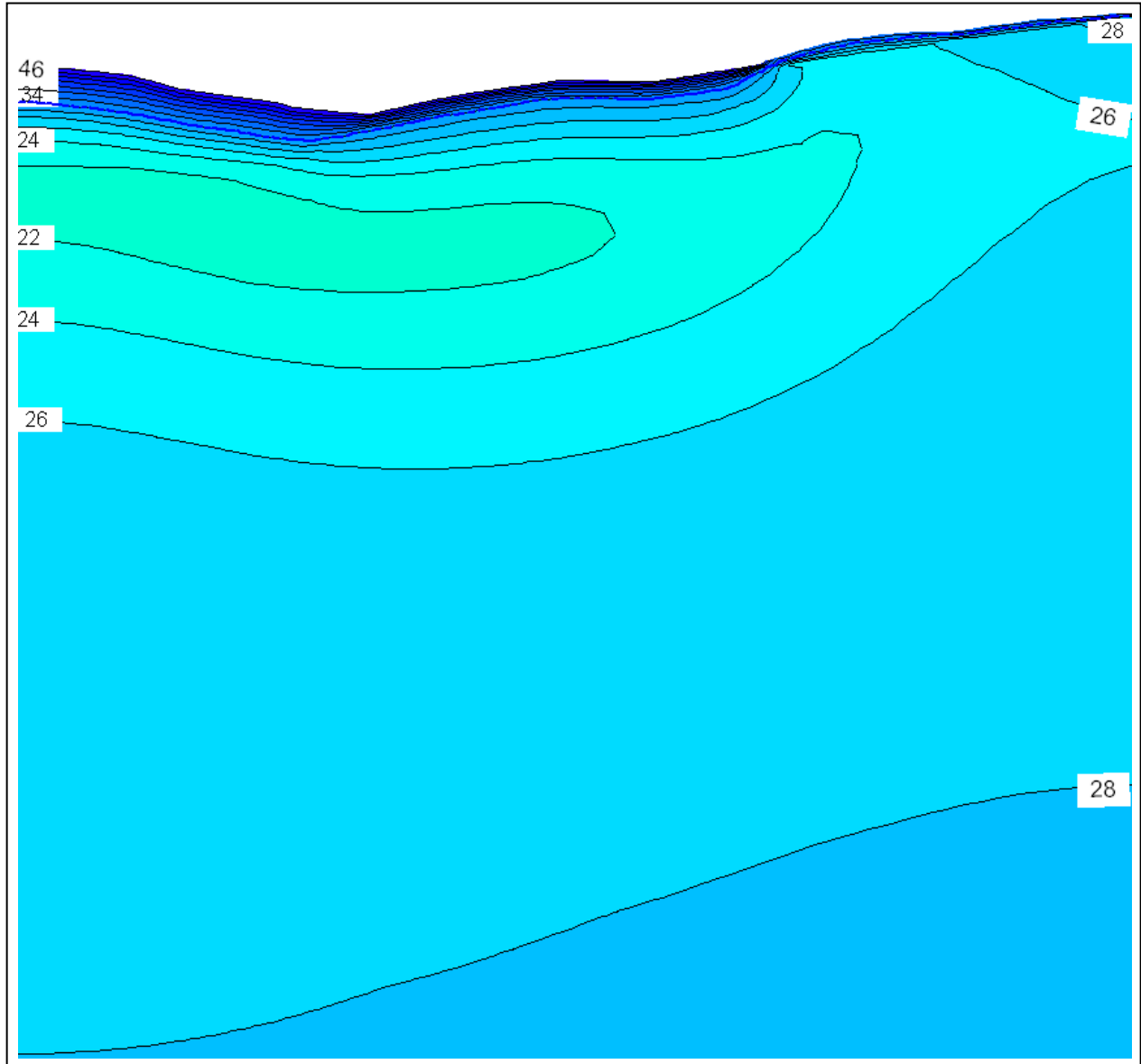
Figure G.2. Thermal modeling results for February 1st, Run 2, Dalton Highway 9 Mile Hill research site. The phase change isotherm is represented as the dashed blue line and the temperature results are shown with a 2°F contour interval.

Figure G.3. Thermal modeling results for March 1st, Run 2, Dalton Highway 9 Mile Hill research site. The phase change isotherm is represented as the dashed blue line and the temperature results are shown with a 2°F contour interval.
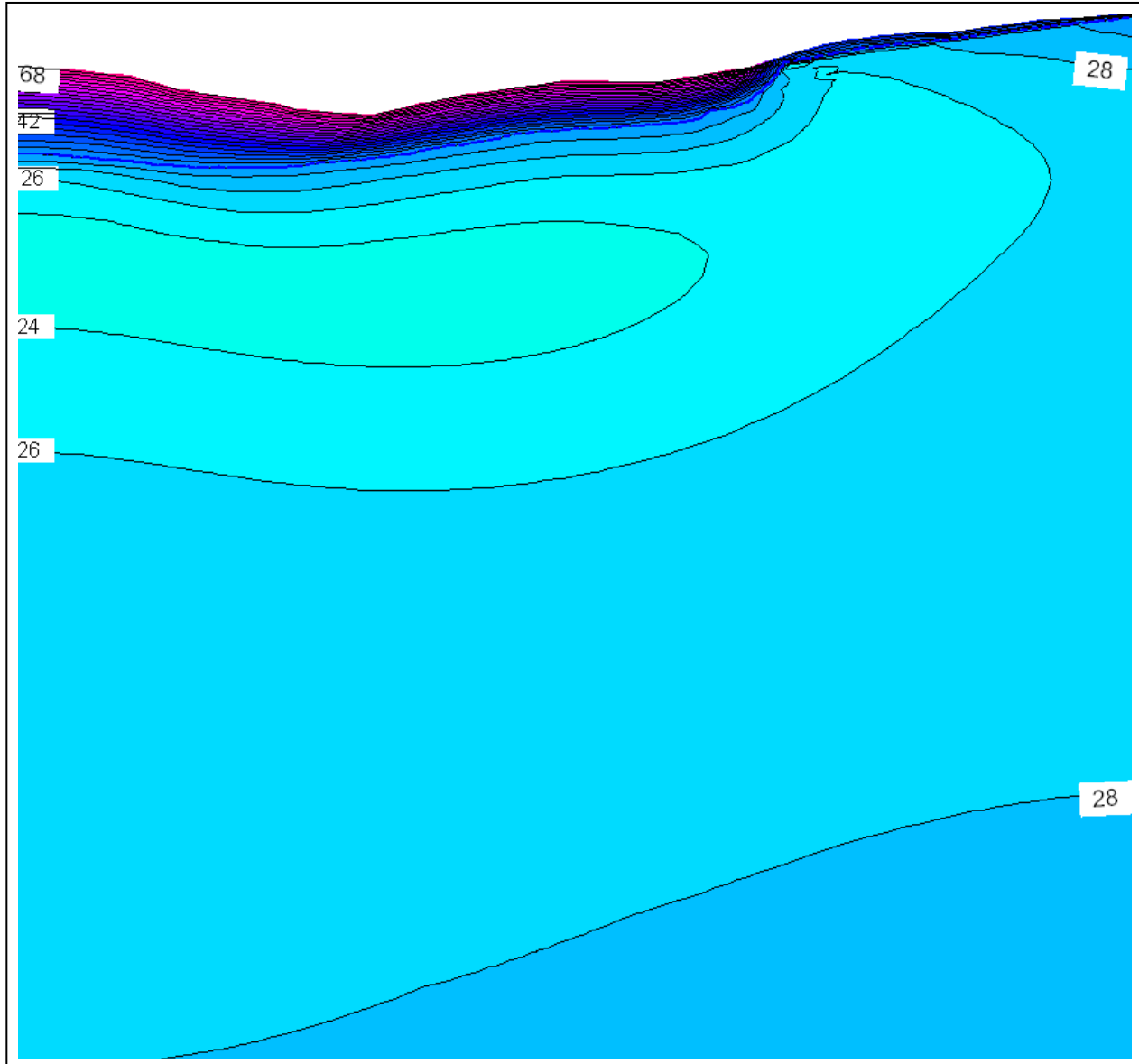
Figure G.4. Thermal modeling results for April 1st, Run 2, Dalton Highway 9 Mile Hill research site. The phase change isotherm is represented as the dashed blue line and the temperature results are shown with a 2°F contour interval.
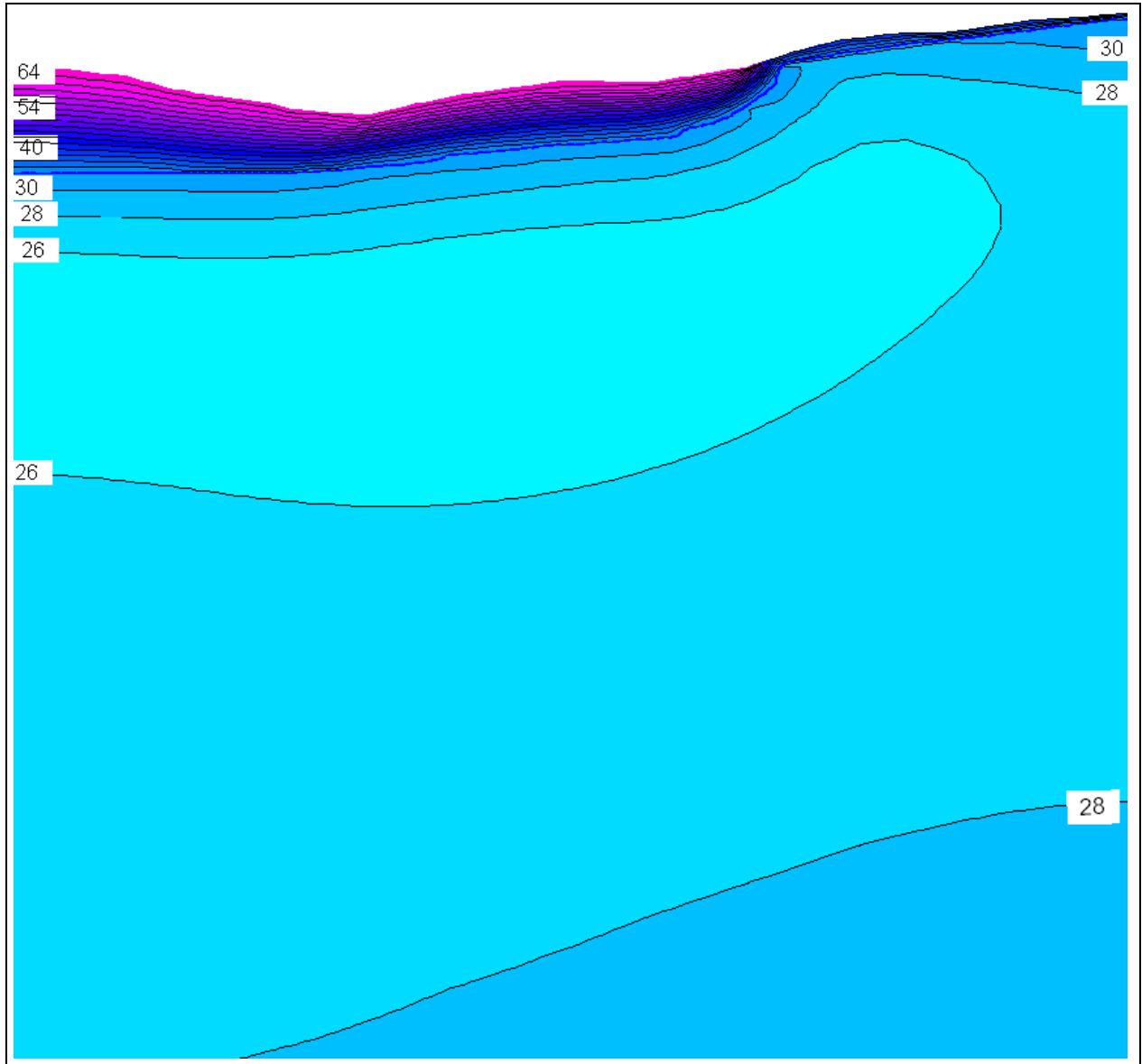
Figure G.5. Thermal modeling results for May 1st, Run 2, Dalton Highway 9 Mile Hill research site. The phase change isotherm is represented as the dashed blue line and the temperature results are shown with a 2°F contour interval.

Figure G.6. Thermal modeling results for June 1st, Run 2, Dalton Highway 9 Mile Hill research site. The phase change isotherm is represented as the dashed blue line and the temperature results are shown with a 2°F contour interval.
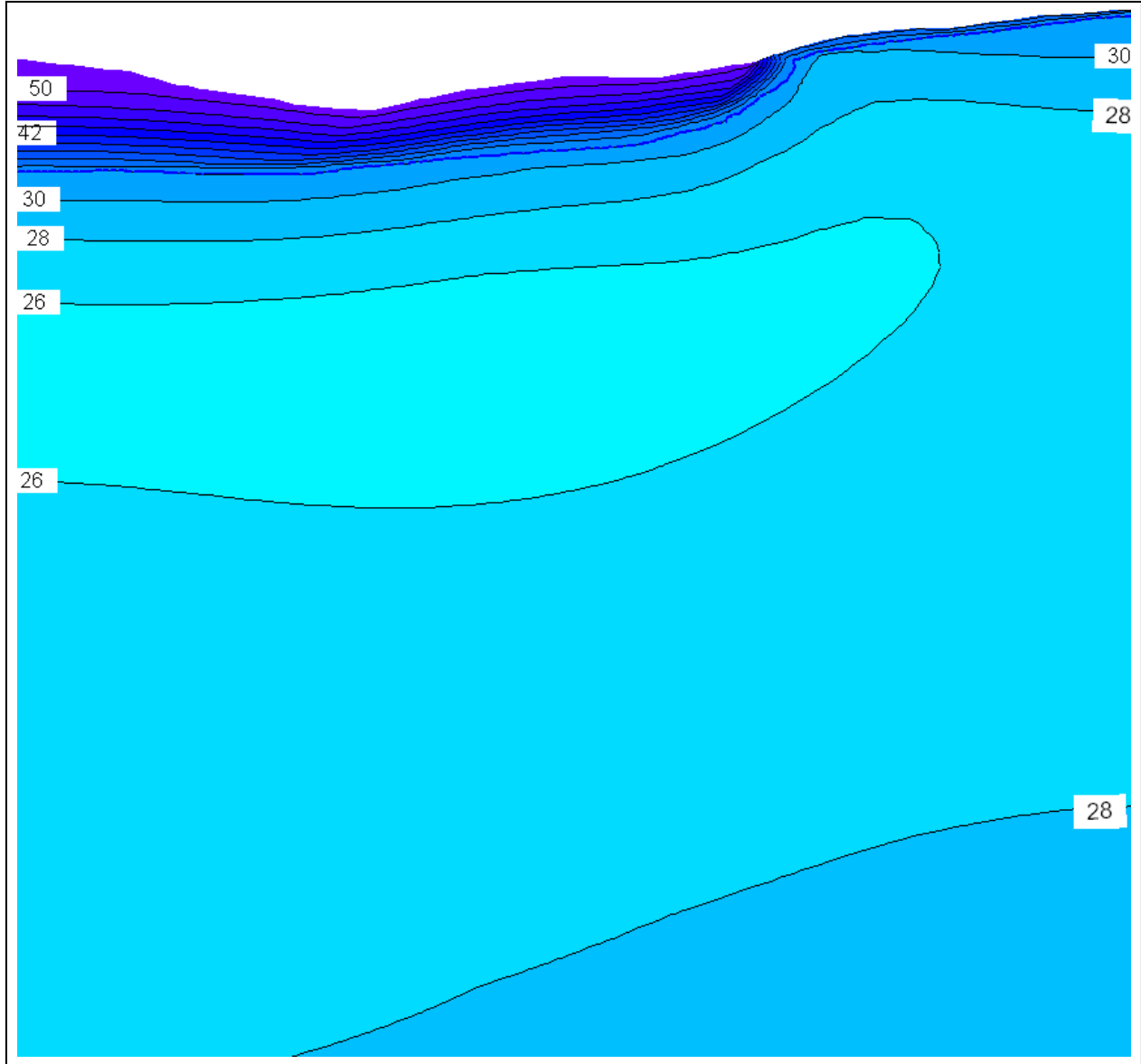
Figure G.7. Thermal modeling results for July 1st, Run 2, Dalton Highway 9 Mile Hill research site. The phase change isotherm is represented as the dashed blue line and the temperature results are shown with a 2°F contour interval.

Figure G.8. Thermal modeling results for August 1st, Run 2, Dalton Highway 9 Mile Hill research site. The phase change isotherm is represented as the dashed blue line and the temperature results are shown with a 2°F contour interval.
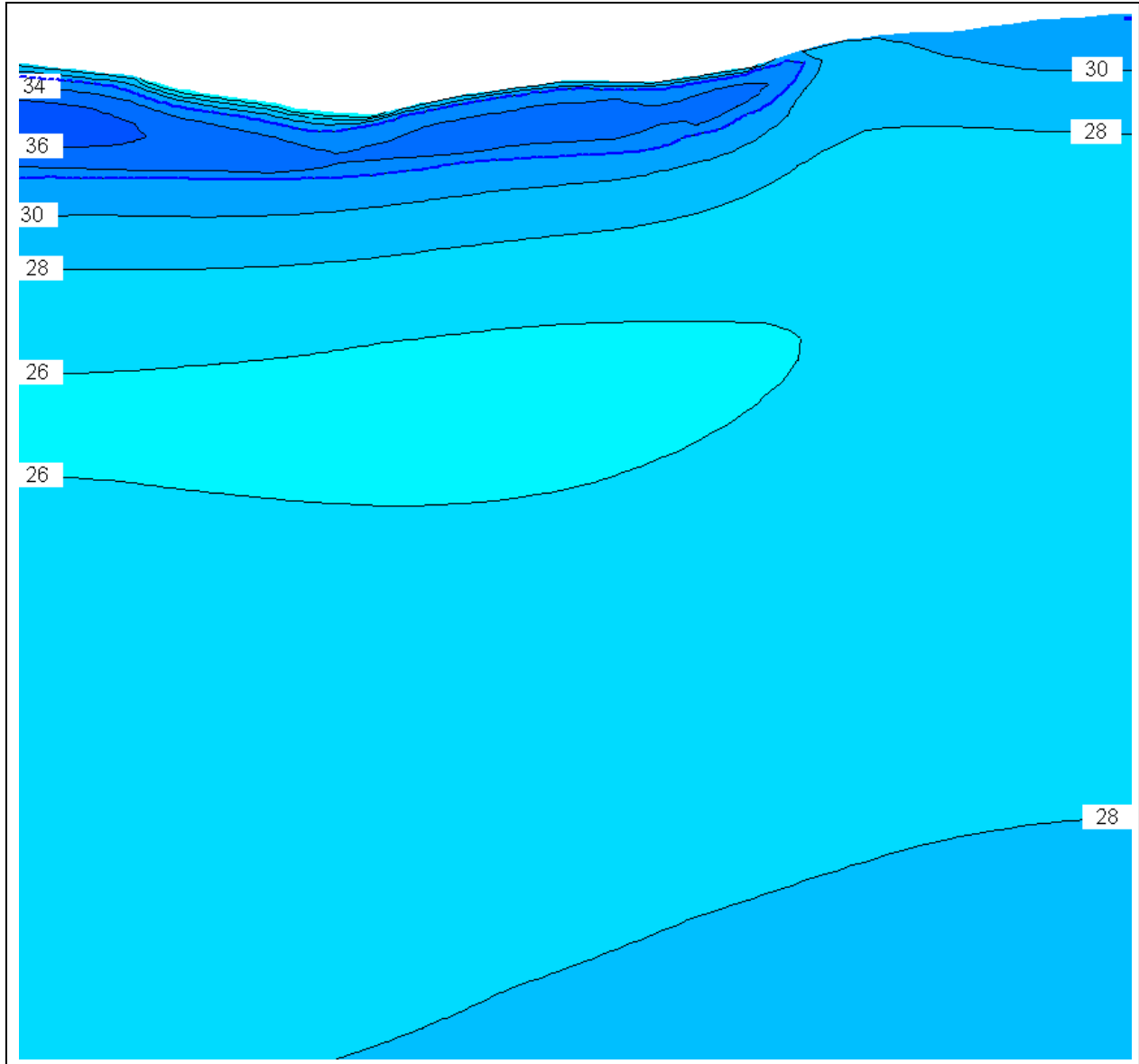
Figure G.9. Thermal modeling results for September 1st, Run 2, Dalton Highway 9 Mile Hill research site. The phase change isotherm is represented as the dashed blue line and the temperature results are shown with a 2°F contour interval.
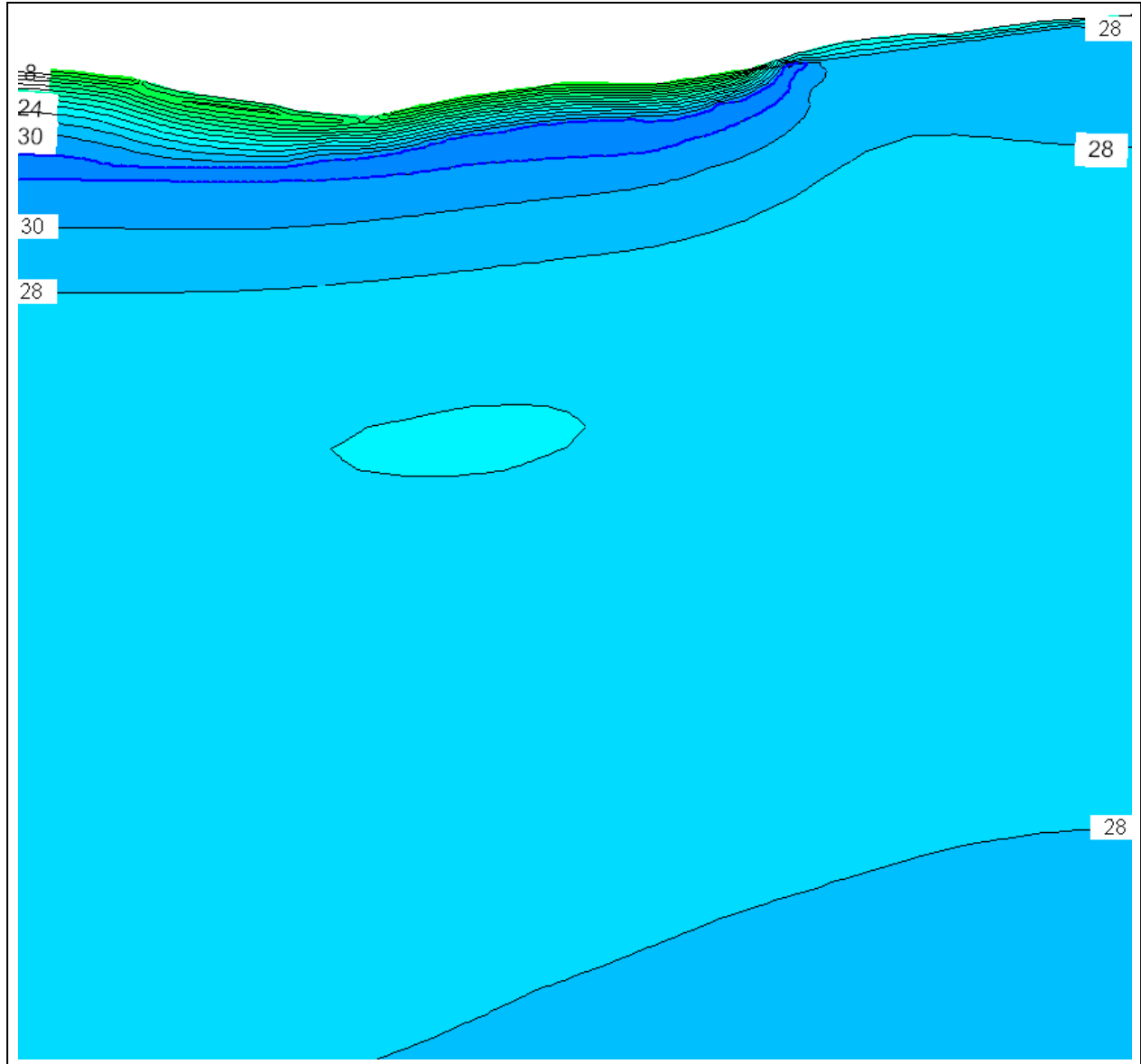
Figure G.10. Thermal modeling results for October 1st, Run 2, Dalton Highway 9 Mile Hill research site. The phase change isotherm is represented as the dashed blue line and the temperature results are shown with a 2°F contour interval.

Figure G.11. Thermal modeling results for November 1st, Run 2, Dalton Highway 9 Mile Hill research site. The phase change isotherm is represented as the dashed blue line and the temperature results are shown with a 2°F contour interval.
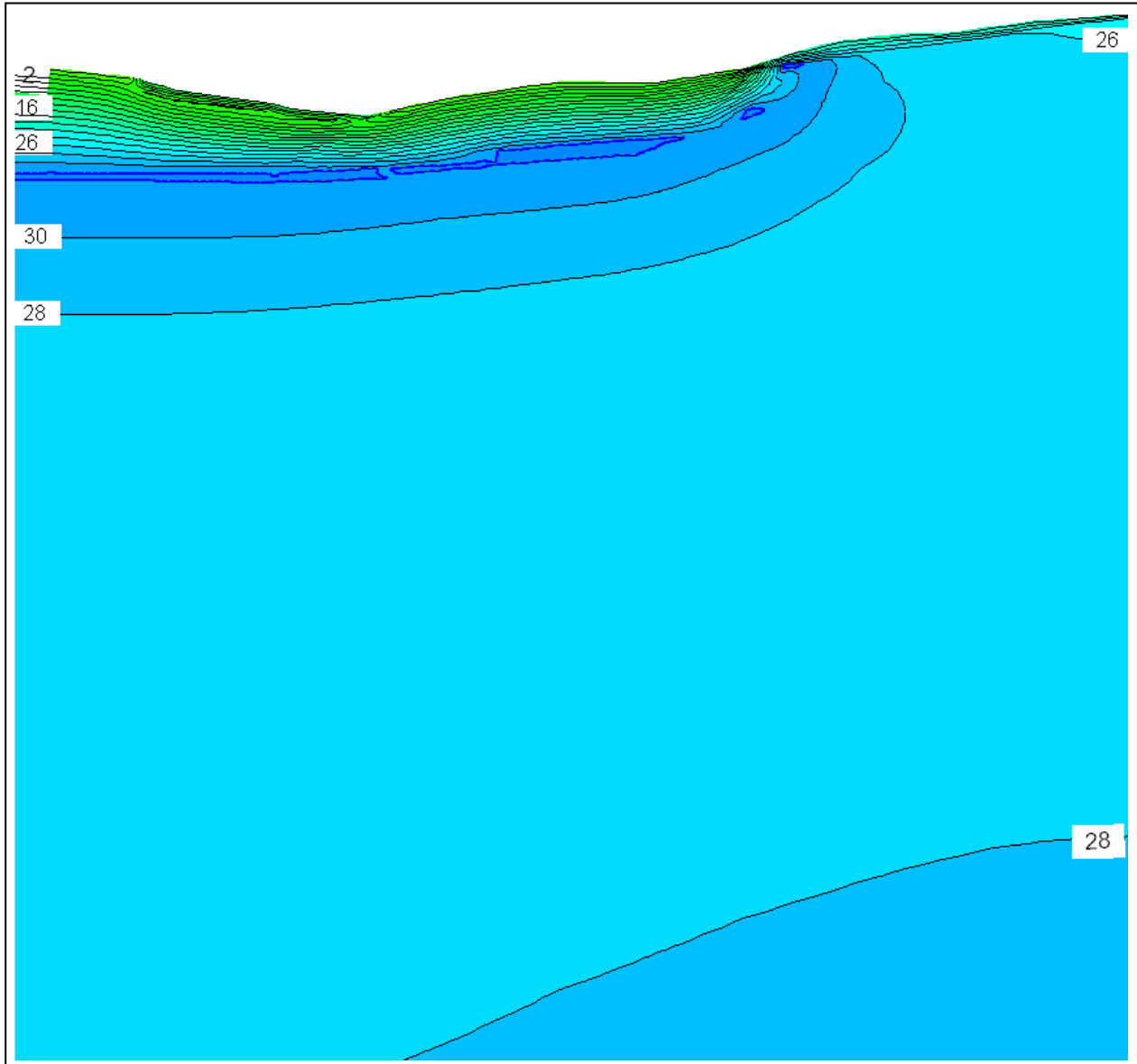
Figure G.12. Thermal modeling results for December 1st, Run 2, Dalton Highway 9 Mile Hill research site. The phase change isotherm is represented as the dashed blue line and the temperature results are shown with a 2°F contour interval.

SELECTING INPUT PARAMETERS FOR THERMAL MODELING OF FROZEN SOIL USING THE TEMP/W PROGRAM

This guide is intended to be used as a supplement to published resources already available from Geo-Slope for TEMP/W. As such, the focus of this guide is not how to run the TEMP/W program, but rather how to choose appropriate input parameters for modeling a typical highway or runway embankment over frozen foundation soils.

Additionally, this guide is written for use with GeoStudio 2004 TEMP/W (Version 6.19). More up-to-date versions of TEMP/W are available and are highly recommended. While the input parameters will not change from version to version, how one enters them may.

Figure H.1 is a screen shot of part of the TEMP/W program, illustrating the typical tools at your disposal when the program first starts. A good practice is to work from left to right across the first tool bar that begins with the *File* menu. Other than saving your document, there is not much to do until the *Set* menu. Here you can change how your document is laid out on the screen, grids, rulers, etc. The most important part is the submenu *Units and Scale* (see Figure H.2). This is where you set the general units that are essential for the rest of the model. All following input parameters need to have units that are consistent with the units chosen in this window.

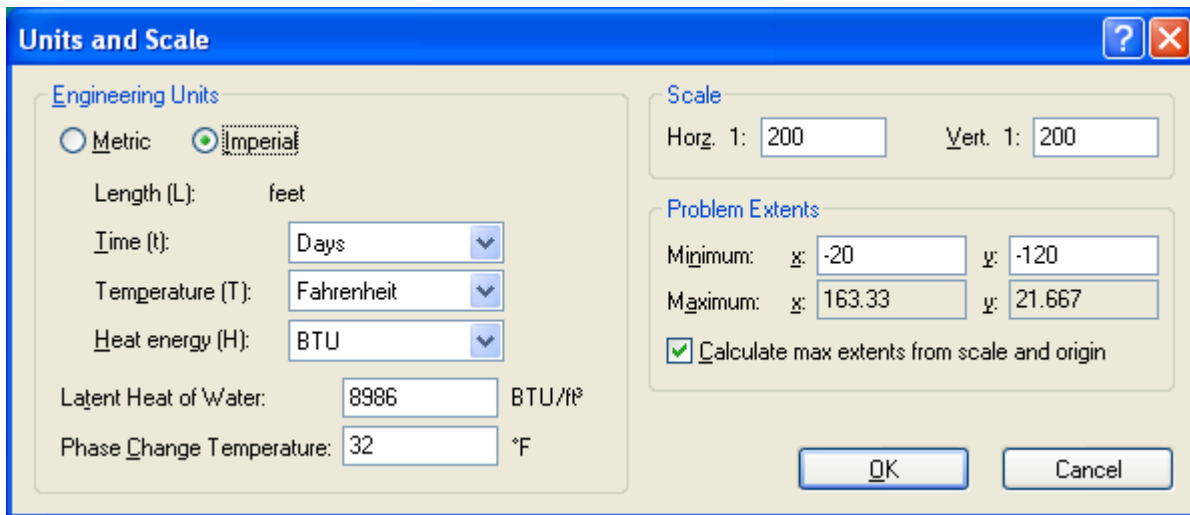Figure H.1. The general toolbars in TEMP/W.

Figure H.2. The *Units and Scale* window in the *Set* menu. It is critical that all other input parameters have units that are consistent with what is specified here.

271

Skipping over the *View* menu, the next essential menu and one which will demand the most attention is the *KeyIn* menu. Figure H.3 is a screen shot of the *KeyIn* menu with all of the submenus shown. The following discussion will work sequentially down this menu.

The first submenu available is *Analysis Settings*. Selecting this will open a window that has five tabs: *Project ID*, *Type*, *Control*, *Convergence*, and *Time*. The *Project ID* tab contains fields for general record-keeping. Under the *Type* tab, it is important to choose "Transient" for the *Analysis Type* for typical embankment analysis. Under *Initial Conditions* you can specify the temperatures from a specific time step in another project as the initial temperature conditions for your new project; however, for most new analyses, this should be left blank. Do not change any of the default parameters under the *Control* and *Convergence* tabs. Figure H.4 is a screen shot of the final tab, *Time*. Here you will specify for how long you want your model to run. A time step will have the units that you specified in *Units and Scale*. For example, in Figure H.2, "Days" are selected for *Time (t)*. Thus, in Figure H.4, each time step will be one day; the total time for the model is 1,825 days or 5 years. This is the suggested minimum amount of time a model should be run, since some time is needed for the model to become thermally stable and adjust to all of the boundary conditions and input parameters. For areas where the underlying permafrost is expected to thaw, 50 years may be suitable for the model time. Unfortunately, a longer model time equates to a larger file and more computing time for your computer. The file size can be reduced by adjusting some of the other values shown in Figure H.4. For example, for the 5 year model, model results are not saved until after the first month (i.e., the *Start Saving at Step* box contains the time step 30). Also, the model results are saved only every 5 days. To reduce the file size of a 50 year model, model results could be saved every year. Keeping the other default values, click the *Generate* button to develop the time steps, which you can view in the box to the lower left.
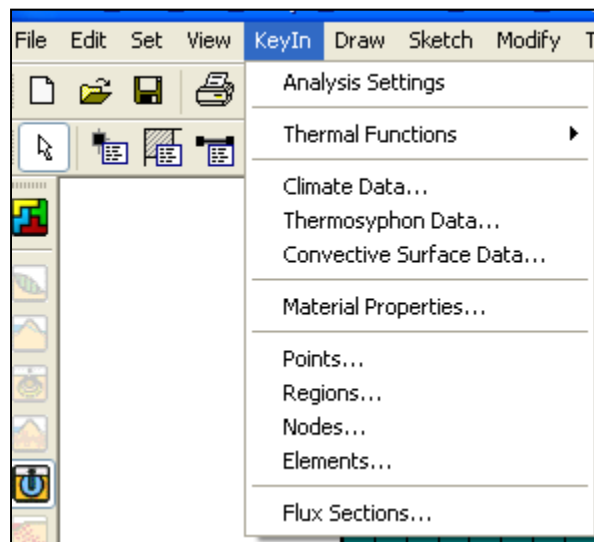

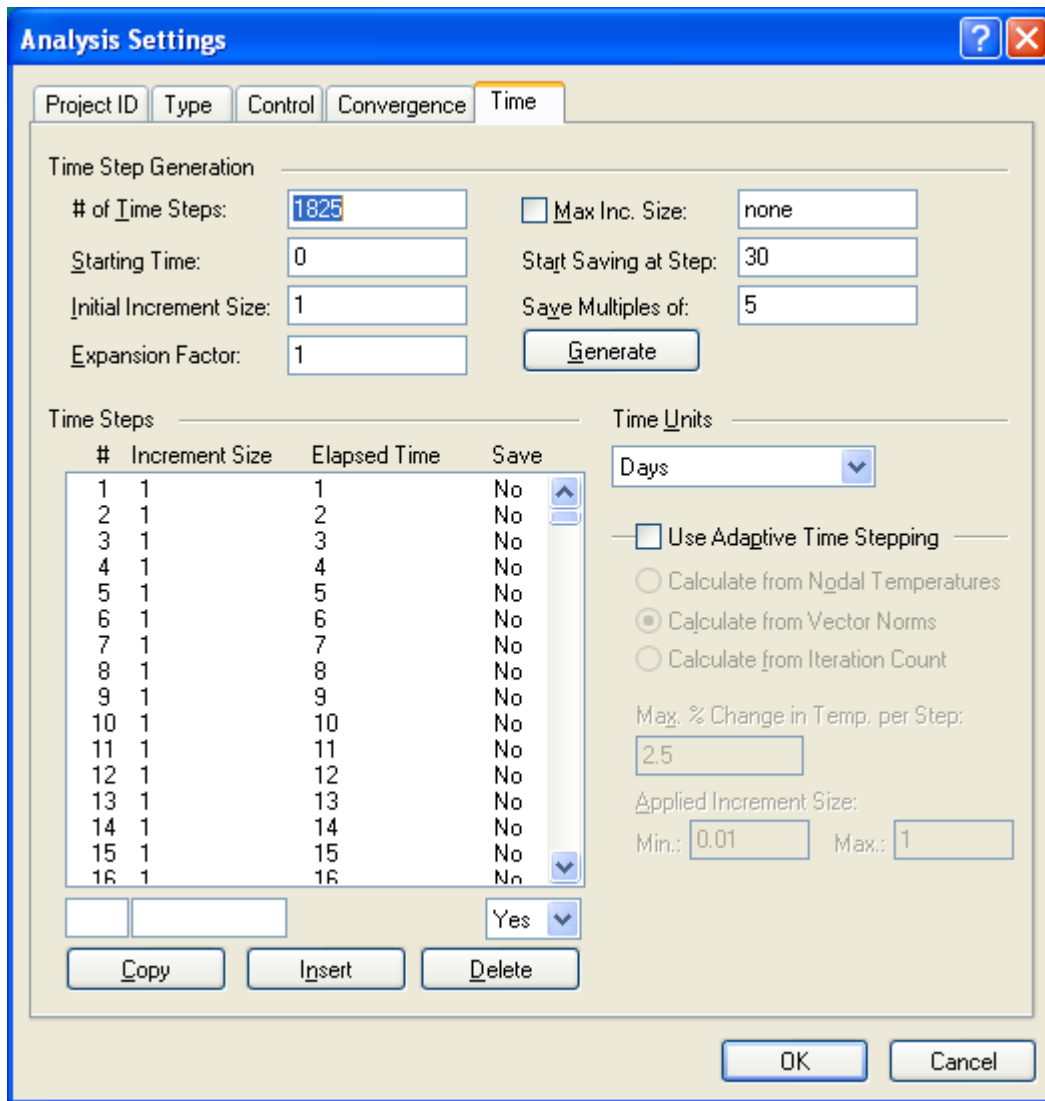Figure H.3. The *KeyIn* menu with drop-down submenus.

Figure H.4. The time step generation tab under *Analysis Settings*.

The next submenu under *KeyIn* is *Thermal Functions*. This submenu has an arrow next to it, which pops out further submenus, each of which is important. The first is *Thermal Conductivity (K vs T)…*. Clicking on this brings up a box where you can create, edit, delete, or import a thermal conductivity function. Once functions are developed, they will appear in the box to the left. Choosing to create a new function will bring up a dialogue box similar to that in Figure H.5. Enter a name for your function for a specific soil type in the *Description* box.

You will need to provide values for both frozen and unfrozen thermal conductivity. If you do not have measured values, you easily can estimate values using charts developed by Kersten (1949). These charts have been republished in other sources, including Andersland and Ladanyi (2004). Care must be taken in choosing the appropriate chart for the soil, i.e. either fine-grained or coarse-grained. The next step in estimating thermal conductivity is to know the moisture content and the dry unit weight, often called dry "density" on the chart. Although moisture content is a test typically run at AK DOT&PF, the determination of dry unit weight is not.
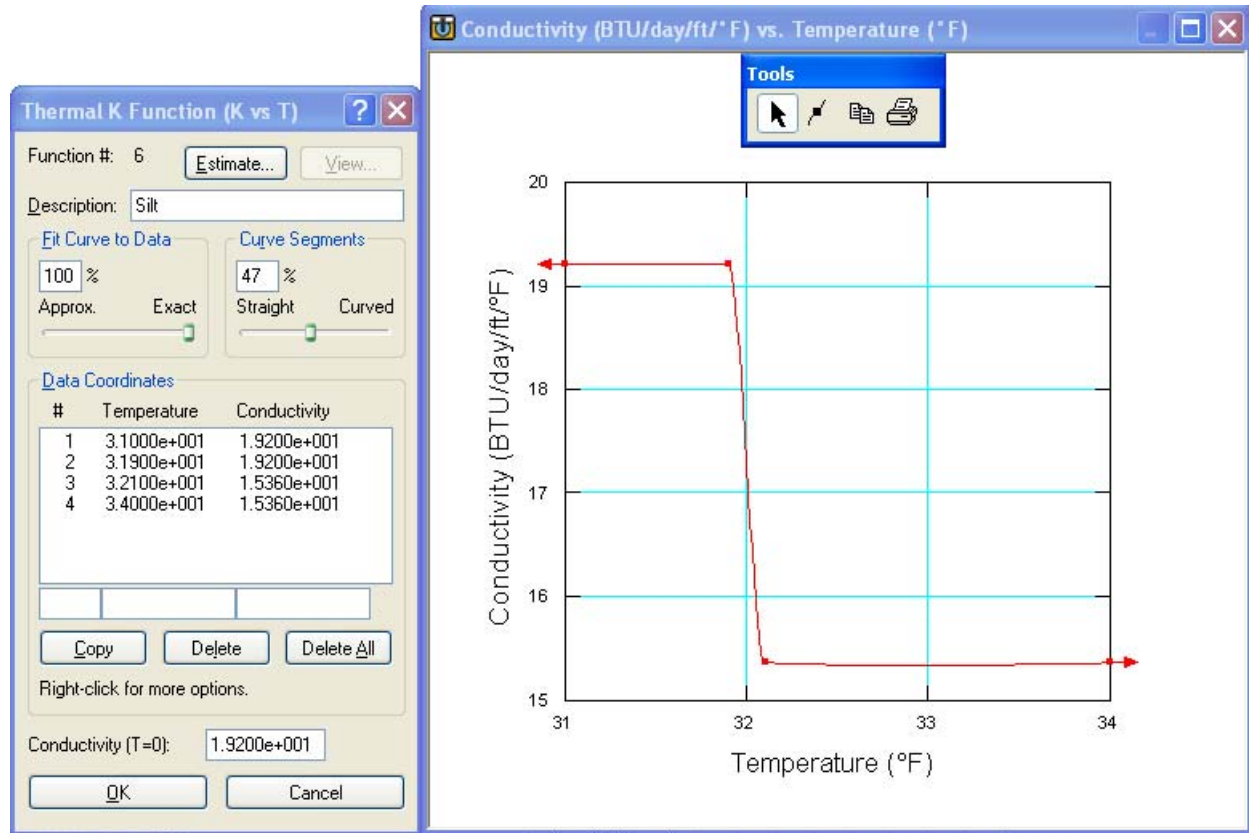
Figure H.5. An example of a thermal conductivity function for silt.

Thus, you will need to look at other references for estimates of this value for your soil. Most soil mechanics books have tables of typical dry unit weights (e.g., Das 1998, Coduto 1999). With approximate values of dry unit weight and soil moisture on hand, estimating the thermal conductivity of the soil is straightforward. This information is then entered into TEMP/W in the input window shown on the left in Figure H.5. Once at least two values are entered, the **View** button can be selected to show a graph of the values (shown on the right in Figure H.5). The program will not allow a vertical segment in any function, so the temperatures chosen must be on either side of 32°F.

Care must be taken for ice-rich soils. First of all, the dry unit weight of an ice-rich soil may be much less than the typical values presented in the literature. This is because most of the volume is ice rather than soil. One way to deal with this is to calculate the thermal conductivity using a geometric mean formula, such as:

$$k_f = k_{ice}^{\%ice} \cdot k_{f_{soil}}^{1-\%ice}$$

The next item under **Thermal Functions** is **Unfrozen W. C.**, standing for unfrozen water content. This function is most critical for fine-grained soils, and especially those with a clay content. An example of the input screen is shown in Figure H.6. The graph to the right in Figure H.6 is the unfrozen water content of a clay. You can use TEMP/W to estimate a function for you by clicking the **Estimate…** button; however, the estimates are not accurate. Otherwise, unfrozen
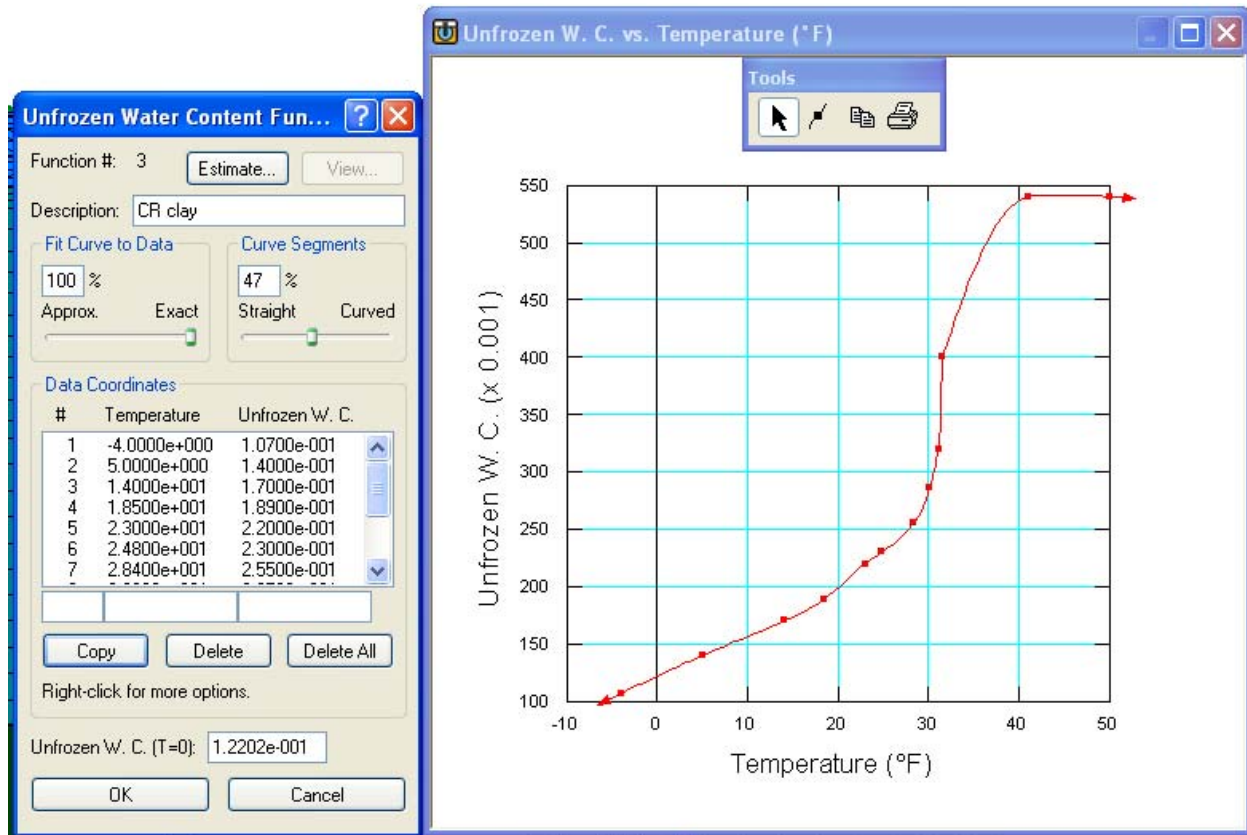
Figure H.6. An example of an unfrozen water content function for clay.

water content data is available in the literature (e.g., Darrow et al. 2009). Ideally, this value is measured for the specific soil being modeled.

Continuing under ***Thermal Functions***, the next selection is ***Boundary Functions***. A boundary function is what is applied as an upper or lower boundary condition in the model. For the lower boundary condition, one may apply a unit flux boundary condition to simulate geothermal heat flow. An average value for this, and in units matching those in Figure H.2, is 0.24 Btu/day·ft^2.

For the upper boundary condition, air temperature can be applied. The boundary condition can be created graphically by moving points in the ***View*** window to simulate a sinusoidal function. For a more accurate boundary function, however, real air temperature data should be used. An internet resource for air temperature data in Alaska is the Western Regional Climate Center (http://www.wrcc.dri.edu/). This site contains historic data for most of the Alaskan communities. However, for some places, the data is spotty and out-of-date. The data for a station can be acquired from the internet site and opened in a spreadsheet program, such as Excel. Then, the data should be averaged to obtain average daily air temperatures for each day of the year. A complete year's worth of data can be copied and pasted in Excel to acquire a multi-year function, the length of which should match the length of the model specified in the ***Analysis Settings***. This data then can be copied and pasted directly into the input window in TEMP/W, saving hours of typing in values by hand. An example of a five-year-long function is shown in Figure H.7.
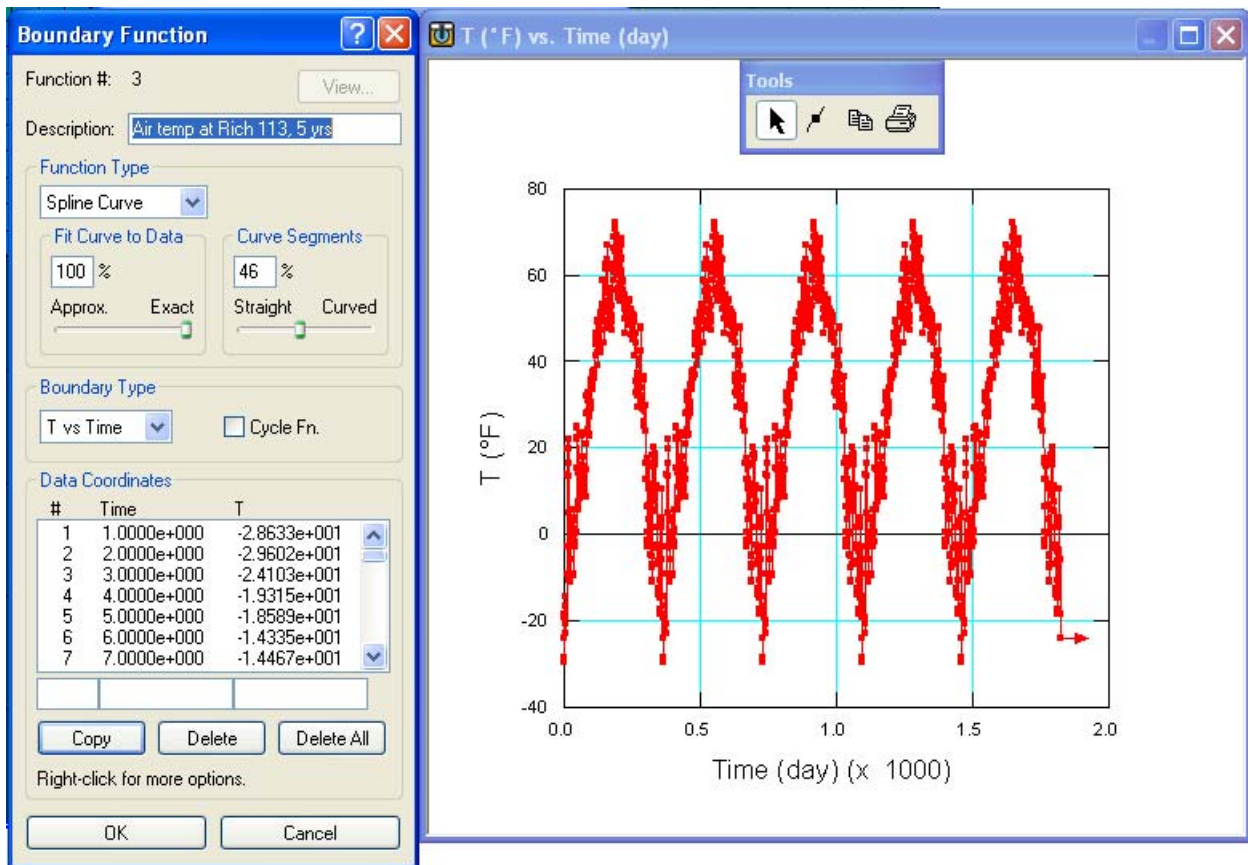
275

Figure H.7. An example of an air temperature boundary condition function.

Going hand-in-hand with the *Boundary Functions* are the *Modifier Functions*. These are the *n*-factors that modify the air temperature to simulate the surface temperature. Typical *n*-factors can be found in the literature (e.g., Andersland and Ladanyi 2004), and should be chosen to match what is on the ground surface. Examples are asphalt, gravel, bare mineral soil, and a spruce forest with sphagnum moss. Care must be taken to adjust the *n*-factors to account for the amount and/or density of snow cover on embankment shoulders and over undisturbed ground. To form a function for a given surface, you must input *n*-factors for conditions both above and below freezing.

Next on the *KeyIn* menu are three input items: *Climate Data…, Thermosyphon Data…,* and *Convective Surface Data…*   These three areas are for more specialized information that is not necessary for most embankment analyses. Thus, they will not be discussed further.

Material Properties… is the next submenu. This is where you will enter the last of the soil properties. Each soil is represented by a row in the *KeyIn Material Properties* window (see Figure H.8). In the 2004 version of TEMP/W, it is handy to record and to be consistent with the order in which you input thermal conductivity and unfrozen water content functions. Once in the *KeyIn Material Properties* window, you will need to recall via their order the relevant function for each soil type (see the second and third columns in Figure H.8). The fourth and fifth columns in Figure H.8 contain the soil's frozen and unfrozen volumetric heat capacity, respectively. These values can be calculated using the following equations:
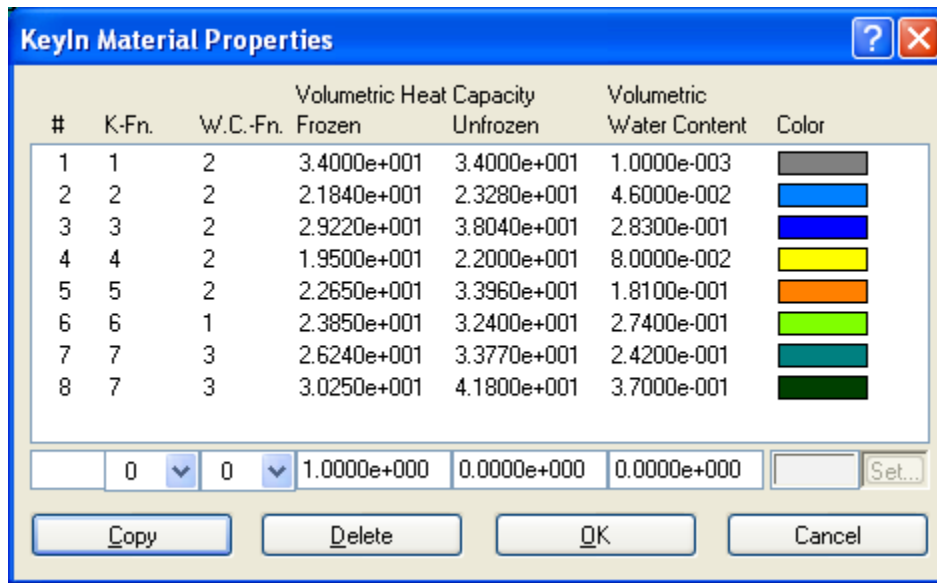
Figure H.8. The *KeyIn Material Properties* window.

$$c_f = \gamma_d[0.17 + 0.5 \cdot (^W/_{100})]$$

$$c_u = \gamma_d[0.17 + (^W/_{100})]$$

where γ_d is the dry unit weight of the soil, and w is the gravimetric water content. These equations have been simplified to include the specific heat of dry soil and the specific heat of water or ice, and values for c_f and c_u are in units of Btu/ft^3·°F. These equations also can be modified to include the unfrozen water content of the soil (see Andersland and Ladanyi (2004) for more information). The sixth column in Figure H.8 contains values for the soil's volumetric water content, θ. This can be calculated from the gravimetric water content using the following equation:

$$\theta = w\frac{\gamma_d}{\gamma_w}$$

where w is the gravimetric moisture content, γ_d is the dry unit weight, and γ_w is the unit weight of water. In the final column in Figure H.8, you can set the color of the soil type for easy recognition in the model.

The remaining submenus in the *KeyIn* menu are for creating the mesh. The TEMP/W manual and lots of practice are the best aids in this endeavor. Happy modeling!